

**„ HYPERBRANCHED POLYETHER POLYOLS
AS BUILDING BLOCKS FOR COMPLEX
MACROMOLECULAR ARCHITECTURES ”**

Dissertation
zur
Erlangung des Grades

„ Doktor der Naturwissenschaften ”

am Fachbereich Chemie, Pharmazie und Geowissenschaften
der Johannes Gutenberg – Universität in Mainz



Emilie Barriau

geboren in Clermont-Ferrand (Frankreich)

Mainz 2005

Tag der mündlichen Prüfung: 21. Dezember 2005

“Penser, ce n'est pas unifier, rendre familière l'apparence sous le visage d'un grand principe. Penser, c'est réapprendre à voir, diriger sa conscience, faire de chaque image un lieu privilégié.”

Albert Camus.

ABSTRACT

The present thesis deals with the development of new branched polymer architectures containing hyperbranched polyglycerol. Materials investigated include hyperbranched oligomers, hyperbranched polyglycerols containing functional initiator-cores at the focal point, well-defined linear-hyperbranched block copolymers and also negatively charged hyperbranched polyelectrolytes.

Hyperbranched oligoglycerols ($DP_n = 7$ and 14) have been synthesized for the first time. The materials show narrow polydispersity (M_w/M_n ca. 1.45) and a very low content in cyclic homopolymers. ^{13}C NMR evidences the dendritic structure of the oligomers and the DB could be calculated (44% and 52%). These new oligoglycerols were compared with the industrial products obtained by polycondensation which exhibit narrow polydispersity ($M_w/M_n < 1.3$) but multimodal distribution in SEC. Detailed ^{13}C NMR and Maldi-ToF studies reveal the presence of branched units and cyclic compounds. In comparison, the hyperbranched oligoglycerols comprise a very low proportion of cyclic homopolymer which render them very interesting materials for biomedical applications for example.

The site isolation of the core moiety in dendritic structure offers intriguing potential with respect to peculiar electro-optical properties. Various initiator-cores (*n*-alkyl amines, UV-absorbing amines and benzophenone) for the ROMBP of glycidol have been tested. The bisglycidolized amine initiator-cores show the best control over the molecular weight and the molecular weight distribution. The photochemical analyses of the naphthalene containing hyperbranched polyglycerols show a slight red shift, a pronounced hypochromic effect (decrease of the intensity of the band) compared with the parent model compound and the formation of a relative compact structure. The benzophenone containing polymers adopt an open structure in polar solvents. The fluorescence measurements show a clear “dendritic effect” on the fluorescence intensities and the quantum yield of the encapsulated benzophenone.

A convenient 3-step strategy has been developed for the preparation of well-defined amphiphilic, linear-hyperbranched block copolymers via hypergrafting. The procedure represents a combination of carbanionic polymerization with the alkoxide-based, controlled ring-opening multibranching polymerization of glycidol. Materials consisting of a polystyrene linear block and a hyperbranched polyglycerol block exhibit narrow polydispersity (1.01-1.02 for 5.4% to 27% wt. PG and 1.74 for 52% wt. PG) with a high grafting efficiency. The strategy was also extended to materials with a linear polyisoprene block.

Detailed investigations of the solution properties of the block copolymers with linear polystyrene blocks show that block copolymer micelles are stabilized by the highly branched block. The morphology of the aggregates is depending on the solvent: in chloroform monodisperse spherical shape aggregates and in toluene ellipsoidal aggregates are formed. On graphite these aggregates show interesting features, giving promising potential applications with respect to the presence of a very dense, functional and stable hyperbranched block.

The bulk morphology of the linear-hyperbranched block copolymers has been investigated. The materials with a linear polyisoprene block only behave like complex liquids due to the low T_g and the disordered nature of both components. For the materials with polystyrene, only the sample with 27% wt. hyperbranched polyglycerol forms some domains showing lamellae.

The preparation of hyperbranched polyelectrolytes was achieved by post-modification of the hydroxyl groups via Michael addition of acrylonitrile, followed by hydrolysis. In aqueous solution materials form large aggregates with size depending on the pH value. After deposition on mica the structures observed by AFM show the coexistence of aggregates and unimers. For the low molecular weight sample (PG 520 $\text{g}\cdot\text{mol}^{-1}$) extended and highly ordered terrace structures were observed. Materials were also successfully employed for the fabrication of composite organic-inorganic multilayer thin films, using electrostatic layer-by-layer self-assembly coupled with chemical vapor deposition.

TABLE OF CONTENTS

1. Introduction	1
1.1. Hyperbranched polymers	1
1.1.1. <i>General concept for the core-dilution/slow addition strategy</i>	2
1.1.2. <i>Polymerization procedure for latent AB₂ monomers</i>	4
1.1.3. <i>Perspectives for hyperbranched polyglycerol</i>	7
1.2. Linear-dendritic block copolymers	9
1.2.1. <i>Linear-dendrimer block copolymers</i>	11
1.2.2. <i>Linear-hyperbranched block copolymers</i>	12
1.3. References	15
2. Objectives	19
2.1. Introduction	19
2.2. Comparison of industrial and hyperbranched oligoglycerols	20
2.3. Incorporation of new functional initiator-cores into hyperbranched polyglycerols	20
2.4. Synthetic routes for linear-hyperbranched amphiphilic block copolymers	21
2.5. Solution properties of linear-hyperbranched amphiphilic block copolymers	22
2.6. Solid-state properties of linear-hyperbranched amphiphilic block copolymers	22
2.7. Negatively charged hyperbranched polyglycerol polyelectrolytes	23
2.8. References	23
3. Comparison of industrial and hyperbranched oligoglycerols	25
3.1. Introduction	25
3.2. Hyperbranched oligoglycerols	26
3.3. Industrial oligoglycerols	30
3.4. Composition of the different materials	34
3.5. Conclusion	41
3.6. Experimental part	42
3.7. References	43
4. Functional initiator-cores for hyperbranched polyglycerols	45
4.1. Introduction	45
4.2. Amines as initiator-cores	47
4.2.1. <i>n-Alkyl amine initiator-cores</i>	49
4.2.2. <i>Photoactive amine initiator-cores</i>	54
4.3. Benzophenone as initiator-core	63

4.4. Conclusion	68
4.5. Experimental part	69
4.5.1. <i>Materials with amines as initiator-cores</i>	69
4.5.2. <i>Materials with benzophenone as initiator-cores</i>	70
4.6. References	71
5. Syntheses of linear-hyperbranched amphiphilic block copolymers	74
5.1. Introduction	74
5.2. Polystyrene- <i>block</i> -(1,2-polybutadiene- <u>hypergrafted</u> -polyglycerol)	75
5.3. Polyisoprene- <i>block</i> -(<u>hyperbranched</u> -polyglycerol)	82
5.4. Conclusion	86
5.5. Experimental part	87
5.5.1. <i>Polystyrene-<i>block</i>-(1,2-polybutadiene-<u>hypergrafted</u>-polyglycerol)</i>	87
5.5.2. <i>Polyisoprene-<i>block</i>-(<u>hyperbranched</u>-polyglycerol)</i>	88
5.6. References	91
6. Solution properties of linear-hyperbranched amphiphilic block copolymers	93
6.1. Introduction	93
6.2. Dynamic and light scattering measurements	94
6.2.1. <i>Measurements in chloroform</i>	95
6.2.2. <i>Measurements in toluene</i>	99
6.3. Atomic force microscopy	102
6.3.1. <i>Deposition from chloroform solution</i>	102
6.3.2. <i>Deposition from toluene solution</i>	103
6.4. Conclusion	107
6.5. References	108
7. Bulk morphology of linear-hyperbranched block copolymers	110
7.1. Introduction	110
7.2. Polyisoprene- <i>block</i> -(<u>hyperbranched</u> -polyglycerol)	111
7.3. Polystyrene- <i>block</i> -(1,2-polybutadiene- <u>hypergrafted</u> -polyglycerol)	115
7.4. Inorganic-organic silica nanohybrids	118
7.5. Conclusion	121
7.6. Experimental part	121
7.7. References	122

8. Negatively charged hyperbranched polyglycerol polyelectrolytes	124
8.1. Introduction	124
8.2. Synthesis	125
8.3. Solution properties	129
8.4. Layer by layer deposition	134
8.5. Conclusion	139
8.6. Experimental part	140
8.7. References	142
9. Summary and conclusions	143
10. Methods and instrumentation	156

SYMBOLS AND ABBREVIATIONS

A ₂	second virial coefficient
ABC	amphiphilic block copolymer
AFM	atomic force microscopy
3-APDMES	3-aminopropyltrimethoxysilane
BA	benzylamine
BAG ₂	biglycidolized benzylamine
BC	block copolymer
b	block
bcc	body centered cubic lattice
BP	benzophenone
BP(OH) ₄	2,2',4,4'tetrahydroxy benzophenone BP(OH) ₄
c	concentration
cca	cyanohydroxycinnamic acid
CVD	chemical vapor deposition
DMF	dimethylformamide
D	dendritic unit / abundance of dendritic unit
D _s , D _p	dendritic unit of polyglycerol attached to a secondary/primary alkoxide
DA	<i>n</i> -dodecylamine
DAG ₂	bisglycidolized <i>n</i> -dodecylamine
DB	degree of branching
DDA	1,12-dodecyl diamine
DDAG ₂	bisglycidolized 1,12-dodecyl diamine
diglyme	diethylene glycol dimethyl ether
Dis	disordered phase
DLS	dynamic light scattering
\overline{DP}_n	average degree of polymerization
DPE	dipiperidinoethane
Dz	z-average of the translational diffusion coefficient
DSC	differential scanning calorimetry
ESI	electron spray ionization
f	composition of block copolymer
f _c	functionality of the initiator-core
[G-x]	generation number of a dendrimer
Glymo	(3-glycidioxypropyl)trimethoxy silane
hg	hypergrafted
HA	<i>n</i> -hexylamine
HAG ₂	bisglycidolized <i>n</i> -hexylamine
HDA	1,6-hexyl diamine
HDAG ₂	bisglycidolized 1,6-hexyl diamine
HMDS	hexamethyldisilazane
HOPG	highly-ordered pyrolytic graphite
IG	inverse gated
K	optical constant
k _B	Boltzmann constant
L	linear unit / abundance of linear unit
L ₁₃	linear L ₁₃ unit of polyglycerol/ abundance of linear L ₁₄ unit
L _{13s} , L _{13p}	linear L ₁₃ unit of polyglycerol attached to a secondary/primary alkoxide

L ₁₄	linear L ₁₄ unit of polyglycerol / abundance of linear L ₁₄ unit
L _{14s} , L _{14p}	linear L ₁₄ unit of polyglycerol attached to a secondary/primary alkoxide
LbL	layer-by-layer
LDBC	linear dendritic block copolymer
LPG	linear polyglycerol
LS	light scattering
MALDI-ToF	matrix-assisted laser desorption ionization - time of flight
M_{app}	apparent molecular weight
\overline{M}_n	number average molecular weight
\overline{M}_p	peak average molecular weight
\overline{M}_w	weight average molecular weight
$\overline{M}_w / \overline{M}_n$	polydispersity
3-MPA	3-mercaptopropionic acid
NMA	naphtylmethylamine
NMAG ₂	bisglycidolized naphtylmethylamine
NMR	nuclear magnetic resonance
ODT	order-to-disorder transition
PB	polybutadiene
PBE	poly(benzyl ether)
PDI	polydispersity
PEI	poly(ethylene imine)
PEO	poly(ethylene oxide)
PG	polyglycerol
PI	polyisoprene
PL	photoluminescence
PPI	poly(propylene imine)
PPO	poly(propylene oxide)
PS	polystyrene
q	scattered vector
R _g	radius of gyration
R _h	hydrodynamic radius
R(θ)	Rayleigh ratio
RI	refractive index
ROMBP	ring-opening multibranching polymerization
SANS	small angle neutron scattering
SAXS	small angle X-ray scattering
SEC	size exclusion chromatography
SPR	surface plasmon resonance
SLS	static light scattering
SMA	slow monomer addition
SSL	strong segregation limit
T	terminal unit / abundance of terminal unit
T _g	glass transition temperature
T _s , T _p	terminal unit of polyglycerol attached to a secondary/primary alkoxide
TEM	transmission electron microscopy
TEMPO	2,2,6,6-tetramethylpiperidine-1-oxyl
TMP	1,1,1-tris(hydroxymethylpropane)

UV-vis	ultra-violet visible
VPO	vapor pressure osmometry
XR	X-ray reflectivity
η_0	viscosity of solvent
λ_{em}^{max}	wavelength of the emission maximum
λ_{max}	maximum wavelength
τ	fluorescent species lifetimes
χ	Flory-Huggins segment-segment interaction parameter
Φ_f	quantum yield

NOMENCLATURE OF POLYMERS

Chapter 3

HBPG_x hyperbranched polyglycerol with $DP_n=x$
SPG_x commercial polyglycerol with $DP_n=x$

Chapter 4

BA-PG polyglycerol with benzylamine as core
BAG₂-PG polyglycerol with bisglycidolized benzylamine as a core
BP-PG_x polyglycerol with benzophenone as core and $DP_n=x$
BP-(PG-Ac)_x acetylated polyglycerol with benzophenone as core and $DP_n=x$
DA-PG polyglycerol with *n*-dodecylamine as core
DAG₂-PG polyglycerol with bisglycidolized *n*-dodecylamine as core
DDA-PG polyglycerol with 1,12-dodecyl diamine as core
DDAG₂-PG polyglycerol with bisglycidolized 1,12-dodecyl diamine as core
HA-PG polyglycerol with *n*-hexylamine as core
HAG₂-PG polyglycerol with bisglycidolized *n*-hexylamine as core
HDA-PG polyglycerol with 1,12-hexyl diamine as core
HDAG₂-PG polyglycerol with bisglycidolized 1,12-hexyl diamine as core
NMA polyglycerol with naphthylmethylamine as core
NMAG₂-PG polyglycerol with bisglycidolized naphthylmethylamine as core

Chapter 5, 6, 7

PS_x-*b*-PB_y polystyrene-*block*-1,2-polybutadiene with $DP_n(S)=x$ and $DP_n(B)=y$
PS_x-*b*-(PB-OH)_y polystyrene-*block*-(hydroxylated 1,2-polybutadiene) with $DP_n(S)=x$ and $DP_n(B-OH)=y$
PS_x-*b*-(PB_y-hg-PG_z) polystyrene-*block*-(1,2-polybutadiene-hypergrafted-polyglycerol) with $DP_n(S)=x$, $DP_n(B)=y$ and $DP_n(G)=z$
PI_x-*b*-LPG_y polyisoprene-*block*-linear polyglycerol with $DP_n(I)=x$ and $DP_n(LG)=y$
PI_x-*b*-(LPG_y-hg-PG_z) polyisoprene -*block*-(linear polyglycerol-hypergrafted-polyglycerol) with $DP_n(I)=x$, $DP_n(LG)=y$ and $DP_n(G)=z$

Chapter 8

HBPG_xCN_y hyperbranched polyglycerol with $DP_n(G)=x$ and *y* nitrile groups
HBPG_x(COO⁻Na⁺)_y hyperbranched polyglycerol with $DP_n(G)=x$ and *y* carboxylic groups
G₄(NH⁺Et₂Cl⁻)₉₆ fourth generation phosphorous dendrimer with 96 end groups

1. Introduction

1.1. Hyperbranched polymers

In the late 1980ies, Kim and Webster introduced the term “hyperbranched polymers” to define dendritic macromolecules with random branch-on-branch topology and compact molecular structures prepared by AB_m -type polycondensation.^{1,2} However, the general notion of these less perfectly branched structures dates back to long time ago. Indeed, Flory first treated the concepts for synthetic hyperbranched polymers based on step-growth polycondensation of multifunctional AB_m type monomers, which contain one A group and m ($m \geq 2$) complementary B groups.³ In the last decade, there has been a renaissance of synthetic hyperbranched macromolecules,⁴⁻⁹ profiting from the fascination created by the perfectly branched dendrimers.

Dendrimers are built up in multi-step “organic” syntheses, either from the core by successive attachment of the branching units (divergent strategy) or from the periphery, resulting in dendrimer segments (dendrons) and final assembly by attachment to the core (convergent strategy).¹⁰ In contrast to dendrimers, hyperbranched polymers are obtained in a single polymerization step, using AB_2 (AB_m) type polyfunctional monomers.

From a topological point of view, hyperbranched polymers are characterized by the peculiarity that there is no connecting line between any two end groups that passes all branching points. This structural factor is well-known and ubiquitously present in naturally occurring dendritic polymers, such as polysaccharides, namely glycogen, amylopectin and dextran.¹¹

Hyperbranched polymers are generally considered to be rather ill-defined because of their broad polydispersity (often exceeding $\overline{M}_w / \overline{M}_n = 5$), which is a consequence of the commonly used step-growth type synthesis. Furthermore, hyperbranched polymers are characterized by a random distribution of functional groups throughout their globular structure.¹² However, this permits the tailoring of their chemical, thermal, rheological properties by simple end-group functionalization and thus provides a powerful tool to design polymers for a wide variety of promising applications.¹³ Hyperbranched polymers are also characterized by the absence of entanglements, which results in low bulk viscosities, contrarily to the linear or star-

branched polymers. Unlike dendrimers,¹⁴ prepared in tedious multistep syntheses, hyperbranched polymers can be easily and more cost-effectively prepared by one-step processes. This synthetic advantage is important point for their use in industrial applications.

Increasing academic and industrial interest has been sparked by the potential for developing advanced nanomaterials, biomaterials, rheology modifiers, structured hydrogels, functional crosslinkers, dental composites and catalytic supports based on the low viscosity combined with high functionality of hyperbranched polymers. To approach dendrimer properties, the usually obtained broad molecular-weight distributions have to be narrowed and new polymerization methodologies are required.

1.1.1. General concept for the core-dilution/slow addition strategy

The crucial issues in the development of well-defined hyperbranched polymers are the the degree of branching (DB) and the control over molecular weights and polydispersity (PD).

Dendrimers do not possess any linear units and therefore just contain dendritic and terminal units. In this perfect case the degree of branching is 1, while for linear polymers it is 0. Accordingly hyperbranched polymers should then have an intermediate DB between 0 and 1 (**Figure 1**).

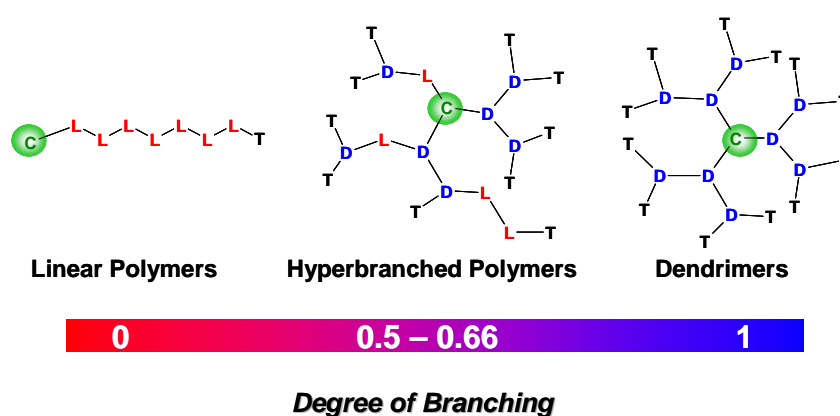


Figure 1. Comparison of polymeric architectures as a function of the degree of branching DB (D, L, T: dendritic, linear and terminal units, respectively).

In this sense, Hawker et al. gave a first definition of the degree of branching for AB₂ monomers in 1991:¹⁵

$$DB_{\text{Fréchet}} = \frac{D + T}{D + T + L} \quad (\text{a})$$

D, L, T represent the relative abundances (%) of the dendritic, linear and terminal units, respectively. It should be noted that in equation (a) the linear direction is also counted as a branching point. This leads to an overestimation of the DB, particularly for low molecular weights.

A theoretical study of the degree of branching in different systems was performed in 1997 by Frey et al.^{16,17} A new expression valid for AB_m (m ≥ 2) type monomers was defined.

$$DB = \frac{2D}{2D + L} \quad (\text{b})$$

In equation (b) the formation of cycles during the polymerization is neglected. The DB is determined by NMR spectroscopy on the basis of low molecular weight model compounds, which possess structures similar to the linear, dendritic and terminal units present in the respective hyperbranched polymer. The DB is obtained by comparison of the intensity of the NMR signals. The main parameters influencing the PDI, the degree of polymerization (\overline{DP}_n) and the DB of hyperbranched polymers (AB_m monomers) were discussed in a computer simulation study.¹⁸ The slow monomer addition of suitable AB_m monomers onto a polyfunctional core allows first of all the control of the molecular weights via the monomer/core ratio and secondly leads to lowering of the polydispersity. At high monomer dilution conditions, achieved via slow monomer addition, it was found that a polydispersity below 1.5 for different core functionalities (from 3 to 12) could be obtained (**Figure 2**). It should be noted that the computer simulation neglects potential deactivation during the polymerization. A parallel theoretical work from Müller et al. confirms the conclusions for the analogous “self condensing vinyl polymerization” of inimer-type structures.¹⁹

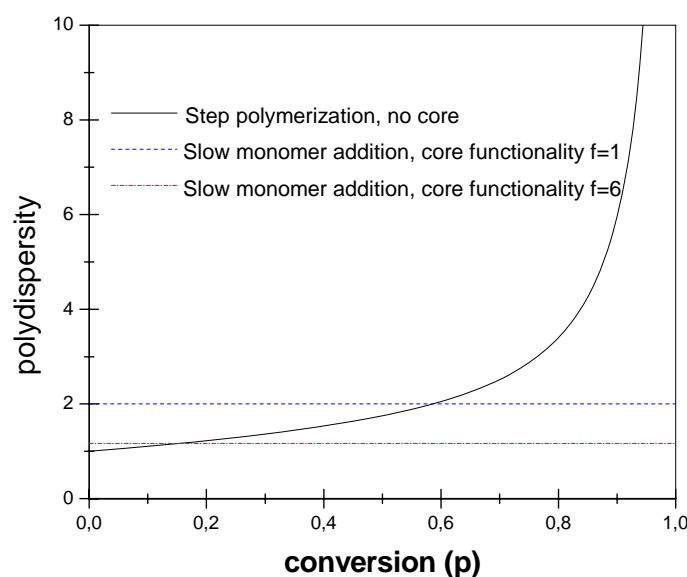


Figure 2. Polydispersity versus conversion (p) for AB_2 monomer in the case of step-growth reaction, and slow monomer addition with arbitrary core functionality values ($f=1$; 6).

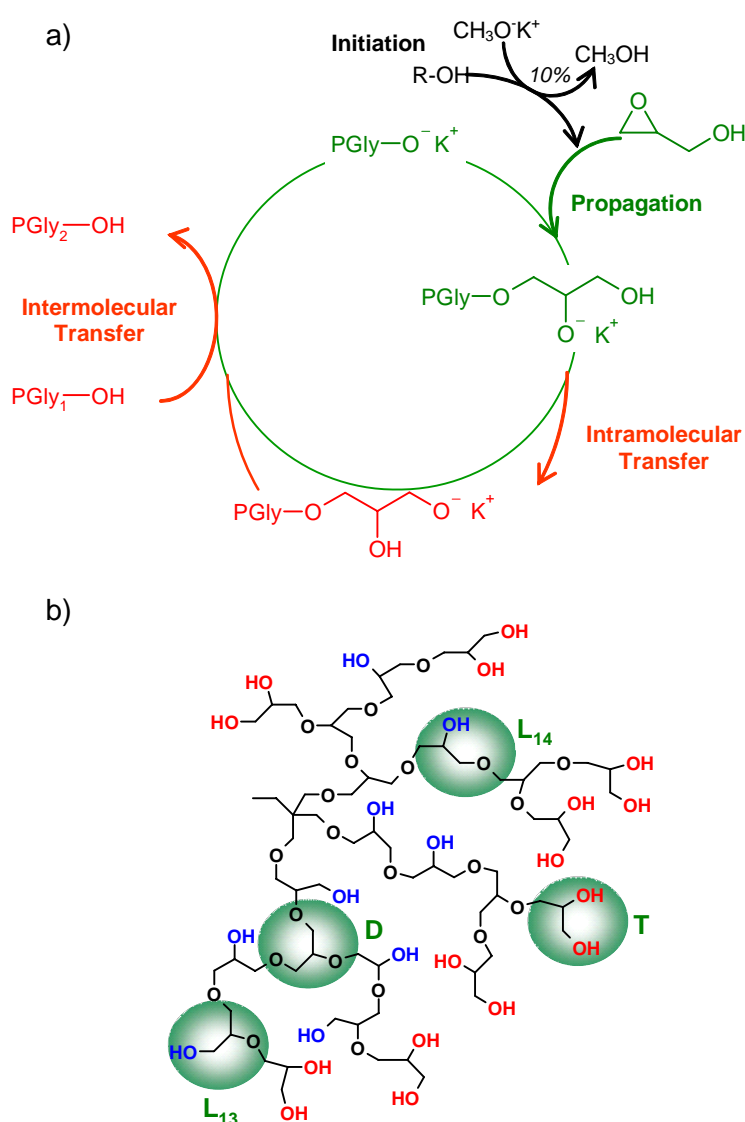
The first example of slow monomer addition was reported in an elegant work by Moore et al.²⁰ The authors polymerized an AB_2 monomer on a B_2 core molecule attached to a solid support. The preparation of hyperbranched polyphenylacetylenes was described, the materials exhibit low polydispersity and minimized amount of homopolymers.²¹ The experiments show the validity of the results from the different simulations: narrow molecular weight distributions from 1.2 to 1.8 for various ratio monomer/core were obtained. Since the hyperbranched molecules grow on the support, this renders intramolecular cyclization impossible.

1.1.2. Polymerization procedure for latent AB_2 monomers

As shown above, the synthesis of well-defined hyperbranched polymers is based on different synthetic requirements, some of which are stringent. One major drawback of polycondensation is the necessity to remove low molecular weight byproducts during the polymerization. In the case of cyclic monomers this synthetic effort can be avoided and the reaction can proceed rapidly to high molecular weights. This technique relies on the use of a “latent AB_2 monomer”, which means that the B

groups take part in the polymerization only after reaction of the A group. The driving force of this polymerization is the ring-opening isomerization.

In the family of the oxiranes, glycidol can be considered as a highly reactive monomer with latent AB₂-monomer structure. This compound has been studied for 40 years by different groups for the preparation of linear polyethers.^{22,23} Vandenberg et al. published the first work on the characterization of these polymeric materials and the branched structures were described briefly.²⁴ Penczek and Dworak presented in 1994 and 1995 the cationic ring-opening polymerization of glycidol leading to hyperbranched polyether polyols.^{25,26}



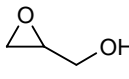
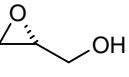
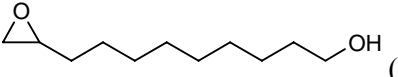
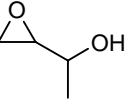
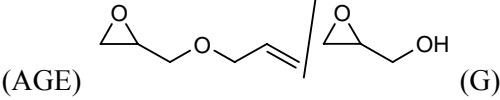
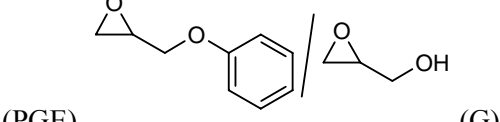
Scheme 1. a) Mechanistic pathway of the base-catalysed ring-opening multibranching polymerization of glycidol. b) Structure of the resulting hyperbranched polyglycerol, which represents only small idealized fragment of the large polymer.

Based on the slow monomer addition approach, glycidol was successfully polymerized via anionic ring-opening multibranching polymerization in 1999.²⁷⁻²⁹ The latent AB₂ monomer is dropwise added onto a partially deprotonated 1,1,1-tris(hydroxymethyl)propane (TMP), representing a trifunctional core-initiator for the polymerization. Due to the fast proton exchange during the polymerization the different chain ends (secondary and primary alcohols) are able to grow simultaneously into a branched structure as shown in **Scheme 1**. The materials obtained are transparent and viscous liquids.

Using ¹³C NMR spectroscopy it was possible to distinguish the dendritic (D), linear (L₁₃, L₁₄) and terminal (T) units and therefore to calculate the degree of branching depending on the molecular weights. As expected from the previous theoretical analyses the degree of branching increases with the degree of polymerization until reaching a *plateau*. The polymers studied in this work exhibited a DB between 0.53 and 0.59 for molar masses between 2,000 and 20,000 g·mol⁻¹ (slightly below the value for ideal slow addition mode) due to the presence of a small fraction of homopolymer. The absolute molecular weight M_n was also determined via vapor pressure osmometry (VPO) in order to confirm the values obtained from NMR spectroscopy. Both methods were found to be in good agreement and confirmed the control over the molecular weight. The apparent polydispersity of the samples was measured by size exclusion chromatography (SEC) and the values were found to be below 1.8, showing that this strategy permits to decrease the polydispersity considerably. The proportion of cycles could be investigated by matrix assisted laser desorption ionization - time of flight (MALDI-ToF) mass spectroscopy. Only a small amount of cyclic products was observed in the low molecular weight range. Based on these first results the experimental strategy was optimized in order to prepare higher molecular weights, and to scale-up the synthesis.³⁰ It was shown that with increasing molecular weights the polydispersity broadens and a second distribution at low molar masses appears, which is ascribed to impeded diffusion of the glycidol monomer with increasing viscosity of the system. This problem was addressed by modification of the geometry of the stirrer leading to more efficient mixing of the reaction mixture. Subsequently, diethylene glycol dimethyl ether (diglyme) was used to dissolve the initiator-core, as high boiling and emulsifying solvent. In this case, the reaction mixture becomes less viscous with molecular weight increase compared to the previous reaction system.

SEC and MALDI-ToF measurements confirmed the disappearance of the low molar mass signal originally due to homopolymerization. According to these new parameters a reactor was built up with the capacity to produce 0.5 to 1 kg of hyperbranched polyglycerol. This represents the first example of larger batch preparation of a well-defined hyperbranched polymer opening new perspectives in this field due to the high functionality and peculiar structure of this type of materials. The presence of a large number of hydroxyl groups throughout the hyperbranched polyglycerols enables vast possibilities of modification using well-established synthetic methodologies.^{31,32} The extension of the concept to other epoxides (**Table 1**) and the applicability of this strategy to achieve complex branched polymers has been studied intensely in recent years. The variety of the materials that can be prepared permits access to a broad range of unprecedented hyperbranched architectures.

Table 1. Monomer structures and SEC data of the resulting hyperbranched polyether polyols

Monomers	\overline{M}_n (g·mol ⁻¹)	$\overline{M}_w / \overline{M}_n$	Ref.
 (G)	1,200-20,000	1.2-3	27-29
 (G*)	1,300-6,900	ca. 1.4	33
 (EUD)	3,000-ca. 30,000	1.1-1.5	34
 (EB)	600-14,000	1.4-2.9	34
 (AGE) / (G)	5,000-6,000	1.2-1.7	35
 (PGE) / (G)	5,800	1.6	35

1.1.3. Perspectives for hyperbranched polyglycerol

The combination of ring-opening multibranching polymerization of glycidol, carried out under slow monomer addition with the versatile epoxide chemistry has provided a useful approach to reactive hyperbranched polyether polyols that can be considered as a modular system for the synthesis of more complex polymer architectures. In

addition to the controllable degree of branching, these hyperbranched polymer architectures generally display unprecedentedly narrow polydispersity ($\overline{M}_w / \overline{M}_n < 1.8$), which renders them unique among the hyperbranched materials. The preparation of these materials on large scale also makes them attractive polymeric materials for industrial application. Their narrow polydispersity is also an attractive parameter when constructing macromolecules that mimic proteins. The functionalization of the hydroxyl end groups permits the preparation of nanocarrier devices, catalytic supports, polymeric liquid crystals³⁶ and hybrid materials for biomineralization³⁷, as shown in **Figure 3**. In view of the remarkable controlled nanostructure of hyperbranched polyglycerols, there is increasing interest in their use as soluble high loading supports for further organic/catalytic reactions,³⁸ as biocompatible protein resistant surfaces³⁹ and as products with therapeutic potential.^{40,41} Some research areas on these materials remain to be investigated, like the introduction of active initiator-cores or macroinitiator-cores at the focal point of the hyperbranched polyglycerols, or the preparation of hyperbranched polyelectrolytes.

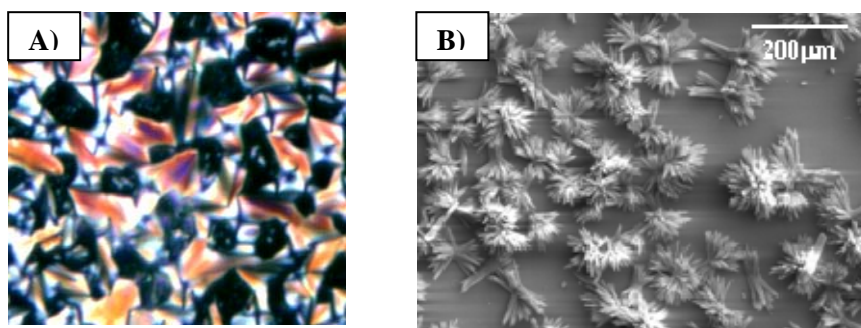
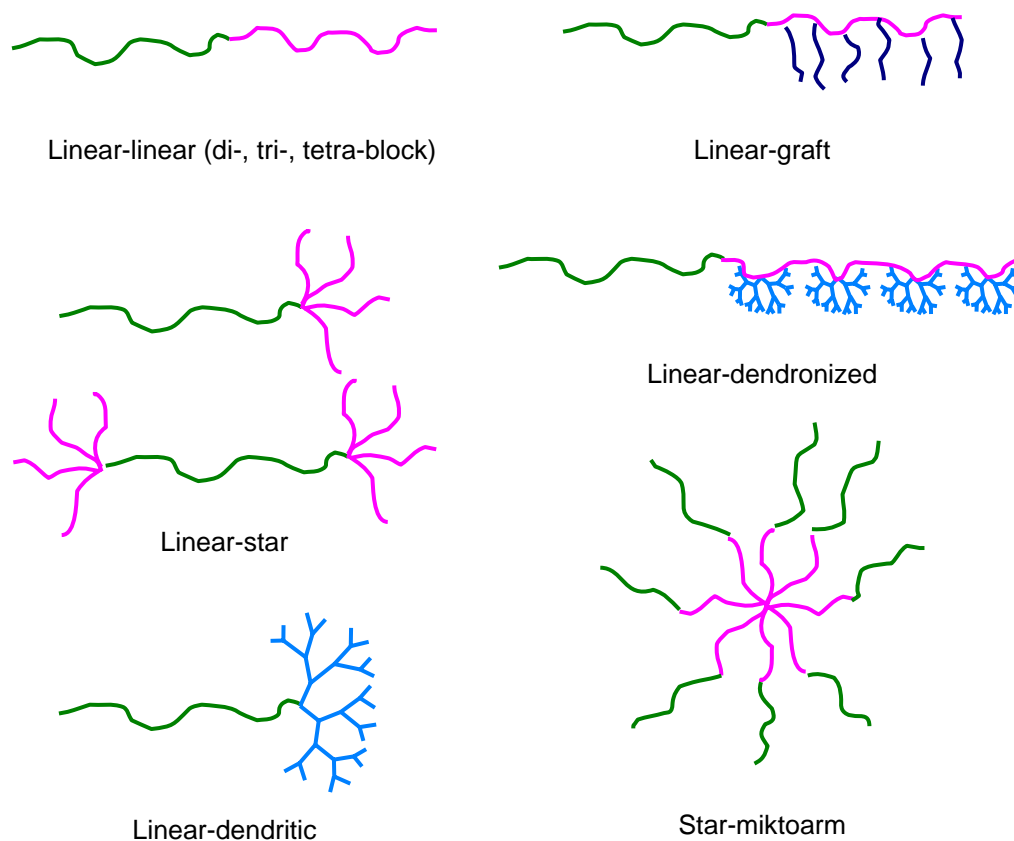


Figure 3: A) Hyperbranched polyglycerol (HBPG₃₃) modified with cyanobiphenyl mesogens HBPG₃₃(C₁₁CB)₉₀ showing a smectic mesophase (90°C). B) Scanning electron micrograph of CaCO₃ crystals of aragonite on an CH₃-terminated self-assembled monolayer surface with adsorbed hyperbranched polyglycerol ($M_n = 5000$ g/mol).

1.2. Linear-dendritic block copolymers

Block copolymers have continued to fascinate both academic polymer scientists as well as industrial researchers since the development of the first living polymer syntheses more than 40 years ago.⁴²⁻⁴⁴ On one hand, this is explained by their intriguing supramolecular organization in bulk as a result of nanophase segregation due to the immiscibility of the chemically different segments.⁴⁵ Furthermore, their organization in solution as well as interfacial and adhesive properties render such materials useful for a vast number of applications, e.g., compatibilization of polymer blends, surface and interface modification of other polymers, encapsulation and release of other compounds, such as drugs.^{46,47} The different architectures of block copolymers developed are illustrated in **Scheme 2**.



Scheme 2: Schematic description of branched block copolymer architectures.

Advanced applications range from the templating of catalytically active transition metal nanoparticles,⁴⁸⁻⁵⁰ the creation of nanometer size patterns⁵¹ and crosslinked

polymer nanostructures^{52,53} to novel electroactive materials. Besides linear AB-diblocks, most commonly ABA-triblock structures have been studied and are also widely applied. In recent years, ABC-triblock copolymers with 3 different, incompatible polymer segments have attracted enormous interest.⁵⁴ The recent advent of “living” and quasi-living polymerization techniques, such as e.g., the TEMPO or Cu-mediated radical polymerization of vinyl monomers has further helped to circumvent the stringent requirements of anionic polymerizations and thus widened the scope of readily available linear polymer building blocks of narrow polydispersity applicable for the synthesis of block copolymers.^{55,56}

The introduction of branches into block copolymers offers additional possibilities regarding both structural complexity and unusual structure-property correlations. In addition, branching leads to substantial changes in the rheological properties. For instance, it has been known for a long time that the melt viscosity decreases drastically for star polymers in comparison to the respective linear analogs.⁵⁷ This peculiarity is exploited in high quality lubricant formulations, using polyisobutylene star polymers.⁵⁸ A variety of other branched polymer architectures has been published, including mikto-arm structures with one long linear block of one type and several shorter segments of different structure,⁵⁹ as well as arborescent-graft structures.⁶⁰

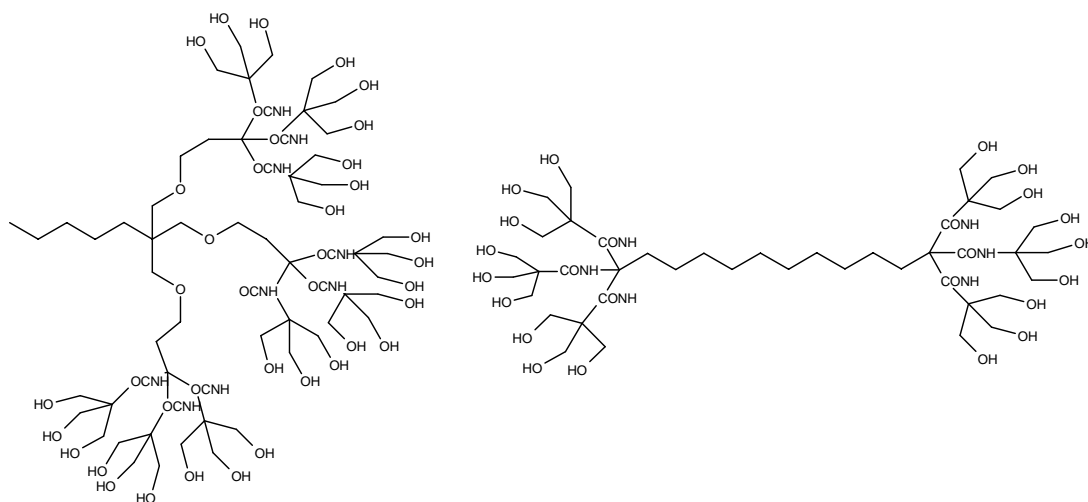
The rapid current development of dendrimers and hyperbranched polymers – cascade-branched structures that are often summarized as “dendritic polymers” - has greatly enhanced the spectrum of potential building blocks for segmented macromolecular architectures. Dendritic structures lead to a compact, globular shape of the macromolecules due to spatial restrictions of the branched topology. In addition, dendritic blocks are unlikely to form entanglements.

Linear-dendrimer block copolymers (designated LDBC)⁶¹ exhibit new properties resulting from such an unusual macromolecular topology. Dendrimer segments may also be attached to polymer chains as side groups (the so-called “dendronized polymers”). An excellent review has been published that elaborates on the consequences of this type of polymer architecture and the resulting properties that are distinctively different from conventional linear block copolymers.⁶²

1.2.1. Linear-dendrimer block copolymers

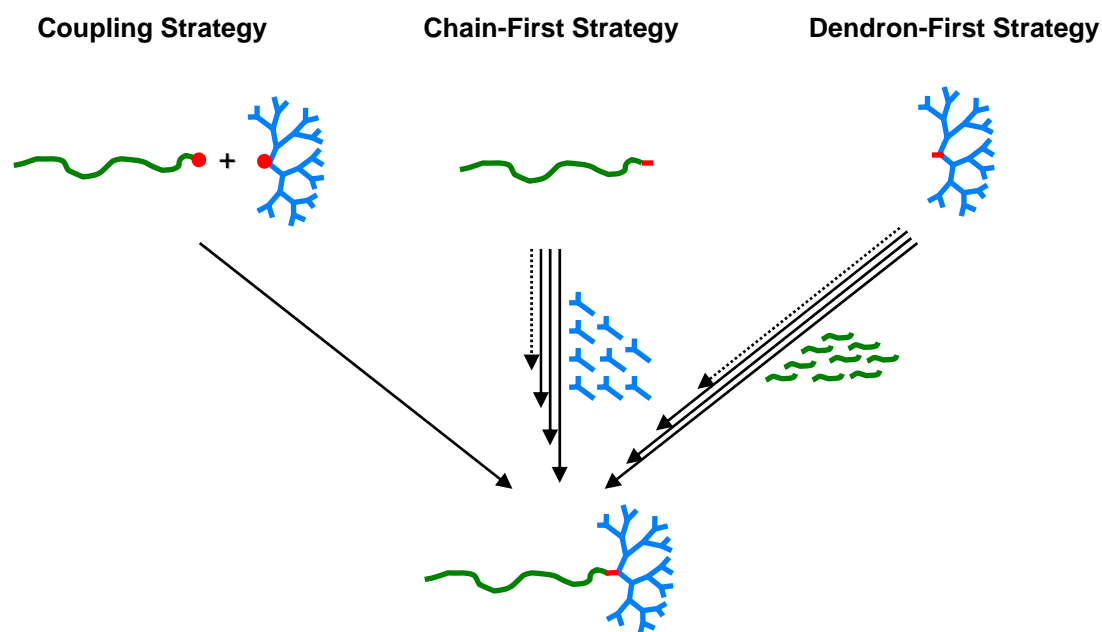
Dendrimers, perfectly branched and highly symmetrical macromolecules, possess a well-defined number of end groups and an interior area offering interesting possibilities for supramolecular chemistry, such as guest uptake and shell-dependent release.⁶³⁻⁶⁶ The multiple end groups of the dendrimers can be functionalized to tailor solubility, surface and interface properties or encapsulation characteristics.⁶⁷⁻⁷⁰ Dendrimers have been used as templates for the formation of metal nanoparticles^{71,72} and are intensely studied with respect to biomedical application in diagnostics and therapy.⁷³

Early works of Newkome on difunctional arborol structures (**Scheme 3**), published between 1985 and 1993 can be considered as an important prelude to the theme of linear-dendrimer hybrid structures.⁷⁴ Low molecular weight cascade molecules and ABA-type structures (“two directional cascade molecules”) with a central, apolar alkyl chain and second generation [G-2] dendrimer segment (“dendron”) termini with up to 9 hydroxyl end groups have been described.⁷⁵ In subsequent works on ABA-type amphiphiles, the structure and flexibility of the central, linear segment was varied and even stiff and apolar oligospiranes have been introduced.^{76,77} A macromolecular aspect of this work is the formation of gels due to hydrogen-bonding of the multiple hydroxyl termini and consequent supramolecular network formation. In this aspect these materials resembled saccharide-based amphiphiles. However, in these early works no polymer segments were employed.



Scheme 3: Newkome's arborols, AB and ABA structures.

Generally, the combination of a dendron with a linear polymer chain to a hybrid linear-dendritic block copolymer is possible via 3 different strategies: (i) coupling of prefabricated dendrons and linear polymer chain; (ii) the “*chain-first*” route and (iii) the “*dendron-first*” strategy. The different pathways are schematically shown in Scheme 5.



Scheme 5: Schematic illustration of the different fundamental strategies for the synthesis of linear-dendrimer block copolymers.

1.2.2. Linear-hyperbranched block copolymers

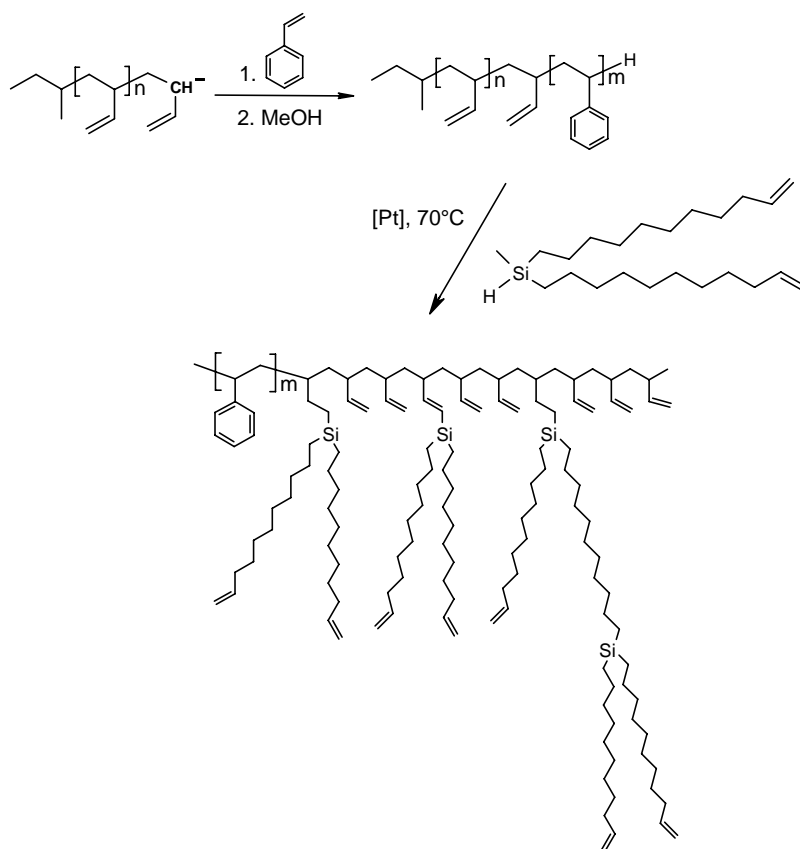
Although LDBC-type structures show many interesting properties, the demanding multi-step preparation strategies required to construct such macromolecular architectures render them interesting study objects, but represent a clear obstacle for real-world application. Motivated by the surge of interest in dendrimers, in recent years also hyperbranched topologies meet increasing interest. However, hyperbranched polymers prepared by the common AB_2 -polycondensation typically show broad polydispersities and $\overline{M}_w / \overline{M}_n$ has been reported to exceed values of 5-10 in many cases.

Thus, a particularly important aspect for the preparation of block copolymers with well-defined supramolecular architecture is a suitable methodology to control the size of the branched block, keeping polydispersity low. It has been suggested to use terminally functional polymers as a monofunctional terminating agent or “macro-

core” for the preparation of linear-hyperbranched block copolymers.⁷⁸⁻⁸⁰ However, since it is well-known cyclization of the focal A-group represents a major side reaction in the synthesis of hyperbranched polymers by polycondensation, preparation of a narrow polydispersity block can not be achieved in this manner.

Knauss et al. grow hyperbranched polymers by subsequent grafting of living, carbanionic chains on a suitable inimer structure.⁸¹ A macromonomer initiator is formed by slow addition of a coupling agent (vinylbenzyl chloride or 4-(chlorodimethylsilyl)styrene) to living polystyrene chains (*sec*-BuLi). A new living chain end is then each time obtained by vinyl addition reaction. This method allows also the controlled addition of styrene units between the branching point by mixing the coupling agent and monomer units in the feed. The materials exhibit a narrow apparent molecular weight distribution with polydispersity between 1.4 and 1.82. One main advantage of this procedure is the existence of only one reactive site. This focal point can initiate the growth of a linear chain by living anionic polymerization after the complete addition of the coupling agent. Interestingly the length of the linear chain was found to depend on the size of the preformed hyperbranched macroinitiator. The macromonomer hyperbranched block shows good efficiency for initiating the linear chain growth. However, this procedure must be carried out with particular precaution due to the high probability of side-reactions by contamination of the environment.

Another new strategy has been developed in recent years, the so called “hypergrafting approach”. This relies on the grafting of branching monomers onto a linear template structure. The grafting of hyperbranched side-chains onto a linear backbone has been investigated in detail in theoretical and synthetic work with respect to the grafting efficiency as well as the resulting structures.⁸² If suitable monomers are employed, the hypergrafting strategy leads to an unusual class of polymer brushes. In order to generate linear-hyperbranched diblock copolymers, a long linear A_n -block is combined with a short polyfunctional B_f -type structure that is used as an initiator-core for the ensuing hypergrafting procedure. In a second “pseudo-living” step, suitably reactive AB_2 monomers are grafted onto the B_f -block.



Scheme 6. Synthesis of linear-hyperbranched polystyrene-*block*-(1,2-polybutadiene-*hypergrafted*-polycarbosilane).

This synthetic approach was first established for the preparation of polystyrene-*block*-(1,2-polybutadiene-*hypergrafted*-polycarbosilane) using alkenyl silane monomers (**Scheme 6**). The grafting efficiency (amount of AB₂ monomer grafted onto the polyfunctional block) was lower than expected (between 30 and 60%) due to intramolecular cyclization of the branched monomers. Nevertheless, the polydispersities were very narrow in the range of 1.02 to 1.07. Morphological studies of these phase-segregated block copolymers show that they can self-assemble nicely in the solid-state. Comparison of the different morphologies for analogous linear block copolymers and the results obtained upon hypergrafting revealed that the macromolecular architecture affects the morphology of the domain borders. It was found that the increase of the size of the hyperbranched block destabilized the lamellar structure towards a more stable cylindrical morphology. These first results are very promising and the extension of this procedure to other architectures like hybrid amphiphilic block copolymer is very challenging, since it will offer the possibility to establish structure-property relationships in solution.

1.3. References

- (1) Kim, Y. H.; Webster, O. W. *Polym. Prepr.* **1988**, 29, 310.
- (2) Kim, Y. H.; Webster, O. W. *J. Am. Chem. Soc.* **1990**, 112, 4592.
- (3) Flory, P. J. *J. Am. Chem. Soc.* **1952**, 74, 2718.
- (4) Kim, Y. H. *J. Polym. Sci. Part A.: Polym. Chem.* **1998**, 36, 1685.
- (5) Sunder, A.; Heinemann, J.; Frey, H. *Chem. Eur. J.* **2000**, 6, 2499.
- (6) Voit, B. *J. Polym. Sci. Part A.: Polym. Chem.* **2000**, 38, 2505.
- (7) Jikei, M.; Kakimoto, M.-a. *Prog. Polym. Sci.* **2001**, 26, 1233.
- (8) Yates, C. R.; Hayes, W. *Eur. Polym. J.* **2004**, 40, 1257.
- (9) Yan, D.; Gao, C. *Prog. Polym. Sci.* **2004**, 29, 183.
- (10) Fréchet, J. M. J.; Tomalia, D. A. *Dendrimers and other Dendritic Polymers*; John Wiley & Sons Ltd, 2001.
- (11) Geddes, R. *Polysaccharides*, Aspinall, G. O. ed.; Academic Press: London, 1985; Vol. 3.
- (12) Flory, P. J. *Principles of polymer Chemistry*; Cornell University Press: Ithaca, NY, 1952.
- (13) Frey, H.; Haag, R. *Mol. Biotechnol.* **2002**, 90, 257.
- (14) Newkome, G. R.; Moorefield, C. N.; Vögtle, F. *Dendrimers and Dendrons*; WILEY-VCH: Weinheim, 2001.
- (15) Hawker, C. J.; Lee, R.; Fréchet, J. M. J. *J. Am. Chem. Soc.* **1991**, 113, 4583.
- (16) Hölter, D.; Frey, H. *Acta Polymer.* **1997**, 48, 298.
- (17) Hölter, D.; Burgath, A.; Frey, H. *Acta Polymer.* **1997**, 48, 310.
- (18) Hanselmann, R.; Hölter, D.; Frey, H. *Macromolecules* **1998**, 31, 3790.
- (19) Radke, W.; Litvinenko, G.; Müller, A. H. E. *Macromolecules* **1998**, 31.
- (20) Bharathi, P.; Moore, J. S. *J. Am. Chem. Soc.* **1997**, 119, 3391.
- (21) Bharathi, P.; Moore, J. S. *Macromolecules* **2000**, 33, 3312.
- (22) Sandler, S. R.; Berg, F. R. *J. Polym. Sci., Polym. Chem. Ed.* **1966**, 4, 1253.
- (23) Tsuruta, T.; Inoue, S.; Koinuma, H. *Makromol. Chem.* **1968**, 112, 58.
- (24) Vandenberg, E. J. *J. Polym. Sc., Polym. Chem. Ed.* **1985**, 23, 915.
- (25) Tokar, R.; Kubisa, P.; Penczek, S. *Macromolecules* **1994**, 27, 320.
- (26) Dworak, A.; Walach, W.; Trzebicka, B. *Macromol. Chem. Phys.* **1995**, 196, 1963.

- (27) Sunder, A.; Hanselmann, R.; Frey, H.; Mülhaupt, R. *Macromolecules* **1999**, *32*, 4240.
- (28) Sunder, A.; Frey, H.; Mülhaupt, R. *Macromol. Symp.* **2000**, *153*, 187.
- (29) Sunder, A.; Mülhaupt, R.; Haag, R.; Frey, H. *Adv. Mater.* **2000**, *12*, 235.
- (30) Kautz, H.; Sunder, A.; Frey, H. *2001 Macromol. Symp.*, *163*, 67.
- (31) Quincy, M. F.; Frey, H. *Abstracts of Papers of the American Chemical Society* **2001**, *221*, U412-U412.
- (32) Maier, S.; Sunder, A.; Frey, H.; Mülhaupt, R. *Macromolecular Rapid Communications* **2000**, *21*, 226-230.
- (33) Sunder, A.; Mülhaupt, R.; Haag, R.; Frey, H. *Macromolecules* **2000**, *33*, 253.
- (34) Kautz, H.; Barriau, E.; Chen, Y.; Collado, M. P.; Wissert, R.; Frey, H. *Pol. Mat. Sci. Eng.* **2003**, *88*, 549.
- (35) Sunder, A.; Türk, H.; Haag, R.; Frey, H. *Macromolecules* **2000**, *33*, 7682.
- (36) Sunder, A.; Quincy, M. F.; Mülhaupt, R.; Frey, H. *Angew. Chem. Int. Ed.* **1999**, *38*, 2928.
- (37) Balz, M.; Barriau, E.; Istratov, V.; Frey, H.; Tremel, W. *Langmuir* **2004**, *21*, 3987.
- (38) Hebel, A.; Haag, R. *J. Org. Chem.* **2002**, *67*, 9452.
- (39) Siegers, C.; Biesalski, M.; Haag, R. *Chem. Eur.J.* **2004**, *10*, 2831.
- (40) Türk, H.; Haag, R.; Alban, S. *Bioconjugate Chem.* **2004**, *15*, 162.
- (41) Kolhe, P.; Khandare, J.; Pillai, O.; Kannan, S.; Lieh-Lai, M.; Kannan, R. *Pharm. Res.* **2004**, *21*, 2185.
- (42) Szwarc, M. *Nature* **1956**, *178*, 1168.
- (43) Szwarc, M. *J. Am. Chem. Soc.* **1956**, *78*, 2657.
- (44) Hadjichristidis, N.; Pispas, S.; Floudas, G. A. *Block copolymers: synthetic strategies, physical properties, and applications*; John Wiley & Sons, Inc.: Hoboken, New Jersey, 2003.
- (45) Huck, W. T. S.; Khan, M. *Abstracts of Papers of the American Chemical Society* **2003**, *225*, U651-U652.
- (46) Förster, S.; Antonietti, M. *Adv. Mater.* **1998**, *10*, 195.
- (47) Förster, S.; Plantenberg, T. *Angew. Chem. Int. Ed.* **2002**, *41*, 688.
- (48) Möller, M.; Spatz, J. P.; Roescher, S.; Mößner, S.; Selvan, S. T.; Klok, H. A. *Macromol. Symp.* **1997**, *117*, 207.

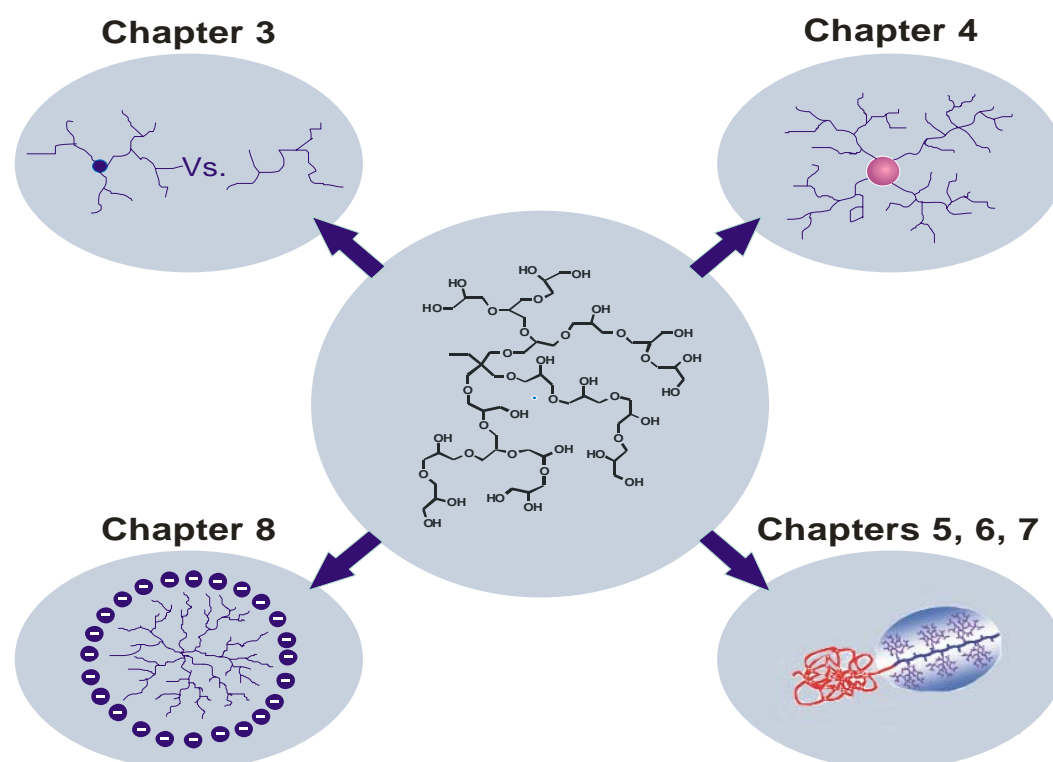
- (49) Antonietti, M.; Förster, S.; Hartmann, J.; Oestreich, S. *Macromolecules* **1996**, *29*, 3800.
- (50) Klingelhöfer, S.; Heitz, W.; Greiner, A.; Oestreich, S.; Förster, S.; Antonietti, M. *J. Am. Chem. Soc.* **1997**, *119*, 10116.
- (51) Subramanian, G.; Manoharan, V. N.; Thorne, J. D.; Pine, D. J. *Adv. Mater.* **1999**, *11*, 1261.
- (52) Remsen, E. E.; Thurmond, K. B.; Wooley, K. L. *Macromolecules* **1999**, *32*, 3685.
- (53) Pan, D.; Turner, J. L.; Wooley, K. L. *Macromolecules* **2004**, *37*, 7109.
- (54) Abetz, V.; Stadler, R.; Leibler, L. *Polym. Bull.* **1996**, *37*, 135.
- (55) Hawker, C. J.; Bosman, A. W.; Harth, E. *Chem. Rev.* **2001**, *101*, 3661.
- (56) Kamigaito, M.; Ando, T.; Sawamoto, M. *Chem. Rev.* **2001**, *101*, 3689.
- (57) Pitsikalis, M.; Pispas, S.; Mays, J. W.; Hadjichristidis, N. *Nonlinear Block Copolymer Architectures*; Springer-Verlag Berlin: Heidelberg, 1998; Vol. 135.
- (58) Kennedy, J. P.; Carter, J. D., 5075389, **1991**.
- (59) Iatrou, H.; Siakali-Kioulafa, E.; Hadjichristidis, N.; Roovers, J.; Mays, J. W. *J. Polym. Sci., Polym. Phys. Ed.* **1995**, *33*, 1925.
- (60) Gauthier, M.; Tichagwa, L.; Downey, J. S.; Gao, S. *Macromolecules* **1996**, *29*, 519.
- (61) Gitsov, I. *Linear-dendritic block copolymers: synthesis and characterization*; Elsevier Science Ltd., 2002; Vol. 5.
- (62) Zhang, A.; Shu, L.; Bo, Z.; Schlüter, A. D. *Macromol. Chem. Phys.* **2003**, *204*, 328.
- (63) Fréchet, J. M. J. *Science* **1994**, *263*, 1710.
- (64) Newkome, G. R.; Moorefield, C. N.; Vögtle, F. *Dendritic Molecules: Concepts, Syntheses, Perspectives*; VCH: Weinheim, 1996.
- (65) Zeng, F.; Zimmerman, S. C. *Chem. Rev.* **1997**, *97*, 1681.
- (66) Matthews, O. A.; Shipway, A. N.; Stoddart, J. F. *Prog. Polym. Sci.* **1998**, *23*, 1.
- (67) Tokuhisa, H.; Crooks, R. M. *Langmuir* **1997**, *13*, 5608.
- (68) Bardaji, M.; Kustos, M.; Caminade, A.-M.; Majoral, J.-P.; Chaudret, B. *Organometallics* **1997**, *16*, 403.
- (69) Alonso, E.; Valerio, C.; Ruiz, J.; Astruc, D. *New J. Chem.* **1997**, *21*, 1139.

- (70) Jansen, J. F. G. A.; Brabander-van den Berg, E. M. M.; Meijer, E. W. *Science* **1994**, *266*, 1226.
- (71) Zhao, M.; Sun, L.; Crooks, R. M. *J. Am. Chem. Soc.* **1998**, *120*, 4877.
- (72) Balogh, L.; Tomalia, D. A. *J. Am. Chem. Soc.* **1998**, *120*, 7355.
- (73) Stiriba, S.-E.; Frey, H.; Haag, R. *Angew. Chem. Int. Ed.* **2002**, *41*, 1329.
- (74) Newkome, G. R.; Yao, Z.-q.; Baker, G. R.; Gupta, V. K. *J. Org. Chem.* **1985**, *50*, 2004.
- (75) Newkome, G. R.; Baker, G. R.; Saunders, M. J.; Russo, P. S.; Gupta, V. K.; Yao, Z.-q.; Miller, J. E.; Bouillion, K. *J. Chem. Soc., Chem. Commun.* **1986**, 752.
- (76) Newkome, G. R.; Baker, G. R.; Arai, S.; Saunders, M. J.; Russo, P. S.; Theriot, K. J.; Moorefield, C. N.; Rogers, L. E.; Miller, J. E.; Lieux, T. R.; Murray, M. E.; Phillips, B.; Pascal, L. *J. Am. Chem. Soc.* **1990**, *112*, 8458.
- (77) Newkome, G. R.; Lin, X.; Yaxiong, C.; Escamilla, G. H. *J. Org. Chem.* **1993**, *58*, 3123.
- (78) Kricheldorf, H. R.; Stukenbrock, T. *J. Polym. Sci. Part A.: Polym. Chem.* **1998**, *36*, 31.
- (79) Baek, J.-B.; Lyons, C. B.; Tan, L.-S. *Polym. Prepr.* **2003**, *44*, 825.
- (80) Cho, C. G.; An, S. G. *Polym. Prepr.* **2003**, 856.
- (81) Al-Muallem, H. A.; Knauss, D. M. *J. Polym. Sci. Part A.: Polym. Chem.* **2001**, *39*, 152.
- (82) Pusel, T.; *Ph. Thesis*, University of Freiburg i. Brsg.: Germany, 2003.

2. Objectives

2.1. Introduction

Hyperbranched polymers have seen a rapid increase of interest since the late 1980ies.¹⁻³ Compared with their perfect cousins, the dendrimers, these materials also show promising potential for multiple applications, since they can be prepared by convenient one-step syntheses. However, only few strategies permit control over molecular weights and molecular weight distribution. One of these strategies is the slow monomer addition technique (SMA), employed for the polymerization of highly reactive AB_m monomers ($m \geq 2$) like glycidol. To date, hyperbranched polyglycerols have been prepared with molecular weights in the range of 2,000 to 20,000 $\text{g}\cdot\text{mol}^{-1}$ with remarkably low polydispersity by this procedure.⁴ The polymers show interesting properties, especially after selective modification of the multiple end groups for applications such as liquid-crystalline materials, hydrogels and phase transfer based on molecular encapsulation.



Scheme 1. Aim and scope of this thesis: “Hyperbranched polyether polyols as building blocks for complex macromolecular architectures”.

The aim and scope of this thesis is the development of new branched polymer architectures on the basis of hyperbranched polyglycerol as building block, such as hyperbranched oligomers, hyperbranched materials containing functional initiator-cores at the focal point, well-defined linear-hyperbranched block copolymers and also negatively charged hyperbranched polyelectrolytes (**Scheme 1**). This is challenging, since most of the targeted topologies are unprecedented in the area of hyperbranched polymers. The respective structure-properties relationship of these materials will be investigated and in some cases compared to dendrimers.

2.2. Comparison of industrial and hyperbranched oligoglycerols

Oligo- and polyglycerols represent widely used products notably for the food, cosmetic and pharmaceutical industries. They are industrially prepared by polycondensation of glycerol or derivatives.⁵ The composition of these industrial products, that are usually of low molecular weight, is a crucial issue, especially for biomedical application, since this could affect the properties of the materials. The aim of chapter 3 is the preparation of new hyperbranched oligomers with molecular weights in the range of 500 - 1,000 g·mol⁻¹ by ring-opening multibranching polymerization of glycidol. These new materials will be characterized with respect to structures and polydispersity. In order to carry out a detailed comparison with technical samples, industrial oligoglycerols obtained from Solvay will also be analyzed. Structures and molecular weights from both approaches will be compared in a systematic manner.

2.3. Incorporation of new functional initiator-cores into hyperbranched polyglycerols

All dendritic structures (dendrimers or hyperbranched polymers) possess a focal point in their interior, although in a hyperbranched structure this may be present in a cyclized form and thus not addressable in a separate manner any more. The site isolation of the core-moiety in a hyperbranched structure offers intriguing potential with respect to peculiar electro-optical properties, catalysis and in many other fields. For example, depending on the polarity of the solvent and the generation number of a dendrimer, changes in the UV-*vis* absorption properties, fluorescence characteristics and correlated conformations of such macromolecules have been observed in the case

of dendrimers.⁶⁻⁸ This generation-dependence of the behavior sites isolated by the dendritic scaffold has also been designated “dendritic effect”. However, to date only four reports describe on the introduction of functionality at the focal point of hyperbranched polymers.⁹⁻¹² Surprisingly, in none of the preceding studies the competing homopolymerization of the AB₂ monomer is discussed, although this is a crucial issue. In chapter 4 various initiator-cores (*n*-alkyl amines, UV-absorbing amines as well as benzophenone) for the ring-opening multibranching polymerization of glycidol have been investigated. The characteristics of the resulting materials will be investigated in detail, placing an emphasis on the extent of incorporation of the initiator-core, using mass spectrometry techniques. In addition, the optical properties of hyperbranched polyglycerols containing a photoactive initiator-core will be studied and the influence of the dendritic architecture on the core properties will be discussed in detail.

2.4. Synthetic routes for linear-hyperbranched amphiphilic block copolymers

The field of amphiphilic block copolymers has been extensively studied, since these materials exhibit promising properties for future nanotechnology and interface modification.^{13,14} Numerous linear amphiphilic AB-diblock copolymer architectures have been reported, but only limited efforts have been described that aim at linear-dendritic architectures with amphiphilic structure.¹⁵ However, the use of perfect dendrimers as building blocks necessitates demanding multistep-syntheses, affords limited quantities of the final material and also limits the molecular weights of the dendritic block to the respective dendrimer generations. In chapter 5 a synthetic strategy for the preparation of amphiphilic block copolymers consisting of a linear and a hyperbranched block will be investigated. A well-defined linear AB-diblock copolymer with a short, polyfunctional B-block that represents a macroinitiator for glycidol will be used. The chemical nature of the blocks will be varied, i.e., polystyrene (high glass transition temperature) and polyisoprene (low glass transition temperature) will be employed as linear units, hydroxylated 1,2-polybutadiene and linear polyglycerol as initiator-core block. In a post-polymerization grafting step, by controlled growth of the hyperbranched structure onto the macroinitiator segment by

slow monomer addition, hyperbranched polymer block with narrow polydispersity may be formed.

2.5. Solution properties of linear-hyperbranched amphiphilic block copolymers

Amphiphilic block copolymers exhibit better control and stability of the self-assembly process compared with low molecular weight surfactants, determined both by the chemical nature and the length of the polymeric blocks. Their aggregation behavior in solution represents a large area of intense research at present.¹⁶ Linear-dendritic amphiphilic block copolymers have been shown to possess unusual properties both in solution and in bulk. It is intriguing to compare the solution properties of such materials with perfectly monodisperse dendrimer block and analogous block copolymers with a somewhat more polydisperse, yet narrow polydispersity hyperbranched block. In chapter 6 the detailed characterization of the structures exhibited in solution (light scattering) and after deposition onto a substrate (atomic force microscopy) by linear hyperbranched polystyrene-*block*-(1,2-polybutadiene)-*hypergrafted*-polyglycerol is to be investigated and described.

2.6. Solid-state properties of linear-hyperbranched amphiphilic block copolymers

The bulk morphology studies of amphiphilic block copolymers containing a perfectly branched block (poly(propylene imine) dendrimer) and a linear block (polystyrene) published by Meijer et al. showed weak segregation.¹⁷ Since hyperbranched polymers exhibit higher polydispersity than dendrimers, it is interesting to compare them with respect to supramolecular structures in the bulk. In chapter 7 of this thesis the solid-state properties of the linear-hyperbranched block copolymers presented in chapter 5 are described. Additionally, the preparation of inorganic-organic nanohybrids using the linear-hyperbranched as structure-directing block copolymer will be discussed.

2.7. Negatively charged hyperbranched polyglycerol polyelectrolytes

Synthetic polyelectrolytes exhibit peculiar properties in aqueous solution, e.g., they may influence the fluid properties of aqueous suspensions and slurries, permit modification of the surface charges of neutral particles via adsorption and strongly interact with ions and colloidal aggregates of opposite charge. The globular shape of dendrimers and their high functionality has attracted considerable interest for the preparation of new types of compact polyelectrolytes.¹⁸ The aim of chapter 8 is the preparation of negatively charged hyperbranched polyelectrolytes via post-modification of the multiple hydroxyl end groups. The properties of these materials in aqueous solution will be explored by various methods. Finally these negatively charged polymers combined with positively charged dendrimers will be investigated with respect to the fabrication of multilayer thin films and hybrid organic/titanium dioxide nanostructures by the layer by layer deposition strategy.

2.8. References

- (1) Sunder, A.; Heinemann, J.; Frey, H. *Chem. Eur. J.* **2000**, *6*, 2499.
- (2) Jikei, M.; Kakimoto, M.-A. *Prog. Polym. Sci.* **2001**, *26*, 1233.
- (3) Yan, D.; Gao, C. *Prog. Polym. Sci.* **2004**, *29*, 183.
- (4) Sunder, A.; Hanselmann, R.; Frey, H.; Mülhaupt, R. *Macromolecules* **1999**, *32*, 4240.
- (5) Behrens, H.; Mieth, G. *Die Nahrung* **1984**, *28*, 815.
- (6) Hawker, C. J.; Wooley, K. L.; Fréchet, J. M. J. *J. Am. Chem. Soc.* **1993**, *115*, 4375.
- (7) Bhyrappa, P.; Young, J. K.; Moore, J. S.; Suslick, K. *J. Am. Chem. Soc.* **1996**, *118*, 5708.
- (8) Vestberg, R.; Nyström, A.; Lindgren, M.; Malmström, E.; Hult, A. *Chem. Mater.* **2004**, *16*, 2794.
- (9) Bernal, D. P.; Bedrossian, L.; Collins, K.; Fossum, E. *Macromolecules* **2003**, *36*, 333.
- (10) Hua, J. L.; Li, B.; Meng, F. S.; Ding, F.; Qian, S. X.; Tian, H. *Polymer* **2004**, *45*, 7143.

- (11) Gittins, P. J.; Alston, J.; Ge, Y.; Twyman, L. J. *Macromolecules* **2004**, *37*, 7428.
- (12) Gittins, P. J.; Twyman, L. J. *J. Am. Chem. Soc.* **2005**, *127*, 1646.
- (13) Förster, S.; Antonietti, M. *Adv. Mater.* **1998**, *10*, 195.
- (14) Forster, S.; Plantenberg, T. *Angew. Chem.-Int. Edit.* **2002**, *41*, 689-714.
- (15) Gitsov, I. *Advances in Dendritic Macromolecules*; Elsevier Science: Amsterdam, 2002; Vol. 5.
- (16) Alexandridis, P.; Lindman, B. *Amphiphilic Block Copolymers: Self-Assembly and Applications*, Elsevier Science BV ed., 1997.
- (17) van Hest, J. C. M.; Delnoye, D. A. P.; Baars, M. W. P. L.; Elissen Román, C.; van Genderen, M. H. P.; Meijer, E. W. *Chem.-Eur. J.* **1996**, *2*, 1616-1626.
- (18) Vögtle, F.; Gestermann, S.; Hesse, R.; Schwoerz, H.; Windisch, B. *Prog. Polym. Sci.* **2000**, *25*, 987.

3. Comparison of industrial and hyperbranched oligoglycerols

3.1. Introduction

Oligoglycerols and their derivatives have been widely used since the beginning of the last century, mainly in the food and the cosmetic industries, but also in pharmaceutical and technical applications. These materials have attracted considerable interest, since they are easy to prepare, to functionalize and they exhibit good biocompatibility.

Academic and industrial reports have detailed various methods for the preparation of both oligoglycerols and polyglycerols. The monomer mostly employed, glycerol, is obtained as product of the hydrolysis or methanolysis of triglycerides. The general strategy is based on the polycondensation of glycerol or derivatives of glycerol with or without catalyst.¹ The reaction efficiency can be enhanced, e.g., by carrying out the reaction under reduced pressure^{2,3} and/or by using catalysts. The use of several acidic catalysts has been reported in industrial patents.^{2,4} Basic catalysts have also been used, mainly potassium hydroxide, sodium hydroxide, alkali metals, various metal oxides and sodium acetate.^{5,6} The resulting materials are a mixture of oligoglycerols or polyglycerols of different chain lengths. The polymerization is commonly terminated by inactivating the catalyst after addition of a stoichiometric amount of neutralizing agent. Therefore, the degree of polymerization mainly depends on the reaction time. The materials can be purified by “bleaching” (i.e. addition of hydrogen peroxide or active coal).⁷ A slightly modified process was developed in 1985 where a derivative of phosphoric acid is used as reducing agent and alkali metal is used as a catalyst.⁸ This combination enhances the selectivity of the chemical reaction with respect to the proportion of side-products. However, to date it is not clearly understood how this method reduces the formation of byproducts.

An alternative route to the polycondensation approach is the anionic ring-opening polymerization of glycidol or derivatives as latent AB₂ monomers. The first polymerizations involving glycidol were reported during the 1960s in the presence of catalysts, but the structure of the resulting materials and the underlying reaction mechanism were not clearly characterized.^{9,10} In 1985 the branched structure of the compounds was first characterized by Vandenberg, but not in a precise manner.¹¹ The

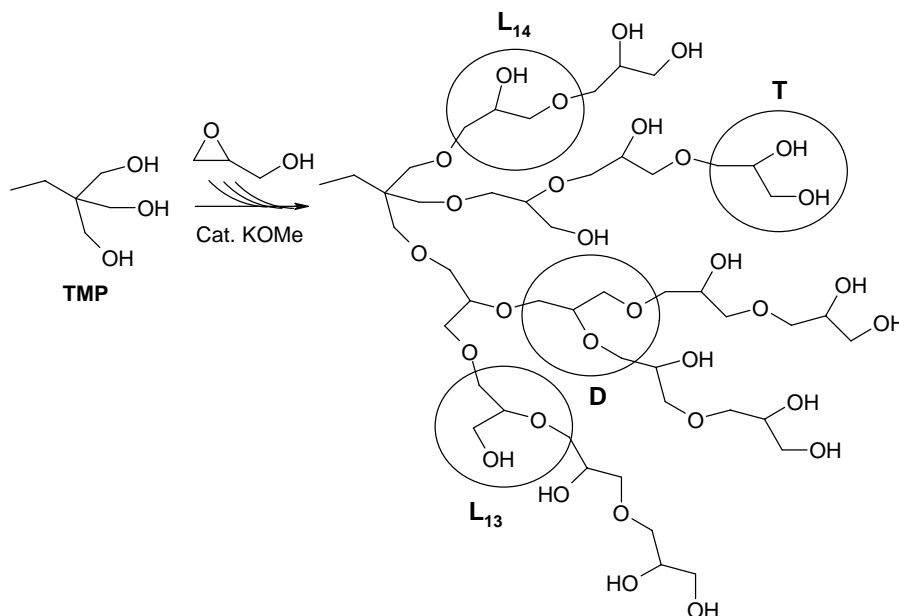
potential of glycidol as a monomer for the preparation of well-defined hyperbranched polyglycerol was first described in 1999 by Frey et al.^{12,13} The strategy is based on the use of a well-defined multifunctional initiator core, activated to a certain extent (10% mol.) with a metal alkoxide and diluted in a high-boiling solvent. Control of molecular weights and molecular weight distribution and a decrease of the formation of cyclic homopolymers (no core incorporated) are achieved by slow monomer addition.^{14,15} This technique permits to keep the concentration of initiator sites higher than the concentration of monomer during the reaction. This strategy was successfully employed for the preparation of hyperbranched polyglycerol with molecular weights ranging from 2,000 to 20,000 g·mol⁻¹. It is known that the synthesis of oligomers via living anionic polymerization is more challenging, since the volume fraction of monomer compared with the volume fraction of the living polymer molecules in this case is high. This affects the equilibrium concentration of monomer and results in a lack of control over the molecular weight distribution.¹⁶ It is interesting to investigate the influence of the degree of polymerization (\overline{DP}_n) on the molecular weights and the polydispersity in the case of hyperbranched oligoglycerols prepared via anionic ring-opening polymerization.

In this chapter, the first preparation of hyperbranched oligoglycerols with molecular weights of 500 and 1,000 g·mol⁻¹ based on the glycidol approach and a comparison of these new materials with the commercially available oligoglycerol⁴ analogs will be reported. The materials have been characterized by size exclusion chromatography (SEC), ¹H NMR and ¹³C NMR spectroscopy, vapor pressure osmometry (VPO) and electron spray ionization (ESI) mass spectrometry.

3.2. Hyperbranched oligoglycerols

The hyperbranched oligoglycerol samples are prepared via ring-opening multibranching polymerization (ROMBP) of glycidol (**Scheme 1**). This AB₂ monomer is an epoxide with one free hydroxyl group. The second initiator group is activated by the ring-opening, promoted by an alkoxide. The polymerization can be controlled by (i) the use of a multifunctional initiator-core (ii) dilution of this initiator in a high-boiling solvent (iii) and slow addition of the monomer into the reaction mixture. Two types of hydroxyl groups are present: primary and secondary. Due to

fast intermolecular and intramolecular proton exchange a hyperbranched architecture is formed. The resulting structural units are dendritic (**D**), terminal (**T**), 1,3-linear (**L₁₃**) and 1,4-linear (**L₁₄**) units, as it has been detailed in the introduction of this thesis



Scheme 1. Synthesis of hyperbranched polyglycerol from glycidol with 1,1,1-tris(hydroxymethyl)propane (TMP) as initiator-core.

The hyperbranched oligoglycerols were experimentally prepared as described in the literature.¹² As expected, the viscosity at the end of the polymerization remains lower than experienced in the syntheses of higher molecular weight hyperbranched polyglycerols. In the following text the hyperbranched oligoglycerols will be named as follows: HBPG₇ (hyperbranched oligoglycerol with a \overline{DP}_n of 7) and HBPG₁₄ (hyperbranched oligoglycerol with a \overline{DP}_n of 14). The hyperbranched oligoglycerols are slightly yellowish, oily materials. The characterization data of the samples are summarized in **Table 1**.

Table 1. Characterization data of hyperbranched oligoglycerols (all molecular weights are given in g·mol⁻¹). [a] calculated from monomer/initiator ratio.

	Theory ^[a]	¹ H NMR	VPO	SEC	
	\overline{M}_n	\overline{M}_n	\overline{M}_n	\overline{M}_n	$\overline{M}_w / \overline{M}_n$
HBPG ₇	500	640	496	650	1.45
HBPG ₁₄	1,000	1,200	976	1,300	1.46

SEC elugrams of the samples are illustrated in **Figure 1**. The SEC chromatography column used was appropriate for low molecular weight polymers (PSS GRAL e4/3/2). Both samples HBPG₇ and HBPG₁₄ show monomodal molecular weight distributions, and exhibit low polydispersity: $\overline{M}_w / \overline{M}_n = 1.45$ and 1.46, respectively. The low viscosity may have aided to keep the molecular weight distribution narrow, due to better diffusion of the monomer in the polymerization medium compared to the synthesis of higher molecular weight materials.

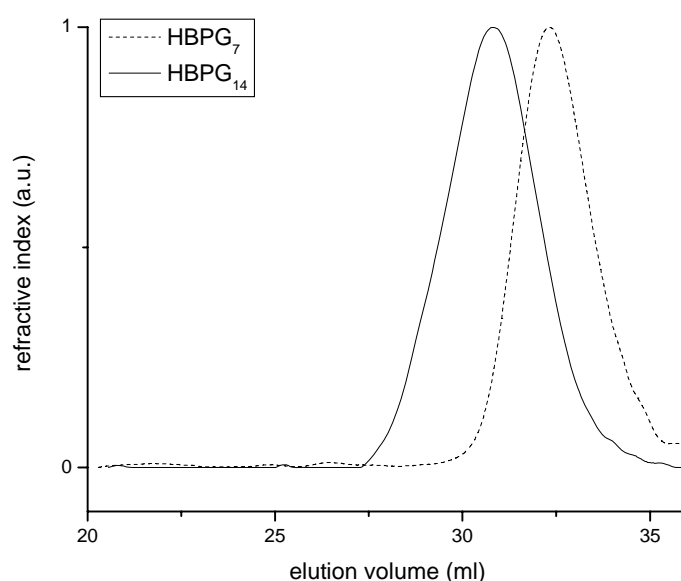


Figure 1. SEC elugrams (refractive index (RI) detection) of hyperbranched oligoglycerols HBPG₇ and HBPG₁₄ with DMF as eluent.

SEC yields information on the relative number average molecular weight M_n and the apparent molecular weight distribution M_w/M_n . Since the measurements are calibrated with linear polymer standards (PS), molecular weights obtained for branched molecules are generally underestimated, because their hydrodynamic volumes are lower. Absolute molecular weights were obtained by two methods: (i) VPO by dividing the product of the slope of the benzil curve and the molar mass of benzil by the slope of the respective polyglycerol curve (ii) ¹H NMR by comparing the intensity of the signals of the initiator-core with the signals of the polyether polyol. The ¹H NMR spectra shown in **Figure 2** evidence the presence of the initiator-core 1,1,1-tris(hydroxymethyl)propane (TMP) with the signals at 0.75 ppm ($\text{CH}_3\text{-CH}_2\text{-}$) and 1.23 ppm ($\text{CH}_3\text{-CH}_2\text{-}$). The other signals of the initiator-core ($\text{-C-CH}_2\text{-OH}$) coincide with the polyether-polyol scaffold between 3.3 and 3.8 ppm. According to computer NMR

simulation (*ACD simulations*) it is possible to distinguish in this same region the methine protons connected to the dendritic **D** (ca. 3.75 ppm) and the linear **L**₁₄ (ca. 3.6 ppm) units. This gives a first indication of the dendritic structure of the samples HBPG₇ and HBPG₁₄, but is not sufficient for determination of the structural composition of the samples.

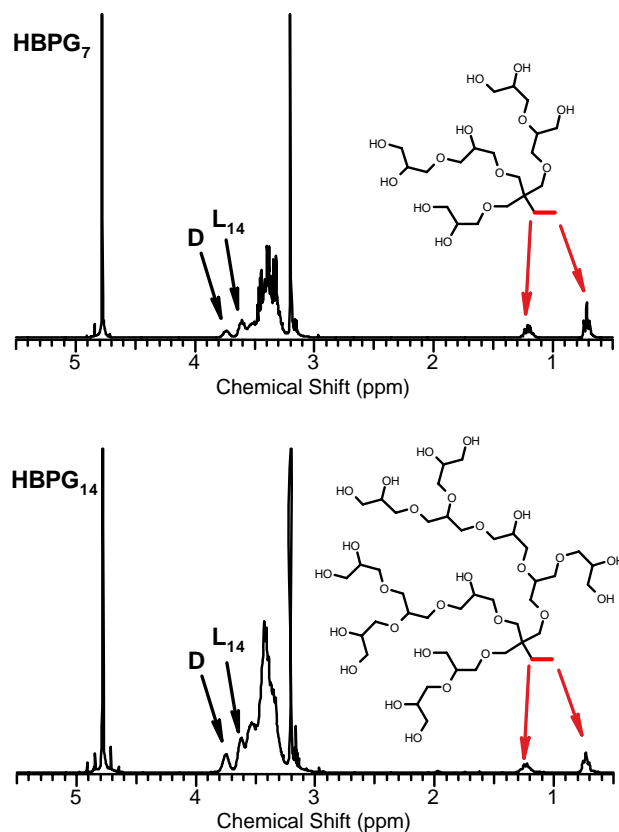


Figure 2. ¹H NMR spectra in d₄-methanol, of the hyperbranched oligoglycerols HBPG₇ (*top*) and HBPG₁₄ (*bottom*).

The molecular weights given in **Table 1** comprise the initiator-core TMP. The values obtained from ¹H NMR and SEC are similar. The difference between the values is not as important as in the case of higher molecular weight hyperbranched polyglycerols. Thus, the hydrodynamic radius of the branched oligomers compared with the linear standards appears to be nearly identical. The results from VPO are slightly below the other values, as it may be expected in view of the sensitivity of this method to traces of low molecular weight impurities. It should also be noted that the molecular weights obtained are in good agreement with the calculated values from monomer/initiator ratios. The number average molecular weight determined by ¹H NMR was used for the calculation of the degree of polymerization (\overline{DP}_n).

In a recent account these samples were characterized by small angle neutron scattering in CD₃OD and D₂O.¹⁷ The results are summarized in **Table 2**. The sizes of the particles and the molar masses of the hyperbranched polyglycerols are similar in the both solvents. Small well-defined entities are present in both solvents, despite the high functionality of hydroxyl groups that could lead to strong aggregation. Apparently, the hyperbranched structure prevents strong irregular aggregation in those solvents. The apparent molar masses (M_{app}) obtained are in good agreement with the values presented in **Table 1**.

Table 2. Apparent molecular weight and radius of gyration for polyglycerols in D₂O and CD₃OD. [a] R_g was calculated from the Guinier approximation.

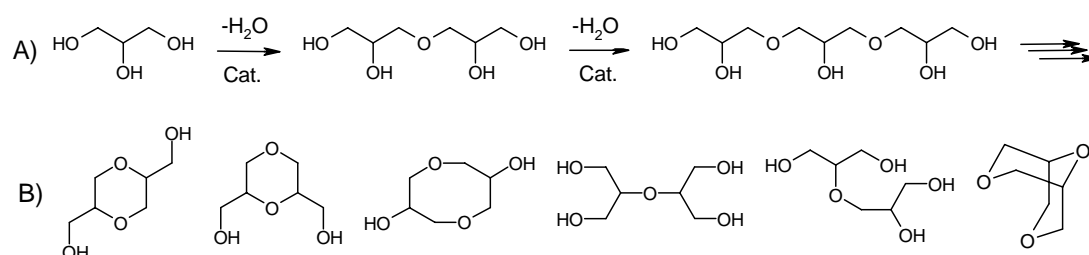
	D ₂ O			CD ₃ OD		
	c (g·mol ⁻¹)	M_{app} (kg·mol ⁻¹)	$R_g^{[a]}$ (nm)	c (g·l ⁻¹)	M_{app} (kg·mol ⁻¹)	$R_g^{[a]}$ (nm)
HBPG ₇	22	0.94	1	23	0.58	-
HBPG ₁₄	22	1.9	1.5	22	1.3	1.3

These results show the possibility to prepare well-defined hyperbranched oligoglycerols (HBPG₇ and HBPG₁₄) in a facile manner by the ring-opening approach. No difficulties were encountered regarding the desired low degrees of polymerization, compared with conventional living anionic polymerization, that leads to rather broad Poisson distributions at low molar mass.¹⁶

3.3. Industrial oligoglycerols

The industrial process for the preparation of oligoglycerol is based on the condensation of glycerol. Glycerol possesses 3 free hydroxyl groups: 2 primary and 1 secondary groups. Obviously, the 2 primary hydroxyls are more likely to react than the secondary ones. The selectivity of the reaction is important, since it is known that glycerol etherification results in a mixture of different isomers.¹ **Scheme 2** summarizes the linear compounds obtainable from the condensation of glycerol or derivatives and the isomers of the so-called “diglycerol”: branched compounds and also cyclic compounds are known to be formed by intramolecular condensation.¹ The proportion of these side-products in the industrial materials is a crucial issue, because

the oligoglycerols are generally modified with fatty acids for the preparation of emulsifying agents as well as other applications. Since all compounds possess different chemical structure, this can affect the properties of the materials, especially for biomedical purposes. The use of catalysts can aid to improve the yield and the selectivity of the reaction with respect to specific products.



Scheme 2. A) linear condensation products of glycerol and B) possible cyclic and branched isomers of diglycerol.

The commercial oligoglycerols used in this study were obtained from Solvay and will be named as follows: SPG₂ (“diglycerol”), SPG₃ (“triglycerol”) and SPG₄ (“tetraglycerol”). The commercially available oligoglycerols are also yellowish and oily materials like the hyperbranched oligoglycerols. Their characterization data are summarized in **Table 3**.

Table 3. Characterization data of commercial oligoglycerols (all molecular weights are given in g·mol⁻¹). [a] calculated for $\overline{DP}_n = 2, 3$ and 4 (\overline{DP}_n depends on the reaction time); [b] \overline{M}_p is the corresponding molecular weight of the maximum(a) of the peak(s) observed in the SEC.

	Theory ^[a]	VPO	SEC		
	\overline{M}_n	\overline{M}_n	\overline{M}_n	$\overline{M}_w / \overline{M}_n$	\overline{M}_p ^[b]
SPG ₂	166	167	115	1.03	120
					180
SPG ₃	240	241	160	1.24	115
					170
					270
SPG ₄	314	295	200	1.26	150
					260

SEC elugrams of the different commercial oligoglycerols are shown in **Figure 3**. The apparent polydispersities of the samples, SPG₂, SPG₃ and SPG₄, are quite narrow, between 1.03 and 1.26. In the case of SPG₂ one peak ($\overline{M}_p = 120 \text{ g}\cdot\text{mol}^{-1}$) and a low molecular weight shoulder (ca. $180 \text{ g}\cdot\text{mol}^{-1}$) are visible, even if the apparent polydispersity is low (1.03). A fraction of condensation products with higher degree of polymerization is also present in the sample. In the case of SPG₃ the elugram shows more clearly the presence of different modes in the sample: 2 peaks with maxima at 115 and $170 \text{ g}\cdot\text{mol}^{-1}$ and, in addition, a shoulder at ca. $270 \text{ g}\cdot\text{mol}^{-1}$. The peak at $\overline{M}_p = 170 \text{ g}\cdot\text{mol}^{-1}$ is the most intense signal; it corresponds to SPG₃ (\overline{DP}_n of 3). For the last sample SPG₄ the elugram shows 2 peaks at 160 and $260 \text{ g}\cdot\text{mol}^{-1}$. SEC elugrams clearly demonstrate that the samples are not well-defined and that different distribution modes exist. The condensation process employed does not permit to control the molecular weight distribution.

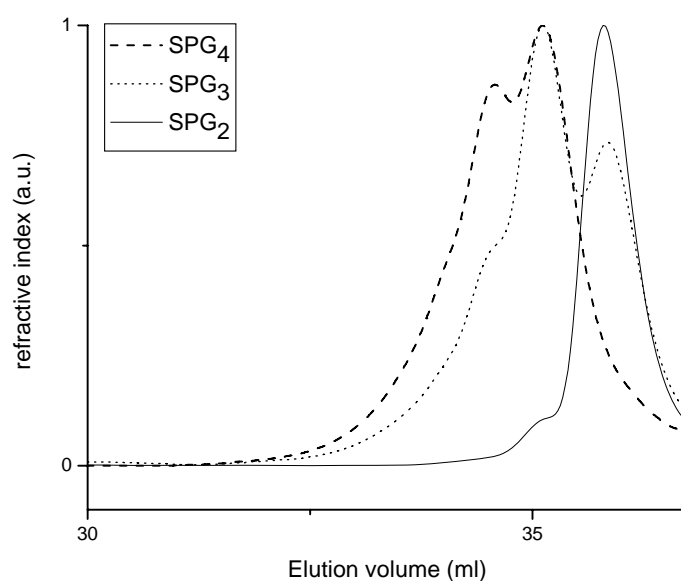


Figure 3. SEC elugrams (refractive index (RI) detection) of commercial samples diglycerol SPG₂, triglycerol SPG₃, tetraglycerol SPG₄ with DMF as eluent.

The absolute number average molecular weight could not be calculated with help from ¹H NMR, because no comparison with end groups or an initiator-core is possible. **Figure 4** shows the ¹H NMR spectra of SPG₂, SPG₃ and SPG₄. The protons of the polyether polyol scaffold are visible between 3.3 and 3.8 ppm. In the case of SPG₂ only the methine protons from the linear L₁₄ units are present. In addition to the

signal corresponding to the linear L_{14} units, the resonance corresponding to dendritic D units is visible in SPG_3 and SPG_4 . This may mean that branched side-products are present in these samples, but it is not possible to obtain a final conclusion on this issue, because 1H NMR is not suitable for the analysis of the different structural units without tedious separation prior to spectroscopic characterization.

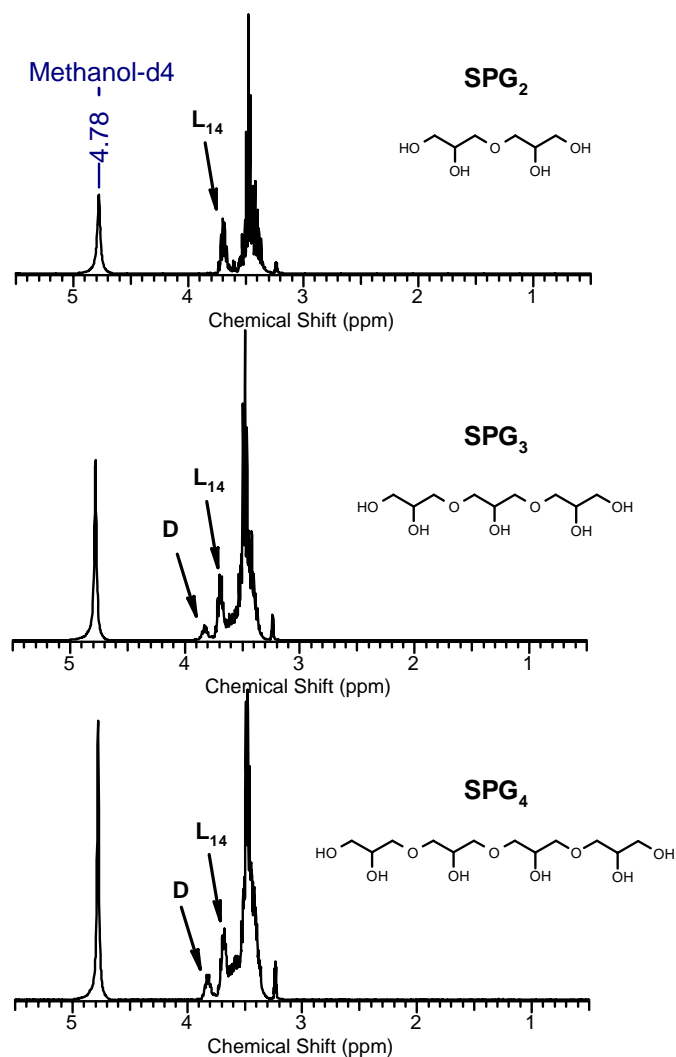


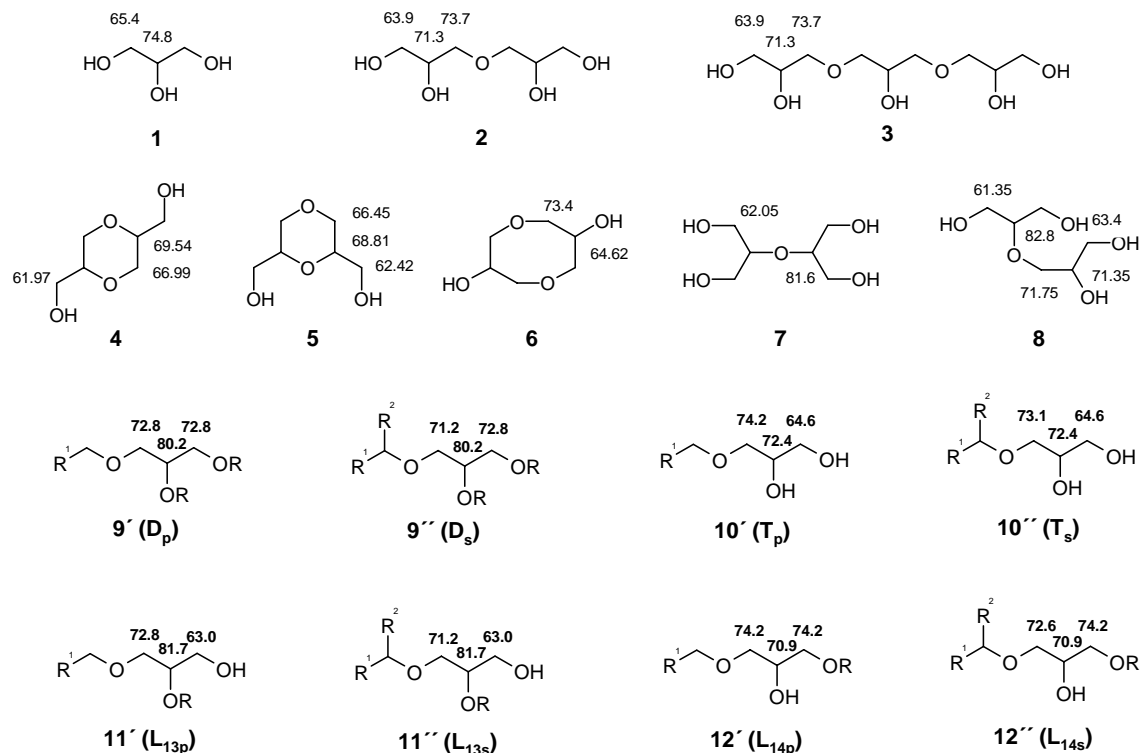
Figure 4. 1H NMR spectra in d_4 -methanol of the different technical oligoglycerol samples: diglycerol SPG_2 (top), triglycerol SPG_3 (middle), tetraglycerol SPG_4 (bottom). Idealized linear structures are given.

The commercial oligoglycerols characterized exhibit narrow molecular weight distributions, but these are not monomodal and not as well-defined as for the hyperbranched glycidol-based oligoglycerols. Due to the multimodal distribution revealed by the elugrams, the values of M_n obtained by SEC and VPO have to be

considered as an estimate. It is interesting to note that the molecular weights are quite similar to the theoretical values.

3.4. Composition of the different materials

SEC and ^1H NMR spectroscopy can not give detailed insight into the composition of the materials with respect to linear, cyclic and branched compounds. As shown in **Figure 2** and **Figure 4**, it is only possible to identify the methine protons connected to linear L_{14} and to dendritic **D** units. Two methods can be employed in order to elucidate the composition of the different samples: ^{13}C NMR spectroscopy and mass spectrometry. The mass spectrometry techniques generally used for the characterization of polymers and/or oligomers are the matrix assisted laser desorption ionization - time of flight (MALDI-ToF) mass spectrometry and the electron spray ionization (ESI) mass spectrometry. The MALDI-ToF technique is limited to masses above $600\text{ g}\cdot\text{mol}^{-1}$, because below this threshold signals interfere with mass peaks from the matrix. Therefore ESI was employed for the characterization of all samples.



Scheme 3. ^{13}C NMR shifts of the possible compounds and units present in commercial and hyperbranched oligoglycerols. Primary dendritic (**D_p**), secondary dendritic (**D_s**), primary terminal (**T_p**), secondary terminal (**T_s**), primary 1,3-linear (**L_{13p}**), secondary 1,3-linear (**L_{13s}**),

primary 1,4-linear (L_{14p}), secondary 1,4-linear (L_{14s}) units were identified in hyperbranched polyglycerol.¹²

Scheme 3 shows the assignments for the different compounds presumably present in the sample. For the compounds **1** to **8** the assignments were obtained by computer simulation (*ACD simulations*). The values for the compounds **9** to **12** have been determined previously by combining the results obtained from standard ^{13}C NMR and DEPT ^{13}C NMR.¹²

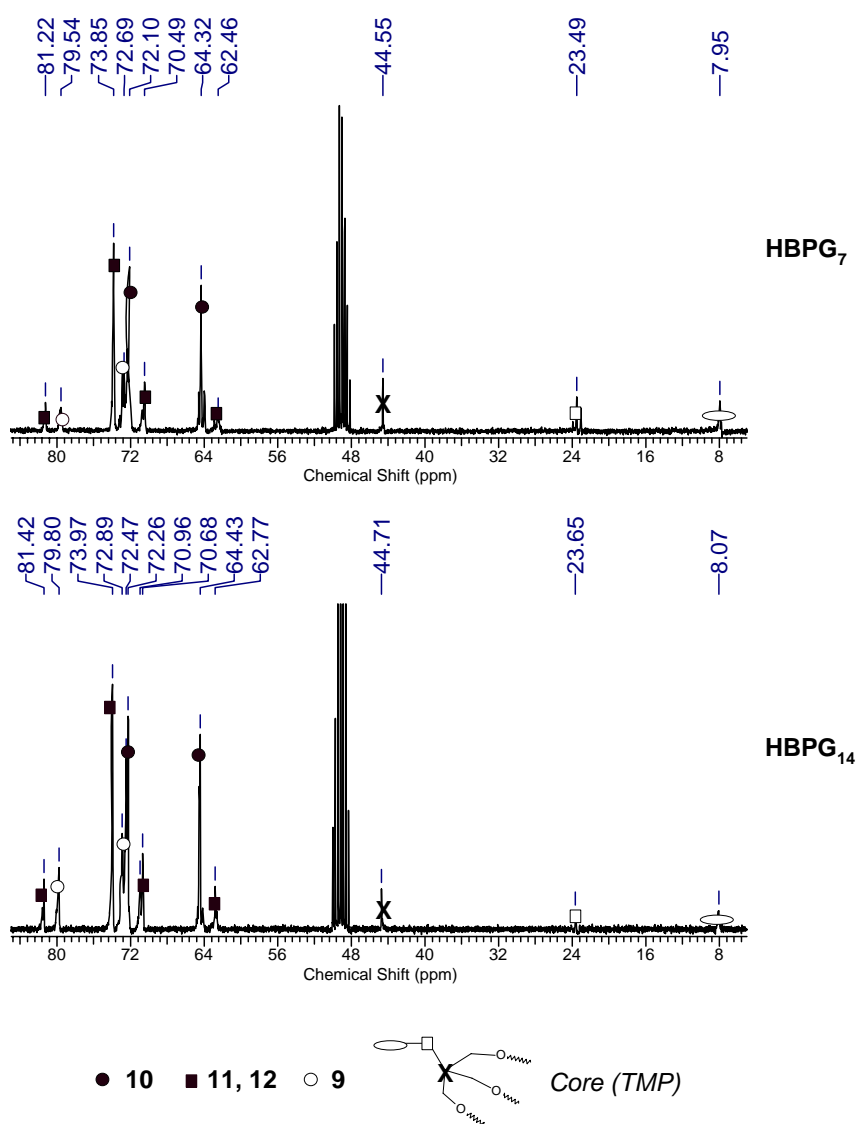


Figure 5. ^{13}C NMR spectra in d_4 -methanol of the hyperbranched oligoglycerol samples: HBPg₇ (top) and HBPg₁₄ (bottom).

Figure 5 shows the ^{13}C NMR spectra of the hyperbranched oligoglycerols prepared via ROMBP of glycidol. The signals corresponding to the initiator-core (TMP) are visible at 44.5 ppm, 23.5 ppm and 8 ppm. Higher molecular weights are generally

more difficult to observe due to their low signal intensities. The rest of the signals ranges between 62 and 81.4 ppm. It is indeed possible to distinguish the different structural units **9**, **10**, **11** and **12**. For both HBPG₇ and HBPG₁₄ the dendritic unit signals (**9**) are clearly present. It is an important observation that at such low DP_n already branching units are formed. The degree of branching (DB) of hyperbranched polyglycerol can be determined by inverse gated (IG) ¹³C NMR spectroscopy.¹² DB is defined theoretically by the following equation:¹⁸

$$DB = \frac{2D}{2D + (L_{13} + L_{14})}$$

where D and L represent the relative abundance (%) of the dendritic and linear units, respectively. From the integrals the relative abundance of the different structural units can be calculated (**Table 4**). DB calculated with the definition given above is 44% for HBPG₇ and 52% for HBPG₁₄. These values are below the ones obtained for higher molecular weight hyperbranched polyglycerols: for HBPG₂₂ DB is 55% and for HBPG₈₃ DB is 59%.¹² The increase of DB with the molecular weight is in good agreement with theoretical expectation.¹⁸⁻²⁰

It is also possible to calculate the \overline{DP}_n from the distribution of structural units, assuming that only propagation onto the core occurs, using the following equation:

$$\overline{DP}_n = \frac{T + L_{13} + L_{14} + D}{T - D} \cdot f_c$$

where f_c is the functionality of the initiator-core (3 for TMP) and T is the relative abundance (%) of the terminal units. The values obtained for \overline{DP}_n are slightly smaller than the ones calculated from ¹H NMR but still in good agreement.

Table 4. Interpretation of ¹³C NMR inverse-gated (IG) spectrum of hyperbranched oligoglycerols HBPG₇ and HBPG₁₄: distribution of structural units.

	Relative abundance				DB	\overline{DP}_n
	D	T	L ₁₃	L ₁₄		
HBPG ₇	10.3%	63.9%	7.9%	17.9%	44%	5.6
HBPG ₁₄	18.9%	45.8%	11.2%	24%	52%	11.2

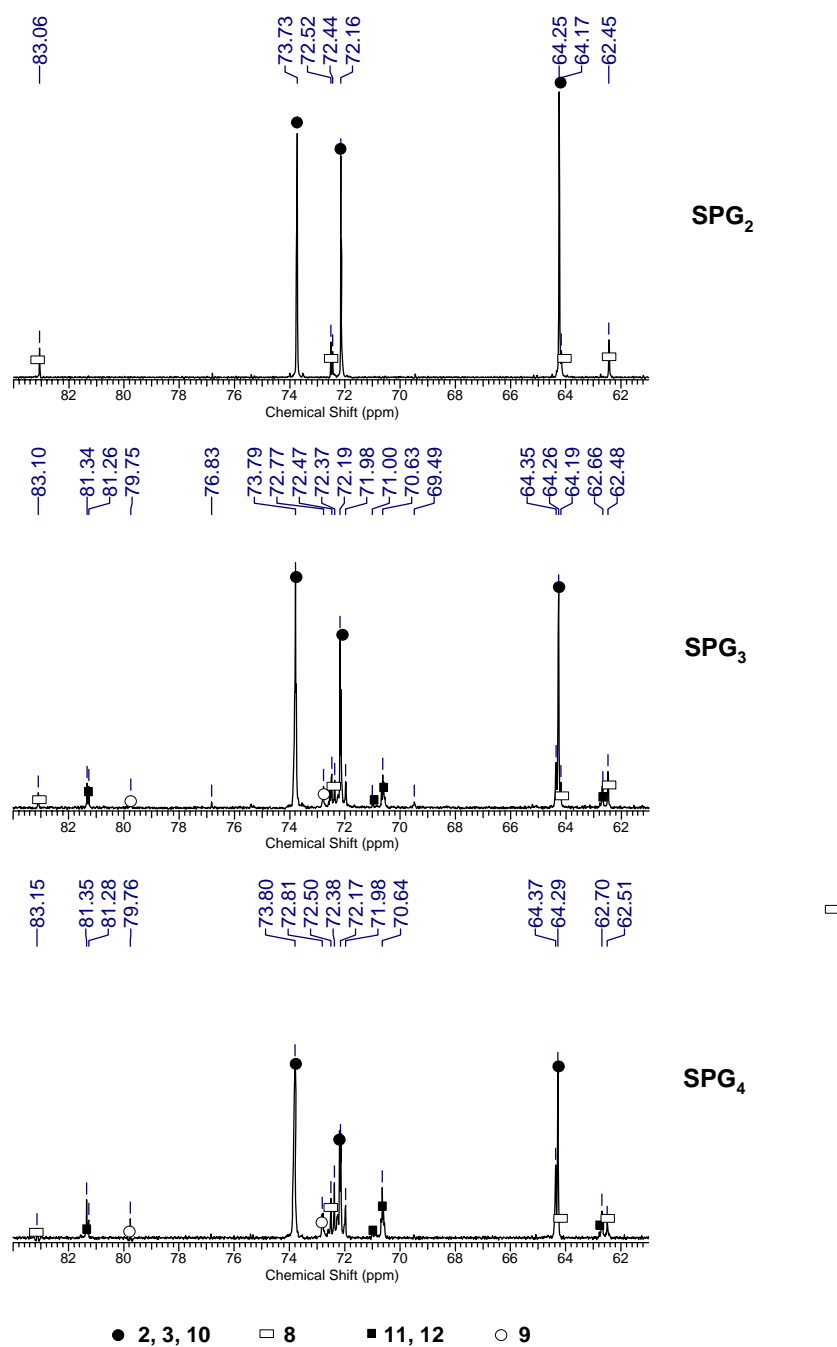
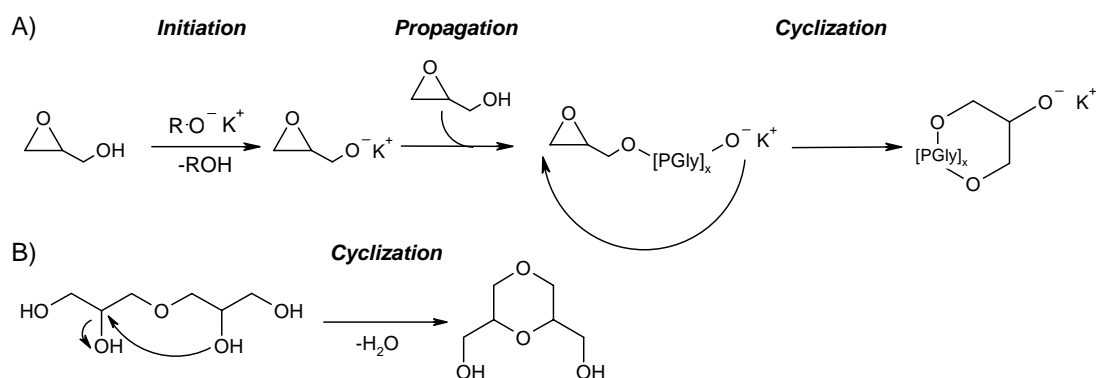


Figure 6. ^{13}C NMR spectra in d_4 -methanol of oligoglycerol samples prepared by polycondensation: diglycerol SPG_2 , triglycerol SPG_3 , tetraglycerol SPG_4 .

The ^{13}C NMR spectra of the commercial oligoglycerol samples are shown in **Figure 6**. For SPG_2 two different species can be identified: the linear oligoglycerols **2**, **3** and **10** (73.73, 72.16, 64.25 ppm), and the compound **8** (83.06, 72.52, 72.44, 64.17, 62.45 ppm), which is branched, because the secondary alcohol condensed with a second glycerol molecule. When the degree of polymerization increases, the number of species also grows. For SPG_3 and SPG_4 the same signals as in the sample SPG_2 are

present: linear oligoglycerol compounds (**2**, **3**, **10**) as well as compound **8**. The other signals correspond to more complex linear units (**11**, **12**) due to the higher DP_n . There are also weak signals corresponding to **9**, i.e., dendritic structural units. Due to the too low intensity of these units it is not possible to calculate the extent of branching in analogy to the hyperbranched polyglycerols. DB is certainly below 10% for the commercial oligoglycerols.

^{13}C NMR can not provide information on the presence or absence of cyclization during the polymerization process. It is not possible to distinguish the cyclic compounds from the others, since they possess the same structural units. Mass spectrometry permits to detect the different compounds in the samples. As explained, ESI was chosen because the samples possess very low masses and MALDI-ToF is not a relevant method in this mass range.



Scheme 4. A) Homopolymerization of glycidol by intramolecular ring-opening, resulting in the formation of cyclic compounds. B) Example of cyclization of diglycerol by intramolecular condensation.

In the case of hyperbranched oligoglycerols the cycles result from the homopolymerization of glycidol, terminated by intramolecular ring-opening as shown in **Scheme 4.A**. The cycles do not comprise any initiator-core. For the commercial oligoglycerols cyclization results from the intramolecular condensation of hydroxyl groups (**Scheme 4.B**). The mass difference in between the cycles and the corresponding non-cyclic condensation products (same $\overline{DP_n}$) is the mass of one molecule of water.

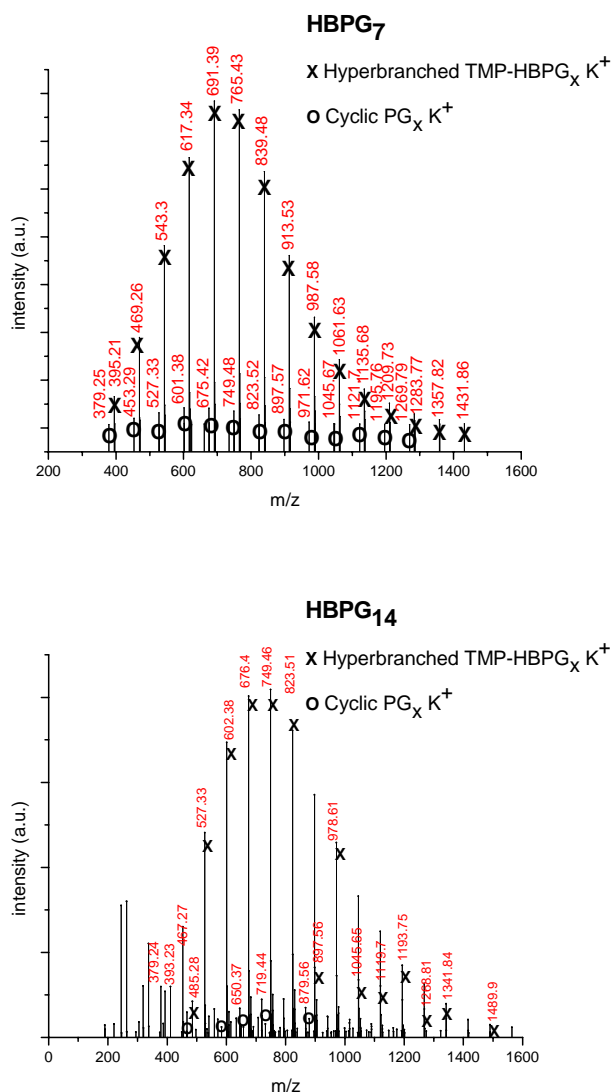
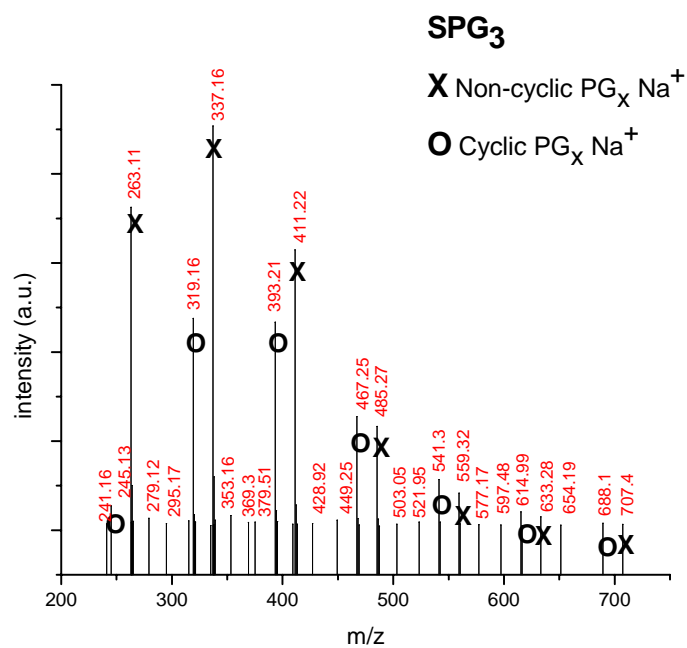
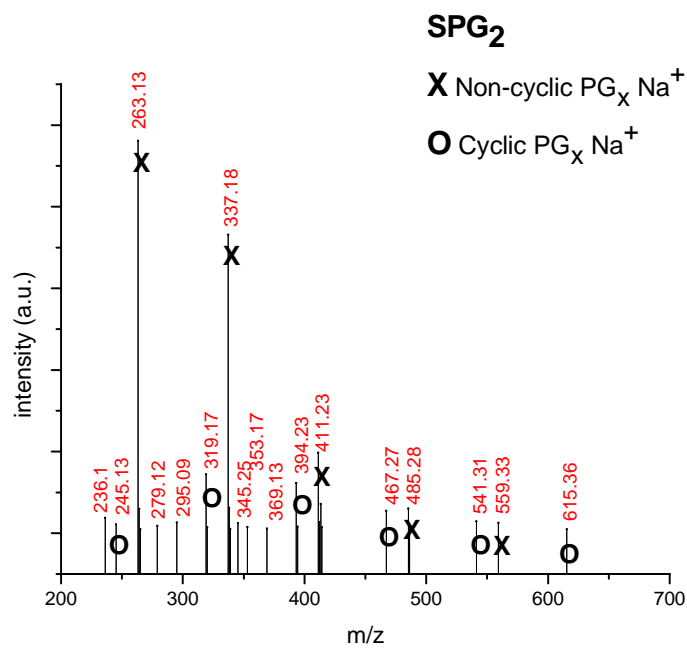


Figure 7. ESI mass spectra (methanol solution $1\text{g}\cdot\text{l}^{-1}$) of hyperbranched oligoglycerol samples prepared: HBPG₇ and HBPG₁₄.

Figure 7 shows the ESI mass spectra of the 2 hyperbranched oligoglycerol samples. It is possible to identify hyperbranched macromolecules with TMP as initiator-core and macromolecules without core (cycles). The intensities of the different signals can yield information on the proportion of the different species. As expected from the slow monomer addition technique the amount of cycles in the hyperbranched oligoglycerol samples is low.



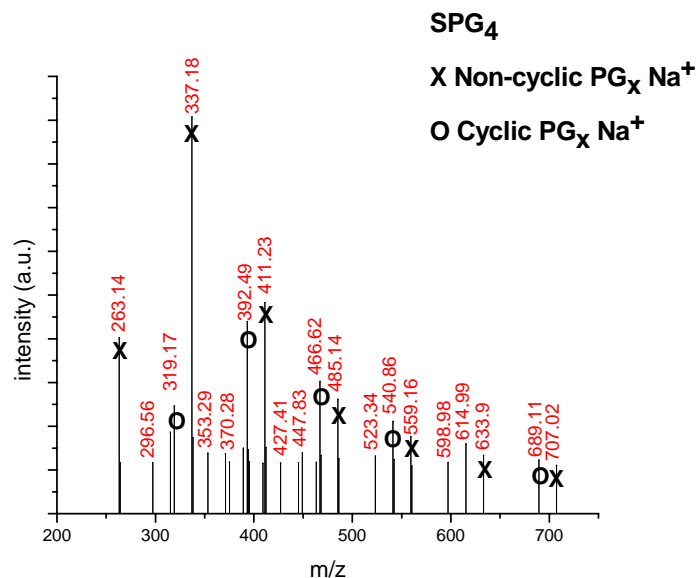


Figure 8. ESI mass spectra (methanol solution $1\text{g}\cdot\text{l}^{-1}$) of commercial oligoglycerol samples prepared by polycondensation: diglycerol SPG_2 , triglycerol SPG_3 , tetraglycerol SPG_4 .

In the case of the commercial oligoglycerols the mass spectra (**Figure 8**) are different from the hyperbranched oligoglycerols' mass spectra (**Figure 7**). The intensities of the cycles compared to the intensities of the non-cyclic oligoglycerols are similar. The proportion of cyclic compounds is higher; the condensation process promotes more intramolecular cyclization. Some signals (between 350 and 450 m/z) in the ESI spectra have not been identified. These may be due to byproducts from the condensation, depending on the procedure employed but it is difficult to conclude because the patent does not give sufficient information on these points.

3.5. Conclusion

Commercial oligoglycerols and hyperbranched oligoglycerols differ with respect to the control over the molecular weight and their composition in linear, branched and cyclic compounds. In the first case, multiple mode elugrams were recorded due to the obvious lack of control during the polycondensation process. ^{13}C NMR studies show the presence of a small amount of dendritic units (below 10%) and ESI measurements reveal a high fraction of cyclic compounds. The composition of the commercial oligoglycerols is not homogeneous and that can affect their properties for various advanced applications.

On the contrary, the hyperbranched oligoglycerol samples show well-defined and monomodal elugrams. These results were supported by a complementary study using SANS.¹⁷ The molecular weight distribution of the hyperbranched oligoglycerols can be controlled via the use of latent AB₂ monomers in combination with the slow monomer addition technique. ¹³C NMR confirms the presence of different units due to the random reaction of the secondary hydroxyl groups. The DB of both samples is 44% and 52%, respectively, which is in good agreement with theory. Additionally ESI experiments show that the materials contain only a small amount of cyclic compounds. The combination of a dendritic architecture and a homogeneous composition offers promising potential for multiple applications, such as biomineralization,²¹ liquid-crystals,²² initiators for star polymers for these new materials.^{23,24} The presence of an initiator-core at the focal point of these oligoglycerols offers additional possibilities. It is feasible to use a functional core with particular properties (electro-optical, pH sensitive etc...) as discussed in the chapter 4 of this thesis.

On the other hand, it has to be mentioned here that glycidol at present is a relatively expensive and toxic monomer, which can limit its application. In a recent account, the ring opening polymerization of glycerol carbonate for the preparation of highly branched polyglycerol has been published. This may be an interesting pathway in order to minimize, at least the toxic and environmental risks.²⁵

3.6. Experimental part

Materials. Diglycerol, triglycerol and tetraglycerol were provided by Solvay as a donation. Acetone, methanol and potassium methoxide were used as received from Fluka. THF and diglyme were obtained from Fluka and distilled over sodium prior to use.

Synthesis of the hyperbranched oligoglycerols. Polymerizations were carried out in a reactor equipped with a mechanical stirrer and a dosing pump under argon atmosphere. TMP (1,1,1-Tris(hydroxymethyl)propane) was used as core-initiator and was partially deprotonated (10%) with potassium methoxide by distilling off the methanol formed. The initiator was dissolved in diglyme and placed in the reactor.

The desired amount of glycidol in THF (1:1) was slowly added. The reaction was carried out at 120°C and THF was evaporated during the polymerization. After completion of the reaction the polymer was dissolved in methanol and was neutralized over a cation-exchange resin (Lewatit K1131). After filtration the polymer was precipitated in acetone and dried at 80°C in vacuo. Polymers were obtained with yields around 90%.

3.7. References

- (1) Behrens, H.; Mieth, G. *Die Nahrung* **1984**, 28, 815.
- (2) Seiden, P.; Bruce, M. J., **1976**, US 3,968,169.
- (3) Bunte, R.; Jeromin, L.; Jordan, V.; Gutsche, B., **1998**, US 5,710,350.
- (4) Dillenburger, H.; Jakobson, G.; Siemanowski, W., **1993**, US 5,243,086.
- (5) Hillion, G.; Stern, R., **1992**, EP 0,518,765.
- (6) Klein, J.; Daute, P.; Hees, U.; Beuer, B., **1993**, DE 4,124,665.
- (7) Babayan, B. V.; Lehman, H., **1972**, US 3,637,774.
- (8) Stuehler, H., **1985**, US 4,551,561.
- (9) Sandler, S. R.; Berg, F. R. *J. Polym. Sci., Polymer. Chem. Ed.* **1966**, 4, 1253.
- (10) Tsuruta, T.; Inoue, S.; Koinuma, H. *Makromol. Chem.* **1968**, 112, 58.
- (11) Vandenberg, E. J. *Polym. Chem. Ed.* **1985**, 23, 915.
- (12) Sunder, A.; Hanselmann, R.; Frey, H.; Mühlhaupt, R. *Macromolecules* **1999**, 32, 4240.
- (13) Sunder, A.; Mühlhaupt, R.; Haag, R.; Frey, H. *Adv. Mater.* **2000**, 12, 235.
- (14) Sunder, A.; Frey, H.; Mühlhaupt, R. *Macromol. Symp.* **2000**, 153, 187.
- (15) Kautz, H.; Sunder, A.; Frey, H. *Macromol. Symp.* **2001**, 163, 67.
- (16) Lee, C. L.; Smid, J.; Szwarc, M. *J. Am. Chem. Soc.* **1963**, 85, 912.
- (17) Garamus, V. M.; Maksimova, T. V.; Kautz, H.; Barriau, E.; Frey, H.; Schlotterbeck, U.; Mecking, S.; Richtering, W. *Macromolecules* **2004**, 37, 8394.
- (18) Hölter, D.; Frey, H. *Acta Polymer.* **1997**, 48, 30.
- (19) Hanselmann, R.; Hölter, D.; Frey, H. *Macromolecules* **1998**, 31, 3790.
- (20) Hölter, D.; Burgath, A.; Frey, H. *Acta Polymer.* **1997**, 48, 298.

- (21) Balz, M.; Barriau, E.; Istratov, V.; Frey, H.; Tremel, W. *Langmuir* **2005**, *21*, 3987.
- (22) Kirsten, J.; *Ph.D. thesis*, Johannes Gutenberg University of Mainz, **2005**.
- (23) Shen, Z.; Chen, Y.; Barriau, E.; Frey, H. *Macromol. Chem. Phys.* **2005**, *submitted*.
- (24) Doycheva, M; Berger-Nicoletti, E.; Frey, H. **2005**, *manuscript in preparation*.
- (25) Rokicki, G.; Rakoczy, P.; Parzuchowski, P.; Sobiecki, M. *Green Chem.* **2005**, *7*, 529.

4. Functional initiator-cores for hyperbranched polyglycerols

4.1. Introduction

Since the first pioneering works on hyperbranched polymers by Flory and others,¹ research on imperfectly branched macromolecules has focused on the preparation and characterization of a broad variety of hyperbranched materials. Gradually, the interest in this field of chemistry has moved towards the introduction of different functional groups at the periphery of the hyperbranched polymers for specific applications.²

As it has been demonstrated for perfectly branched dendrimers, the site isolation of the core moiety in a dendritic scaffold is of great interest with respect to optical properties and for catalysis. In this context, a solvatochromic chromophore (4-(*N,N*-dimethylamino)-1-nitrobenzene) was introduced at the focal point of a polybenzylether dendrimer by Fréchet et al.³ Depending on the polarity of the solvent and the generation number of the dendrimer, changes in the UV-visible absorption features of the encapsulated photoactive core as well as a transition in the morphology of the macromolecule from an extended to a more globular structure were observed. It has also been demonstrated that Manganese and Zinc-porphyrins coated by a dendritic structure exhibit better stability and improved regioselectivity in catalytic processes.^{4,5}

To date only few examples have been reported that deal with this issue and hyperbranched polymers. Fossum et al. investigated the effect of an enhanced core reactivity on molecular weight, polydispersity and degree of branching.⁶ The authors showed for the case of hyperbranched poly(arylene ether phosphine)s that the cores with the highest reactivity provided the best control over the molecular weight of the hyperbranched materials obtained in a polycondensation-type procedure.

Concerning the introduction of functionality in the core, two approaches have been reported so far: the direct copolymerization of a functional, active core and the post-polymerization modification of the core subsequent to the formation of the dendritic structure. Tian et al. used a modified triphenylamine as core for the polymerization of a conjugated hyperbranched polymer.⁷ The hyperbranched architecture had an influence on both UV-absorption and fluorescence properties of the core. Post-polymerization modification of the core was employed for an aromatic hyperbranched polyester that was reported to possess one nitrophenyl ester group at its focal point.^{8,9}

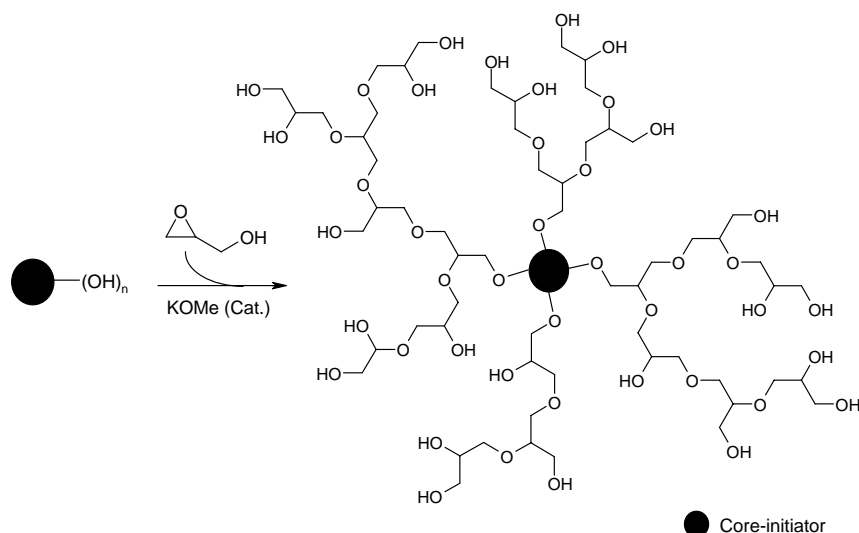
Reaction of this active ester with amines was followed by NMR and UV spectroscopy. One major drawback of the latter method is the limitation to relatively low molecular weights due to the difficult access to the core at high molecular weights.

Surprisingly, in most of these works the competing homopolymerization of the branching monomer is not discussed.¹⁰ However, this is a central point in the determination of the properties of the core in the hyperbranched structure, since for simple statistical reasons, the majority of the hyperbranched macromolecules are unlikely to possess a core unit in a conventional AB_m -type polycondensation. Žagar and Žigon published an elegant work on the characterization of commercially available hyperbranched polyesters obtained from AB_2 monomer and B_3 functional core molecule in 2002.¹¹ Clearly, detailed mass spectroscopy is crucial to identify the presence of “coreless” homopolymers, because the overall molecular weight and the degree of branching are only slightly affected. NMR and conventional SEC measurements are not sufficient to confirm the incorporation of an initiator-core in a dendritic structure, as it will be demonstrated in this section of the thesis.

This chapter reports on the incorporation of different initiator-cores into hyperbranched polyglycerols. The employed cores are structurally different, including mono- and bifunctional *n*-alkyl amines as well as photoactive cores, such as benzylamine and 1-naphthylmethylamine. In particular, the effect of core-variation on both molecular weights and final molecular weight distribution is discussed. In addition, the detection and analysis of non-cored glycidol homopolymer fractions is presented, using MALDI-ToF mass spectroscopy as a major characterization technique. Furthermore, a typical triplet photosensitizer 2,2',4,4'-tetrahydroxy benzophenone $BP(OH)_4$ is employed as initiator-core. All hyperbranched polyglycerols containing photoactive cores are analyzed using UV-visible and fluorescence spectroscopy in both stationary and time-resolved modes in order to establish the effect of the photoactive core microenvironment in hyperbranched macromolecules of varying molecular weights. Finally, the presence of a “dendritic effect” in the hyperbranched structure will be discussed on the basis of the data obtained.

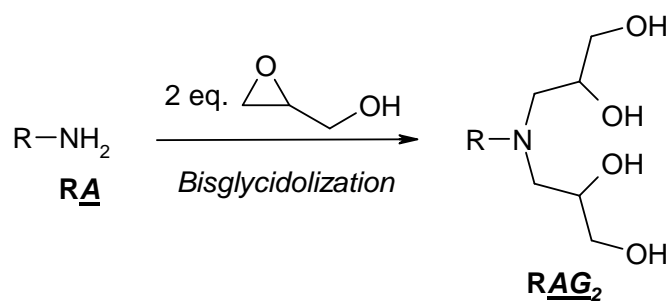
4.2. Amines as initiator-cores

The ring-opening multibranching polymerization (ROMBP) of glycidol is initiated by the reaction with an alkoxide, as illustrated in **Scheme 1**. Due to fast proton exchange, intermolecular and intramolecular transfers take place, leading to uniform growth at all functionalities, as detailed in previous work.¹²



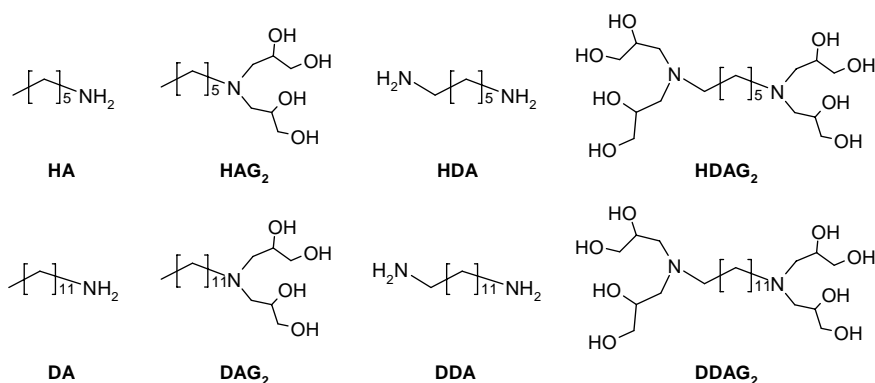
Scheme 1. Structure of hyperbranched polyglycerol with an initiator-core at its focal point.

Suitable initiators are compounds containing at least three hydroxyl groups. Since primary amines are known to react rapidly with epoxides, they also represent suitable initiators for the polymerization of glycidol. Initiation of the polymerization of glycidol by an amine (*in situ*) in the presence of a deprotonating agent (i.e. potassium *tert*-butoxide) that propagates the ROMBP represents one possibility. An interesting alternative is the bisglycidolization of the amine prior to the polymerization (**Scheme 2**).

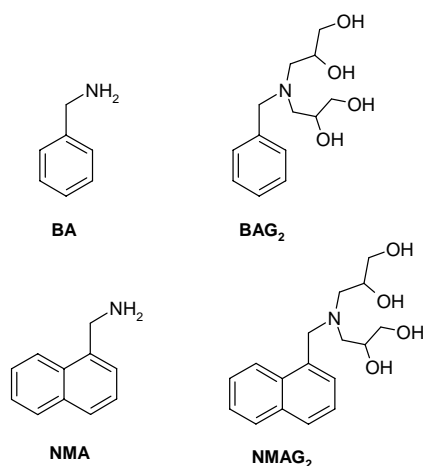


Scheme 2. Bisglycidolization of the amine initiator-cores.

The preparation of linear-dendritic nonionic surfactants using an amino-terminated linear poly(propylene oxide) block (Jeffamine) as macroinitiator-core was reported in previous work.^{13,14} A systematic comparison of the direct use of amines as initiator-cores by *in situ* glycidolization with well-defined bisglycidolized amines is presented here. The initiator-cores used can be divided in two categories: the *n*-alkyl amines (**Scheme 3**) and the photoactive amines (**Scheme 4**). For that purpose, the length and the functionality of the aliphatic amines have been varied: *n*-hexylamine (HA), 1,6-hexyldiamine (HDA), *n*-dodecylamine (DA) and 1,12-dodecyldiamine (DDA). Two photoactive compounds were used as core: benzylamine (BA) and naphthylmethylamine (NMA). RAG₂ corresponds to the bisglycidolized amines.



Scheme 3. *n*-Alkyl amine initiator-cores used in this work.



Scheme 4. Photoactive amine initiator-cores employed in this work.

4.2.1. *n*-Alkyl amines initiator-cores

In the case of the *n*-alkyl amines, polymerizations were carried out in order to achieve a theoretical molecular weight of 2,000 g·mol⁻¹. The different data obtained are summarized in **Table 1**. The resulting materials have been fully characterized by NMR spectroscopy, SEC and MALDI-ToF mass spectrometry. The relative \overline{M}_n values determined by SEC are believed to be underestimated, since linear polymer standards (polystyrene) were used for calibration. In order to obtain absolute values, \overline{M}_n was also calculated from the ¹H NMR spectra by comparison of the signals of the core moieties and the signals of the polyether polyol scaffold. To this end, we have to assume that all hyperbranched species present possess a core unit. However, this assumption will be confirmed only later with detailed MALDI-ToF studies (*vide infra*).

Table 1. Characterization data of hyperbranched polyglycerol samples with *n*-alkyl amine initiator-cores prepared with a theoretical molecular weight of 2,000 g·mol⁻¹. [a] \overline{M}_n in g·mol⁻¹; [b] NCS: no core signals visible in ¹H NMR-spectra.

	Core	¹ H NMR	SEC	
		$\overline{M}_n^{[a]}$	$\overline{M}_n^{[a]}$	$\overline{M}_w / \overline{M}_n$
1	No core	-	2,700	5.4
2	TMP	2,300	1,900	1.6
3	HA	NCS ^[b]	14,652	11.2
4	HAG ₂	6,800	5,600	1.5
5	HDA	3,500	1,110	3.6
6	HDAG ₂	3,100	2,850	1.65
7	DA	25,980	9,350	2.1
8	DAG ₂	4,500	2,000	1.5
9	DDA	6,200	3,340	5.4
10	DDAG ₂	3,580	1,500+(aggreg.)	1.9

The characterization data summarized in **Table 1** point to interesting conclusions, particularly with respect to the effects of bisglycidolization. As expected and mentioned in previous work, polymerization experiments of glycidol without core (but under slow monomer addition-conditions) leads to materials of high apparent

polydispersity (above 5) and obviously no control over molecular weights can be achieved in this case.

Clearly, when *n*-alkyl amines are employed directly, the molecular weights are much higher than expected and the apparent polydispersity of these materials broadens, in some cases exceeding values of $\overline{M}_w / \overline{M}_n = 5$ or even 10. Thus, the polymerization cannot be controlled via this strategy. In contrast, all polymerizations initiated by bisglycidolized amines lead to well-defined hyperbranched polymers with apparent polydispersities in the range of $\overline{M}_w / \overline{M}_n = 1.5 - 1.9$. We explain this observation by the inhomogeneous start of the polymerization in the case of the direct use of the amines. Indeed, two classes of reactions take place in the amine system, the bisglycidolization as well as the concurrent propagation via the hydroxyl groups. Thus, the cores do not grow homogeneously due to these competing reactions.

It is important to note that both NMR spectroscopy and SEC are not appropriate methods to differentiate between macromolecules carrying an initiator-core and the hyperbranched homopolymers. As pointed out before, this results in an error for molecular weight calculations based on NMR signal intensities, because the signals from the polyether polyol scaffold do not solely correspond to species carrying a core. Additional methods are required in order to make a conclusive statement on the composition of the samples. Thus, detailed MALDI-ToF mass spectrometry is mandatory to confirm core attachment of the macromolecular structure present.^{15,16}

Due to intermolecular proton exchange, undesired homopolymerization of glycidol may take place, even if glycidol is added very slowly. In the case of incomplete core attachment two different series of hyperbranched polymers may be encountered in the final samples: (i) homopolymer of glycidol, (ii) hyperbranched polyglycerol with an amine derivative as core. All the samples were processed in the same manner using cyanohydroxycinnamic acid (cca) as matrix and lithium chloride as cationization agent. **Figure 1** shows typical MALDI-ToF spectra of two polymer samples (**7**, **8**), one prepared from the DA-core and the other one from the DAG₂ initiator-core. Both spectra show striking differences, in spite of the apparent similarity of the final product. Of course, when using MALDI-ToF spectra for detailed characterization, it is important to verify, whether the spectra obtained are actually representative of the complete distribution of species actually present in the sample. It should be noted here that MALDI-ToF mass spectrometry is not a quantitative method and that the

intensity of the signals gives only an estimate of the fraction of species present. The average molecular weight will also not be determined by MALDI-ToF due to mass discrimination. Indeed, depending on molecular weight and chemical composition the macromolecules do not exhibit the same ionization and desorption probability. It is reasonable to believe that the low molecular weight species will undergo desorption more easily than the high molecular weight macromolecules. Nevertheless, with MALDI-ToF it is possible to confirm or dispute the presence or absence of homopolymers. This is crucial to confirm the incorporation of the initiator-cores.

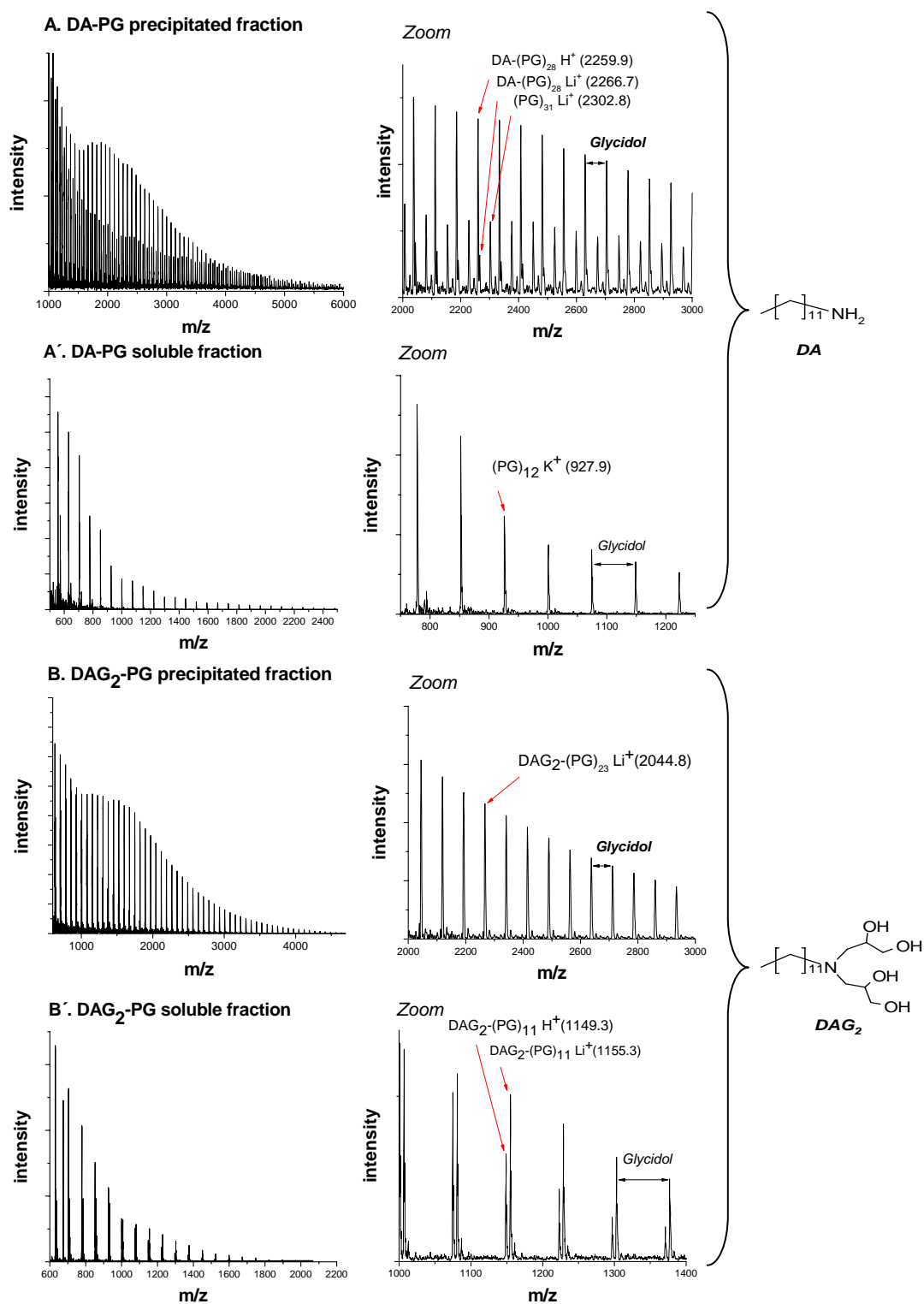


Figure 1. MALDI-ToF mass spectra of hyperbranched polyglycerols obtained with dodecylamine (sample 7: A. precipitated fraction, A'. soluble fraction) and bisglycidolized dodecylamine (sample 8: B. precipitated fraction, B'. soluble fraction) initiator-cores.

In the case of sample **8** a molecular weight calculation based on the ^1H NMR spectrum gives a value of $4,500\text{ g}\cdot\text{mol}^{-1}$ for \overline{M}_n , which is larger than the \overline{M}_n obtained from the SEC elugram at $2,000\text{ g}\cdot\text{mol}^{-1}$. As mentioned above, the difference is mainly due to the fact that the calibration is carried out with linear polymer standards (PS). The hydrodynamic radius of a dendritic macromolecule is smaller than that of a linear polymer with the same molecular weight. The MALDI-ToF spectrum of sample **8** (**Figure 1**) shows signals up to $5,000\text{ g}\cdot\text{mol}^{-1}$. Thus, a large fraction of the molecular weight distribution can be detected. The formation of cyclic homopolymer is more likely to occur at the beginning of the reaction at the low molecular weight level. When the overall molecular weight and thus the number of growing chain ends increase in the batch, the viscosity also increases. The probability that a monomer added reacts with another unreacted monomer present is very limited under SMA-conditions. For sample **7** the difference between the molecular weight \overline{M}_n from ^1H NMR ($26,000\text{ g}\cdot\text{mol}^{-1}$) and from SEC ($9,350\text{ g}\cdot\text{mol}^{-1}$) is very large. This probably could mean that the fraction of homopolymer is higher in this sample than in sample **8**.

The MALDI-ToF spectrum of the sample **7** using the amine (DA) directly as initiator reveals the presence of hyperbranched polyglycerol homopolymer macromolecules ($\text{PG}_x\text{ M}^+$) with high intensity in the molecular weight region from $2,000$ to $3,000\text{ g}\cdot\text{mol}^{-1}$ as well as the formation of hyperbranched polymer with DA as a core ($\text{DA-PG}_y\text{ M}^+$). In pronounced contrast, the spectrum of the sample **8** initiated with bisglycidolized amine (DAG_2) shows only the presence of polymer with incorporated initiator-core in the molecular weight range of 500 to $4,500\text{ g}\cdot\text{mol}^{-1}$. Also in this case, based on the other characterization data, it can be concluded that this is representative of the whole sample.

All materials were precipitated in acetone/methanol, when the monomer addition was complete. After each polymer precipitation step, the solution of acetone/methanol was evaporated and the soluble fraction was also isolated. MALDI-ToF spectra (**Figure 1**) of both the precipitated polymer fractions as well as the material in the soluble fractions were recorded. Interestingly, we observed that in the case of DA initiator-core (A') the soluble fraction was mainly composed of homopolymer, presumably cycles. This means, that via precipitation some low molecular weight cyclic homopolymer can be separated from the hyperbranched polymer. Again, in

pronounced contrast for the DAG₂ initiator-core no homopolymer fraction was observed in the soluble fraction (B') as well as in the precipitated fraction (B). These results are in excellent agreement with the conclusions made above on the direct use of the *n*-alkyl amines as initiator-cores, because they lead to a larger extent of homopolymerization than the *n*-alkyl bisglycidolized amines.

The different bisglycidolized *n*-alkyl amines employed vary in the length of their alkyl chain and the number of functional groups (monoamine vs. diamine). The results summarized in **Table 1** confirm that the control over the molecular weight depends on the length of the aliphatic amine. Very clearly, the C₁₂ amine leads to better control of the molecular weight than the C₆ amine. This can be explained by the fact that the initiator solution (bisglycidolized amine, potassium *tert*-butylate and diglyme as high boiling point solvent) is more homogeneous with increasing length of the alkyl chain of the amine, as observed in the reaction setup. Furthermore, in the case of the cores carrying longer aliphatic chains the fraction of homopolymer in the precipitated material is negligible. This suggests that the longest aliphatic amines are better initiators due to their higher stability (higher boiling point, sublimation of the amines at the top of the reactor is then more unlikely to happen) and their better solubility in diglyme.

4.2.2. Photoactive amine initiator-cores

Samples with photoactive initiator-cores, namely benzylamine (BA) and 1-naphthyl-methylamine (NMA) have also been prepared. Introducing these cores into the hyperbranched structure was expected to provide fundamental information about the shielding effect provided by the hyperbranched polymer “shell” and to establish the nature of the chromophore microenvironment in hyperbranched polyglycerols in dependence of molecular weight in different media. This is of relevance for designing easily accessible, yet encapsulated dye-cores that may act as photosensitizers.

The characterization results of hyperbranched polyglycerol with benzylamine initiator-cores are shown in **Table 2**. A series of samples of different molecular weight were prepared, starting from BA and from bisglycidolized benzylamine (BAG₂). Molecular weight control and also the width of the molecular weight distribution is unsatisfactory with BA as initiator-core (**11**, **13**, **15**). The molecular

weights are higher than the theoretical values determined from the monomer/initiator-core ratio, and the weight distribution is broad (in the range of 2.4 - 3.5). All samples of BAG₂ (**12**, **14**, **16**) exhibit better molecular weight control and a narrow apparent polydispersity (1.8). This is in agreement with the results presented for the *n*-alkyl amines. Again, it is important to note that only the well-defined bisglycidolized amine initiators permit controlled polymerization of glycidol and provide narrow polydispersity.

Table 2. Characterization data of hyperbranched polyglycerol samples with benzylamine initiator-cores. [a] \overline{M}_n in g·mol⁻¹; [b] NCS: no core signals detectable in ¹H NMR-spectra.

	Core	Theory	¹ H NMR	SEC	
		$\overline{M}_n^{[a]}$	$\overline{M}_n^{[a]}$	$\overline{M}_n^{[a]}$	$\overline{M}_w / \overline{M}_n$
11	BA	1,000	8,460	1,690	2.4
12	BAG ₂	1,000	1,560	1,200	1.8
13	BA	2,000	4,200	2,100	3.3
14	BAG ₂	2,000	3,290	2,900	1.8
15	BA	5,000	NCS ^[b]	67,400	3.5
16	BAG ₂	5,000	5,400	3,300	1.8

Figure 2 shows the MALDI-TOF spectra in the case of the benzylamine initiator-cores BA (sample **13**: C and C') and BAG₂ (sample **14**: D and D') for a theoretical molecular weight of 2,000 g·mol⁻¹. Both spectra from the precipitated fractions do not exhibit any homopolymer peaks, but the soluble fraction of the BA polymer clearly shows signals that are assigned to core-less material. In this case, precipitation is efficient to separate the cycles and the core-containing hyperbranched polymer, presumably because of their pronounced polarity difference.

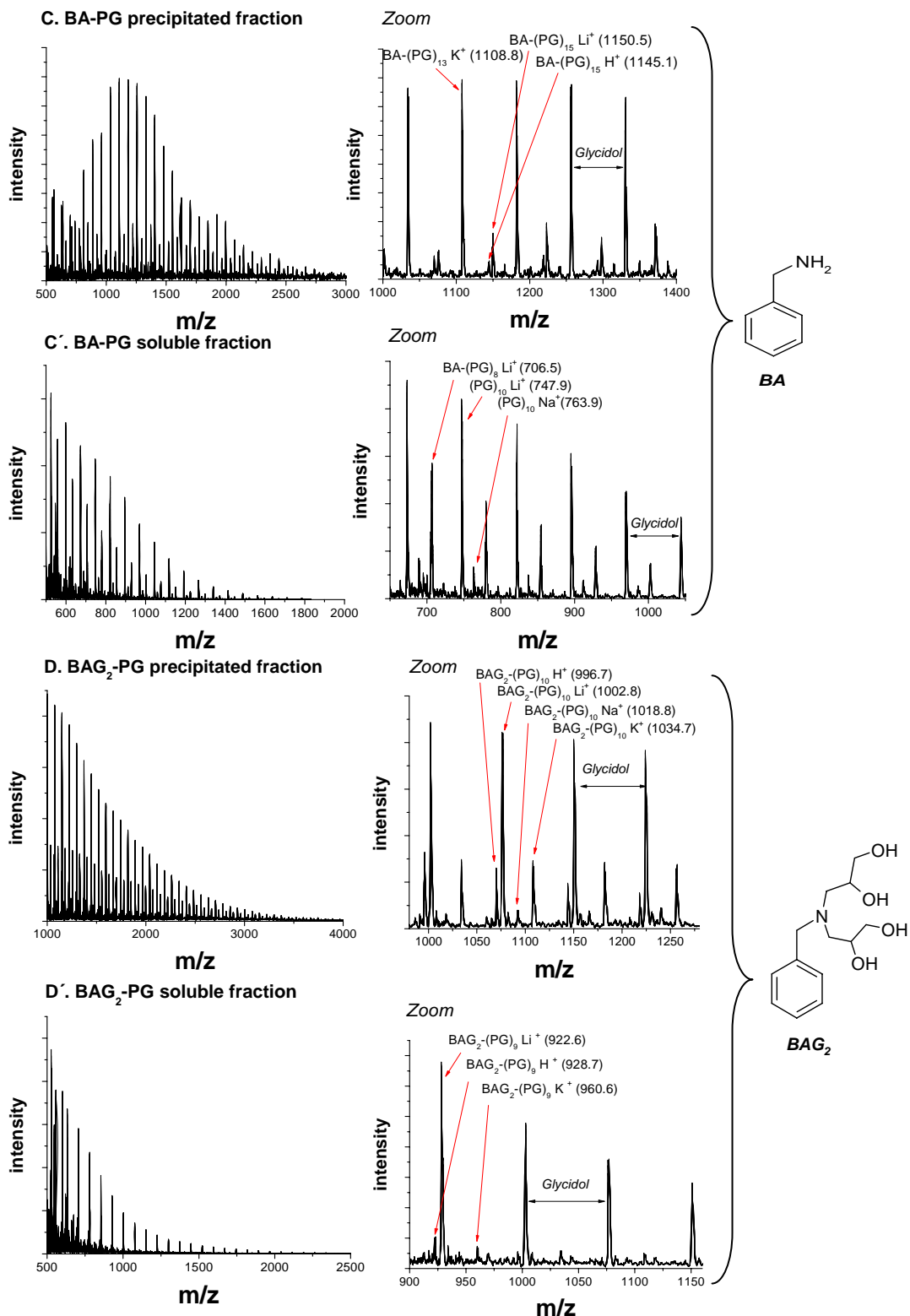


Figure 2. MALDI-ToF mass spectra of hyperbranched polyglycerols obtained with benzylamine BA (sample 13: C. precipitated fraction, C'. soluble fraction) and bisglycidolized benzylamine BAG₂ (sample 14: D precipitated fraction, D'. soluble fraction) initiator-cores.

Naphthalene has been intensely studied with respect to its photochemical and photophysical properties. This compound represents the most simple polynuclear aromatic structure available and it exhibits a rich vibronic structure in its electronic transitions compared to benzene.¹⁷⁻²¹ The samples prepared with 1-naphthylmethylamine as initiator-core are listed in **Table 3**. Results show that NMAG₂ provides good control over the molecular weight. However it should be noted that the apparent polydispersity with NMAG₂ is higher than in the case of *n*-alkyl amines and benzylamine. This can most probably be explained by the fact that this initiator-core is less soluble than the others.

Table 3. Characterization data of hyperbranched polyglycerol samples with 1-naphthylmethylamine initiator-cores. [a] \overline{M}_n in g·mol⁻¹.

	Core	¹ H NMR	SEC	
		$\overline{M}_n^{[a]}$	$\overline{M}_n^{[a]}$	$\overline{M}_w / \overline{M}_n$
17	NMA	10,150	17,504	2.83
18	NMAG ₂	8,360	9,100	2.5
19	NMAG ₂	4,400	3,200	2

As it was previously pointed out in this chapter, a number of potential technological applications have been proposed for hyperbranched polymers, and therefore a significant effort has been directed towards understanding their physical and chemical properties in solution as well as in bulk.² Functional ‘probe’-labelled macromolecular structures, in particular in dendrimers and linear polymers, have proven to be an informative means facilitating the detailed investigation of their properties.²²⁻²⁶ In this regard, naphthalene, a rigid aromatic hydrocarbon with π, π^* configuration of the singlet state S₁, is an excellent probe for the study of a hyperbranched polyglycerol microenvironment because of its sensitive solvatochromic shifts and measurable fluorescence.

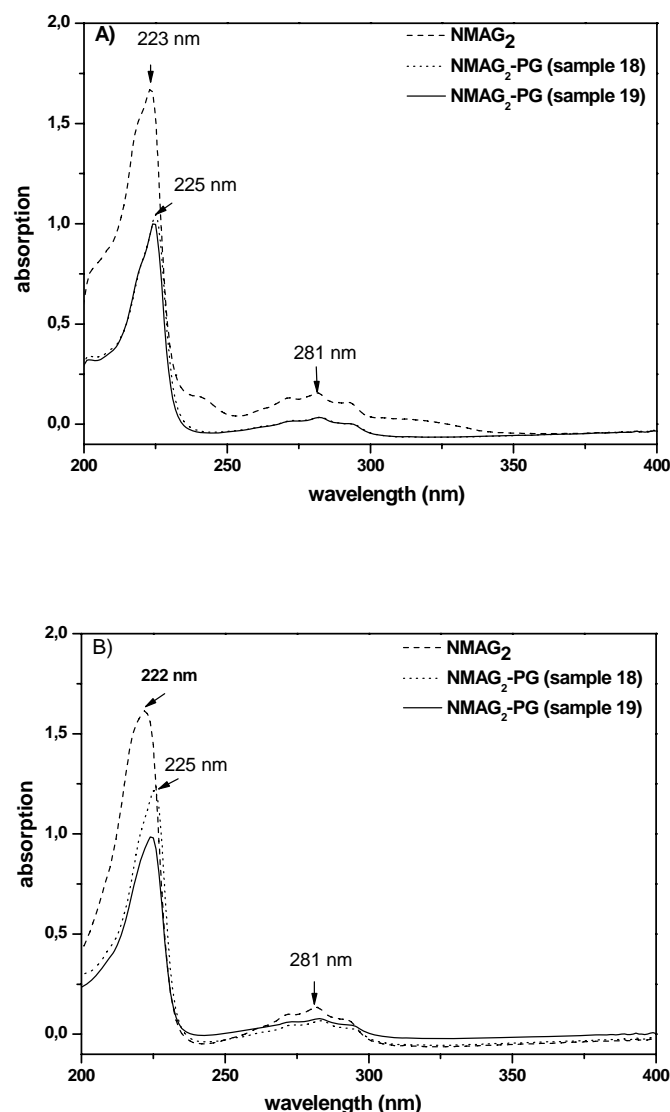


Figure 3. UV-vis spectra of N MAG₂, hyperbranched polyglycerols with N MAG₂ as initiator-core (**18**, **19**) recorded at 298K: A) in methanol; B) in Millipore water. The solutions measured have been prepared at fixed naphthalene concentration 10⁻⁵M.

UV-vis spectroscopy. **Figure 3** shows the UV-vis spectra of the core N MAG₂ and hyperbranched polyglycerols with N MAG₂ as initiator-core (**18**, **19**) in both methanol and water. For a systematic comparison the solutions were prepared with fixed concentration of the absorbing chromophore, naphthalene, at 10⁻⁵M. It should be noted that because of the different solubility of the prepared polyols (**18**, **19**) only in methanol or water, the UV-vis measurements had to be carried out in these solvents, which display slightly different polarity (normalized transition energy values as empirical parameters of solvent polarity, E_T^N , for methanol ca. 0.790 and ca. 1.000 for

water). In the absorption spectra of both hyperbranched polymers, four characteristic bands were observed, one pronounced in the far UV-region (225 nm) due to the conjugation of the naphthalene group and three other weak bands in the UV region (270, 281, 296 nm) attributed to the π,π^* - transition of the naphthalene. The absorption in the UV showed a very small red-shift of 2 to 3 ± 0.5 nm in methanol and water, respectively, compared to the model compound, i.e., bisglycidolized 1-naphthyl-methylamine core (222-223 nm). This is also accompanied by a significant hypochromic shift (decrease of the intensity of the band) at $\lambda_{\max}=225$ nm. For the hyperbranched polyglycerols containing a naphthalene-core, the absence of any kind of a strong peak broadening or shift in the absorption spectra compared to the model compound, suggests that the focal naphthalene is well-separated from the branched polyether segments with very weak electron coupling in the ground state.

Steady state and lifetime fluorescence spectroscopy. The emission spectra of bisglycidolized methylnaphthalene amine, NMAG₂ and hyperbranched polyglycerols with NMAG₂ as initiator-core **18**, **19** are depicted in **Figure 4. Table 4** summarizes the corresponding wavelengths of the emission maxima ($\lambda_{\text{em}}^{\text{max}}$), the quantum yields (Φ_f) and the fluorescent species lifetimes (τ). The compounds **18** and **19** in methanol display the same emission spectra (322 nm) upon excitation of the naphthalene core at 296 nm as the naphthalene core-initiator (322 nm) with only a small hypochromic shift. This excludes the formation of excimer species. This small decrease of the emission band i.e., hypochromic shift observed in methanol becomes larger in water. The emission intensity of NMAG₂ in water ($\Phi_f = 0.14$) is 10 times larger than for hyperbranched polymers **18** and **19** (ca. $\Phi_f = 0.013$ and 0.015 , respectively). It should be noted that naphthalene alone fluoresces with a moderate quantum yield ($\Phi_f \sim 0.20$), however, the presence of an amine group as substituent at the backbone permits the quenching of its excited fluorophore by electron transfer promoted by the amine group.²⁷ It appears that in methanol hyperbranched polymers **18** and **19** adopt a somewhat more compact structure than in water. This induces the formation of a hydrophobic pocket for NMA, inaccessible for water, which is known as hydrogen-donor solvent (formation of hydrogen bonds with the amine group). This prevents static quenching and results in higher emission of naphthalene, as observed in the case of NMAG₂ in water.^{28,29}

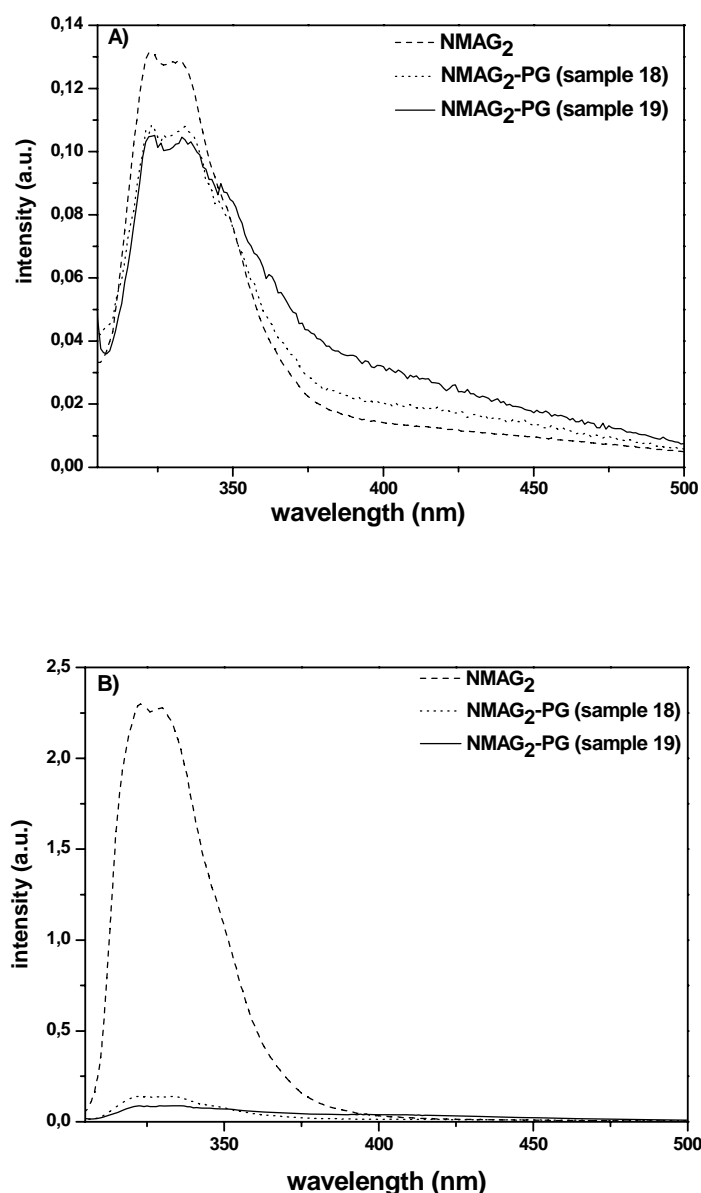


Figure 4. Fluorescence emission spectra at excitation wavelength $\lambda_{\text{exc}} = 296$ nm of NMAG₂, hyperbranched polyglycerols with NMAG₂ as initiator-core (**18**, **19**) at 298K: A) in methanol; B) in Millipore water. The samples were prepared at fixed absorption, $\text{Abs}(\lambda_{\text{max}}=296\text{nm}) = 0.3$.

The lifetime of the fluorescent species summarized in **Table 4** as well as the corresponding kinetic spectra shown in **Figure 5** recorded in methanol support our conclusion that the hyperbranched polymers **18** and **19** adopt a more compact structure than in water. In methanol, the singlet lifetimes are less than 2.3 ns and they are twice longer in water (ca. 4.9 ns). The accessibility of water (hydrogen-bonding solvent) to the core unit enhances the fluorescence emission of the probe via hydrogen

bonding interaction with amine electrons. N_{MAG}₂ in water displayed a long lifetime ($\tau = 12$ ns), 6 times longer than in methanol.

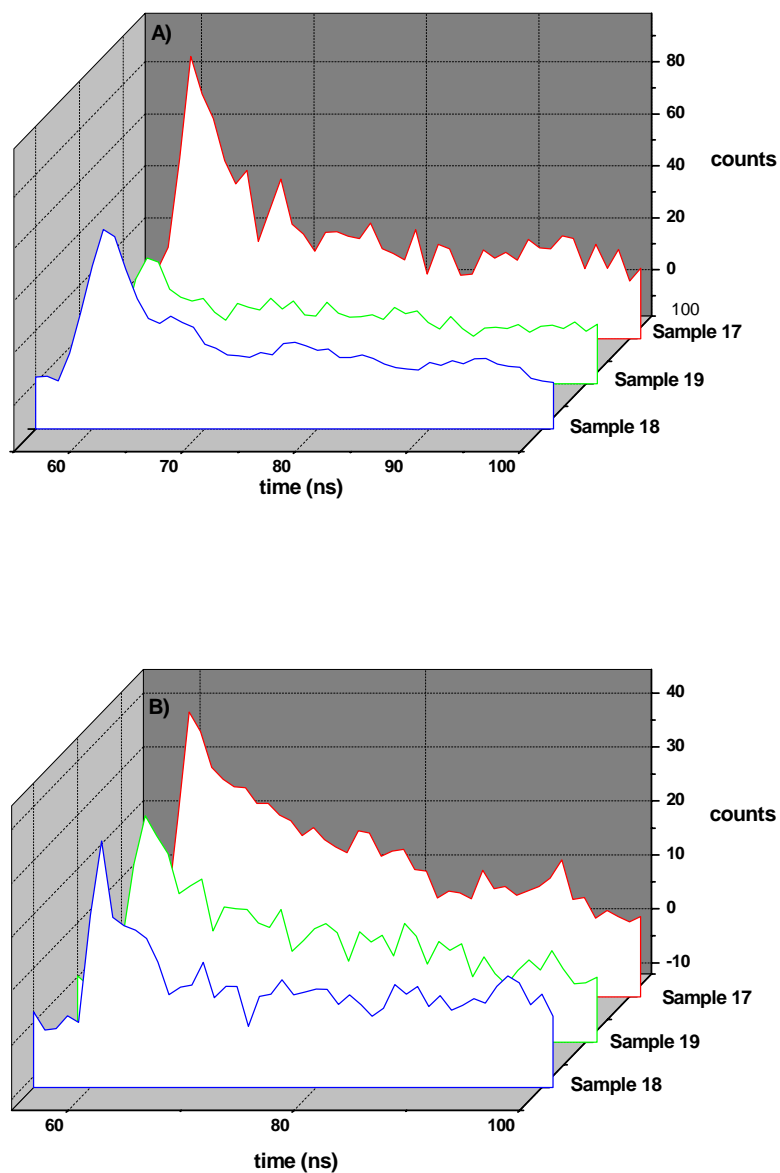


Figure 5. Time resolved fluorescence decay spectra at excitation wavelength $\lambda_{exc} = 296$ nm and $\lambda_{em} = 322$ nm of N_{MAG}₂, hyperbranched polyglycerols with N_{MAG}₂ as initiator-core with fixed $Abs_{296} = 0.3$ at 298K (17, 18, 19): A) in methanol; B) in Millipore water.

Table 4. Photophysical Parameters of NMAG₂ and hyperbranched polyglycerols with NMAG₂ as initiator-core (Abs₂₉₆ = 0.3) at 298K. All wavelengths are given with an accuracy of ±0.5 nm.

	MeOH			H ₂ O			H ₂ O (pH=2)	
	λ_{em}^{max} (nm)	ϕ_f	τ_f (ns)	λ_{em}^{max} (nm)	ϕ_f	τ_f (ns)	ϕ_f	τ_f (ns)
17	322	0.012	2.0	323	0.14	12	0.20	18.4
18	322	0.016	2.1	323	0.015	4.9	0.19	25.7
19	322	0.013	2.3	323	0.013	4.6	0.21	23.4

Steady State Fluorescence-pH Dependence. The amino-groups in proximity of the core offer the possibility to study the pH-dependence of the UV-absorption properties. **Figure 6** shows the dependence of the fluorescence spectra of the hyperbranched polymers **18** and **19** on pH. The corresponding lifetimes and quantum yields of the protonated species are presented in **Table 4** for comparison with those performed at pH 7. The protonation state of the hyperbranched polymers containing naphthalene cores strongly influences their fluorescence emission spectra. Upon decrease of the pH-values of the aqueous solutions of the polymers, a pronounced increase in the fluorescence intensity (not in the shape of the fluorescence absorption) is observed. This is due to protonation of the amine, which renders the electron transfer from the amine to the naphthalene singlet state impossible. Remarkably, the quantum yields of NMAG₂ ($\Phi_f=0.20$) and **18** ($\Phi_f=0.21$) and **19** ($\Phi_f=0.19$), measured at pH=2 are higher by an order of magnitude than those recorded at pH 7.5. The same tendency was observed for the lifetime of the fluorescent species, which lives 10 times longer than at neutral pH.

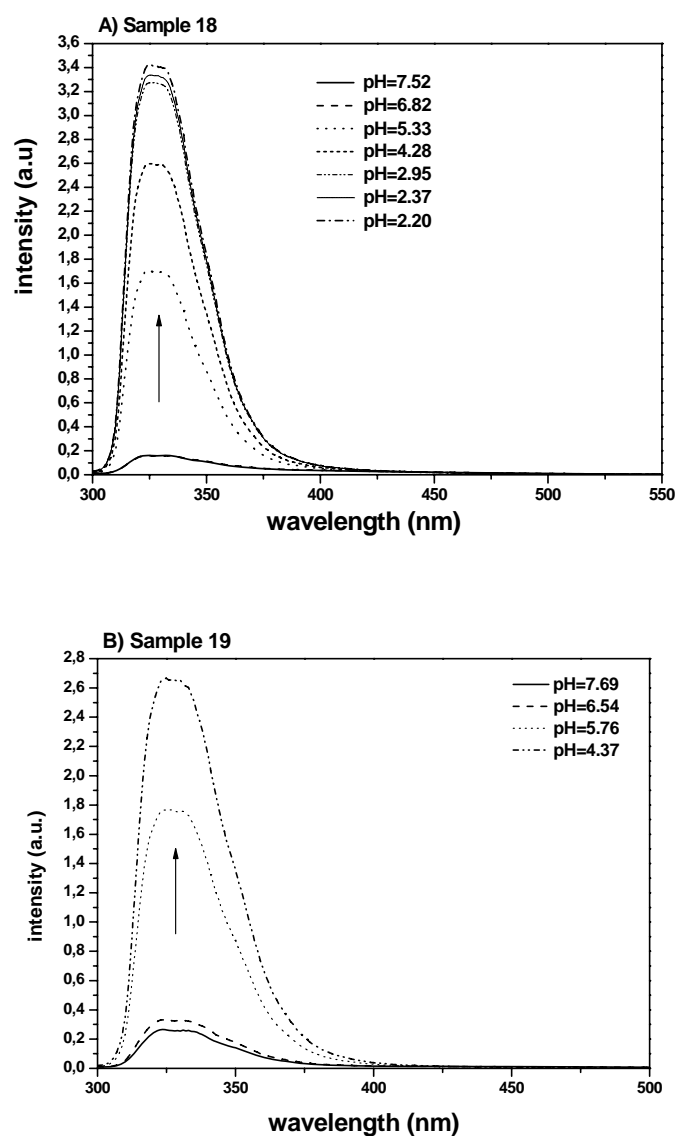
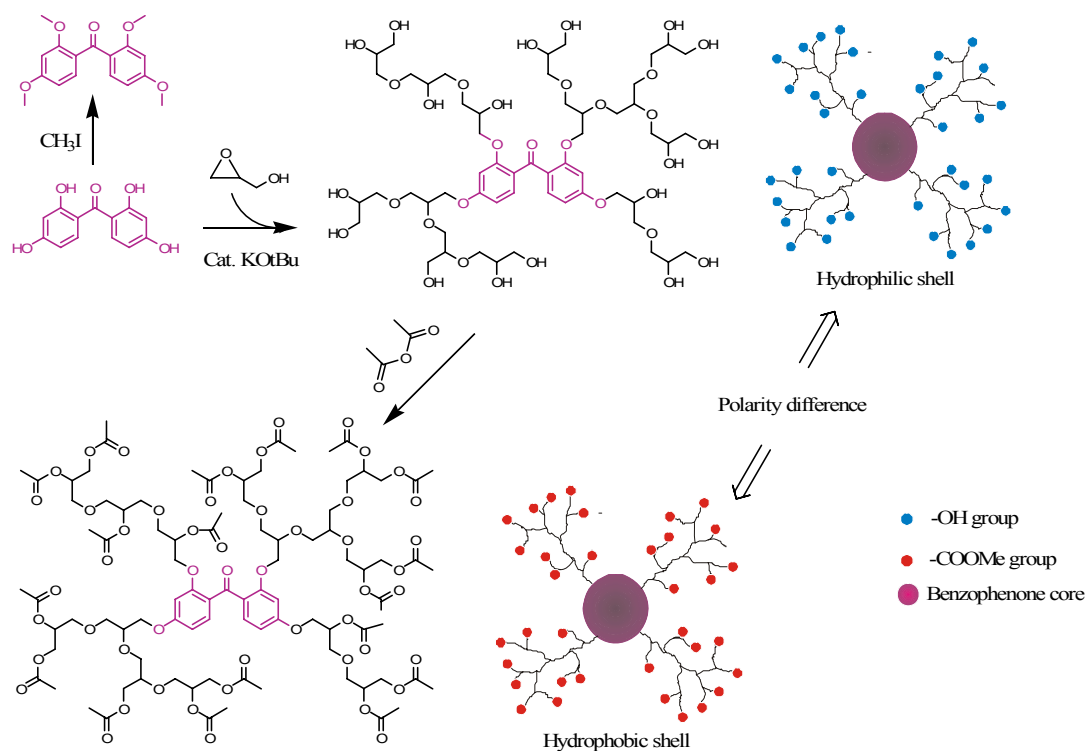


Figure 6. Fluorescence emission spectra of hyperbranched polyglycerols with NMAG_2 as initiator-core fixed at ($\text{Abs}_{296} = 0.3$) excitation wavelength $\lambda_{\text{exc}} = 296 \text{ nm}$, in NaCl (0.1M) aqueous solution recorded at 298K as a function of pH: A) sample **18**; B) sample **19**.

4.3. Benzophenone as initiator-core

A typical triplet photosensitizer has also been employed as initiator-core, 2,2',4,4'-tetrahydroxy benzophenone $\text{BP}(\text{OH})_4$.²¹ The synthetic strategy is presented in **Scheme 5**. In order to investigate the photo-optical properties depending on the polarity of the materials, the hydroxyl end groups were post-modified by acetylation. Two series of samples have been prepared: (i) hyperbranched polyglycerols containing a benzophenone core (BP-PG) and (ii) acetylated hyperbranched polyglycerol samples containing a benzophenone core (BP-(PG-Ac)).



Scheme 5. Synthesis of hyperbranched polyglycerols containing a benzophenone core, post-modification of the end groups and methylation of the benzophenone used as initiator-core.

The ROMBP of glycidol is in this case initiated by four aromatic hydroxyl groups. The reactivity of these initiator-groups is not as high as the reactivity of the hydroxyl groups of the aliphatic polyols usually employed. Therefore, the initiator-core was partially deprotonated to a higher extent (20%) with potassium *tert*-butoxide. The results of the synthesis are summarized in **Table 5**. The polydispersity of the 3 samples prepared was narrow. In the case of a tetrafunctional core, the expected polydispersity would be 1.25 according to theory.

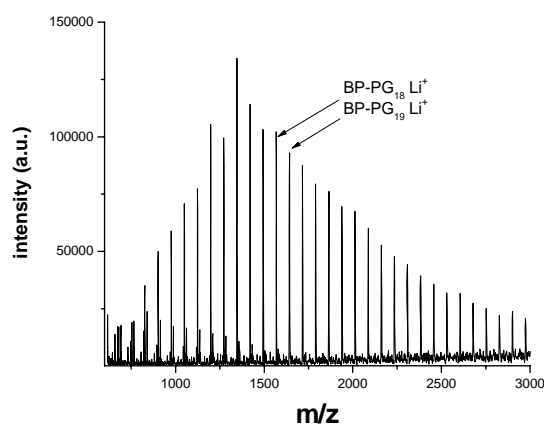


Figure 7. MALDI-ToF mass spectrum of hyperbranched polyglycerols with 2,2',4,4'-tetrahydroxybenzophenone BP-PG₈₀.

The MALDI-ToF mass spectrum presented in **Figure 7** confirms the attachment of the benzophenone to the hyperbranched polyglycerol. Masses corresponding to non-cored homopolymers were not detected. Thus, quantitative incorporation of the core is achieved.

Table 5. Photophysical parameters of the hyperbranched polyethers containing a benzophenone core, recorded at the same absorption value (Abs= 0.3) of the prepared solutions at 298K. All wavelengths are ± 0.5 nm. [a] from ^1H NMR calculations; [b] from SEC; [c] branching effect known in the case of dendrimers as “dendritic effect” is calculated for the same solvent as follows: $\Delta\lambda$ (nm)= $\lambda_{\text{max}}(\text{BP}-(\text{PG}-\text{Ac})_{113})-\lambda_{\text{max}}(\text{BP}(\text{OMe})_4)$; [d] the same branching effect is calculated for emission data: $\Delta\lambda$ (nm)= $\lambda_{\text{em}}(\text{BP}-(\text{PG}-\text{Ac})_{113})-\lambda_{\text{em}}(\text{BP}(\text{OMe})_4)$; [e] values used for the branching effect $\Delta\lambda$ (nm) determination.

	\overline{M}_n ^[a] ($g \cdot mol^{-1}$)	$\overline{M}_w / \overline{M}_n$ ^[b]	CH ₃ CN	CH ₃ OH		ϕ_f
			λ_{max} ^[c] (nm)	λ_{max} ^[c] (nm)	λ_{emi} ^[d] (nm)	
BP(OMe) ₄	302	1	308	311 ^[e]	480 ^[e]	0.004
BP-PG ₂₁	1,520	1.5	-	310	468	0.01
BP-(PG-Ac) ₂₁	2,120	-	304	310	455	0.01
BP-PG ₈₀	5,850	1.8	-	309	454	0.02
BP-(PG-Ac) ₈₀	8,874	-	303	309	447	0.02
BP-PG ₁₁₃	8,340	2	-	307	451	0.03
BP-(PG-Ac) ₁₁₃	12,908	-	302	307 ^[e]	436 ^[e]	0.03

The UV-vis spectra of these new hyperbranched polyglycerols containing benzophenone as a core have been recorded in two solvents with different polarity, i.e., methanol and acetonitrile. It is well known that environmental polarity is important in controlling red or blue-shifts of the benzophenone chromophore (S_1 : n, π^* configuration). The UV-vis spectra of the single alkylated chromophore (model compound) and the hyperbranched polymers are shown in **Figure 8**, and the absorption maxima for the solvatochromic chromophore are listed in **Table 5**. In the absorption spectra of the model chromophore BP(OMe)₄³⁰ and hyperbranched polymers BP-PG₂₁, BP-PG₈₀ and BP-PG₁₁₃ as well as their acetylated derivatives BP-(PG-Ac)₂₁, BP-(PG-Ac)₈₀ and BP-(PG-Ac)₁₁₃ in methanol, two pronounced and distinct bands in the UV region (278 and 310 nm), are observed. A slight blue shift (ca. -4 nm) was detected for the UV-vis spectra of the obtained polymers in comparison with the simple tetraalkoxy core. The measurements recorded in a less polar solvent (i.e. CH₃CN) showed a small blue shift of up to -6 nm for BP-(PG-Ac)₂₁, BP-(PG-Ac)₈₀ and BP-(PG-Ac)₁₁₃ (302 nm), as compared to 2,2',4,4'-tetramethoxybenzophenone (308 nm). Absorption maxima and molar extinction

coefficients increase with the molecular weight of the hyperbranched structure. The absence of a drastic influence on the absorption spectra of the benzophenone core can be attributed to the rather open structure of the hyperbranched macromolecules in polar solvents (i.e CH₃OH, CH₃CN). This prevents close contact of the branches with the benzophenone core.

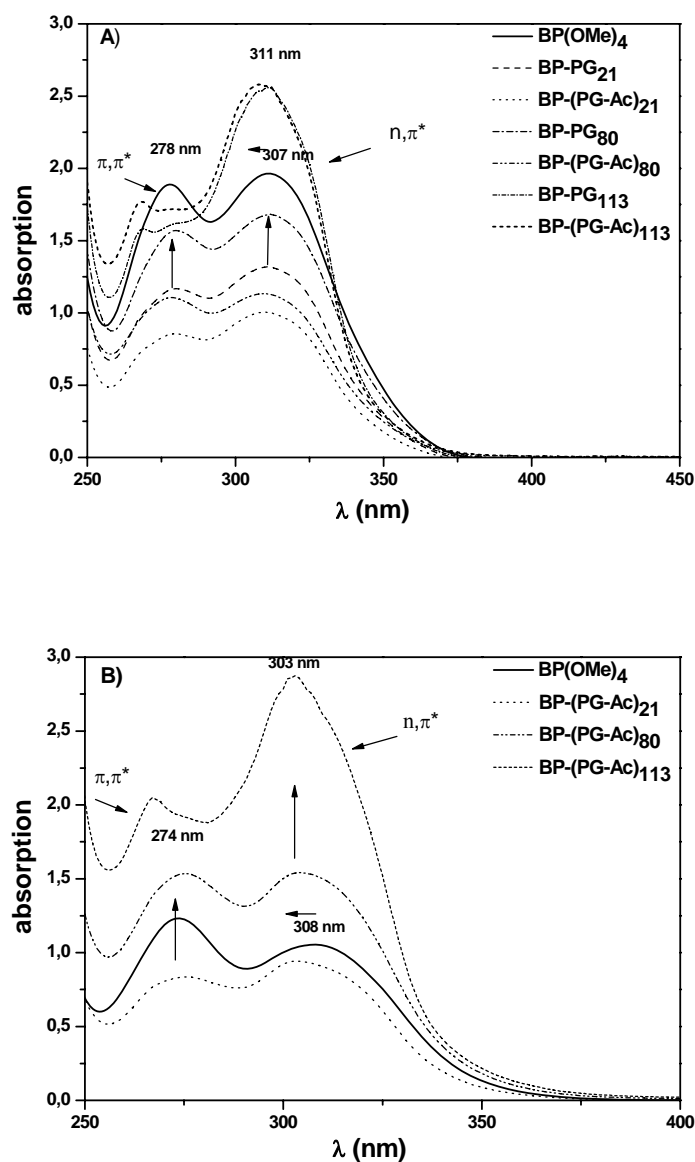


Figure 8. UV-vis spectra of hyperbranched polyglycerols containing benzophenone core normalized to [BP]= 10⁻⁴M at 298K: in methanol (*top*) and in acetonitrile (*bottom*).

The fluorescence spectra of BP(OMe)₄ and hyperbranched polymers BP-PG₂₁, BP-PG₈₀ and BP-PG₁₁₃ as well as the acetylated derivatives BP-(PG-Ac)₂₁, BP-(PG-Ac)₈₀ and BP-(PG-Ac)₁₁₃ were obtained upon excitation of the benzophenone core at 355

nm in methanol. For systematic comparison of the emission response to the excitation wavelength, all samples were prepared in such a manner that the photoactive chromophore absorbs the same energy (i.e. $Abs_{355}(BP) = 0.3$). The emission spectra are displayed in **Figure 9**, and the emission maxima as well their respective quantum yields are presented in **Table 5**. Strikingly, an increase of the emission intensity was observed upon increase of the molecular weight (comparison with the weak fluorescence displayed by the simple model 2,2',4,4'-tetramethoxybenzophenone). The emission spectra of the high molecular weight hyperbranched polymer BP-(PG-Ac)₁₁₃, display a negative blue shift (436 nm) compared to the emission of the parent benzophenone (480 nm). A strong increase of the fluorescence intensity of the benzophenone core at the emission maximum is observed with increasing molecular weight of the hyperbranched polymer. The quantum yield of the fluorescence (Φ_f) of the hyperbranched polymers (298K) is lower than 0.03. These values are similar to those obtained for amphiphilic polar aliphatic polyester-based dendrimers containing a benzophenone core, reported recently by Fréchet and Hecht²³ and photophysically studied by Shiraishi et al.³¹ The limited solubility of the prepared hyperbranched polymers in apolar solvents such as cyclohexane, did not permit a detailed analysis of the behavior in solvents with different polarity. However, a clear “dendritic effect” was observed in the fluorescence intensities and quantum yield of the encapsulated benzophenone compared with the methylated BP(OMe)₄ model compound.

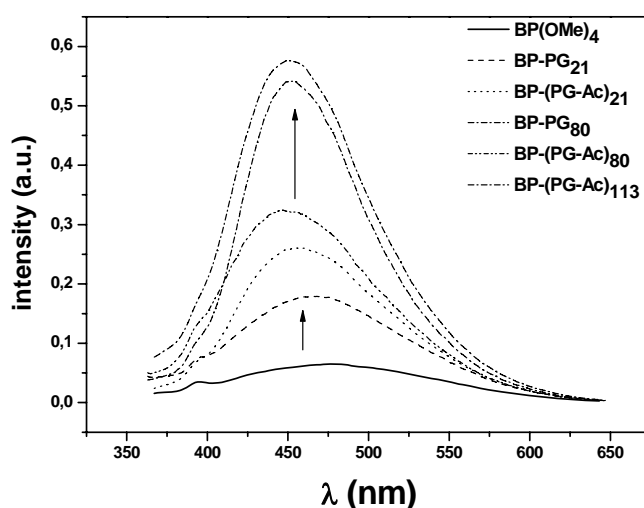


Figure 9. Fluorescence emission spectra at excitation wavelength $\lambda_{exc} = 355$ nm of hyperbranched polyglycerols containing benzophenone core in methanol, normalized at $Abs_{355}(BP) = 0.3$.

4.4. Conclusion

Hyperbranched polyglycerols with different initiator-cores have been prepared both directly from amine-terminated compounds and from bisglycidolized amines in order to compare both methods with respect to molecular weights and polydispersity of the hyperbranched products. Various *n*-alkyl amines (mono- and bifunctional) and photoactive cores (benzylamine and 1-naphthylmethylamine) were used to establish a simple method. ¹H NMR spectra and size exclusion chromatography (SEC) elugrams show improved control over the molecular weights, when using the bisglycidolized amines vs. the unmodified amines. Molecular weights and polydispersity of the hyperbranched polyglycerols prepared with these initiator-cores were in the range of 1,600 to 8,400 g·mol⁻¹ and of 1.5 to 2.5, respectively. Via MALDI-ToF mass spectrometry the presence of hyperbranched polymers containing an initiator-core and cycles of homopolymers was confirmed for the hyperbranched polyglycerols prepared directly with the amine initiator-cores. In the case of the materials with bisglycidolized core-initiators no core-less homopolymer fraction was detected.

UV-visible, steady state and time-resolved fluorescence spectroscopy as well as pH-dependent fluorescence have been applied to confirm the of the naphthalene probe and to determine the influence of the surrounding hyperbranched polyether polyols on the optical and electronic properties of the naphthalene core. A slight red shift and pronounced hypochromic shift in the hyperbranched UV-spectra compared with the low molecular weight model compound BP(OMe)₄ have been observed. No electronic interactions between the polyglycerol branches and naphthalene occurred in the ground state. Fluorescence spectroscopy indicates the formation of relative compact structure with a possible hydrophobic pocket for the naphthalene, inaccessible for hydrogen-donor solvents. Access of hydrogen-solvents to the core increases the fluorescence emission of the probe due to hydrogen interaction with amine electrons. At acidic pH, the fluorescence emission of the hyperbranched polymers increased strongly, pointing at rigid and compact structures.

In addition to these experiments a tetrahydroxy benzophenone was also employed as core-initiator. The hyperbranched polyglycerol containing benzophenone were characterized with respect to molecular weights and molecular weight distribution. The samples show relatively narrow polydispersity (1.5 < PDI < 2) for a range of molecular weights from 1,500 to 8,300 g·mol⁻¹. UV-vis experiments support the

adoption of an open structure of the hyperbranched macromolecules in polar solvents. This appears to prevent close contact of the branches with the benzophenone core. However, it is a striking observation that the fluorescence shows a clear “dendritic effect” with respect to the fluorescence intensities and quantum yields of the encapsulated benzophenone compared with the low molecular model compound. These first results are very promising, since the hyperbranched polymers with a benzophenone core exhibits analogous properties as upon incorporation into a perfectly branched dendrimer structure.

4.5. Experimental part

4.5.1. Materials with amines as initiator-cores

Materials. n-Hexylamine (HA), 1,6-hexyldiamine (HDA), n-dodecylamine (DA), 1,12-dodecyldiamine (DA), benzylamine (BA) and 1-naphthylmethylamine (NMA) were purchased from Acros. Dichloromethane, acetone, methanol and *tert*-butoxide were used as received from Fluka. THF and diglyme were obtained from Fluka and distilled over sodium prior to use.

Initiator-cores preparation. All amines except NMA were all purified prior to use via recrystallization or distillation. The bisglycidolization was carried out under normal atmosphere by adding 2 equivalents of distilled glycidol to the amine dissolved in dichloromethane at room temperature and stirred for 4 additional hours. After completion of the reaction dichloromethane was removed.

Polymerizations with amines initiator-core. Polymerizations were carried out according to the literature⁶ via slow monomer addition onto the core-initiator. The core-initiators were 10%-deprotonated using potassium *tert*-butoxide and were used directly for the polymerization. After completion of the addition the polymer was dissolved in methanol and precipitated twice in acetone. The precipitated polymer was dried in vacuum at 80°C for 2 days. The acetone/methanol fraction was evaporated and the isolated product was dried as described above. The different products obtained were characterized.

¹H NMR of the materials (300 MHz, d₄-methanol, 25°C):

n-Hexylamine-PG: $\delta = 3.9\text{-}3.3$ ppm (CH₃(CH₂)₄CH₂N-**PG**), 2.6 ppm (CH₃(CH₂)₄**CH₂**N-PG), 1.4-1.2 ppm (CH₃(**CH₂**)₄CH₂N-PG), 0.9 ppm (**CH₃**(CH₂)₄CH₂N-PG).

1,6-Hexyldiamine-PG: $\delta = 3.9\text{-}3.3$ ppm (**PG**-NCH₂(CH₂)₄CH₂N-**PG**), 2.6 ppm (PG-N**CH₂**(CH₂)₄**CH₂**N-PG), 1.4-1.2 ppm (PG-NCH₂(**CH₂**)₄CH₂N-PG).

n-Dodecylamine-PG: $\delta = 3.9\text{-}3.3$ ppm (CH₃(CH₂)₁₀CH₂N-**PG**), 2.6 ppm (CH₃(**CH₂**)₁₀CH₂N-PG), 1.4-1.2 ppm (CH₃(**CH₂**)₁₀CH₂N-PG), 0.9 ppm (**CH₃**(CH₂)₁₀CH₂N-PG).

1,12-Dodecyldiamine-PG: $\delta = 3.9\text{-}3.3$ ppm (**PG**-NCH₂(CH₂)₁₀CH₂N-**PG**), 2.6 ppm (PG-N**CH₂**(CH₂)₁₀**CH₂**N-PG), 1.4-1.2 ppm (PG-NCH₂(**CH₂**)₁₀CH₂N-PG).

Benzylamine-PG: $\delta = 7.1\text{-}7.3$ ppm (C₆**H₅**CH₂N-PG), 3.9-3.3 ppm (**PG**-N**CH₂**(CH₂)₁₀CH₂N-**PG**).

1-Naphthylmethylamine-PG: $\delta = 8.3, 7.9, 7.5$ ppm (**C₁₀H₇**-CH₂-PG) 3.9-3.3 ppm (C₁₀H₇-**CH₂**-**PG**).

4.5.2. Materials with benzophenone as initiator-cores

Materials. 2,2',4,4'-tetrahydroxybenzophenone, acetic anhydride and chloroform were purchased from Acros Organics. The rest of the chemicals are the same as in section 4.5.1.

Polymerizations with benzophenone. Polymerizations were carried out according to literature via slow monomer addition onto the 2,2',4,4'-tetrahydroxybenzophenone (purchased by Acros Organics). The core-initiator was 20%-deprotonated using potassium *tert*-butoxide and was used directly for the polymerization. After completion of the addition the polymer was dissolved in acetone and precipitated twice in acetone. The precipitated polymer was dried in vacuum at 80°C for 2 days. The acetone/methanol fraction was evaporated and the isolated rest was dried as described above. The different products were characterized.

Acetylation of the hyperbranched polyglycerol. BP-PG₂₁, BP-PG₈₀ or BP-PG₁₁₃ was mixed with acetic anhydride (6 eq. relative to the hydroxyl groups of PG). The

mixture was stirred at 120°C for 6h. After removing most of the volatile under vacuum, the residual was dissolved in 100 ml of chloroform. Around 50 ml of 10% NaOH aq. was added to the solution. The mixture was stirred violently at room temperature for 1-2h. After separating the two phases, the organic phase was washed twice by 10% NaOH aq. and several times by water until the pH=7. The organic phase was dried by anhydrous Na₂SO₄. After removing the volatile, the residue was kept at 60°C in vacuum oven overnight. The fully acetylated BP-PG (BP-(PG-Ac)₂₁, BP-(PG-Ac)₈₀ and BP-(PG-Ac)₁₁₃) was obtained.

¹H NMR (300MHz, 25 °C):

Benzophenone-PG: (d₄-methanol) δ = 7.3, 7.2 and 6.4 ppm (d, s, d benzophenone core), 3.7-3.3 ppm (m, -**CH₂CHO**-(**CH₂O**-) hyperbranched polyglycerol).

Acetylated benzophenone-PG: (d₃-chloroform) δ = 7.3, 7.2 and 6.4 ppm (d, s, d benzophenone core), 5 ppm (m, -**CH**-(O-C=O-CH₃))(CH₂-O-C=O-CH₃), 4-4.5 ppm (m, -CH-(O-C=O-CH₃))(**CH₂**-O-C=O-CH₃)) acetylated hyperbranched polyglycerol), 3.25-3.75 ppm (m, -**CH₂CHO**-(**CH₂O**-) acetylated hyperbranched polyglycerol backbone), 2 ppm (m, -CH-(O-C=O-**CH₃**))(CH₂-O-C=O-**CH₃**)) acetylated hyperbranched polyglycerol).

4.6. References

- (1) Flory, P. J. *J. Am. Chem. Soc.* **1952**, *74*, 2718.
- (2) Gao, C.; Yan, D. *Prog. Polym. Sci.* **2004**, *29*, 183.
- (3) Hawker, C. J.; Wooley, K. L.; Fréchet, J. M. J. *J. Am. Chem. Soc.* **1993**, *115*, 4375.
- (4) Bhyrappa, P.; Young, J. K.; Moore, J. S.; Suslick, K. *J. Am. Chem. Soc.* **1996**, *118*, 5708.
- (5) Vestberg, R.; Nyström, A.; Lindgren, M.; Malmström, E.; Hult, A. *Chem. Mater.* **2004**, *16*, 2794.
- (6) Bernal, D. P.; Bedrossian, L.; Collins, K.; Fossum, E. *Macromolecules* **2003**, *36*, 333.
- (7) Hua, J. L.; Li, B.; Meng, F. S.; Ding, F.; Qian, S. X.; Tian, H. *Polymer* **2004**, *45*, 7143.

- (8) Gittins, P. J.; Alston, J.; Ge, Y.; Twyman, L. J. *Macromolecules* **2004**, *37*, 7428.
- (9) Gittins, P. J.; Twyman, L. J. *J. Am. Chem. Soc.* **2005**, *127*, 1646.
- (10) Burgath, A.; Sunder, A.; Frey, H. *Macromol. Chem. Phys.* **2000**, *201*, 782.
- (11) Žagar, E.; Žigon, M. *Macromolecules* **2002**, *35*, 9913.
- (12) Sunder, A.; Hanselmann, R.; Frey, H.; Mülhaupt, R. *Macromolecules* **1999**, *32*, 4240.
- (13) Istratov, V.; Kautz, H.; Kim, Y.-K.; Schubert, R.; Frey, H. *Tetrahedron* **2003**, *59*, 4017.
- (14) Nieberle, J.; Frey, H. *Manuscript in preparation* **2005**.
- (15) Gooden, J. K.; Gross, M. L.; Mueller, A.; Stefanescu, A. D.; Wooley, K. L. *J. Am. Chem. Soc.* **1998**, *120*, 10180.
- (16) Clausnitzer, C.; Voit, B.; Komber, H.; Voigt, D. *Macromolecules* **2003**, *36*, 7065.
- (17) Cai, X.; Hara, M.; Kawai, K.; Tojo, S.; Majima, T. *Chem. Commun.* **2003**, *2*, 222.
- (18) Negri, F.; Zgierski, M. Z. *J. Chem. Phys.* **1997**, *107*, 4827.
- (19) Pina, F.; Lima, J. C.; Lodeiro, C.; Seixas de Melo, J.; Díaz, P.; Albelda, M. T.; García-Espana, E. *J. Chem. Phys. A* **2002**, *106*, 8207.
- (20) Albelda, M. T.; García-Espana, E.; Gil, L.; Lima, J. C.; Lodeiro, C.; Seixas de Melo, J.; Melo, M. J.; Parola, A. J.; Pina, F.; Soriano, C. *J. Chem. Phys. B* **2003**, *107*, 6573.
- (21) Turro, N. J. *Modern Molecular Photochemistry*; University Science Books: Sausalito, CA, 1999.
- (22) Balzani, V.; Campagna, S.; Denti, G.; Juris, A.; Serroni, S.; Venturi, M. *Acc. Chem. Res.* **1998**, *31*, 26.
- (23) Hecht, S.; Fréchet, J. M. J. *Angew. Chem. Int. Ed.* **2001**, *40*, 74.
- (24) Devadoos, C.; Bharathi, P.; Moore, J. S. *J. Am. Chem. Soc.* **1996**, *118*, 9635.
- (25) Wang, B.-B.; Zhang, X.; Jia, X.-R.; Li, Z.-C.; Ji, Y.; Yang, L.; Wei, Y. *J. Am. Chem. Soc.* **2004**, *126*, 15180.
- (26) Baker, L. A.; Crooks, R. M. *Macromolecules* **2000**, *33*, 9034.
- (27) Valeur, B. *Molecular Fluorescence Principles and Applications*; Wiley-VCH: Weinheim, 2002.
- (28) Smith, D. K.; Müller, L. *Chem. Commun.* **1999**, 1915.

- (29) Koenig, S.; Müller, L.; Smith, D. K. *Chem. Eur. J.* **2001**, *7*, 979.
- (30) Pastor Pérez, L.; University of Valencia, 2005.
- (31) Shiraishi, Y.; Kooizumi, H.; Hirai, T. *J. Phys. Chem. B* **2005**, *109*, 8580.

5. Syntheses of linear-hyperbranched amphiphilic block copolymers

5.1. Introduction

Amphiphilic block copolymers offer promising potential with respect to the formation of supramolecular structures in solution^{1,2} that may serve e.g., as nanoreactors or templates for nanometer size objects.³ Also their interfacial properties can be exploited, e.g., for the preparation of organic/inorganic hybrid structures, in biomineralization as well as for materials with novel optic, magnetic and catalytic properties. Excellent recent reviews describe the enormous potential in this field.^{4,5}

Although a large variety of linear amphiphilic AB-diblock copolymer architectures has been reported, to date only limited efforts have been described that aim at linear-dendritic architectures with amphiphilic structure. In these works, a linear chain is combined with a dendrimer block, as summarized in a recent review.⁶ Various reports have detailed the divergent construction of polar dendron blocks on a suitably reactive chain end. For instance, Meijer et al. reported an elegant synthesis of poly(styrene)-*b*-poly(propylene imine) (PS-*b*-PPI) linear-dendrimer architectures that were quaternized to afford an amphiphilic block copolymer.^{7,8} Fréchet, Gitsov et al. pioneered the coupling of an apolar poly(benzyl ether) (PBE) dendrimer block with a polar, linear poly(ethylene oxide) (PEO) chain⁹ as well as the design of dendrimers as macroinitiators for a linear block.¹⁰ However, the use of perfect dendrimers as building blocks necessitates demanding multistep-syntheses, affords limited quantities of the final material and also limits the molecular weights of the dendritic block to the respective dendrimer generations. Therefore, the development of synthetic strategies for the preparation of amphiphilic linear-dendritic architectures with somewhat lower structural perfection, yet narrow molecular weight distribution represents an important challenge.

The synthesis of hyperbranched polymers based on multifunctional AB_m-type polycondensation has long been known to lead to materials with high polydispersity and uncontrolled molecular weights and is unsuitable for the construction of well-defined blocks.¹¹ However, calculations by Müller et al.¹² as well as simulation results by Frey et al.¹³ demonstrated that slow addition of highly reactive monomers to

suitable core molecules leads to pseudo chain growth conditions and thereby permits to circumvent the theoretical limitations of multifunctional polycondensation. The concept has been verified by the synthesis of polyglycerols (PG) of narrow polydispersity¹⁴ as well as by the preparation of well-defined poly(phenylacetylene) in elegant work by Moore and coworkers.¹⁵

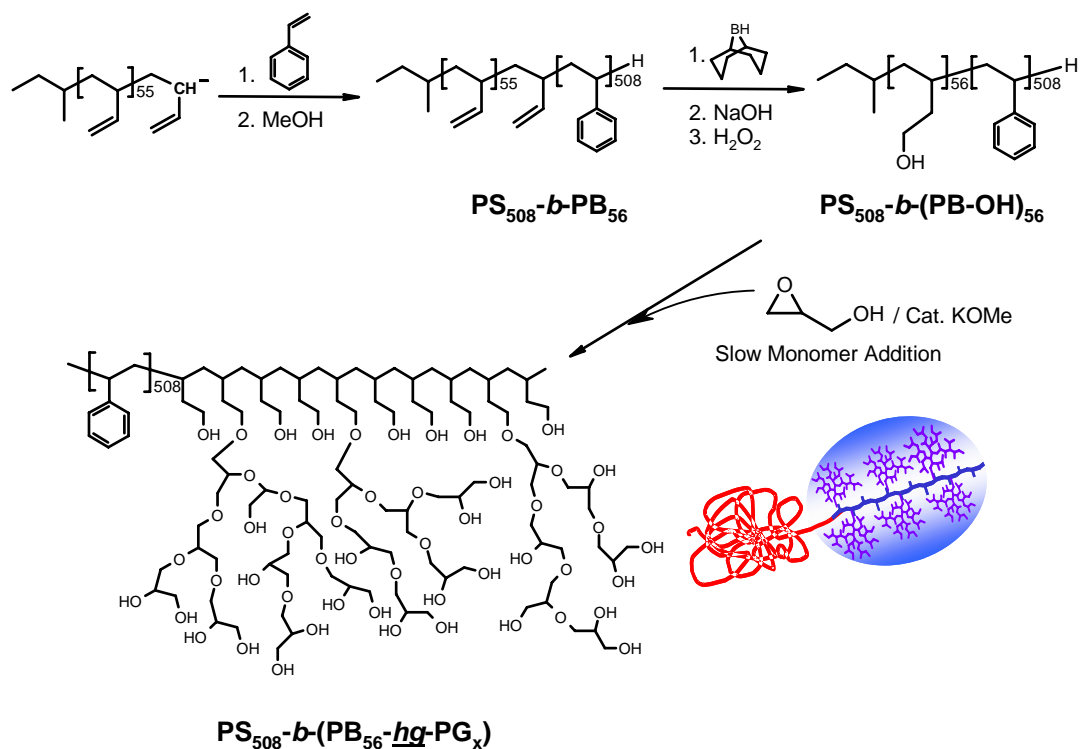
A first account of a general strategy permitting the preparation of linear-hyperbranched diblock copolymers was given in 2002.¹⁶ The concept is based on a well-defined linear AB-diblock copolymer with a short, polyfunctional B-block that represents a macroinitiator for AB₂-type monomers. In a post-polymerization grafting step, by controlled growth of the hyperbranched structure (slow monomer addition) onto the macroinitiator segment, a narrow polydispersity hyperbranched polymer block is formed. It is important to note that the mere presence of one functional group at the chain end would result both in insufficient attachment of the hyperbranched structure to the linear chain as well as a lack of control, resulting in increased polydispersity.¹³ The basic principle has been demonstrated in a first example by the preparation of poly(styrene)-*b*-hb-polycarbosilane block copolymer.¹⁷ Linear-hyperbranched structures with a linear poly(propylene oxide) (PPO) block and a hyperbranched polyglycerol segment have recently been described on the basis of a bisglycidolized, tetra-hydroxy functional PPO-amine.¹⁸

In this chapter, a general synthetic concept will be described for a novel type of well-defined amphiphilic block copolymer with a linear apolar chain and a hydrophilic hyperbranched polyglycerol block.

5.2. Polystyrene-*block*-(1,2-polybutadiene-hypergrafted-polyglycerol)

The general synthetic strategy employed for this work is shown in **Scheme 1**. The linear block copolymer macroinitiator PS₅₀₈-*b*-(PB-OH)₅₆ (PS = polystyrene, PB-OH = hydroxylated 1,2-polybutadiene, poly(hydroxyethyl)ethylene) used in this work for the synthesis of the linear-hyperbranched block copolymers has been prepared by anionic polymerization and subsequent hydroboration, as described by Gronski and coworkers.^{19,20} Obviously, narrow polydispersity of the linear AB-diblock copolymer PS₅₀₈-*b*-(PB-OH)₅₆ is an important prerequisite. The block copolymer macroinitiator exhibits a polydispersity of 1.01. Control of the fraction of desired 1,2-incorporation

in the polybutadiene block was achieved by the use of dipiperidinoethane (DPE) as mediator in the polymerization and by solvent variation and strict temperature control. In this manner, the fraction of undesired 1,4-structures was less than 3 % ($^1\text{H NMR}$). In a second step, hydroboration was employed to convert the vinyl groups fully to 2-hydroxyethyl structures.¹⁹ The reaction leads to full conversion under mild conditions.



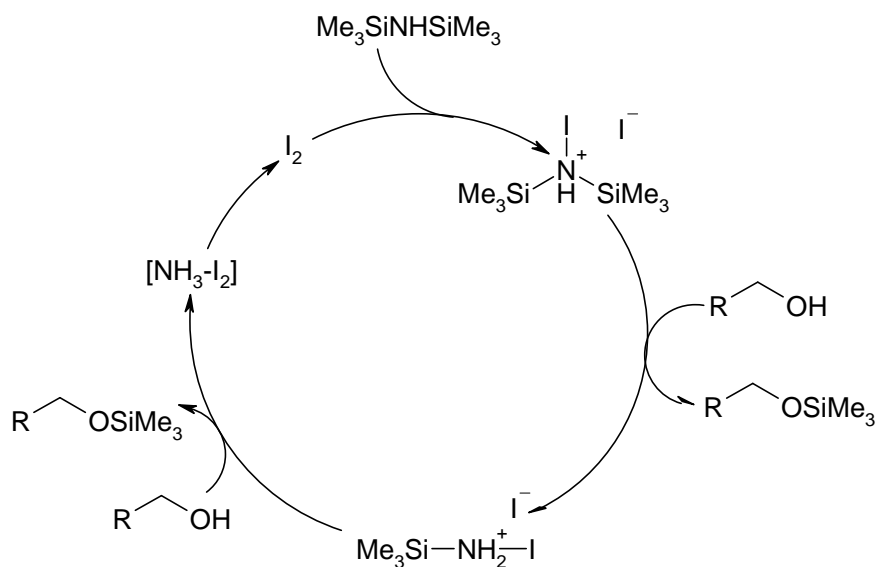
Scheme 1. Synthetic strategy for the preparation of PS₅₀₈-b-(PB₅₆-hg-PG_x).

Subsequent grafting of the hyperbranched polyglycerol structure from the hydroxylated PB-block was achieved in analogy to the synthesis of hyperbranched polyglycerol homopolymers.¹⁴ The PS₅₀₈-b-(PB-OH)₅₆ was dissolved in diglyme and deprotonated to an extent of 10 %. Subsequently, glycidol was slowly added via a syringe pump in the course of 2-3 hours. The amount of glycidol depended on the desired size of the hyperbranched polyglycerol block.

During the polymerization the reaction mixture remained homogeneous at all times for short polyglycerol blocks. Interestingly, when a larger block of polyglycerol was hypergrafted (*hg*), a turbid appearance of the reaction mixture could be observed at the end of the polymerization. After completion of the polymerization, solvents were removed and the crude product was analyzed. Size exclusion chromatography (SEC) traces revealed the presence of a minor low molecular weight fraction and a major high molecular weight product. The crude product was redissolved and precipitated

twice into methanol. The high molecular weight fraction isolated after precipitation i.e., the linear-hyperbranched block copolymer was obtained either as a white, solid powder or as a rubbery material, clearly depending on the molecular weight of the hyperbranched, flexible polyglycerol block. In the following text, PS₅₀₈-*b*-(PB₅₆-*hg*-PG_x) will be employed to designate the linear-hyperbranched block copolymers. The methanol-soluble fraction was dried, and a low viscosity, transparent product in a rather small quantity was isolated.

Based on theory,¹⁴ one expects a narrow molecular weight distribution for the block copolymers, since slow monomer addition conditions are used. In addition, there are ca. 60 potential initiator groups for the hypergrafted structure per macromolecule, leading to the control of the molecular weight distributions of the branched side chains. As it is common for amphiphilic block copolymers, SEC measurements of the materials in chloroform revealed strong aggregation. The main distribution mode found at molecular weights of 10⁶ g·mol⁻¹ in the case of the sample PS₅₀₈-*b*-(PB₅₆-*hg*-PG₈₆), for instance, is clearly due to aggregates. In order to obtain reliable information on the actual molecular weight distribution, the polymer samples were persilylated with hexamethyldisilazane, applying an efficient silylation method recently published by Karimi and Golshani as illustrated in **Scheme 2**.²¹



Scheme 2. General Procedure for silylation of alcohols using hexamethyldisilazane (HMDS) catalyzed with I_2 .

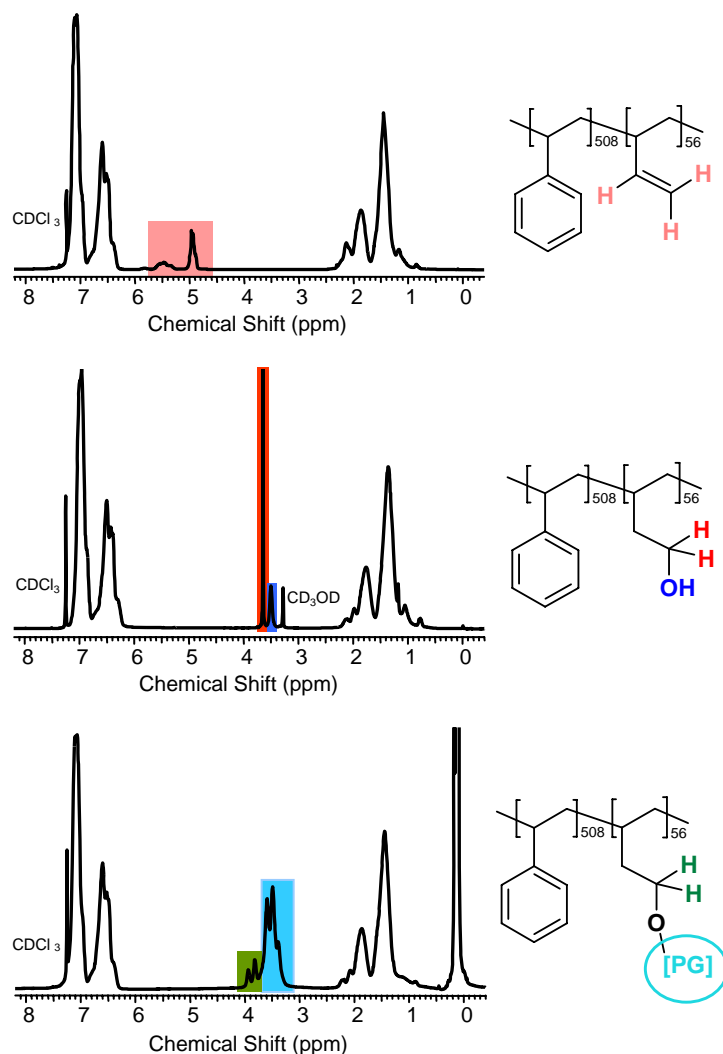


Figure 1. ^1H NMR-spectra in CDCl_3 of $\text{PS}_{508}\text{-}b\text{-PB}_{56}$ (top), $\text{PS}_{508}\text{-}b\text{-}(\text{PB-OH})_{56}$ employed as macroinitiator (middle); persilylated $\text{PS}_{508}\text{-}b\text{-}(\text{PB}_{56}\text{-hg-PG}_{280})$ (bottom).

^1H NMR data (**Figure 1**) of the different samples evidence attachment of the hyperbranched polyglycerol block to the macroinitiator and permit to determine molecular weights by comparing the integral of the aromatic protons of the PS block and the protons of PG (subtracting the methylene protons of the PB-OH hydroxyethyl moiety).

The grafting efficiency, defined by the amount of glycidol grafted onto the block copolymer compared with the amount of glycidol added, has also been calculated from the NMR integrals. The values were in the range of 60-76 % and thus quite high compared with carbosilane monomers studied previously.²² The desired grafting of glycidol onto the block copolymer backbone competes with homopolymerization of glycidol and subsequent cyclization of the oligoglycerols formed, preventing attachment to the block copolymer. However, due to its good solubility in methanol,

the low molecular weight fraction could be conveniently separated from the grafted block copolymer. Detailed MALDI-ToF analysis showed that this low molecular weight fraction consisted of cyclic oligo- and polyglycerol homopolymer. Unfortunately, unreacted hydroxyl groups at the hydroxylated polybutadiene backbone can not be differentiated from the end groups of the hyperbranched polyglycerol block by NMR spectroscopy, rendering precise determination of the fraction of reacted backbone groups impossible.

Table 1: Characterization data of the macroinitiator and the linear-hyperbranched block copolymers. SEC and ^1H NMR were performed on persilylated samples. [a] Values from SEC include the TMS groups; [b] values in $\text{g}\cdot\text{mol}^{-1}$.

	SEC ^[a]		^1H NMR		
	$\overline{M}_n^{[b]}$	$\overline{M}_w / \overline{M}_n$	$\overline{M}_n^{[b]}$	wt. % PG	% Grafting
PS ₅₀₈ - <i>b</i> -PB ₅₆	56,790	1.01	52,873 (PS) 3,017 (PB)	-	-
PS ₅₀₈ - <i>b</i> -(PB-OH) ₅₆ ^[a]	52,900	1.01	56,840	-	-
PS ₅₀₈ - <i>b</i> -(PB ₅₆ - <i>hg</i> -PG ₄₄) ^[a]	56,000	1.02	60,100	5.4%	60%
PS ₅₀₈ - <i>b</i> -(PB ₅₆ - <i>hg</i> -PG ₈₆) ^[a]	56,760	1.02	63,140	10%	65%
PS ₅₀₈ - <i>b</i> -(PB ₅₆ - <i>hg</i> -PG ₂₈₀) ^[a]	70,700	1.02	77,580	27%	65%
PS ₅₀₈ - <i>b</i> -(PB ₅₆ - <i>hg</i> -PG ₈₄₀)	120,640	1.74	119,020	52%	76%

SEC measurements of the persilylated polymers showed extremely narrow apparent molecular weight distributions for all samples, as summarized in **Table 1**. Furthermore, the molecular weight increase with increasing amount of glycidol added is obvious from SEC results. It should be noted that the apparent molecular weights determined by SEC for the persilylated samples are strongly underestimated, even though the molecular weight values include the TMS groups. This is obvious from a comparison of SEC with NMR-data and is explained by the highly branched and therefore compact structure.

A sample with a very large hyperbranched block (52 wt. %) has also been prepared, PS₅₀₈-*b*-(PB₅₆-*hg*-PG₈₄₀). This material was not soluble in CHCl₃ any more, but in DMF. SEC investigation does not reveal any aggregation in DMF and an increase of the polydispersity was observed. However the polydispersity remained fairly low

(1.74), considering the molecular weight of the hyperbranched block. This result confirms that the strategy employed leads to well-defined architectures even at high molecular weight.

The hyperbranched block comprises dendritic, linear and terminal units due to the random structure. The degree of branching DB was defined theoretically for AB_m (m≥2) type monomers by Frey et al.^{23,24} D, L represent the relative abundance (%) of the dendritic, linear units, respectively.

$$DB = \frac{2D}{2D + L}$$

In this equation the formation of cycles during the polymerization is neglected. The DB is determined by NMR spectroscopy on the basis of low molecular weight model compounds, which possess similar structures to the linear, dendritic and terminal units present in the respective hyperbranched polymer. The DB is obtained by comparison of the intensity of the NMR signals.

The extent of branching in the case of hyperbranched polyglycerol can be determined by inverse gated (IG) ¹³C NMR spectroscopy.¹⁴ For the linear hyperbranched block copolymers the difficulty was to record spectra, where the PG block was visible due to first the high viscosity of the solution and the predominance of the polystyrene block. In **Figure 2** the ¹³C NMR in d₇-DMF (high boiling point solvent) of the sample with the highest weight fraction of the hyperbranched polyglycerol block (PS₅₀₈-*b*-(PB₅₆-*hg*-PG₈₄₀)) is shown. The signals at 124, 128 and 146 ppm correspond to the polystyrene block and at 42-44 and 60 ppm to the 1,2-polybutadiene block. The presence of the hyperbranched block (polyether polyol) can be evidenced by the signals between 64 and 81 ppm. An enlarged of the ¹³C NMR spectrum was obtained in the shift region of the hyperbranched polyglycerol block. The expected resonances corresponding to the different structural units (D, T, L₁₃, L₁₄) can be clearly discerned (**Figure 2**).

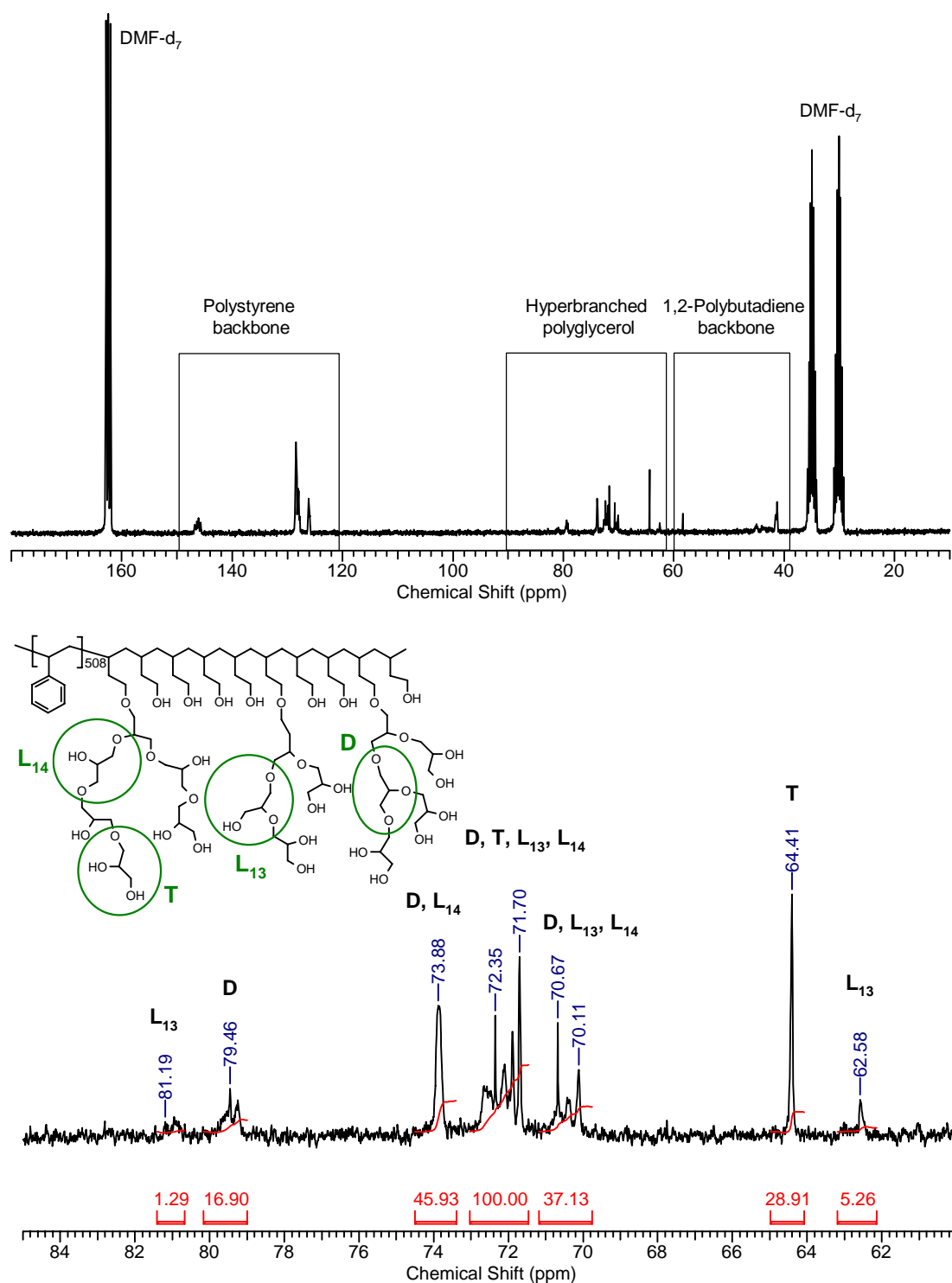


Figure 2. ^{13}C NMR inverse gated (IG) spectrum in DMF-d_7 of $\text{PS}_{508}\text{-}b\text{-}(\text{PB}_{56}\text{-}hg\text{-}\text{PG}_{840})$ (top) and zoom of the area between 60 and 85 ppm (bottom). D, L, T represent the dendritic, linear and terminal units.

From the integrals the relative abundance of the different structural units can be calculated (**Table 2**). The degree of branching calculated with the definition given above is 51%. This is comparable to the values obtained with hyperbranched

polyglycerol (53% to 59%). This is however below the theoretical value (66%) for an AB₂ monomer polymerization carried out in slow monomer addition mode.¹² On the other hand, the formation of dendritic units clearly confirms the expected hypergrafted structure.

Table 2: Interpretation of ¹³C NMR inverse-gated (IG) spectrum of PS₅₀₈-*b*-(PB₅₆-hg-PG₈₄₀): distribution of structural units.

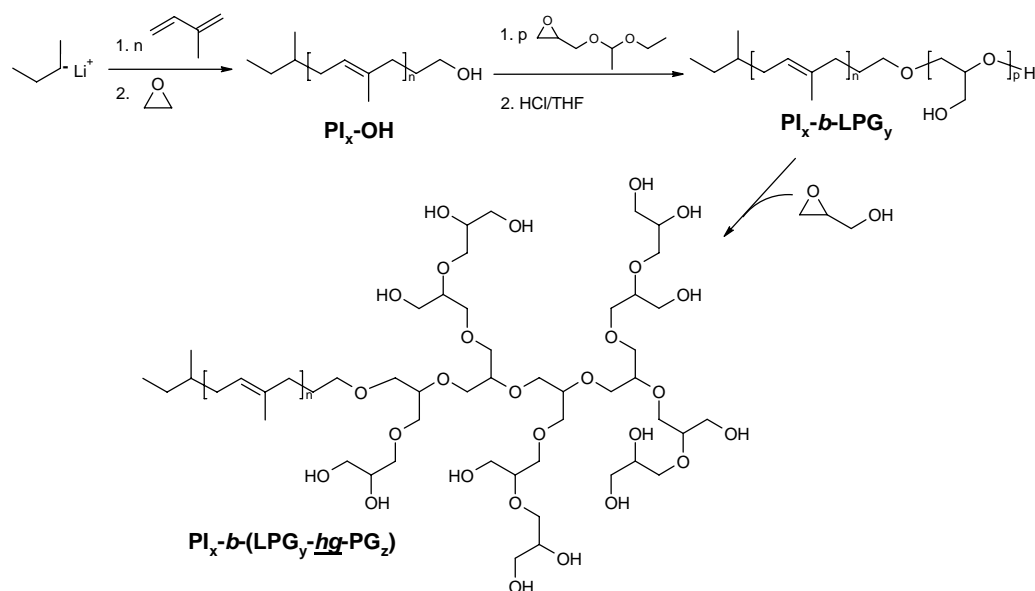
Structural unit	Relative abundance (%)
D	21.5%
T	36.8%
L ₁₃	6.7%
L ₁₄	34.9%

5.3. Polyisoprene-*block*-(hyperbranched-polyglycerol)

A series of amphiphilic block copolymers with a low glass transition temperature linear block (polyisoprene PI) has also been prepared, using a slightly modified strategy. The materials are liquid-like and their bulk morphology and their application for the preparation of silica inorganic-organic nanohybrids will be discussed later in chapter 7.

The hypergrafting technique illustrated above with the polystyrene-*block*-(1,2-polybutadiene-hypergrafted-polyglycerol) permits the synthesis of well-defined block copolymers. The short multifunctional block plays a key role in the control over the molecular weight. Indeed the initiator functionality is a crucial parameter, as it is also shown for bisglycidolized amines in chapter 4. In this first example a hydroxylated polybutadiene block was used as initiator block. It would be interesting, based on this strategy, to use a linear initiator block with the same chemical nature as the hyperbranched block. Linear polyglycerol (LPG) can be obtained via ring-opening polymerization of a glycidol protected with an acetal (ethoxy ethyl glycidyl ether) followed by cleavage of the protecting group under acidic conditions.^{25,26} The polymerization of the protected monomer can be initiated by an alkoxide and the molecular weight is limited to 15,000-20,000 g·mol⁻¹. A hydroxyl-terminated polyisoprene prepared via anionic polymerization was used as macroinitiator for the

polymerization of the protected glycidol monomer, as shown in **Scheme 3**. Polyisoprene was synthesized using *sec*-butyllithium as initiator and terminated by ethylene oxide. The polymer was carefully precipitated and dried prior to deprotonation with potassium hydride. The short linear PG-block was then grown onto polyisoprene via slow monomer addition of the protected glycidol. Deprotection was accomplished under acidic conditions.



Scheme 3. Synthetic strategy for the preparation of polyisoprene-*block*-(hyperbranched-polyglycerol) (PI_x-*b*-(LPG_y-hg-PG_z)).

The functionalized polyisoprene with the linear polyglycerol block (PI_x-*b*-LPG_y) was characterized by SEC and ¹H NMR. **Figure 4** shows the ¹H NMR spectrum of PI_x-*b*-LPG_y before and after deprotection. The signals of the polyisoprene are in the range of 4.6 to 5.8 ppm (protons of the double bonds) and from 0.84 to 2.2 ppm (methyl and methylene protons), respectively. The linear polyglycerol block resonances can be assigned from 3.3 to 3.6 ppm, and the protons corresponding to the acetal in the case of the protected block overlap with PI protons between 0.84 and 2.2 ppm. Therefore, after deprotection the integration value decreases in this area. The number average value of the molecular weight (\overline{M}_n) can be calculated by comparing the integration of the protons from the double bonds of PI and the integration of the PG protons, (subtracting the protons of the ethylene oxide unit). The molecular weight of PI was obtained from SEC, because the end groups are not visible for \overline{M}_n of 4,000 and 11,000 g·mol⁻¹. After hypergrafting of glycidol onto the linear polyglycerol block, the integrals were also compared and the molecular weight could be calculated.

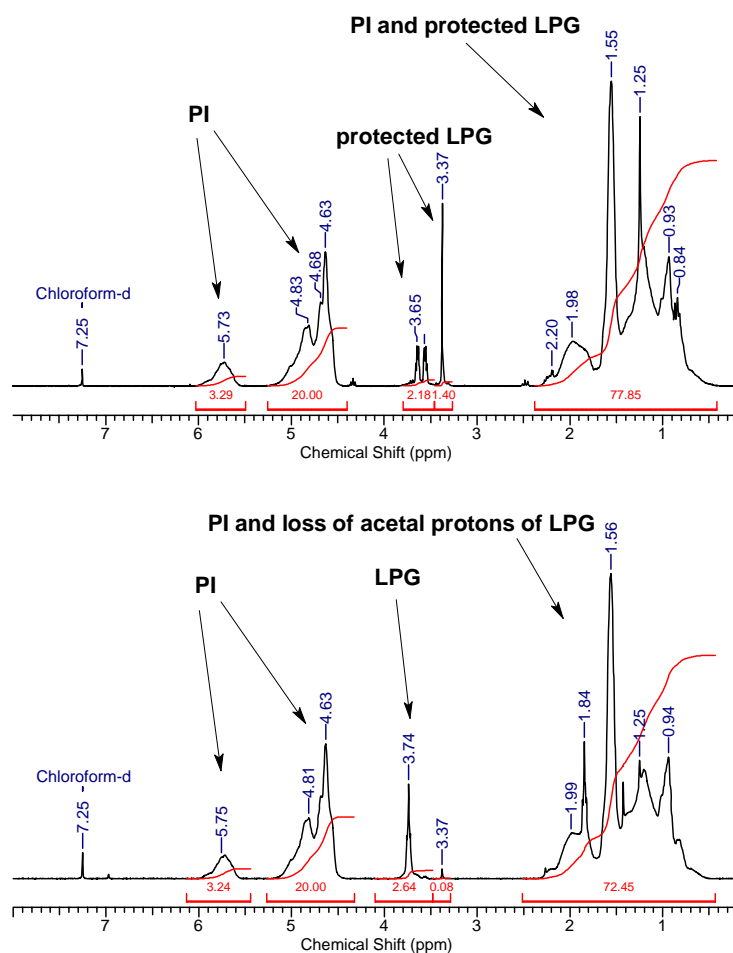


Figure 4. ¹H NMR spectra in CDCl₃ of (top) polyisoprene-*block*-(linear protected polyglycerol) (PI_x-*b*-(protected LPG)_y) and of (bottom) polyisoprene-*block*-(linear protected polyglycerol) (PI_x-*b*-LPG_y).

A series of samples with different block length of polyisoprene was prepared and characterized by SEC and ¹H NMR. The results are summarized in **Table 2**. PI samples with a degree of polymerization of 60 and 162, respectively, have been functionalized with linear polyglycerol. Compared with the polystyrene-containing block copolymers the linear initiator block is relatively small. The degree of polymerization of the linear polyglycerol block should not exceed 10% of the degree of polymerization of the linear PI block in order to prepare block copolymers with different amount of the hyperbranched block in the subsequent step. To this end, the hydroxyl-terminated PI was dissolved in THF and deprotonated with an excess of potassium hydride for at least one day. Then it was filtrated, placed in the reactor and protected glycidol was slowly added. The polydispersity stays narrow after functionalization with the short linear polyglycerol block (cf. **Table 2** PI₆₀-*b*-LPG₄ and PI₁₆₂-*b*-LPG₅). Polyglycerol homopolymer formed during the reaction was rinsed

off during the deprotection, because it stays soluble in the polar solvent, while the block copolymer was precipitated in it. The work-up for these materials was rendered difficult because they are liquid like due to the low glass transition temperatures of the both blocks. Therefore the block copolymers were precipitated in cold methanol and for some of them left at low temperature for an extended period of time before to be isolated.

The hyperbranched block was grown onto this macroinitiator as described above for PS-*b*-(PB-*hg*-PG). For a systematic study samples with a weight fraction of the polyglycerol block (linear and hyperbranched) of 10%, 20% and 30% have been prepared. Some aggregation could be seen in the SEC curves, and therefore the concentration was lowered for the measurements. Remarkably, the polydispersity of the linear-hyperbranched block copolymers remains below $\overline{M}_w / \overline{M}_n = 1.4$, which is reasonably well-defined for such a systems (cf. **Table 2**). The series of sample prepared with the macroinitiator PI₁₆₂-*b*-LPG₅ exhibits even lower polydispersity than the one prepared with PI₆₀-*b*-LPG₄. It is very illustrative to notice the effect of the small change of the functionality of the short initiator block. Together with the results presented above for the PS-*b*-(LPG-*hg*-PG) materials this is in agreement with the theoretical expectation of the polydispersity ($\overline{M}_w / \overline{M}_n = 1 + 1/f$, *f* being the initiator functionality). This is a strong validation of the relevance of the hypergrafting strategy for the preparation of well-defined hybrid block copolymers.

Table 2. Characterization data of the linear-hyperbranched block copolymers polyisoprene-*block*-(*hyperbranched*-polyglycerol). [a] PI_{*x*}-*b*-(LPG_{*y*}-*hg*-PG_{*z*}): *x*, *y* and *z* are the degrees of polymerization of the initial poly(isoprene); of the short linear polyglycerol block (LPG) used for the initiation of the ROMBP of glycidol; and of the *hypergrafted*-polyglycerol block (*hg*-PG) respectively; [b] values obtained from ¹H NMR; [c] values obtained from SEC.

Samples ^[a]	\overline{M}_n ^[b]	$\overline{M}_w / \overline{M}_n$ ^[c]	wt. % PG	% grafting
PI ₆₀ - <i>b</i> -LPG ₄	4,477	1.07	-	-
PI ₆₀ - <i>b</i> -(LPG ₄ - <i>hg</i> -PG ₄)	4,778	1.22	13%	50%
PI ₆₀ - <i>b</i> -(LPG ₄ - <i>hg</i> -PG ₁₀)	5,181	1.3	20%	51%
PI ₆₀ - <i>b</i> -(LPG ₄ - <i>hg</i> -PG ₁₉)	5,895	1.4	30%	51%
PI ₁₆₂ - <i>b</i> -LPG ₅	11,485	1.05	-	-
PI ₁₆₂ - <i>b</i> -(LPG ₅ - <i>hg</i> -PG ₁₅)	12,616	1.1	12%	55%
PI ₁₆₂ - <i>b</i> -(LPG ₅ - <i>hg</i> -PG ₄₀)	14,435	1.2	23%	55%
PI ₁₆₂ - <i>b</i> -(LPG ₅ - <i>hg</i> -PG ₅₉)	15,878	1.13	30%	56%

In **Table 2**, the grafting efficiency is also summarized. The values increase with the length of the initiator block (up to 4-5% between PI₆₀-*b*-LPG₄ and PI₁₆₂-*b*-LPG₅ sample series). The values are generally lower than for the polystyrene-based samples. This can be explained by the lower concentration of initiator groups at the start of the reaction and this is in good agreement with the observation made above on the crucial effect of the functionality of the macroinitiator on molecular weight control and molecular weight distribution. Unfortunately the degree of branching could not be calculated, because the signals (¹³C NMR) for the polyglycerol block were too weak (in the noise level). With higher molecular weight samples the signals are easier to observe (see section 5.2).

5.4. Conclusion

A convenient 3-step strategy has been developed for the preparation of well-defined amphiphilic, linear-hyperbranched block copolymers via hypergrafting. 2 different systems have been explored and synthetic pathways developed: (i) polystyrene-*block*-(1,2-polybutadiene-*hypergrafted*-polyglycerol) and (ii) polyisoprene-*block*-(*hyperbranched*-polyglycerol). The polystyrene-based materials described represent the first example of high molecular weight amphiphilic linear-dendritic block copolymers. The procedure is based on a combination of carbanionic polymerization with the alkoxide-based, controlled ring-opening multibranching polymerization of glycidol. The materials prepared exhibit narrow polydispersity over a wide range of molecular weights and compositions ($\overline{M}_w / \overline{M}_n = 1.1$ to 1.4). It should be emphasized, that in contrast to linear block copolymers the linear-hyperbranched block copolymers described here do not only exhibit polydispersity with respect to molecular weight. Even macromolecules possessing the same \overline{M}_n will be characterized by additional structural isomerism, i.e., broad structural variability, in pronounced contrast to linear-dendrimer block copolymers.

This strategy was extended to lower molecular weight amphiphilic block copolymers with polyisoprene as linear block. In a first step linear polyglycerol block as initiator block was grown at the end of the polyisoprene block. The diblock copolymer prepared has the advantage of possessing an initiator block with the same chemical

structure as the hyperbranched block hypergrafted subsequently. Materials with relatively narrow polydispersity and good molecular weight control could be prepared. Of course it is intriguing to study whether there is supramolecular order in solution and in bulk (chapters 6, 7).

These two examples show that the hypergrafting strategy is a versatile method. It is of interest to prepare ABA structures with this strategy, in which the A blocks will also possess a hyperbranched topology. This would be a perfect analogy to the so-called dumbbell triblock copolymers. Work in this direction is in progress.

5.5. Experimental part

5.5.1. Polystyrene-block-(1,2-polybutadiene-hypergrafted-polyglycerol)

Materials. For the preparation of the macroinitiator all solvents were used as commercial p.a. quality. Cyclohexane, THF purchased from Roth and styrene purchased from Aldrich were dried by conventional methods under argon and freshly distilled prior to use. 1,3-butadiene was pre-dried under vacuum in a brass tube integrated in the reactor equipment that contained molecular sieve and an external heating source of approx. 200 °C. The exact concentration of 1,3M *sec*-BuLi in hexane acquired from Fluka was determined by the Gilman procedure prior to use.²⁷ The indicator 4,5-methylenphenanthrene (MPT) and the ligand complex 1,2-dipiperidinoethane (DPE) were purchased from Aldrich and used without further purification. Methanol (high purity) purchased from Riedel de Haën was degassed several times under argon via the freeze-thaw method.

For the synthesis of the hyperbranched block, potassium methylate was purchased by Fluka. Glycidol (Degussa) was distilled prior to polymerization and kept under Argon. THF and diglyme were distilled from sodium; methanol was used without further purification. For the silylation 1,1,1,3,3,3-hexadimethylsilazane 98%, iodine and sodium disulfide were purchased by Acros. Dichloromethane was used as received.

Syntheses of the materials. The macroinitiator consisting of a linear poly(styrene) block and a linear hydroxylated 1,2-polybutadiene block was prepared as described by

Gronski et al.^{19,20} As described in the literature¹⁴, for the synthesis of hyperbranched polyglycerol homopolymers, the hyperbranched block was obtained by slow monomer addition. Polymerizations were carried out in a reactor equipped with a mechanical stirrer and a dosing pump placed under argon atmosphere. The macroinitiator containing 56 OH groups was 10% deprotonated with potassium methyllate. The activated macronitiator was dissolved in 20 ml Diglyme, heated up to 120 °C and placed in the reactor. The amount of macroinitiator was chosen according to the desired monomer/initiator ratio. Glycidol was dissolved in THF and was slowly added at 120 °C. After completion of the reaction the product was neutralized with a cationic-exchange resin, dried in a first step to characterize the crude product. Then the crude product was twice precipitated in cold methanol and dried for an extended period at 80 °C in vacuo. Yields: 70-80 %.

For further characterization the linear-hyperbranched block copolymers were persilylated according to an elegant synthesis reported by Karimi and Golshani²¹ using a disilazane compound in the presence of iodine. The reaction was followed by FT-IR until the disappearance of the OH-band. After completion of the silylation, the persilylated compound was purified by dialysis in chloroform for 3 days and then dried in vacuo at 80 °C.

¹H NMR (400 MHz, d₁-CDCl₃, 25 °C).

PS₅₀₈-b-PB₅₆: δ = 7.5-6.3 ppm (m, -C₆H₅ PS), 5.5 ppm (m, -CH=CH₂ PB), 4.95 ppm (q, -CH=CH₂ PB), 2.4-0.75 ppm (m, -CH₂-CH- PS and PB backbone).

PS₅₀₈-b-(PB-OH)₅₆: δ = 7.5-6.3 ppm (m, -C₆H₅ PS), 3.64 ppm (m, -CH₂-CH₂OH PB), 3.51 ppm (s, -CH₂CH₂OH PB), 2.4-0.75 ppm (m, -CH₂-CH- PS and PB backbone).

Persilylated PS₅₀₈-b-(PB₅₆-hg-PG_x): 7.5-6.3 ppm (m, -C₆H₅ PS), 3.94-3.82 ppm (m, -CH₂-CH₂-O-Si(CH₃)₃ PB; -CH₂-CH₂-O-[PG] PB), 3.7-3.3 ppm (m, -CH₂CHO-(CH₂O-) PG), 0.45-0 ppm (m, -CH₂CH₂OSi(CH₃)₃ PB and -O-Si(CH₃)₃ PG).

5.5.2. Polyisoprene-block-(hyperbranched-polyglycerol)

Materials. Prior to use THF from Acros was purified via cryo-transfer from a purple potassium/benzophenone solution and cyclohexane supplied Acros from a red living

polystyrene. Isoprene (Acros) was stored over CaH_2 until used. methanol, chloroform, and other common solvents or reagents were purchased from Acros and used as received. *sec*-butyllithium (1.6M, Acros) was used as received. The concentration of the initiator was determined by the Gilman procedure.²⁷ Ethylene oxide (EO) ($\geq 99.8\%$, Aldrich) was used without further purification. All degassing and cryo transfer procedures were done using liquid nitrogen. Potassium hydride suspended in oil was purchased by Acros and was rinsed several times with THF prior to use. Ethoxy ethyl glycidyl ether (acetal protected glycidol) was prepared according to literature.²⁵ For the synthesis of the hyperbranched block, potassium *tert*-butylate was purchased by Fluka. Glycidol (Degussa) was distilled prior to polymerization and kept under Argon. THF and diglyme were distilled from sodium; methanol was used without further purification.

Preparation of linear polyisoprene. The polymerization was performed in a 1l glass reactor containing a 100 ml flask with living PS (closed by a Teflon tap), a magnetic glass stirrer, a rubber septum. The glass reactor was connected to a high vacuum line (10^{-7} mbar) containing a graduated ampoule and the flasks with the solvents and reagents. The reactor was evacuated ($10^{-6} - 10^{-7}$ mbar) and rinsed with a living polystyrene solution via several cryo-transfer cycles procedures. Then a vacuum of $10^{-6} - 10^{-7}$ mbar was established and the graduated ampoule was flame dried with a heating gun. After cooling Isoprene (20 to 25 ml) was cryo-transferred into the graduated ampoule. Cyclohexane was placed into the reactor via cryo-transfer. For a typical polymerization the amount of solvent was chosen such that the monomer concentration was ca. 10% vol. The reactor was kept under liquid nitrogen and the solvents in the reactor were degassed under vacuum ($10^{-6} - 10^{-7}$ mbar) for at least 30 minutes. The reactor was closed and heated to room temperature and then cooled again with an ice bath to 0°C . The desired amount of *sec*-butyllithium was introduced with a gastight Hamilton syringe through the rubber septum. After 5-10 min the mixture was heated to 40°C to start the polymerization and kept at this temperature for ca. 12 hours. After completion of the polymerization the reactor was cooled down slowly to -10°C . Then 25 ml of dried THF were cryo-transferred and as the temperature is increasing to room temperature a light yellow color indicative for the living carbanions appeared (not visible with pure cyclohexane). The solution is again cooled down to -10°C . Approximately 5 ml (0.1 mole) of EO were cryo-transferred

to the graduated ampoule and then to the reactor. The solution was heated to room temperature and kept after the disappearance of the color for an additional half an hour stirring. The reaction was quenched with 5 ml methanol. The polymer was precipitated twice from a THF solution in methanol.

Preparation of linear polyisoprene-block-(linear polyglycerol). The polymer obtained above was dissolved in THF and deprotonated with an excess of potassium hydride under argon atmosphere. The mixture was kept stirring in a sealed flask with an argon filled balloon for one day. Then it was filtered and placed in a reactor equipped with a mechanical stirrer and a dosing pump. The activated polyisoprene was dissolved in diglyme, and heated up to 120 °C. THF was then distilled off from the reactor via a distillation bridge. The amount of macroinitiator was chosen according to the desired monomer/initiator ratio. Ethoxy ethyl glycidyl ether was dissolved in THF and was slowly added at 120 °C. After completion of the reaction the product was neutralized with a cationic-exchange resin (Lewatit K1131). Then the crude product was twice precipitated in cold methanol from a THF solution and dried for an extended period at 60 °C in vacuo.

Preparation of linear poly(isoprene)-block-(hyperbranched-polyglycerol).

Polymerizations were carried out in the same reactor as above. The macroinitiator was 10% deprotonated with potassium *tert*-butylate. The activated macroinitiator was dissolved in 20 ml Diglyme, heated up to 120 °C and placed in the reactor. The amount of macroinitiator was chosen according to the desired monomer/initiator ratio. Glycidol was dissolved in THF and was slowly added at 120 °C. After completion of the reaction the product was neutralized with a cationic-exchange resin and dried in a first step to characterize the crude product. Then the crude product was twice precipitated in cold methanol (it was necessary for some samples to place the precipitated solution in the freezer for one day due to the liquid-like material obtained) and dried for an extended period at 60 °C in vacuo.

$^1\text{H NMR}$ (400 MHz, $d_1\text{-CDCl}_3$, 25 °C).

PI_x-OH: $\delta=5.3$ ppm (m, $-\text{CH}_2\text{-C}(\text{CH}_3)=\underline{\text{CH}}\text{CH}_2$ 1,4-PI), $\delta=4.9$ ppm (m, $-\text{CH}_2\text{-CH}(\text{CH}_3\text{C}=\underline{\text{CH}}_2)$ 3,4-PI), $\delta=3.7$ ppm (m, $\text{C}\underline{\text{H}}_2\text{CH}_2\text{OH}$ EO when visible), $\delta=3.5$ ppm (m, $\text{CH}_2\text{C}\underline{\text{H}}_2\text{OH}$ EO when visible), $\delta=2.2\text{-}0.8$ ppm (m, $-\text{C}\underline{\text{H}}_2\text{-C}(\underline{\text{C}}\underline{\text{H}}_3)=\text{CHC}\underline{\text{H}}_2$ PI).

PI_x-b-LPG_y: $\delta=5.3$ ppm (m, $-\text{CH}_2\text{-C}(\text{CH}_3)=\underline{\text{CH}}\text{CH}_2$ 1,4-PI), $\delta=4.9\text{-}4.6$ ppm (m, $-\text{CH}_2\text{-CH}(\text{CH}_3\text{C}=\underline{\text{CH}}_2)$ 3,4-PI), $\delta=3.3\text{-}3.7$ ppm (m, $\text{C}\underline{\text{H}}_2\text{C}\underline{\text{H}}_2\text{OH}$ EO and $-\text{C}\underline{\text{H}}_2\text{-C}\underline{\text{H}}_2(\underline{\text{C}}\underline{\text{H}}_2\text{-O-C}\underline{\text{H}}(\text{CH}_3)\text{-O}\underline{\text{C}}\underline{\text{H}}_2\text{CH}_3)\text{-O-}$ acetal LPG), $\delta=2.2\text{-}0.8$ ppm (m, $-\text{C}\underline{\text{H}}_2\text{-C}(\underline{\text{C}}\underline{\text{H}}_3)=\text{CHC}\underline{\text{H}}_2$ PI and $-\text{CH}_2\text{-CH}_2(\text{CH}_2\text{-O-CH}(\underline{\text{C}}\underline{\text{H}}_3)\text{-OCH}_2\underline{\text{C}}\underline{\text{H}}_3)\text{-O-}$ acetal LPG).

PI_x-b-(LPG_y-hg-PG_z): $\delta=5.3$ ppm (m, $-\text{CH}_2\text{-C}(\text{CH}_3)=\underline{\text{CH}}\text{CH}_2$ 1,4-PI), $\delta=4.9\text{-}4.6$ ppm (m, $-\text{CH}_2\text{-CH}(\text{CH}_3\text{C}=\underline{\text{CH}}_2)$ 3,4-PI), $\delta=3.3\text{-}3.7$ ppm (m, $\text{C}\underline{\text{H}}_2\text{C}\underline{\text{H}}_2\text{OH}$ EO and $-\text{C}\underline{\text{H}}_2\text{-C}\underline{\text{H}}_2(\underline{\text{C}}\underline{\text{H}}_2\text{-OH})\text{-O-}$ LPG), $\delta=2.2\text{-}0.8$ ppm (m, $-\text{C}\underline{\text{H}}_2\text{-C}(\underline{\text{C}}\underline{\text{H}}_3)=\text{CHC}\underline{\text{H}}_2$ PI).

5.6. References

- (1) Yu, K.; Zhang, L. F.; Eisenberg, A. *Langmuir* **1996**, *12*, 5980.
- (2) Moffitt, M.; Vali, H.; Eisenberg, A. *Chem. Mater.* **1998**, *10*, 1021.
- (3) Göltner, C.; Cölfen, H.; Antonietti, M. *Chem. Unserer. Zeit* **1999**, *33*, 200.
- (4) Förster, S.; Antonietti, M. *Adv. Mater.* **1998**, *10*, 195.
- (5) Förster, S.; Plantenberg, T. *Angew. Chem.-Int. Edit.* **2002**, *41*, 689.
- (6) Gitsov, I. *Advances in Dendritic Macromolecules*; Elsevier Science: Amsterdam, 2002; Vol. 5.
- (7) van Hest, J. C. M.; Delnoye, D. A. P.; Baars, M. W. P. L.; van Genderen, M. H. P.; Meijer, E. W. *Science* **1995**, *268*, 1592.
- (8) van Hest, J. C. M.; Baars, M. W. P. L.; Elissen-Román, C.; van Genderen, M. H. P.; Meijer, E. W. *Macromolecules* **1995**, *28*, 6689.
- (9) Gitsov, I.; Wooley, K. L.; Fréchet, J. M. J. *Angew. Chem.-Int. Edit.* **1992**, *31*, 1200.
- (10) Gitsov, I.; Ivanova, P. T.; Fréchet, J. M. J. *Macromol. Rap. Commun.* **1994**, *15*, 387.
- (11) Flory, P. J. *J. Am. Chem. Soc.* **1952**, *74*, 2718.
- (12) Radke, W.; Litvinenko, G.; Müller, A. H. E. *Macromolecules* **1998**, *31*, 239.
- (13) Hanselmann, R.; Höltner, D.; Frey, H. *Macromolecules* **1998**, *31*, 3790.

- (14) Sunder, A.; Hanselmann, R.; Frey, H.; Mülhaupt, R. *Macromolecules* **1999**, *32*, 4240.
- (15) Barathi, P.; Moore, J. S. *Macromolecules* **1997**, *32*, 4240.
- (16) Pusel, T.; *Ph.D. Thesis*, University of Freiburg/Brsg: Germany, 2002.
- (17) García Marcos, A.; Pusel, T.; de Juan de Casrto, B.; Geppert, S.; Thomann, R.; Gronski, W.; Frey, H. *Polym. Prepr.* **2003**, *44*, 534.
- (18) Istratov, I.; Kautz, H.; Kim, Y. K.; Schubert, R.; Frey, H. *Tetrahedron* **2003**, *59*, 4017.
- (19) Adams, J.; Sängler, J.; Tefehne, C.; Gronski, W. *Macromol. Rap. Commun.* **1994**, *15*, 879.
- (20) Sängler, J.; Tefehne, C.; Lay, R.; Gronski, W. *Polym. Bull.* **1996**, *36*, 19.
- (21) Karimi, B.; Golshani, B. *J. Org. Chem.* **2000**, *65*, 7228.
- (22) García Marcos, A.; Pusel, T.; Thomann, R.; Pakula, T.; Okrasa, L.; Geppert, S.; Gronski, W.; Frey, H. *Macromolecules* **2005**, *submitted*.
- (23) Hölter, D.; Frey, H. *Acta Polymer.* **1997**, *48*, 298.
- (24) Hölter, D.; Burgath, A.; Frey, H. *Acta Polymer.* **1997**, *48*, 359.
- (25) Fitton, A.; Hill, J.; Jane, D.; Miller, R. *Synthesis* **1987**, 1140.
- (26) Taton, D.; Le Borgne, A.; Sepulchre, M.; Spassky, N. *Macromol. Rap. Commun.* **1994**, *195*, 139.
- (27) Gilman, H.; Haubein, A. H. *J. Am. Chem. Soc.* **1944**, *66*, 1515.

6. Solution properties of linear-hyperbranched amphiphilic block copolymers

6.1. Introduction

Commonly, amphiphilic block copolymers (ABCs) are distinguished from low molecular weight surfactants, since they exhibit better control of the self-assembly process determined both by the chemical nature and the length of the polymeric blocks. The associated superstructures formed in solution are also more stable, i.e., less dynamic due to additional steric and electrosteric stabilization effects. Currently, there is a vivid interest in ABCs in the context of nanotechnology, and numerous studies related to their aggregation behavior in solution have been reported. Various authors have summarized the state of the art for these systems in reviews.¹⁻³

Linear dendritic block copolymers (LDBC) have been shown to possess unusual properties both in solution and in bulk. In a selective solvent, such block copolymers show self-assembly, leading to the formation of spherical micelles or in some cases more complex supramolecular structures, e.g., cylindrical micelles or vesicles. As suggested by Meijer et al., polymers with dendritic head groups may represent an amphiphile intermediate between traditional organic surfactants and amphiphilic block copolymers, with the size of the latter and the shape of the former.⁴ The materials developed and studied by Meijer's group consisted of a polystyrene (PS) linear chain and a hydrophilic poly(propylene imine) (PPI) dendrimer block, PS-*block-(dend-PPI)_n*. Light scattering techniques were applied to study the structure of the supramolecular aggregates. The authors interpreted^{4,5} the self-assembly behavior observed for their linear dendritic block copolymers in terms of the theory of Israelachvili,⁶ which is based on the size-dependent type of aggregation (geometry of the aggregates given by the packing parameter $P=V(a_0 \cdot l_0)$). The PS-*block-(dend-PPI)_n* from generation number [G-3] to [G-5] show a generation-dependant increase of the radius of gyration (R_g) from planar bilayers through vesicles [G-3] and rodlike micelles [G-4] to spherical micelles [G-5]. Unfortunately the other generations show clustered structures due to electrostatic interaction. This is an important limitation in the study of this type of LDBC. DLS results were supported by transmission electron microscopy (TEM) results. However the images obtained are not always clear, but

some information can be collected. No structural transition was observed with dilution indicating that aggregates of these diblock copolymers are very stable.

Kim et al.⁷ and Sommerdijk et al.⁸ also reported some DLS data on amphiphilic linear-dendrimer constructs based on poly(ethylene oxide) (PEO) and branched polycarbosilanes. The radii of gyration increase with the generation number of the dendritic block, but only generations up to [G-3] were measured, which does not give the possibility to conclude on a systematic dendritic block effect. The authors of the study suggested the presence of secondary micellar aggregation, because values between 170 and 190 nm were obtained as the length of a fully extended PEO-*block-(dend-polycarbosilane)* is around 100 Å. Zhu et al. reported diameters of aggregates between 40 and 70 nm for the poly(N-isopropylacrylamide)-*block-(dend-poly(benzyl ether))* hybrid copolymers.⁹ Again, TEM of these materials did not show clear structures. The diameters of spherical aggregates ranged between 30 and 60 nm. Entangled nanotubes with identical diameter seem to lead to a single spherical aggregate primarily formed and then going to measure several micrometers.

The aim of this chapter is the detailed characterization of the structures exhibited by linear-hyperbranched polystyrene-*block-(1,2-polybutadiene-hypergrafted-polyglycerol)* in solution, emphasizing their peculiarity brought about by the dendritic segment. Self-assembly, onset of micellization, the dimensions and the structure of the micelles will be discussed.

6.2. Dynamic and static light scattering measurements

Dynamic light scattering (DLS) and static light scattering (SLS) in two different solvents (chloroform and toluene) have been performed on the macroinitiator polystyrene-*block-(hydroxylated-1,2-polybutadiene)* (PS₅₀₈-*b*-(PB-OH)₅₆) and polystyrene-*block-(1,2-polybutadiene-hypergrafted-polyglycerol)* (PS₅₀₈-*b*-(PB₅₆-*hg*-PG_x) samples. The synthesis of the materials has been presented in chapter 5. The sample with 52% wt. of polyglycerol block was not investigated, because it shows only good solubility in dimethylformamide at very dilute concentration. In aqueous solution, turbidity is observed, and dissolution is only achieved in the ultrasonic bath (large aggregates).

The hydrodynamic radii (R_h) were calculated by applying the Stokes-Einstein equation. The z-average of the translational diffusion constant D_z is defined as follow:

$$D_z = \frac{k_B T}{6\pi\eta_0} \left\langle \frac{1}{R_h} \right\rangle$$

where k_B is the Boltzmann factor, T is the temperature in Kelvin (K) and η_0 the viscosity of the solvent. The radii of gyration (R_g) and the weight average molecular weight ($\overline{M_w}$) were obtained from the Zimm equation¹⁰ (static light scattering):

$$\frac{Kc}{R(\theta)} = \frac{1}{M_w} \left(1 + \frac{1}{3} q^2 \langle R_g^2 \rangle_z \right) + 2A_2c + \dots$$

where K is the optical constant, c the concentration, $R(\theta)$ the Rayleigh ratio as a function of scattering angle, q the scattering vector and A_2 the second virial coefficient.

The ρ ratio is a dimensionless quantity defined by:

$$\rho = \frac{\langle R_g^2 \rangle_z^{1/2}}{\langle R_h^{-1} \rangle_z^{-1}}$$

This ratio gives information on the geometry of the aggregates.¹¹

6.2.1. Measurements in chloroform

The samples were dissolved in chloroform and measurements were performed at 5 different concentrations. For clarification, the solutions were passed through 0.2 μm pore size Millex LCR filters into dust-free cylindrical cuvettes. As shown in **Figure 1**, the samples could not be measured at the same concentrations. For some concentrations large aggregates were formed and the solution could not pass through the filter or the scattered intensity was too high to perform the measurement. The concentration of the macroinitiator PS-*b*-(PB-OH)₅₆ solution had to be reduced from 1 $\text{g}\cdot\text{l}^{-1}$ to 0.1 $\text{g}\cdot\text{l}^{-1}$. The chloroform solution of PS₅₀₈-*b*-(PB₅₆-hg-PG₈₆) was also dilute, but at a higher concentration (0.6 $\text{g}\cdot\text{l}^{-1}$). Only with the sample PS₅₀₈-*b*-(PB₅₆-hg-PG₂₈₀) the measurements could start with a concentration of 1.5 $\text{g}\cdot\text{l}^{-1}$. This first observation is contradictory to expectation. The macroinitiator possesses only a short block of hydroxylated polybutadiene (5.3% wt.) and a long linear polystyrene chain, but it seems that the system is not well-organized, and big clusters of aggregates are

formed. As the weight fraction of hypergrafted polyglycerol increases, the solubility increases and the size of the aggregates remains constant over a range of concentrations from $1.5 \text{ g}\cdot\text{l}^{-1}$ to $0.2 \text{ g}\cdot\text{l}^{-1}$. This can be explained by three factors: (i) the high solvation surface of the hyperbranched block (ii) the presence of hydrogen bonds (iii) the strong phase segregation of the both blocks.

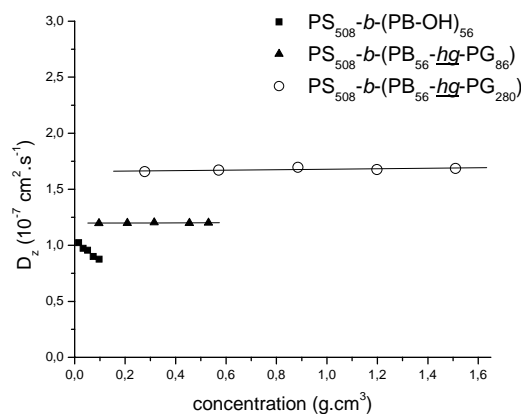


Figure 1. Dynamic light scattering data: z-average of the translational diffusion constant D_z plotted as a function of the concentration in chloroform for the macroinitiator $\text{PS}_{508}\text{-}b\text{-(PB-OH)}_{56}$ and the $\text{PS}_{508}\text{-}b\text{-(PB}_{56}\text{-hg-PG}_x)$ samples.

The results of the dynamic and static light scattering are summarized in **Table 1**. The three samples measured show a dramatic difference. The hydrodynamic radius of the macroinitiator $\text{PS}_{508}\text{-}b\text{-(PB-OH)}_{56}$ is 36.3 nm and its radius of gyration 153 nm. The ratio ρ was not calculated, because the polydispersity of the aggregates is too large. \overline{M}_w is estimated to be $59.8 \cdot 10^6 \text{ g}\cdot\text{mol}^{-1}$ and the second virial coefficient is negative. These results confirm the formation of large and not very well-defined aggregates. The presence of 56 OH groups seems to be insufficient to stabilize micelles and too high for the dilution of the independent unimers.

When 86 units of glycidol are hypergrafted onto the hydroxylated 1,2-polybutadiene block, the size of the aggregates becomes smaller, R_h is 31.6 nm, R_g is 110 nm and \overline{M}_w is $2.8 \cdot 10^6 \text{ g}\cdot\text{mol}^{-1}$. However, again these results can not be taken as real values, because they first reflect the broad size distribution of the aggregates.

The last sample $\text{PS}_{508}\text{-}b\text{-(PB}_{56}\text{-hg-PG}_{280})$ contains 280 units of polyglycerol, which corresponds to 27% weight fraction in the amphiphilic block copolymer. In this case the light scattering results show the formation of well-defined aggregates with R_h of 22.8 nm, R_g of 25.2 nm and a corresponding ρ -ratio of 1.1. According to these results

the aggregated structures show spherical shapes with a relatively narrow polydispersity in chloroform.

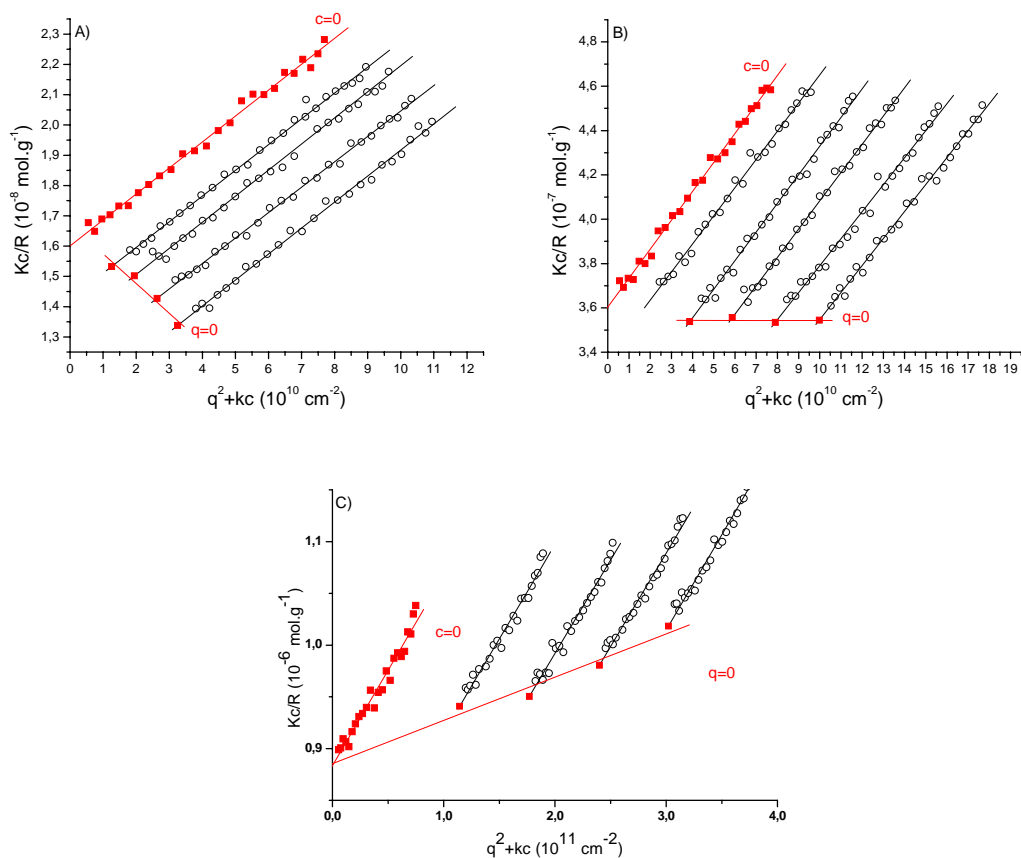


Figure 2. Zimm-plots of A) PS₅₀₈-*b*-(PB₅₆-*hg*-PG₈₆); B) PS₅₀₈-*b*-(PB-OH)₅₆; C) PS₅₀₈-*b*-(PB₅₆-*hg*-PG₂₈₀) in CHCl₃ at 293K.

Figure 2 gives the Zimm plots of the three samples discussed. The extrapolated curves ($c=0$ and $q=0$) are plotted in red. Their intersection permits to calculate the weight average molecular weight of the aggregates. As discussed above, it is possible to see, here graphically, that the sample with the higher content of polyglycerol PS₅₀₈-*b*-(PB₅₆-*hg*-PG₂₈₀) shows a better control in the self-assembly than the other samples, PS₅₀₈-*b*-(PB-OH)₅₆ and PS₅₀₈-*b*-(PB₅₆-*hg*-PG₂₈₀) because the intersection of the curves fits only perfectly for this sample.

Table 1. Results from static and dynamic light scattering measurements in chloroform at 293K for the macroinitiator PS₅₀₈-*b*-(PB-OH)₅₆, PS₅₀₈-*b*-(PB₅₆-*hg*-PG₈₆) and PS₅₀₈-*b*-(PB₅₆-*hg*-PG₂₈₀) after extrapolation to c=0 and q=0 according to Zimm.¹⁰

	DLS			SLS		
	D _z	$\langle 1/R_h \rangle_z^{-1}$	ρ	$\langle R_g^2 \rangle_z^{1/2}$	\overline{M}_w	A ₂
	(cm ² .s ⁻¹)	(nm)		(nm)	(g.mol ⁻¹)	(mol.cm ³ .g ⁻²)
PS ₅₀₈ - <i>b</i> -(PB-OH) ₅₆	1.0438·10 ⁻⁷	36.28	-	153	59.8·10 ⁶	-1.96·10 ⁻⁵
PS ₅₀₈ - <i>b</i> -(PB ₅₆ - <i>hg</i> -PG ₈₆)	1.1974·10 ⁻⁷	31.63	-	110	2.82·10 ⁶	2.28·10 ⁻⁷
PS ₅₀₈ - <i>b</i> -(PB ₅₆ - <i>hg</i> -PG ₂₈₀)	1.6583·10 ⁻⁷	22.8	1.1	25.2	1.1·10 ⁶	5.04·10 ⁻⁶

In order to determine the average number of aggregation, single macromolecules have to be isolated in a solvent. The first method would be to find a common solvent for both blocks, which prevents aggregation. Dimethylformamide (DMF) would be a good candidate, since polystyrene and polyglycerol are soluble in this solvent. Unfortunately, the DLS and SLS measurements show aggregation for the three samples presented in **Table 1**.

In chapter 5, the PS₅₀₈-*b*-(PB₅₆-*hg*-PG_x) samples were persilylated in order to overcome the aggregation problems during size exclusion chromatography measurements, in order to determine the polydispersity and the molecular weight of the samples. After persilylation both blocks possess a similar polarity and can be analyzed in a non polar solvent such as chloroform. The persilylated samples were investigated by DLS and SLS. The results again show aggregation, and it was not possible to determine the size of the macromolecules in solution even after fractionation with a preparative chromatography set-up. SEC is not as sensitive to the presence of aggregated structures as LS. The interactions of the sample with the column as well as the hydrodynamic shearing forces also reduce the formation of aggregates. The conditions in the cuvettes during DLS and SLS measurements are different and some latent aggregation due to some remaining hydroxyl groups is apparently sufficient to disturb the measurements.

Table 2: Estimation of the average aggregation number Z in chloroform by comparing the M_n obtained from ^1H NMR for the single macromolecules (chapter 5) and the M_w from SLS for the aggregated macromolecules. \overline{M}_n and \overline{M}_w are given in $\text{g}\cdot\text{mol}^{-1}$.

	\overline{M}_n	\overline{M}_w	Z
	^1H NMR	SLS	
PS ₅₀₈ - <i>b</i> -(PB-OH) ₅₆	56,840	$59.8\cdot 10^6$	1050
PS ₅₀₈ - <i>b</i> -(PB ₅₆ - <i>hg</i> -PG ₈₆)	63,140	$2.82\cdot 10^6$	44
PS ₅₀₈ - <i>b</i> -(PB ₅₆ - <i>hg</i> -PG ₂₈₀)	77,580	$1.1\cdot 10^6$	14

It is only possible to estimate the average aggregation number by using the results for the single macromolecules reported in chapter 5. The values from SEC can not be used because firstly they include the TMS groups and secondly measurements are calibrated with linear polymer standards (PS). The absolute M_n values obtained from ^1H NMR are used, because the polydispersity of the samples is so low (1.01-1.02) that the difference between M_w and M_n is minimal. The estimated aggregation number Z is calculated by dividing the M_w obtained for the aggregated macromolecules by M_n obtained by ^1H NMR for the single macromolecules. The results are given in **Table 2**. It is important to stress that these calculated values only give a rough estimate. The aggregation number increases as the fraction of the polyglycerol block decreases. An increase of the hyperbranched block size leads to a higher stability of the aggregates by involving fewer macromolecules than for lower content of polyglycerol. In the case of the macroinitiator PS₅₀₈-*b*-(PB-OH)₅₆ Z is very large, which confirms the formation of big aggregates.

6.2.2. Measurements in toluene

The influence of the nature of the solvent on the aggregates was studied by performing the same light scattering experiments in a non-polar solvent, i.e., toluene. Surprisingly, the macroinitiator was badly soluble in toluene and no measurements could be carried out. The solution was sonicated for extended periods without success. Also, the samples were first dissolved in chloroform and then placed in toluene, but this procedure did not improve the solubility, when the second solvent was slowly removed.

The two samples containing 86 and 280 units of glycidol, respectively, could be dissolved in toluene starting at a concentration of $0.4 \text{ g}\cdot\text{l}^{-1}$ for the first one and $0.5 \text{ g}\cdot\text{l}^{-1}$ for the second one. In **Figure 3** (*top*) the dependence of the diffusion coefficient D_z is plotted versus the concentration of the sample in toluene. For both cases there is no dependence of D_z on the concentration, which means that the aggregates are stable. From the static light scattering data the Zimm plots (**Figure 3**, *bottom*) show quite good accordance for the extrapolated functions of $\text{PS}_{508}\text{-}b\text{-(PB}_{56}\text{-}hg\text{-PG}_{280})$, but this is not the case for $\text{PS}_{508}\text{-}b\text{-(PB}_{56}\text{-}hg\text{-PG}_{86})$.

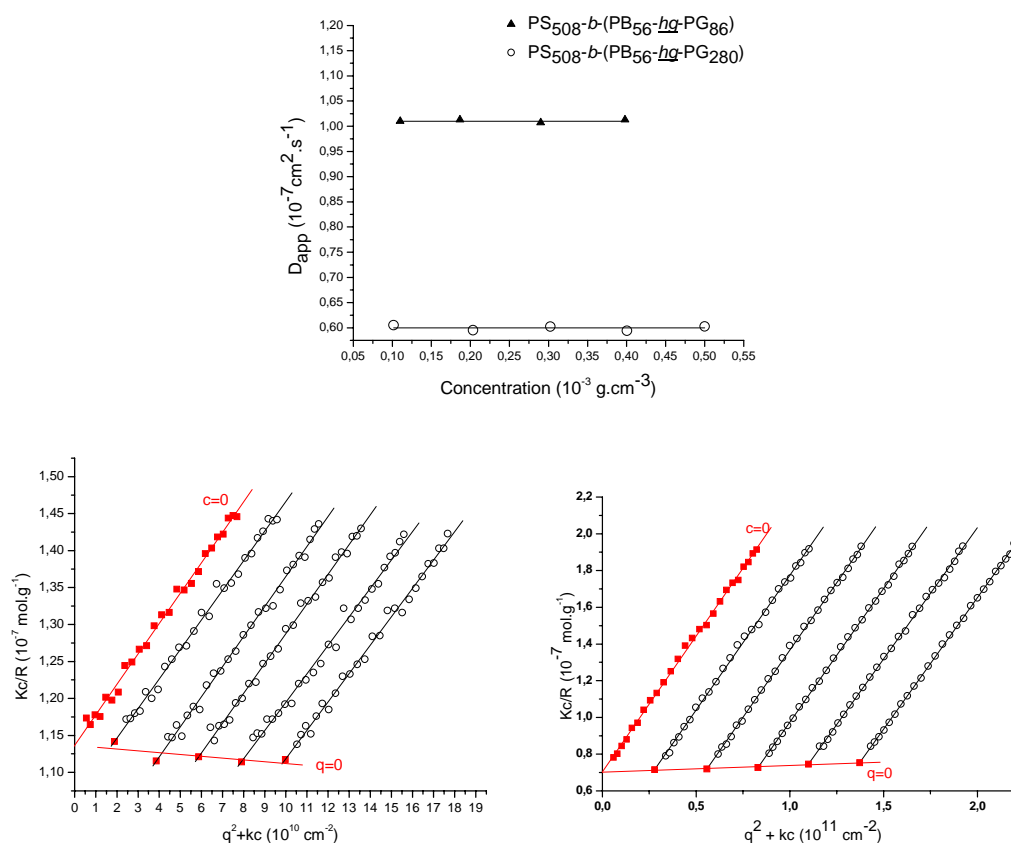


Figure 3. Dynamic light scattering data (*top*): z-average of the translational diffusion constant D_z plotted as a function of the concentration in toluene for the $\text{PS}_{508}\text{-}b\text{-(PB}_{56}\text{-}hg\text{-PG}_x)$ samples and static light scattering data (*bottom*): Zimm plots in toluene of $\text{PS}_{508}\text{-}b\text{-(PB}_{56}\text{-}hg\text{-PG}_{86})$ (*left*) and for $\text{PS}_{508}\text{-}b\text{-(PB}_{56}\text{-}hg\text{-PG}_x)$ (*right*).

All results of DLS and SLS measurements are summarized in **Table 3**. The influence of the solvent on both the size and the morphology of the aggregates in solution is obvious. The sample $\text{PS}_{508}\text{-}b\text{-(PB}_{56}\text{-}hg\text{-PG}_{86})$ shows again low polydispersity as in chloroform and the values of R_h and R_g estimated can not be taken into account. This confirms the fact that an increase of the fraction of hyperbranched polyglycerol leads

to an optimum for the self-assembly in solution, as suggested already in the first section.

Table 3. Results from static and dynamic light scattering measurements in toluene at 293K for the macroinitiator sample PS₅₀₈-*b*-(PB₅₆-*hg*-PG₈₆) and PS₅₀₈-*b*-(PB₅₆-*hg*-PG₂₈₀) after extrapolation to c=0 and q=0 according to Zimm.¹⁰

	DLS			SLS		
	D _z	$\langle 1/R_h \rangle_z^{-1}$	ρ	$\langle R_g^2 \rangle_z^{1/2}$	\overline{M}_w	A ₂
	(cm ² .s ⁻¹)	(nm)		(nm)	(g.mol ⁻¹)	(mol.cm ³ .g ⁻²)
PS ₅₀₈ - <i>b</i> -(PB ₅₆ - <i>hg</i> -PG ₈₆)	1.01·10 ⁻⁷	36.7	-	108	8.8·10 ⁶	4.88·10 ⁻⁶
PS ₅₀₈ - <i>b</i> -(PB ₅₆ - <i>hg</i> -PG ₂₈₀)	5.818·10 ⁻⁸	60.7	1.3	79.6	14.25·10 ⁶	5.04·10 ⁻⁶

According to the ρ ratio, the aggregated structures of PS₅₀₈-*b*-(PB₅₆-*hg*-PG₂₈₀) show an ellipsoidal morphology of a higher polydispersity than in chloroform. This is potentially due to the presence of cylindrical micelle structures. The size of the micelles is larger than in the previous solvent, which can be explained by the difference of polarity.

Table 4. Estimation of the average aggregation number Z in toluene by comparing the M_n obtained from ¹H NMR for the single macromolecules (chapter 5) and the M_w from SLS for the aggregated macromolecules. \overline{M}_n and \overline{M}_w are given in g·mol⁻¹.

	\overline{M}_n	\overline{M}_w	Z
	¹ H NMR	SLS	
PS ₅₀₈ - <i>b</i> -(PB ₅₆ - <i>hg</i> -PG ₈₆)	63,140	8.8·10 ⁶	139
PS ₅₀₈ - <i>b</i> -(PB ₅₆ - <i>hg</i> -PG ₂₈₀)	77,580	14.25·10 ⁶	183

The average aggregation numbers in toluene are given in **Table 4**. The estimated values are higher than in chloroform, because the aggregates are larger. The average aggregation number is less affected by the size of the polyglycerol block than in chloroform.

6.3. Atomic force microscopy measurements

In order to visualize micellar aggregates after deposition, atomic force microscopy (AFM) were performed. Different solutions in chloroform and toluene were prepared and then spin-cast on a substrate.

6.3.1. Deposition from chloroform solution

An AFM-micrograph of the sample PS₅₀₈-*b*-(PB₅₆-*hg* PG₂₈₀) deposited from chloroform solution onto graphite (HOPG) is shown in **Figure 4**. The solution concentration was set at 0.5 g·l⁻¹ in order to realize a homogeneous coverage of the surface of the substrate by the micellar structures. The concentration was also lowered and no major difference was observed, except for a decrease of the coverage of the surface. For higher concentrations the aggregates agglomerate and it was difficult to isolate them.

The structures present on the surface are spherical-like, and some of them agglomerate. From the height profile the diameter of the structures is estimated to be 58 nm, and the height 2 nm. The light scattering results presented above show the presence of spherical aggregates in chloroform solution. In this respect the structures observed on the surface by AFM may have been present in solution. The change of the size of the aggregates may be due to the surface interaction. However, the morphology remains the same.

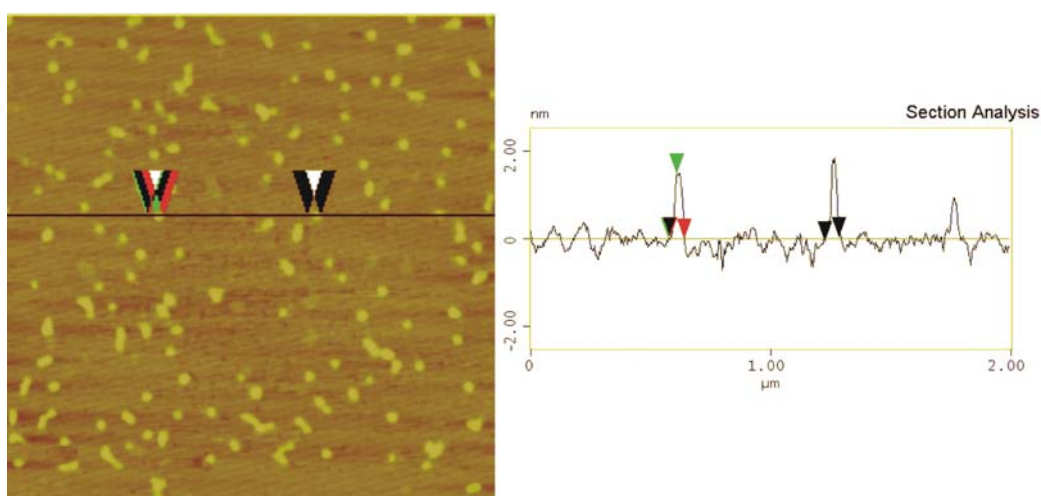
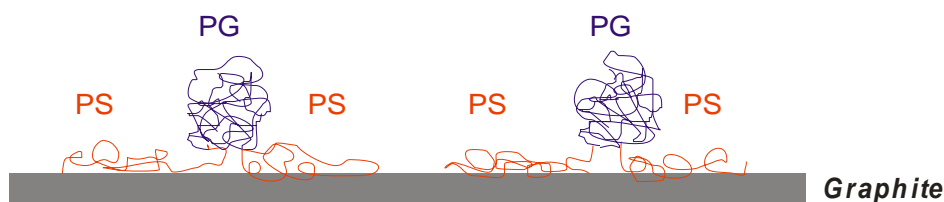


Figure 4. AFM-micrograph (*left*) with corresponding height profile (*right*) of PS₅₀₈-*b*-(PB₅₆-*hg* PG₂₈₀) from a chloroform solution (0.5 g·l⁻¹) on a graphite substrate (tapping mode).

6.3.2. Deposition from toluene solution

In the AFM-micrograph (**Figure 5**) micellar core-shell structures are observed after toluene solution casting. Like from chloroform solution the concentration was set at $0.5 \text{ g}\cdot\text{l}^{-1}$. The surface of the substrate was mainly covered after deposition. These superstructures consist of a polystyrene shell that interacts with the apolar graphite surface and a hyperbranched, highly polar polyglycerol core that is likely to show repulsive interaction with the apolar surface as illustrated in **Scheme 1**. As the aggregates are deposited on the surface, the spherical micelles adopt an open morphology. Such core-shell superstructures appear, when one of the blocks is strongly adsorbed and forms a tightly bound monomolecular layer on the surface, while monomer units of the other block are incompatible with the surface.

Similar surface patterns were first observed experimentally for linear block copolymers in thin films formed by adsorption of symmetrical polystyrene-*block*-poly(2-vinyl-pyridine) (PS-*b*-P2VP) copolymers from a dilute nonselective solvent onto a mica substrate.^{12,13} For the copolymer PS₃₀₀-*b*-P2VP₃₀₀ a polystyrene core cluster with a height of 5 nm surrounded by a P2VP shell with a height of 1 nm was measured.



Scheme 1: Schematic illustration of core-shell structures after deposition from toluene solution onto graphite.

Preliminary experiments with mica have been performed, but no superstructures could be observed. In the case of mica polyglycerol would be adsorbed stronger on the surface than the polystyrene block. This means that the interaction with the surface plays a key role for the deposition of these aggregates. This phenomenon was reported in different works on block copolymer micelles. The interaction of copolymers with a surface can lead to essential changes in the morphology or even to its disappearance.¹⁴⁻¹⁶

For both samples the same kind of superstructures can be observed. In the case of PS₅₀₈-*b*-(PB₅₆-*hg* PG₈₆) (**Figure 5 top**), the superstructures are more polydisperse. The micrograph shows different types of aggregates, i.e., the system did not reach an equilibrium state and the core-shell superstructures coexist with other structures. The morphology of the aggregates after deposition on the surface does not depend on the size of the polar hyperbranched block but the size distribution is highly molecular weight dependent.

The sample PS₅₀₈-*b*-(PB₅₆-*hg*-PG₂₈₀) shows very well-defined structures on the graphite surface (**Figure 5 bottom**). The height of the core region was estimated to be 4 nm from the AFM surface profile, confirming the presence of a dense and highly functional core. This result suggests that the core is very dense because the structures result from the aggregation of a lot of single macromolecules. The height of the shell region is more difficult to estimate, it is between 0.5 and 1.5 nm. These values are similar to the ones obtained with PS₃₀₀-*b*-P2VP₃₀₀ from a nonselective solvent. It is possible to see some interactions between some micellar structures.

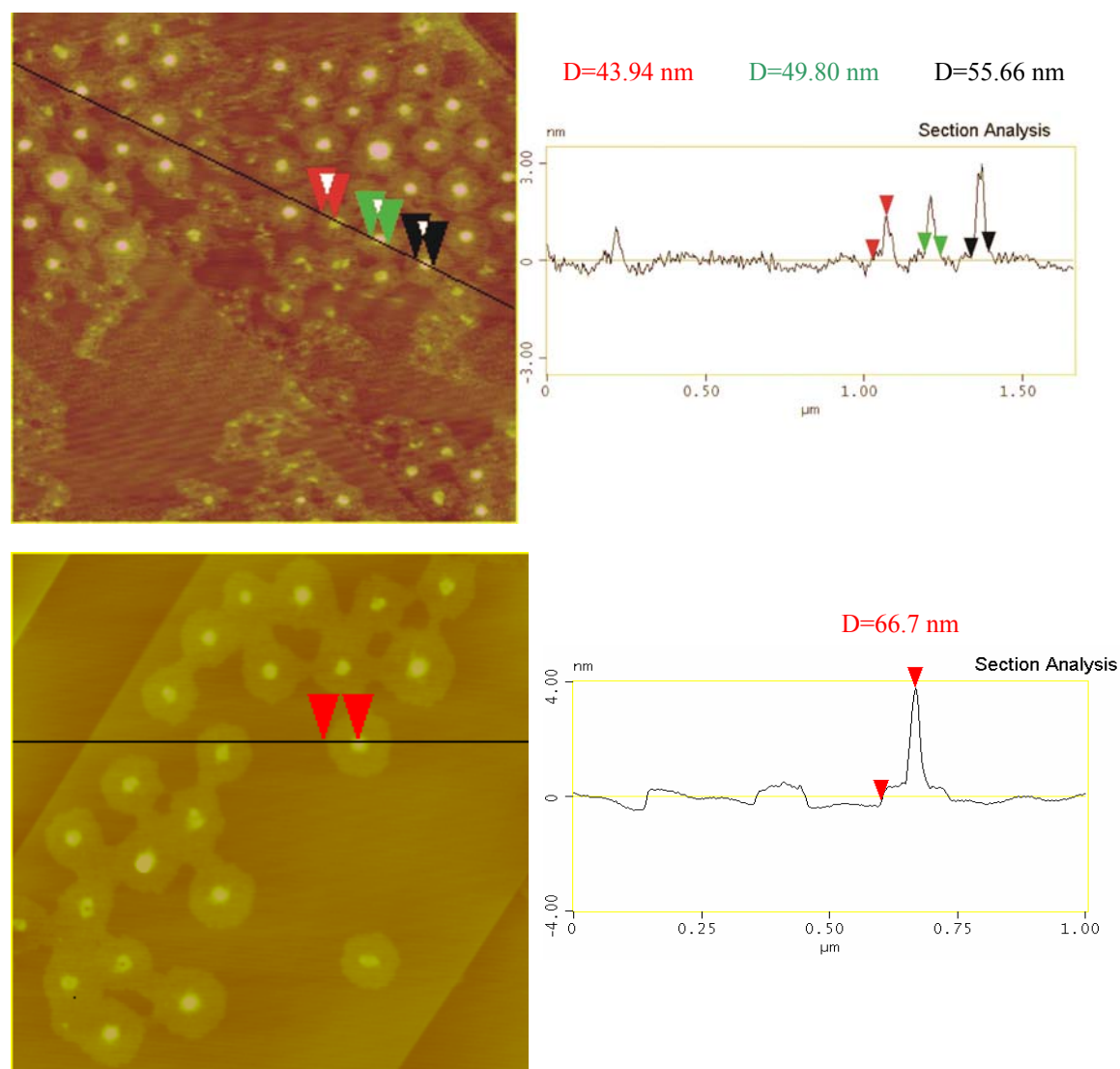


Figure 5. AFM-micrographs (left) with corresponding high profile (right) of PS₅₀₈-*b*-(PB₅₆-*hg* PG₈₆) (*top*) and of PS₅₀₈-*b*-(PB₅₆-*hg* PG₂₈₀) (*bottom*) from a toluene solution (0.5 g·l⁻¹) on a graphite substrate (tapping mode).

Taking into account the high stability of the polyether-polyol scaffold, deposition of the block copolymer micelles appears to be suitable for the generation of ordered arrays of nanosize hydrophilic domains on surfaces. Such domains are of interest with respect to biomineralization, the formation of small noble metal or semiconductor structures as well as biomedical applications. The preparation of chemically heterogeneous nanomosaic using lateral phase separation has been reported by several groups in 1996.^{17,18} These materials have been applied for the preparation of nanopatterns with gold nanoparticles using them as masks for lithographic techniques after etching.¹⁹⁻²¹ **Figure 6** shows the preparation of nanoarrays using the sample PS₅₀₈-*b*-(PB₅₆-*hg* PG₂₈₀) after deposition on graphite from a 1.5 g·l⁻¹ toluene solution.

The AFM micrograph shows some hexagonally packed domains but the overall surface is not perfectly ordered as evidenced by the Fourier Transform (**Figure 6**). Only one periodicity in a small length scale is present and no other preferred directions are detected. This experiment represents a first attempt for the preparation of ordered 2D-colloidal nanoarrays using the new linear-hyperbranched amphiphilic block copolymers presented in this thesis. Further investigations will have to be performed in the future in order to prepare ordered nanomosaic structures.

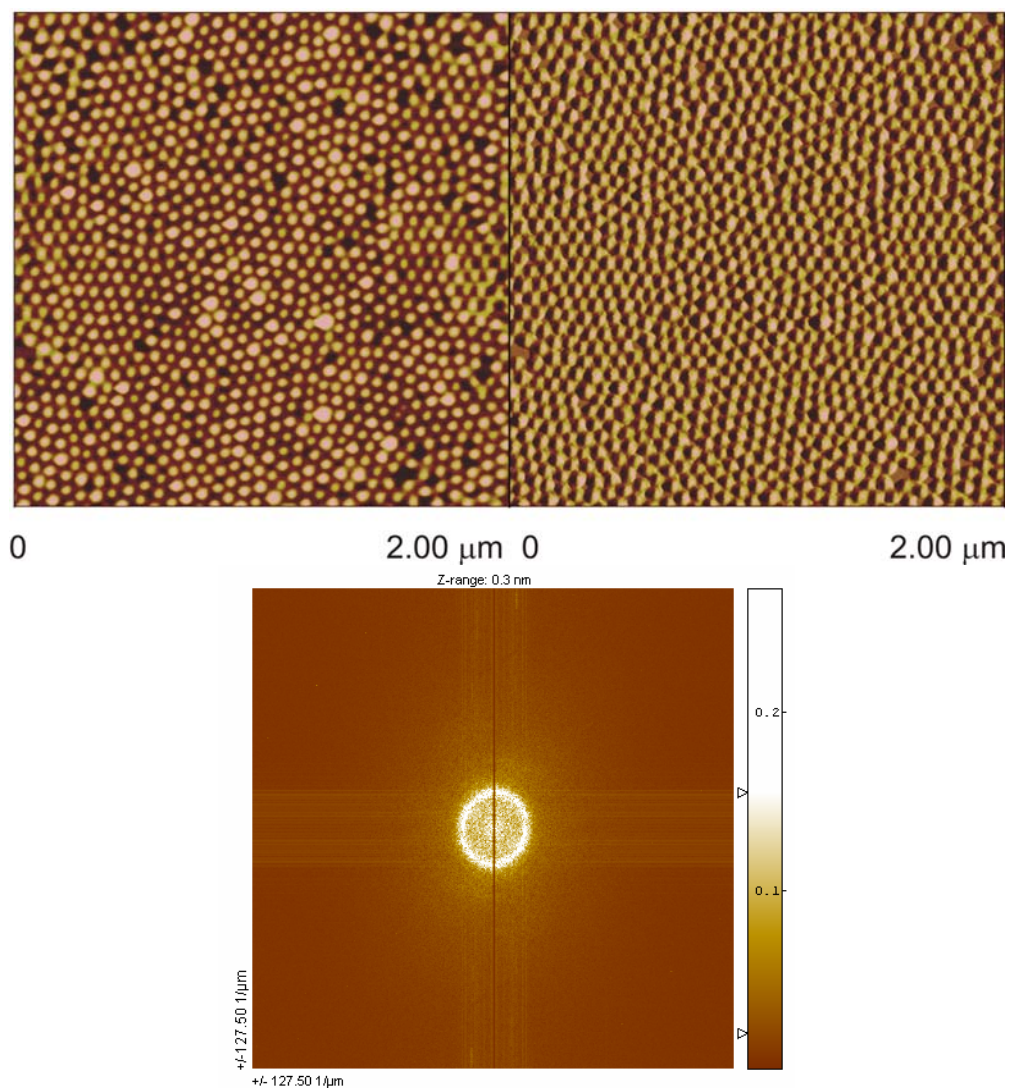


Figure 6. AFM-micrograph (*top*) of PS₅₀₈-*b*-(PB₅₆-*hg* PG₂₈₀) from a toluene solution (1.5 g.l⁻¹) on a graphite substrate (tapping mode) and the corresponding Fourier Transform (*bottom*) obtained with the software Capture.

6.4. Conclusion

One may assume that due to the complex distribution of topological isomers present even for the same molecular weight, hyperbranched materials are unlikely to form ordered supramolecular structures. However, detailed investigation shows that as the hyperbranched polyglycerol block fraction increases to an optimum weight fraction, the macromolecules form block copolymer micelles of homogeneous size in apolar solvents (chloroform and toluene). Presumably the block copolymer micelles are stabilized by the highly branched block.

The amphiphilic block copolymers show different behavior in different solvents. The size of the aggregates is smaller in chloroform than in toluene. The polarity of the solvent can influence the self-assembly mechanism. The morphology of the aggregates is also depending on the solvent: in chloroform monodisperse spherical shape aggregates and in toluene ellipsoidal aggregates (and some cylindrical aggregates) are formed.

The structures of these aggregates on the surface (graphite) show interesting features, enabling promising potential applications in respect to the presence of a highly dense, functional and stable hyperbranched block. Deposition from chloroform leads to dense spherical micelles but with relatively broad polydispersity. From toluene it leads to the formation of well-defined core-shell structures. The shell consists of the polystyrene block and the core of the hyperbranched polyglycerol block. The sample with 27% wt. PG (PS₅₀₈-*b*-(PB₅₆-*hg*-PG₂₈₀) shows very homogeneous superstructures on graphite surface. The diameter of the structures is estimated to be 66 nm, the height of the core region to be 4 nm and the shell to be between 0.5 and 1.5 nm. By increasing the concentration it was possible to prepare an ultrathin film with the presence of hexagonally packed domains. This is a promising result for the preparation of ordered nanoarrays by using the self-assembly behavior of these novel linear-hyperbranched block copolymers.

6.5. References

- (1) Alexandridis, P.; Lindman, B. *Amphiphilic Block Copolymers: Self-Assembly and Applications*, Elsevier Science BV ed., 1997.
- (2) Forster, S.; Plantenberg, T. *Angew. Chem.-Int. Edit.* **2002**, *41*, 689-714.
- (3) Förster, S.; Antonietti, M. *Adv. Mater.* **1998**, *10*, 195.
- (4) van Hest, J. C. M.; Delnoye, D. A. P.; Baars, M. W. P. L.; van Genderen, M. H. P.; Meijer, E. W. *Science* **1995**, *268*, 1592-1595.
- (5) van Hest, J. C. M.; Delnoye, D. A. P.; Baars, M. W. P. L.; Elissen Román, C.; van Genderen, M. H. P.; Meijer, E. W. *Chem.-Eur. J.* **1996**, *2*, 1616-1626.
- (6) Israelachvili, J. N.; Mitchell, D. J.; Ninham, B. W. *J. Chem. Soc. Faraday Trans. 2* **1976**, *72*, 1525.
- (7) Chang, Y. Y.; Kim, C. *J. Polym. Sci. Pol. Chem.* **2001**, *39*, 918-926.
- (8) Cornelissen, J. J. L. M.; van Heerbeek, R.; Kamer, P. C. J.; Reek, J. N. H.; Sommerdijk, N. A. J. M.; Nolte, R. J. M. *Adv. Mater.* **2002**, *14*, 489-+.
- (9) Zhu, L. Y.; Zhu, G.; Li, M. Z.; Wang, E.; Zhu, R.; Qi, X. *Eur. Pol. J.* **2002**, *38*, 2503.
- (10) Zimm, B. H. *J. Chem. Phys.* **1948**, *16*, 1099.
- (11) Burchard, W.; Richtering, W. *Progr. Colloid & Polymer Sci* **1989**, *80*, 151.
- (12) Spatz, J. P.; Roescher, A.; Sheiko, S.; Krausch, G.; Möller, M. *Adv. Mater.* **1995**, *8*, 731.
- (13) Spatz, J. P.; Möller, M.; Noeske, M.; Behm, R. J.; Pietralla, M. *Macromolecules* **1997**, *30*, 3874.
- (14) Anastasiadis, S.; Russell, T. P.; Satija, S. K.; Majkrzak, C. F. *Phys. Rev. Lett.* **1989**, *62*, 1852.
- (15) Bates, F. S.; Fredrickson, G. H. *Annu. Rev. Phys. Chem.* **1990**, *41*, 525.
- (16) Radzilowski, L.; Carvalho, B.; Thomas, E. *J. Polym. Sci. B* **1996**, *34*, 3081.
- (17) Spatz, J. P.; Sheiko, S.; Möller, M. *Adv. Mater.* **1996**, *8*, 513.
- (18) Li, Z.; Liu, W.; Rafailovich, M. H.; Sokolov, J.; Khougaz, K.; Eisenberg, A.; Lennox, R. B.; Krausch, G. *J. Am. Chem. Soc.* **1996**, *118*, 10892.
- (19) Selvan, S. T.; Spatz, J. P.; Klok, H.-A.; Möller, M. *Adv. Mater.* **1998**, *10*, 132.
- (20) Potemkin, I. I.; Kramarenko, E. Y.; Khokhlov, A. R.; Winkler, R. G.; Reineker, P.; Eibeck, A.; Spatz, J. P.; Möller, M. *Langmuir* **1999**, *15*, 7290.

- (21) Mössmer, S.; Spatz, J. P.; Möller, M.; Aberle, T.; Schmidt, J.; Burchard, W.
Macromolecules **2000**, *33*, 4791.

7. Bulk morphology of linear-hyperbranched block copolymers

7.1 Introduction

The bulk morphology and nanophase segregation of block copolymers is a large area of interest.¹⁻⁴ It is a great challenge to be able to control the size and shape of nano-objects as well as nanopatterns. The most common block copolymers studied in this context are AB, ABA, AB_n structures with linear blocks A and B. Small angle X-ray scattering (SAXS), differential scanning calorimetry (DSC) and imaging methods such as transmission electron microscopy (TEM) and atomic force microscopy (AFM) are indispensable to understand the bulk and surface assembly behavior of block copolymers.

It has been established that two main parameters influence the bulk morphology: the product of the Flory-Huggins segment-segment interaction parameter χ and the degree of polymerization \overline{DP}_n ($\chi \overline{DP}_n$), as well as the composition, characterized by f . For $\chi N \leq 10$ a disordered phase (Dis) can be observed due to the dominance of the entropic terms. Oppositely, when $\chi N > 10$, the enthalpic terms are dominant and this results in an order-to-disorder transition (ODT). In this latter case depending on the composition and other factors like copolymer architecture, fluctuation effects and conformational asymmetry the phases vary from spheres over cylinders to lamellae, inverted cylinders and inverted spheres.

Linear-dendritic block copolymers possess a peculiar macromolecular architecture compared with conventional linear block copolymers. Both the size and the shape of the dendritic block can influence the bulk morphology, and these parameters can easily be tuned by varying the generation number and the nature of the periphery, for example. The few examples of bulk morphologies of amphiphilic block copolymers containing a dendrimer block and a linear block studied to date show weak segregation, as in the case of polystyrene-*block*-(*dend*-poly(propylene imine)).^{5,6}

In this chapter DSC will be used to study the thermal behavior of linear-hyperbranched block copolymers consisting of a conventional linear block, polystyrene or polyisoprene, and a hyperbranched polyglycerol block. SAXS will be used to determine whether or not periodic nanosegregated polymer domains are

formed and also to study the size of these domains. TEM will be employed to directly observe potential phase-segregated domain morphologies.

7.2 Polyisoprene-*block*-(hyperbranched-polyglycerol)

The linear-hyperbranched block copolymers polyisoprene-*block*-(hyperbranched-polyglycerol) (PI_x-*b*-(LPG_y-hg-PG_z)) have already been characterized with respect to synthesis and molecular properties in chapter 5. Primarily the thermal behavior of the samples has been studied by differential scanning calorimetry (DSC) in order to determine whether phase segregation occurs. In these materials both blocks are flexible and amorphous. Linear poly(isoprene) exhibits a glass transition temperature (T_g) at around -60°C and hyperbranched polyglycerol at around -20°C. In the case of phase segregation, two distinct T_gs are visible and in the case of phase mixing only one glass transition is expected.

Table 1. Results from the DSC measurements after heating-cooling-heating cycle (10°C/min).

	T _{g1} (°C)	T _{g2} (°C)	Comment
PI ₆₀ - <i>b</i> -LPG ₄	-63	-	-
PI ₆₀ - <i>b</i> -(LPG ₄ - <u>hg</u> -PG ₄)	-63	-16	Phase segregation
PI ₆₀ - <i>b</i> -(LPG ₄ - <u>hg</u> -PG ₁₀)	-63	-20	Phase segregation
PI ₆₀ - <i>b</i> -(LPG ₄ - <u>hg</u> -PG ₁₉)	-62	-20	Phase segregation
PI ₁₆₂ - <i>b</i> -LPG ₅	-63	-	-
PI ₁₆₂ - <i>b</i> -(LPG ₅ - <u>hg</u> -PG ₁₅)	-65	-25	Phase segregation
PI ₁₆₂ - <i>b</i> -(LPG ₅ - <u>hg</u> -PG ₄₀)	-62	-20	Phase segregation
PI ₁₆₂ - <i>b</i> -(LPG ₅ - <u>hg</u> -PG ₅₉)	-62	-20	Phase segregation

The results from the DSC curves after a heating-cooling-heating cycle (heating and cooling rates 10°C/min) are summarized in **Table 1**. It should be noted that the T_{g1} of the linear polyisoprene block is predominant (high fraction of PI) compared with the T_{g2} of the hyperbranched polyglycerol block. This phenomenon is presumably due to the fraction of the respective blocks. However, hydrogen bonds of different quality due to the multiple end groups of the hyperbranched block may also influence this behavior. For all the block copolymer samples phase segregation takes place. This

means that the incompatibility between both blocks is strong enough to induce immiscibility in the bulk, similar as in PI-*b*-PEO block copolymers.

Conventional SAXS was used to probe the microstructures of these samples. The scattering data are presented as a function of the scattering vector q . In the case of microstructural periodicities first order and higher order reflections can be identified. The samples were all measured in a sealed capillary placed in a vacuum chamber. They could be annealed by applying a defined temperature range and the length of the distance between the detector and the sample was varied from 40 cm to 80 cm.

Figure 1 gives the SAXS diffractograms of a series of materials with a polyisoprene linear block with $DP_n=60$ and with various weight fractions of the hyperbranched polyglycerol block where taken at room temperature after annealing (see below). All curves show a first-order peak at 6.7 nm for PI₆₀-*b*-(LPG₄-*hg*-PG₄), at 6.98 nm for PI₆₀-*b*-(LPG₄-*hg*-PG₁₀) and at 7.16 nm for PI₆₀-*b*-(LPG₄-*hg*-PG₁₉). This first order is illustrated by a ring (**Figure 2.D**) in the image of the detector. It can clearly be observed that the periodicity of this pattern increases only slightly with the weight fraction of the hyperbranched block. This can tentatively be explained by the fact that the increase in size of the dendritic block occurs in several directions, whereas in the case of a linear block it happens only in one direction. For this reason the spatial extension of the branched block is less affected by the degree of polymerization.

The presence of a first order reflection permits to conclude that there is supramolecular organization in the materials. However, this is not sufficient to determine the periodicity of the samples. Various methods have been employed in order to improve the self-assembly of the materials. First of all the samples were heated to enhance chain mobility and then cooled down slowly to stabilize the respective chain arrangement. The temperature was increased up to 100°C and then decreased slowly to -10°C, which is still above both glass transitions T_{g1} and T_{g2} . However, the chains should be less mobile than at 100°C. Above 60-70°C the hydrogen bonds formed by the hyperbranched polyglycerol block gradually weaken, as it is evident from infra-red spectroscopy (-OH bond), which could also help to generate the supramolecular arrangement. **Figure 2.A** shows the result of the annealing experiments. Unfortunately no further orders appear and only the scattering intensity of the first-order peak increased. The system may be problematic with respect to ordering due to the bulky shape of the hyperbranched block

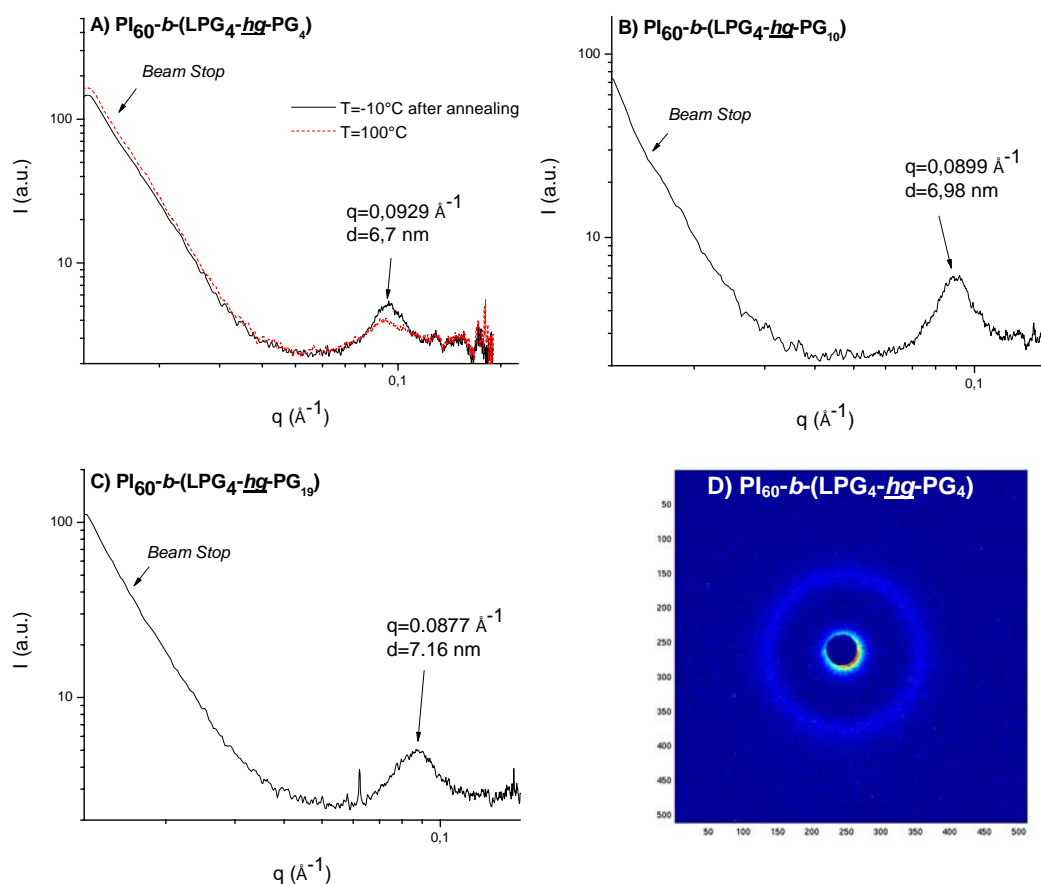


Figure 1. Small angle X-ray scattering (SAXS) diffractograms of A) $\text{PI}_{60}\text{-}b\text{-}(\text{LPG}_4\text{-}hg\text{-}\text{PG}_4)$; B) $\text{PI}_{60}\text{-}b\text{-}(\text{LPG}_4\text{-}hg\text{-}\text{PG}_{10})$; C) $\text{PI}_{60}\text{-}b\text{-}(\text{LPG}_4\text{-}hg\text{-}\text{PG}_{19})$. D) is the scattering pattern of $\text{PI}_{60}\text{-}b\text{-}(\text{LPG}_4\text{-}hg\text{-}\text{PG}_4)$ before integration.

The SAXS diffractograms of the block copolymer samples with PI_{162} are shown in **Figure 2**. Like for the PI_{60} samples a first-order peak is detected and the characteristic length ranges from 11.6 to 11.8 nm. This spacing increases with the size of the linear polyisoprene block, as expected. The samples were also annealed, as shown in **Figure 2.B** and no higher order reflections could be detected by this method. Like above the system may be frustrated.

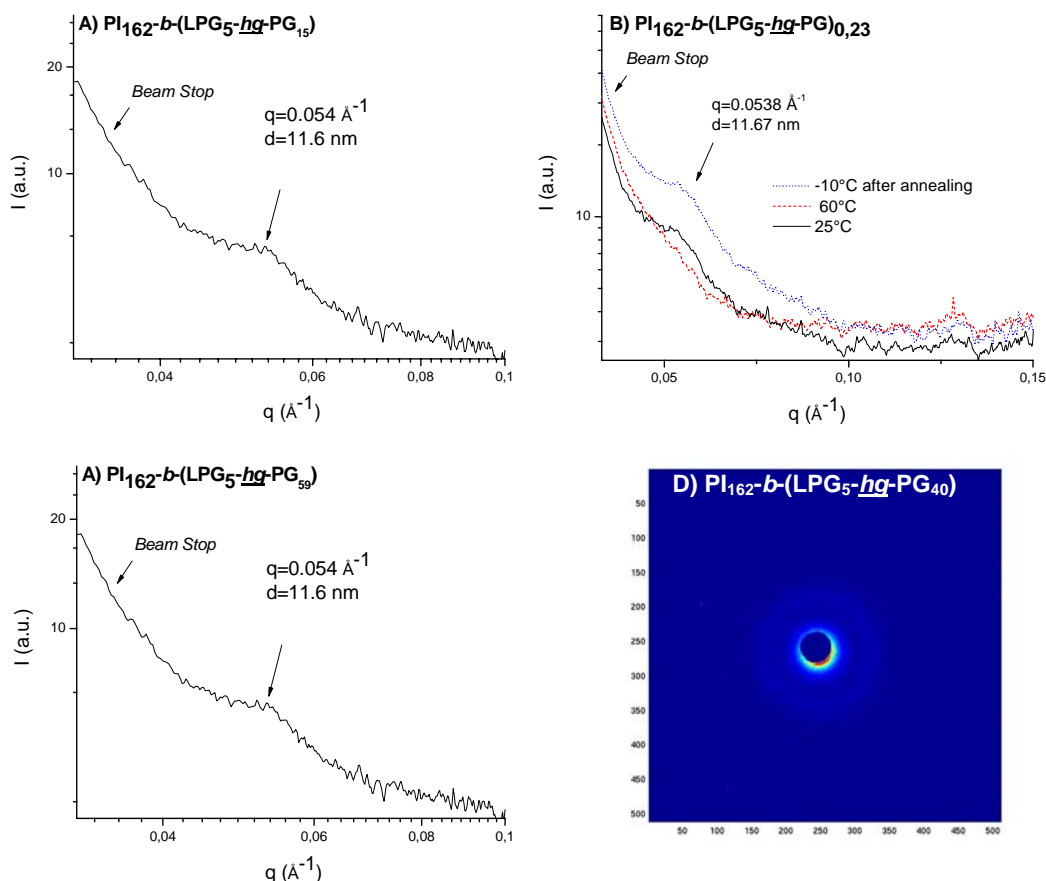


Figure 2. Small angle X-ray scattering (SAXS) diffractograms of A) $\text{PI}_{162}\text{-}b\text{-}(\text{LPG}_5\text{-}hg\text{-}\text{PG}_{15})$; B) $\text{PI}_{162}\text{-}b\text{-}(\text{LPG}_5\text{-}hg\text{-}\text{PG}_{40})$; C) $\text{PI}_{162}\text{-}b\text{-}(\text{LPG}_5\text{-}hg\text{-}\text{PG}_{59})$. D) is the scattering pattern of $\text{PI}_{162}\text{-}b\text{-}(\text{LPG}_5\text{-}hg\text{-}\text{PG}_{40})$ before integration.

The different data obtained with the $\text{PI}_x\text{-}b\text{-}(\text{LPG}_y\text{-}hg\text{-}\text{PG}_z)$ samples only give information on one periodicity present in the material. This is unfortunately not sufficient to determine any type of morphology. In the literature no examples of linear-dendritic block copolymers with polyisoprene as linear block are present. At least it is possible to compare this system with a linear AB diblock copolymer analog, polyisoprene-block-poly(ethylene oxide) ($\text{PI}\text{-}b\text{-}\text{PEO}$). The solid-state behavior of $\text{PI}\text{-}b\text{-}\text{PEO}$ has been studied and the phase diagram has been established in 2001.⁷ Five different ordered phases have been identified. According to these results the following samples (based on the composition of the BC) would have the following morphologies: $\text{PI}_{162}\text{-}b\text{-}(\text{LPG}_5\text{-}hg\text{-}\text{PG}_{15})$ a body-centered cubic lattice (bcc) and $\text{PI}_{162}\text{-}b\text{-}(\text{LPG}_5\text{-}hg\text{-}\text{PG}_{59})$ a hexagonal phase. However, in none of these samples an ordered phase was observed. Both systems differ in the architecture and also in their thermal behavior. PEO is a semicrystalline polymer and hyperbranched PG is an amorphous polymer. In the case of $\text{PI}_x\text{-}b\text{-}(\text{LPG}_y\text{-}hg\text{-}\text{PG}_z)$, both blocks are amorphous and at room

temperature they are above their T_g . The combination of the bulky polar head group and thermal behavior (amorphous state) may prevent the system from relaxing. In summary, these materials behave more like a complex liquid with some polydomain structures and no longer range correlation.

7.3 Polystyrene-*block*-(1,2-polybutadiene-hypergrafted-polyglycerol)

The polystyrene-*block*-(linear polyglycerol-hypergrafted-polyglycerol) samples presented in section 5.2 have also been characterized in their solid state by DSC, SAXS and TEM. The materials are solid and become slightly viscous as the weight fraction of the hyperbranched block increases. The polymers could be investigated in glass capillaries via X-ray diffraction measurements. All samples were annealed prior to measurements: heated up to 150°C (at 5°C/min) and then cooled down slowly to room temperature. The number average molecular weights of the samples ranges from 60,100 to 77,580 g·mol⁻¹. According to the DSC results all of the amphiphilic block copolymers show phase segregation (**Table 2**).

Table 2. Results from the DSC measurements after heating-cooling-heating cycle (10°C/min).

	T_{g1} (°C)	T_{g2} (°C)	Comment
PS ₅₀₈ - <i>b</i> -(PB-OH) ₅₆		107	-
PS ₅₀₈ - <i>b</i> -(PB ₅₆ - <u>hg</u> -PG ₄₄)	-12	61	Phase segregation
PS ₅₀₈ - <i>b</i> -(PB ₅₆ - <u>hg</u> -PG ₈₆)	-25	71	Phase segregation
PS ₅₀₈ - <i>b</i> -(PB ₅₆ - <u>hg</u> -PG ₂₈₀)	-25	40	Phase segregation

Figure 3 shows the SAXS diffractogram of the sample PS₅₀₈-*b*-(PB₅₆-hg-PG₄₄). Bragg reflection peaks are visible, but they are weak and located within the beam-stop. They suggest the presence of an ordered morphology in the sample, but this is not sufficient. The sample was stained with osmium tetroxide to introduce contrast in the electron beam of TEM. However, it was not possible to visualize any clear morphological arrangement. These observations may indicate that the sample is not within the strong segregation limit (SSL).

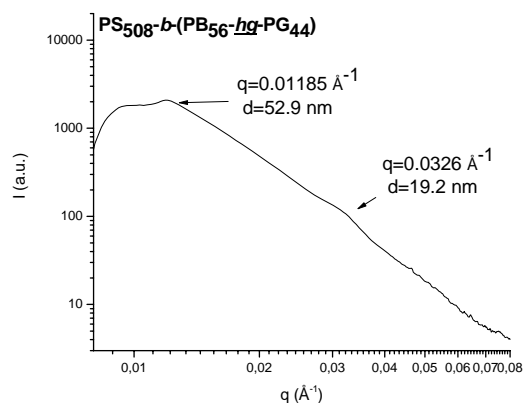


Figure 3. Small angle X-ray scattering (SAXS) diffractograms of $PS_{508}\text{-}b\text{-}(PB_{56}\text{-}hg\text{-}PG_{44})$ with a sample-detector distance of 80 cm.

For the next sample $PS_{508}\text{-}b\text{-}(PB_{56}\text{-}hg\text{-}PG_{86})$, SAXS and TEM were performed (**Figure 4**). Three reflections are detected by SAXS. In the TEM image the light regions correspond to the hyperbranched polyglycerol block and the darker areas to the linear polystyrene-block. The micrograph is similar to a disordered, phase-segregated morphology. A similar image was obtained for a [G-4.5] poly(ethylene oxide)-*block*-(*dend*-poly(ethylene imine)) by Hammond et al.⁸ The disordered phase in this linear-dendrimer system is found for higher dendrimer weight fraction than in the case of the sample $PS_{508}\text{-}b\text{-}(PB_{56}\text{-}hg\text{-}PG_{86})$. The nature of the segments in the both systems is different. Various parameters depending on the composition of the block copolymers may influence the self-assembly mechanism.

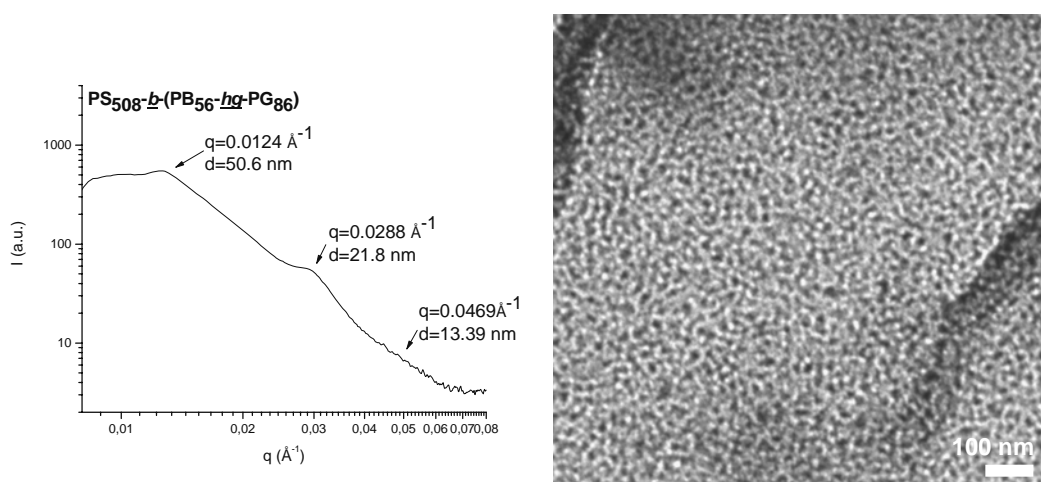


Figure 4. Small angle X-ray scattering diffractograms (*left*) and transmission electron microscopy (*right*) after staining with osmium tetroxide and dry cutting of $PS_{508}\text{-}b\text{-}(PB_{56}\text{-}hg\text{-}PG_{86})$.

The last sample $\text{PS}_{508}\text{-}b\text{-(PB}_{56}\text{-}hg\text{-PG}_{280})$ shows well-developed order and SAXS reflections up to the fourth order could be detected. The TEM micrograph (**Figure 5**) after staining of the sample supports the presence of some domains with regular lamellar structure. It is interesting to note that the linear-hyperbranched amphiphilic block copolymer $\text{PS}_{508}\text{-}b\text{-(PB}_{56}\text{-}hg\text{-PG}_{280})$ presented here has the ability to order in the bulk. This is surprising since the hyperbranched polyglycerol block is a strongly hydrogen-bonding structure, which can impede the self-assembly in the solid-state. A comparison with literature shows that for $\text{PS-}b\text{-(dend-PPI)}$, an analogous linear-dendrimer system, an increase of the size of the polar head group induced phase separation, which could be detected for the generations [G-4] and [G-5].⁶ Unfortunately the authors did not publish detailed results on the solid-state morphology beyond these claims.

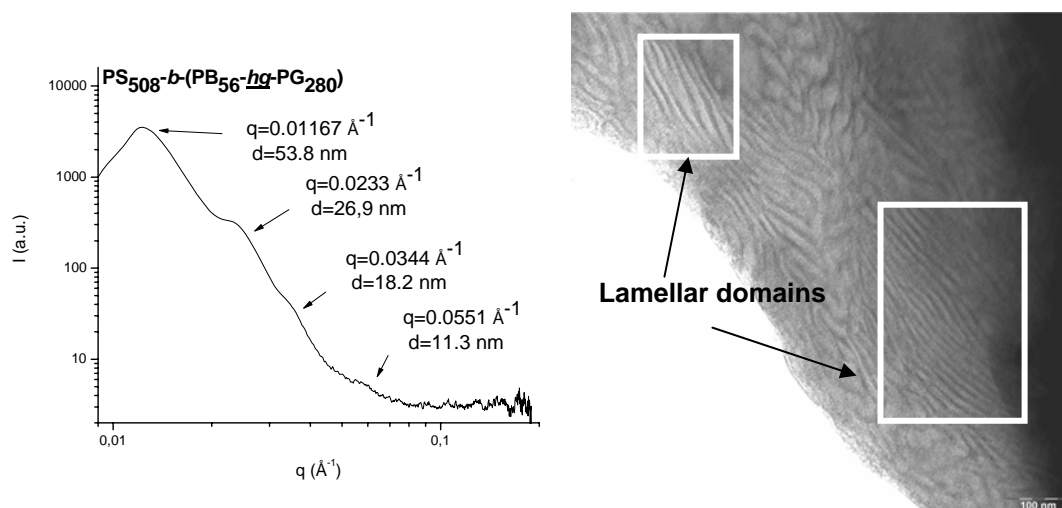


Figure 5. Small angle X-ray scattering diffractograms (*left*) and transmission electron microscopy (*right*) after staining with osmium tetroxide and dry cutting of $\text{PS}_{508}\text{-}b\text{-(PB}_{56}\text{-}hg\text{-PG}_{280})$.

The theoretical and experimental values for the d^* -spacing of the different orders in the case of a lamellae morphology are given in **Table 2**. TEM micrograph shows lamellar domains perpendicular to the surface. The lamellar long period is determined to be 53.8 nm, which is reasonable when taking into account the molecular weight of the sample ($77,580 \text{ g}\cdot\text{mol}^{-1}$).

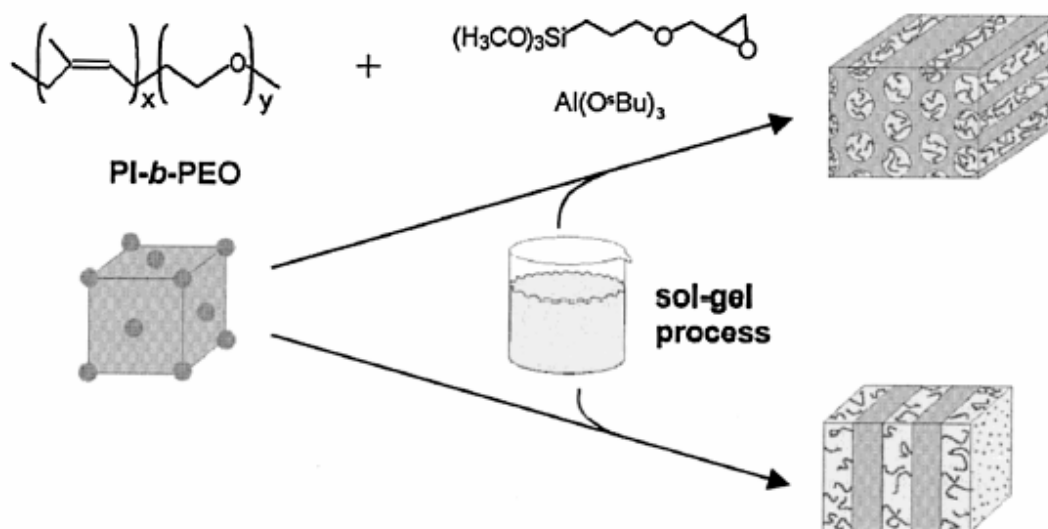
Table 2. Theoretical and experimental values of the d^* -spacing for the lamellae morphology of PS₅₀₈-*b*-(PB₅₆-*hg*-PG₂₈₀) according to Bragg.

Order	Theoretical d^*	Experimental d^*
1	53.8 nm	53.8 nm
2	26.9 nm	26.9 nm
3	17.9 nm	18.2 nm
4	13.45 nm	11.9 nm

7.4 Inorganic-organic silica nanohybrids

One of the most investigated areas of research in material science is the control of the size and the shape of inorganic materials like in the biomineralization.⁹ Different pathways for the preparation of organic-inorganic hybrid materials (nanohybrids) were developed recently. A convenient strategy is the use of block copolymers as structural templates for the preparation of nanohybrids. For example silica nanohybrids can be fabricated by using PI-*b*-PEO block copolymers as structure-directing molecules. As mentioned above, PI-*b*-PEO materials are known as well-organized phase-segregated block copolymers. The strategy is based on the amphiphilic character of the block copolymers and the low glass transition temperature of the hydrophobic PI-block. The fabrication of the nano-objects is a multi-step synthesis: (i) formation of a sol-gel mixture containing the inorganic compound, (ii) dispersion or solvation of the block copolymer in the mixture, (iii) deposition on a substrate, evaporation of the solvents and curing of the film. As the inorganic part is in contact with the self-assembled block copolymer, it will swell only one block selectively. The film is finally cured in order to degrade the block copolymer and a highly ordered pattern of inorganic is observed. The block copolymer will direct the subsequent organization of the inorganic depending on its morphology.

This method is well established for silica systems employing (3-glycidioxypropyl)trimethoxysilane (Glymo) and aluminum sec-butoxide (Al(OsBu)₃) as sol-gel mixture and PI-*b*-PEO block copolymer (**Scheme 1**). Variation of the architecture of the block copolymer remains an interesting point, since it can lead to new morphologies.



Scheme 1. Schematic drawing of Wiesner's approach for synthesizing ordered hybrid materials: morphology of the precursor polymer (*left*); resulting morphologies after addition of various amounts of metal alkoxides (*right*). (Simon, P. F. W.; Ulrich, R.; Spiess, H. W.; Wiesner, U. *Chem. Mater.* **2001**, 13, 3464).

The linear-hyperbranched $\text{PI}_x\text{-b}(\text{LPG}_y\text{-hg-PG}_z)$ samples presented in chapter 5 were used for the preparation of hybrid materials with Glymo and $\text{Al}(\text{O}^i\text{Bu})_3$. The experiments were performed at Cornell University (USA) as part of a scientific collaboration. As shown above, the materials did not show high order in the solid-state, which renders the fabrication of ordered silica nanostructures more difficult. Different parameters were varied during this study: concentration, size of the inorganic particles (diameters from 3 to 10 nm) as well as the solvent evaporation process.

Figure 6 (top) shows the AFM micrograph of the film formed after deposition of the sol-gel mixture and the block copolymer $\text{PI}_{162}\text{-b}(\text{LPG}_5\text{-hg-PG}_{40})$. The film is very heterogeneous, and no ordered domains are observed. Clearly, the inorganic part is not incorporated in the hyperbranched polyglycerol block (phase segregation between the silica particles and the block copolymer was observed). The block copolymer seems to form very large aggregates on the surface. After the heat treatment at 500°C the block copolymer is removed and only the randomly distributed silica particles remain on the surface (**Figure 6** bottom). One possible explanation may be that the high density of the hyperbranched block prevents the swelling of the inorganic fraction in this block. The silica particles (even for 3 nm diameter) are too large to enter into the multiple branches of polyglycerol and phase-segregation takes place. The experiments were repeated with the precursor molecules and not the silica

particles (from the sol-gel mixture). Unfortunately other parameters were affected by these changes like the kinetics of the reaction between Glymo and $\text{Al}(\text{OsBu})_3$ and no arranged pattern could be obtained.

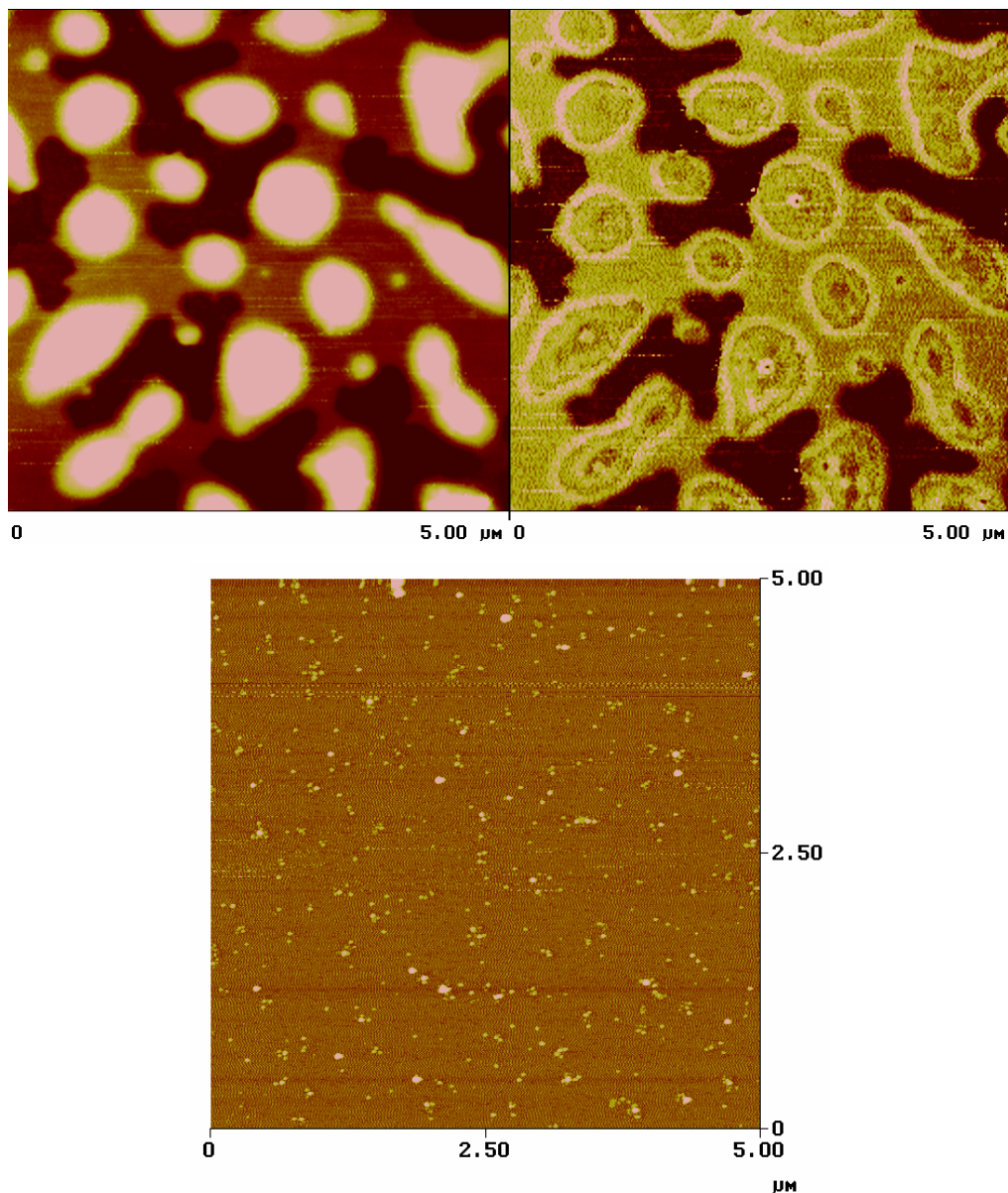


Figure 6. AFM micrograph of the film formed $\text{PI}_{162}\text{-}b\text{-}(\text{LPG}_5\text{-}hg\text{-}\text{PG}_{40})$ in presence of the inorganic (Glymo and $\text{Al}(\text{OsBu})_3$) (*top*) and after removal of the block copolymer by heat treatment (*bottom*) (mica, tapping mode).

7.5 Conclusion

The bulk morphology of the linear-hyperbranched block copolymer consisting of a linear polyisoprene or polystyrene block and a hyperbranched polyglycerol block has been investigated. The linear-hyperbranched block copolymers containing polyisoprene only show one reflection in SAXS measurements which means that the materials did not form ordered morphology in the solid-state. These materials behave like complex liquids due to the low T_g and the disordered nature of both components. The bulk morphology of the polystyrene-block-(1,2-polybutadiene-hg-polyglycerol) samples has also been investigated. Only the sample with 27% wt. hyperbranched polyglycerol forms some domains showing lamellae. Like in solution well-defined structures are achieved with increasing ratio of the hyperbranched block. The same observation was already reported for the linear-dendrimer system (PS-*b*-(*dend*-PPI)), an analogous block copolymer.⁶ Finally the fabrication of inorganic nano-objects using PI_x -*b*-(LPG_y-hg-PG_z) materials as structure-directing block copolymers has been reported. Unfortunately these block copolymers were not suitable for this application, since the branches may impede the integration of the inorganic in the hydrophilic block (high density).

These preliminary results on the self-assembly of amphiphilic linear-hyperbranched block copolymers in bulk are very interesting, since it is the first study on such materials. These materials organize nicely in solution (chapter 6) due to the presence of highly multifunctional hydrophilic block and due to the specific architecture of the branched block resembling to low molecular weight surfactants. Since the hyperbranched polyglycerol block is bulky and possesses dense hydroxyl groups, it is difficult for the structure to self-organize in bulk.

7.6 Experimental part

Materials. (3-glycidyloxypropyl)trimethoxy silane (Glymo) and aluminum *sec*-butoxide ($Al(O\textit{s}Bu)_3$) were purchased by Aldrich and placed under controlled nitrogen atmosphere in a glove box. Potassium chloride, THF, chloroform and 0.01M acid chloride were used as received from Aldrich.

Preparation of nanohybrids. 0.5 g of the block copolymer was dissolved in 5g chloroform and 5 g THF (solution A). The solution was stirred for an hour. 5.3 g of Glymo and 1.4 g of $\text{Al}(\text{OsBu})_3$ were stirred together in a beaker placed in an ice-bath (solution B). 0.04 g of KCl is added to the solution B. After 5 minutes stirring 0.27 ml of 0.01M acid chloride HCl is added and the solution B is stirred for 15 minutes. The solution is warmed up to room temperature (about 15 minutes). Then 1.7 ml of 0.01M HCl is added again and the solution B is kept stirring for 20 minutes more. Finally 2ml of solution B are removed with a syringe. A filter (Millipore 0.45 μm) is placed at the end of the syringe.

The desired amount of solution B (depending of the composition of the block copolymer and the expected morphology) is then added to the solution A containing the block copolymer. This final solution is stirred for an hour and then pour into a petri-dish (aluminum, teflon or glass) cover with aluminum foil with many holes. The solvent is evaporated on the hotplate at 50°C during 1 hour or until all the solvent is gone.

The material is then backed an additional hour at 130°C in vacuum oven. The film can be characterized using SAXS or TEM. To visualize only the inorganic part the film is heated up to 500°C for 4 hours and then slowly cooled down.

7.7 References

- (1) Bates, F. S.; Fredrickson, G. H. *Phys. Today*. **1999**, 32-38.
- (2) Hamley, I. *The Physics of Block Copolymers*; Oxford University Press: Oxford, U.K., 1998.
- (3) Calleja, F. J. B.; Roslaniec, Z. *Block Copolymers*; Marcel Dekker, 2000.
- (4) Bates, F. S.; Fredrickson, G. H. *Annu. Rev. Phys. Chem.* **1990**, *41*, 525.
- (5) van Hest, J. C. M.; Baars, M.; van Genderen, M. H. P.; Meijer, E. W. *Science* **1995**, *168*, 1592.
- (6) van Hest, J. C. M.; Delnoye, D. A. P.; Baars, M.; Elissen-Román, C.; van Genderen, M. H. P.; Meijer, E. W. *Chem. Eur. J.* **1996**, *2*, 1616.
- (7) Floudas, G.; Vazaiou, B.; Schipper, F.; Ulrich, R.; Wiesner, U.; Iatrou, H.; Hadjichristidis, N. *Macromolecules* **2001**, *34*, 2947.

- (8) Santini, C. M. B.; Johnson, M. A.; Boedicker, J. Q.; Hatton, T. A.; Hammond, P. T. *J. Polym. Sci., Part A: Polym. Chem.* **2004**, *42*, 2784.
- (9) Lowenstam, H. A.; Weiner, S. *Biomineralisation*; Oxford University Press: New York, 1989.

8. Negatively charged hyperbranched polyglycerol polyelectrolytes

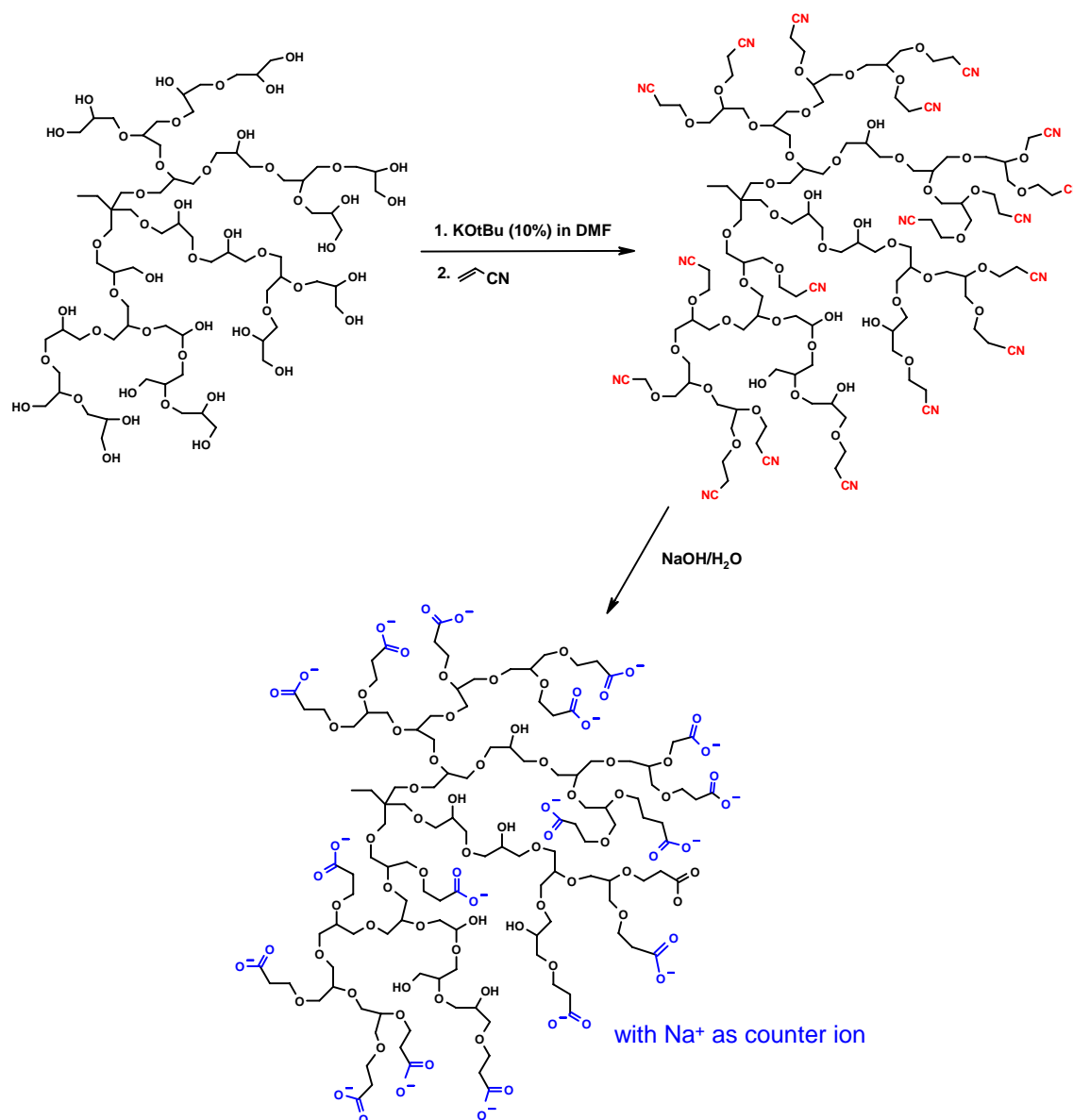
8.1. Introduction

Macromolecules carrying electrostatic charges (negative or positive) are commonly termed “polyelectrolytes”. These materials are important in numerous areas, e.g., to control the stability and rheology of complex fluids. In nature, many important biological molecules (proteins, DNA...) are polyelectrolytes. They play a major role in regulation reactions and also in biomineralization processes. The development of polyelectrolytes has become a topic of broad interest, since these polymers exhibit particular properties in aqueous solution by influencing the fluid characteristics of aqueous suspensions and slurries, modification of the surface charge of neutral particles via adsorption, and strong interaction with ions and colloidal aggregates of opposite charge. They find applications in various domains: coatings, thickeners, dispersants, soap and detergent additives, ion-exchange resins etc...

Functional dendrimers have been extensively developed with respect to specific properties.¹ In addition to the multi-step synthesis for the preparation of dendrimers, functionalization of the periphery has to be highly efficient and selective. Polyamino dendrimers (poly(propylene imines))²⁻⁴ were successfully converted into polynitriles via Michael addition. The dendrimer-periphery could be fully converted and a subsequent hydrolysis step leads to carboxylic groups. The method has been reported to be successful for the preparation of amphiphilic linear-dendritic block copolymers.⁵ In this chapter a convenient pathway for the modification of the hydroxyl end groups of hyperbranched polyglycerol into carboxylic acid groups will be presented. The solution properties of these new hyperbranched polyelectrolytes in aqueous solution will be discussed. Finally these materials will be used for the preparation of ultrathin multilayer films and hybrid organic/titanium dioxide nanostructures by the layer by layer deposition strategy.

8.2. Synthesis

Hyperbranched polyglycerol can easily be modified via the hydroxyl end groups. The reactions employed for the functionalization should lead to a high degree of conversion, the compounds have to stay soluble in the medium and the work-up has to be convenient. Modification into carboxylic groups was achieved via Michael addition reaction followed by hydrolysis, as shown in **Scheme 1**.



Scheme 1. Synthesis of carboxylated hyperbranched polyglycerol via Michael addition followed by hydrolysis.

In the first step the hydroxyl groups are converted into nitrile groups, and the polymeric materials obtained are hydrophobic. Hyperbranched polyglycerol was dissolved in DMF and partially deprotonated (10% mol. of the hydroxyl groups). The

reaction was carried out in a reactor with a double envelope in order to regulate the temperature. During addition of acrylonitrile the temperature was kept under 0°C in order to control the reaction. The materials were precipitated twice from acetone solution into methanol. The products are viscous and brown. The glass transition temperature of the polymer is not affected by the functionalization; it stays around -20°C.

In the second step, the nitrile groups are hydrolyzed with hydrogen peroxide in presence of sodium hydroxide and the materials become soluble in aqueous solution. The carboxylated products are then precipitated in diethyl ether. The carboxylated hyperbranched polyglycerols are solid, yellow materials. They were purified by dialysis in water.

Figure 1.A shows the different ^1H NMR spectra of hyperbranched polyglycerol. The signals between 3.3 and 3.8 ppm are assigned to the polyether protons. Resonances at 0.8 ppm are due to the methyl group, and signals at 1.3 ppm stem from the methylene group of the initiator-core TMP. After the Michael addition reaction the 2 protons next to the nitrile group are visible at 2.7 ppm (**Figure 1.B**). This signal is shifted to 2.4 ppm after hydrolysis (**Figure 1.C**). Elemental analysis has also been performed in order to trace the percentage of nitrogen before and after hydrolysis.

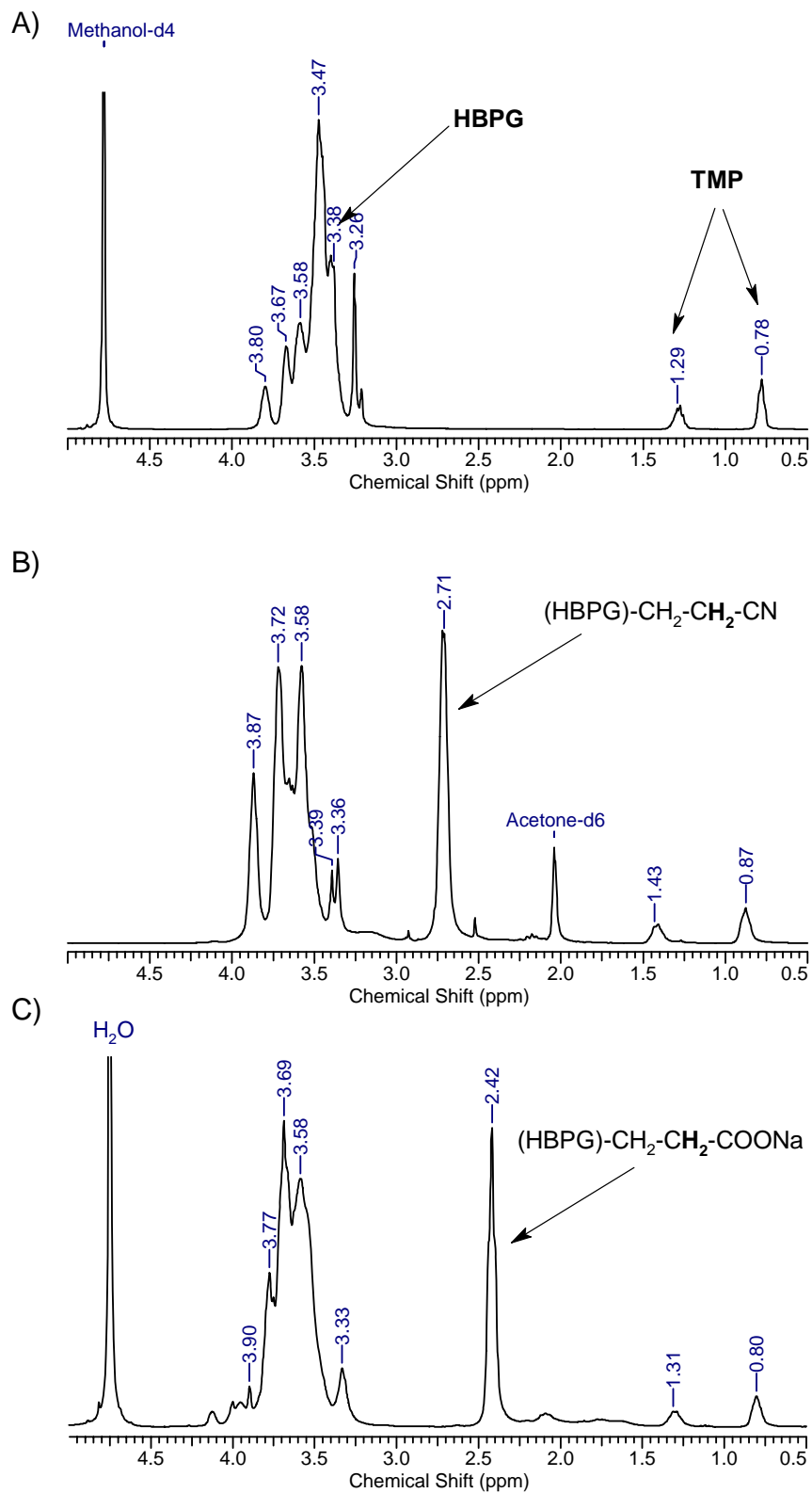


Figure 1. ¹H NMR spectra of A) PG₁₅ in d₄-methanol and B) HBPG₁₅CN₁₃ in d₆-acetone-; C) sample 2 in D₂O.

The ^{13}C NMR spectrum of the carboxylated hyperbranched polyglycerol (Figure 2) also shows the expected signals: 180 ppm for the carboxylic group and 37 ppm for the carbon next to this group.

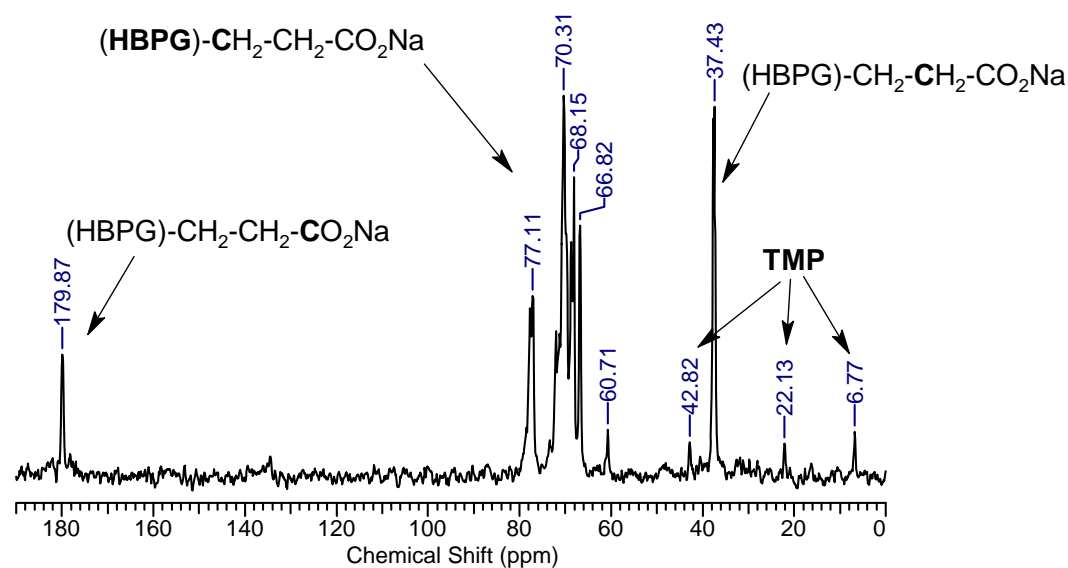


Figure 2. ^{13}C NMR spectrum of sample 2 in D_2O .

A series of hyperbranched polyglycerols with different molecular weights were functionalized (**Table 1**). For the samples 1 and 2 the degree of modification is between 80 and 90% and around 90% for the samples 3 and 4 (higher molecular weights). As expected, the degree of conversion decreases as the molecular weight increases. The reaction of the hydroxyl of the interior of the hyperbranched architecture is more difficult than of the ones present at the periphery. They are less accessible and this phenomenon is affected by the molecular weight, similar to the difficulties encountered when functionalizing the interior of dendrimer structures. In this context, it is interesting to note that the samples possess some remaining hydroxyl groups. This can be interesting in the case of encapsulation applications. These groups may act, e.g., as anchors for guest molecules.

The hyperbranched polynitriles are also interesting for the conversion into other functional groups such as amine groups after reduction. This is then the analogue of the PPI dendrimers.²⁻⁴ This strategy was realized for the preparation of polyamines and positively charged hyperbranched polyelectrolytes with polyammonium structures.

Table 1. Characterization data of the carboxylated hyperbranched polyglycerols (HBPG). The values have been obtained from ^1H NMR spectra; \overline{M}_n values are given in $\text{g}\cdot\text{mol}^{-1}$.

	HBPG		Carboxylated HBPG		% Modif.
	\overline{M}_n	OH groups/polymer	COO^-Na^+ groups/polymer	\overline{M}_n	
1	520	8.2	6.4	970	78%
2	1,030	15.1	13.5	2,280	89,4%
3	2,880	40.1	22.5	4,140	56,1%
4	6,480	89.7	55	10,220	62%

8.3. Solution properties

The solution properties of these hyperbranched polyelectrolytes have been studied by dynamic light scattering (DLS) and atomic force microscopy (AFM). All samples exhibit good solubility in aqueous solution at a large range of pH values. As the molecular weight increases, the solubility in methanol decreases (effects of the multiple charges).

The DLS results for the sample **3** are summarized in **Table 2**. At basic, neutral and acidic pH the data always show two modes of distribution. It seems that in solution the unimolecular hyperbranched carboxylated polymers (D_1), unimers, coexist with large aggregates (D_2). The values of D_1 have to be taken carefully, because they are extrapolated for D_0 in a domain near the noise level of the equipment. It is only possible to conclude that these unimers do not show any strong dependence on concentration and pH.

The second size distribution (D_2), aggregates, shows a clear dependence on pH and concentration. The carboxylic groups become more dissociated, as the pH decreases, which leads to a decrease of the size of the aggregates. Clearly, the charges promote aggregation, which is a consequence of enhanced amphiphilicity of the resulting structures. The concentration also influences the size of the aggregates, but this effect is not as strong as the influence of the pH value. Measurements at lower concentration (until 0.02 g/l) did not permit to observe only the unimers' mode. Aggregation is a dominant mechanism even at low concentration.

Table 2. Dynamic light scattering data of the carboxylated hyperbranched polyglycerol sample **3**. D_1 and D_2 correspond to the unimolecular and the aggregates of the hyperbranched carboxylated polymers.

Concentration ($g \cdot l^{-1}$)	pH	D_1 (nm)	D_2 (nm)
2	10	1.8	168.9
2	7	2.4	138.5
2	2	1.1	98.2
1	10	4.3	152.9
1	7	9.3	105.6
1	2	2.5	73.6

Tapping-mode AFM measurements for the samples **1** (**Figure 3**) and **3** (**Figure 4**) were performed after deposition on mica, a negatively charged substrate. The sample solutions were prepared at different pH in all cases at the concentration of $1 \text{ g} \cdot \text{l}^{-1}$ and spin-coated. Sample **1** (from HBPG $520 \text{ g} \cdot \text{mol}^{-1}$) in acidic conditions shows very small conglomerates of spherical particles (2-3 nm in height), sometimes with beads-on-string morphology. This aggregation occurs in solution, as the DLS results show. At pH 2, unimers are more collapsed (and therefore higher – 2-3 nm), presumably due to intramolecular hydrogen bonding. At pH 7 small particles, the AFM-images show structures less than 1 nm in height co-existing with large aggregates (10 nm in height). Unimers display extended conformation, since they are partially ionized (several Å in height). At pH 10 formations of extended and highly ordered terrace structures of about 1.5 nm in the height can be observed. Fragments of bilayers are also observed. Obviously, such terraces form upon evaporation of solvent for sample **1**. Similar structures do not exist at pH 7. This shows that for ordered aggregation the macromolecules should be in the fully extended (open) conformation to minimize intramolecular interaction, which leads to a collapse of the unimers and maximizes intermolecular interactions. All measurements were performed on a strongly charged substrate and in the case of charged materials (at pH 10 and partially at pH 7) adsorption is not favorable onto a surface with similar charges. This may explain why the surface is not fully covered with the first monolayer as the next monolayer already starts to be formed. Also this adsorption mode (adsorption onto similarly charged surface) can strongly complicate the mechanism of adsorption and its interpretation. The formation of a rather flat monolayer is unprecedented in the area of

hyperbranched polymers. And this is certainly a consequence of the low polydispersity of the materials.

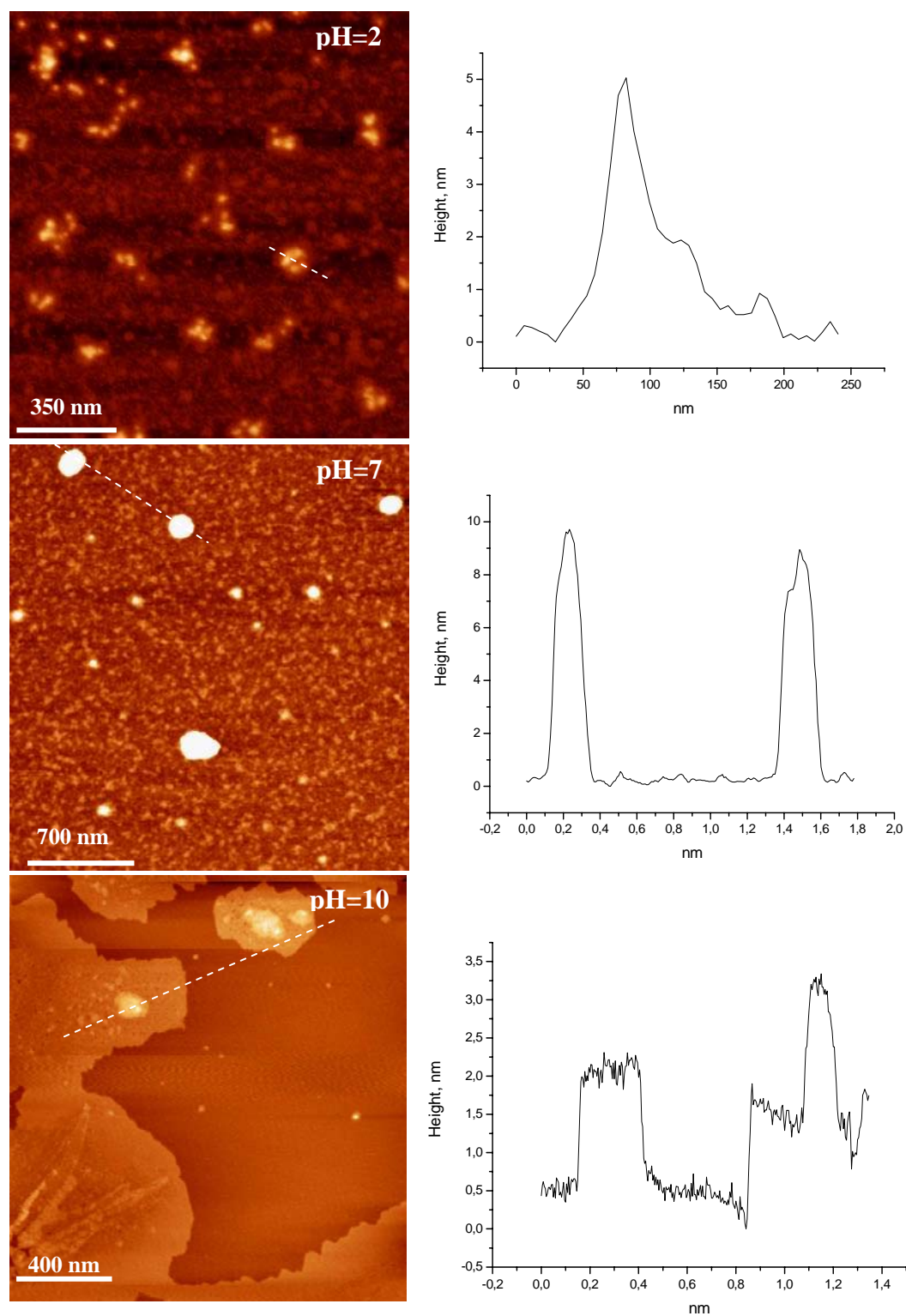


Figure 3. AFM-micrograph (*left*) with corresponding height profile (*right*) of sample 1 (from HBPG $520 \text{ g}\cdot\text{mol}^{-1}$) from an aqueous solution ($1 \text{ g}\cdot\text{l}^{-1}$) at different pH (2, 7 and 10) on a mica substrate (tapping mode).

The sample **3** (from HBPG 2,880 g·mol⁻¹) forms aggregates upon adsorption at pH 2 (diameter is about 100-300 nm, height is about 3-5nm). These structures are arranged not regular (particularly regarding their distance) as charged micelles. On the other hand, the pattern observed can not be the result of coincidental adsorption. Also this arrangement can not be driven by charge repulsions, since the carboxylic acid groups are not ionized at pH 2, nor because of excluded volume interaction, since the distance between them is too large (ordering can occur in the case of closely packed particles). Therefore this material may either be molecularly dissolved in solution at pH 2 or exist as loosely connected swollen aggregates and may initially adsorb onto the surface. Thus, it covers the surface more or less fully. Then, upon water evaporation the material does not undergo only Z-collapse (in the vertical direction that leads to the dense layer) but also X-Y (lateral) collapse (“dewetting” like process). Thus, the film forms islands and their shrinkage occurs more or less with the same rate. In the case of toroids shrinkage may occur simultaneously from the center and from the periphery of the islands. Driving force can be strong inter/intramolecular attractions between carboxylic groups and polyether moieties. This mechanism is not sufficient to form intermolecular aggregates in the case of lower molecular weight (sample **1**).

At pH 7, sample **3** forms larger aggregates (up to 15 nm high), which exist in solution. These structures are not well-defined. They usually consist of a dense core and extended, stabilized shell. In this case these are low-density aggregates; the ratio diameter/height (500 nm large and 15 nm high) is 33, if assuming a near spherical geometry and merely Z-collapse upon drying. For Z-collapse of dense micelles the diameter/height ratio is usually considerably lower, for example 3.33 for polystyrene-*block*-poly(2-vinylpyridine).

In basic conditions smaller aggregates are observed, but they are arranged somewhat surprisingly: several particles of very different diameters are localized in close proximity, but are not connected to each other in most cases. Between such “populations” empty spaces are observed. This might reflect breaking of larger aggregates that existed in solution during the deposition onto several smaller ones.

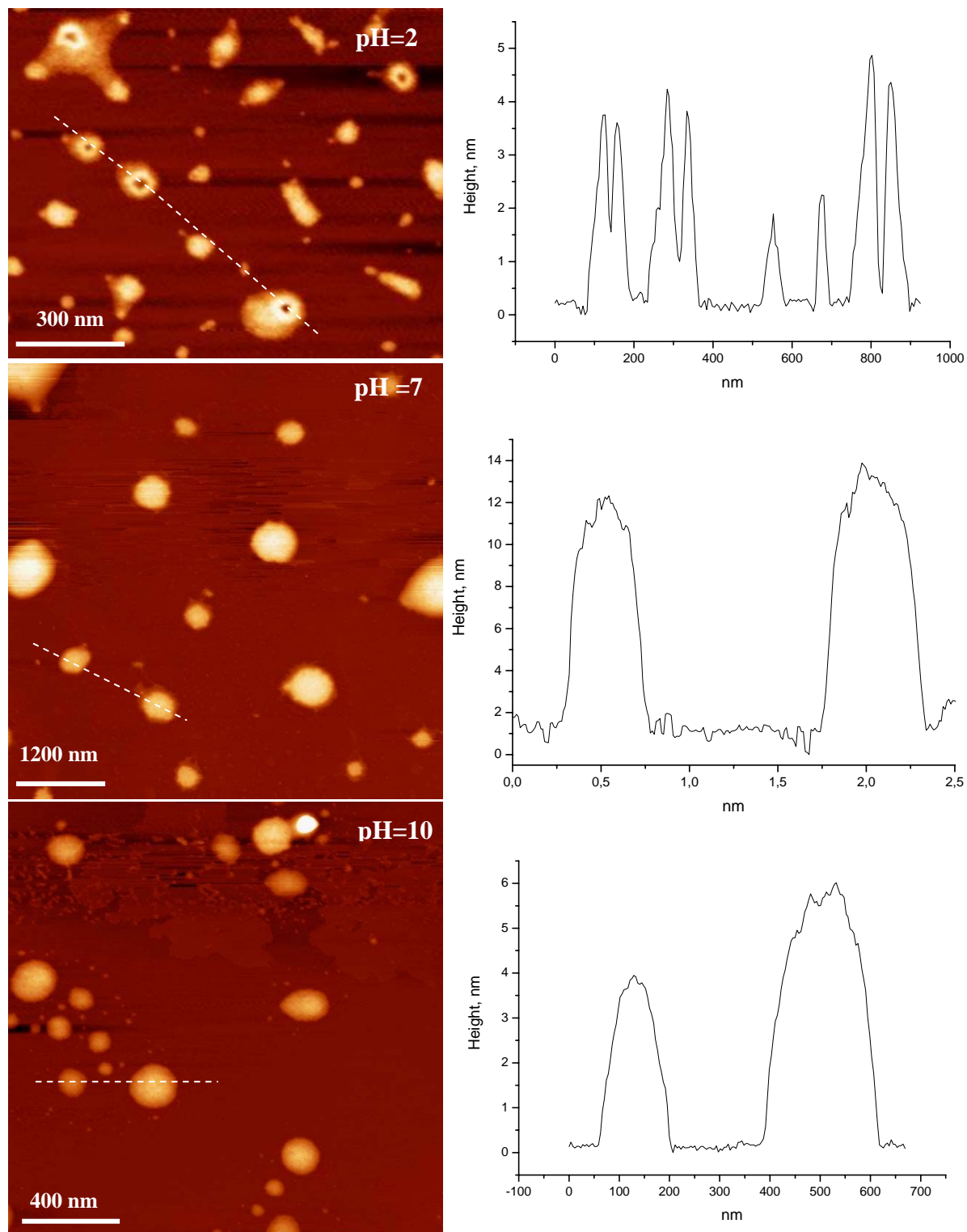
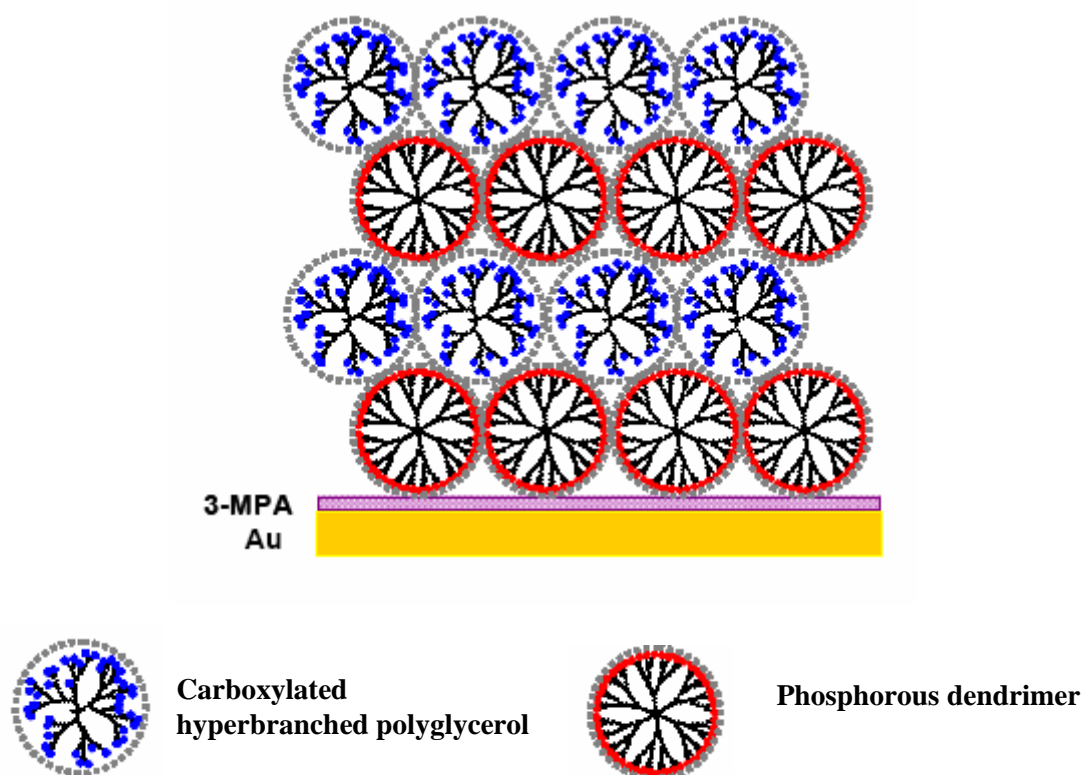


Figure 4. AFM-micrograph (*left*) with corresponding height profile (*right*) of sample 3 (from HBPG $2,880 \text{ g}\cdot\text{mol}^{-1}$) from an aqueous solution ($1 \text{ g}\cdot\text{l}^{-1}$) at different pH (2, 7 and 10), deposited on mica substrate (tapping mode).

8.4 Layer by layer deposition

Recently, the use of charged dendrimers as building blocks for the preparation of molecularly thin multilayer films driven by electrostatic layer-by-layer (LbL) self-assembly⁶⁻¹⁰ have been developed. However, the applications of such dendrimers for multilayers architectures or as templates for hybrid nanostructured materials are still limited.^{11,12}

In this section a route to the fabrication of multilayer thin films and hybrid organic/TiO₂ nanostructures by the LbL strategy combined with chemical vapor deposition (CVD) is described, using positively charged phosphorous dendrimers and negatively charged hyperbranched polyglycerols as building blocks. Such hybrid nanoarchitectures may find potential application in catalysis, sensors, optics and optoelectronics.¹³⁻¹⁵ Fabrication of the multilayer films was monitored by Surface Plasmon Resonance (SPR) spectroscopy, UV-visible spectroscopy, and X-ray reflectivity (XR) measurement. The physical properties of the hybrid films were investigated in terms of fluorescence characteristics. A schematic diagram of a multilayer composed of G₄(NH⁺Et₂Cl)₉₆ (fourth generation phosphorous dendrimer) and HBPG₅₀(COO⁻Na⁺)₄₄ (carboxylated hyperbranched polyglycerols with $\overline{DP}_n = 50$ and 44 carboxylic groups) is shown in **Scheme 2**. The G₄(NH⁺Et₂Cl)₉₆/HBPG₅₀(COO⁻Na⁺)₄₄ multilayers were prepared as follows: a gold layer was modified by adsorption of 3-MPA from an aqueous solution, providing a negatively charged surface onto which the first G₄(NH⁺Et₂Cl)₉₆ layer readily adsorbs. The substrate thus prepared was first immersed in a G₄(NH⁺Et₂Cl)₉₆ solution of a concentration $\sim 1.0 \text{ mg}\cdot\text{ml}^{-1}$ for 30 min, followed by 10 min rinsing with water. A HBPG₅₀(COO⁻Na⁺)₄₄ solution with the same concentration was then added into the sample-containing flow cell. After 50 min given for adsorption a rinsing step of 10 min was performed. The G₄(NH⁺Et₂Cl)₉₆ and HBPG₅₀(COO⁻Na⁺)₄₄ adsorption steps were repeated four times each to build multilayers on the Au-substrate.



Scheme 2. Schematic illustration of a multilayer composed of positively charged dendrimers and negatively charged hyperbranched polymers fabricated by layer-by-layer self-assembly onto a gold (Au) substrate modified by 3-mercaptopropionic acid (3-MPA).

The consecutive alternating deposition steps were monitored by in-situ SPR spectroscopy and the resulting kinetic mode SPR curve is shown in **Figure 5.A**. The red and blue curves indicate the addition of $G_4(\text{NH}^+\text{Et}_2\text{Cl})_{96}$ and that of $\text{HBPG}_{50}(\text{COO}^-\text{Na}^+)_{44}$, respectively. In between, the samples were carefully washed with deionized water (indicated by arrows) by which physically adsorbed molecules were removed, leading to a small decrease in intensity. It is clearly observed that the addition of each layer leads to a regular increase of the reflectivity up to 4 bilayers. **Figure 5.B** shows the scan mode SPR curves obtained from the stepwise, alternating deposition. The first scan curve (sky blue line) is due to the adsorption of 3-MPA on the Au surface. The red and blue curves indicate the addition of $G_4(\text{NH}^+\text{Et}_2\text{Cl})_{96}$ and that of $\text{HBPG}_{50}(\text{COO}^-\text{Na}^+)_{44}$, respectively. It is clearly observed that the addition of each layer leads to a regular increase of the resonance angle. The accumulated shift of resonance angle was converted into the geometrical film thickness with the refractive index of the dendrimer being ~ 1.457 and by assuming the index of HBP ~ 1.5 . The results are plotted as a function of the number of deposition step as shown in **Figure 5.C**. The plot shows a linear increase in film thickness during the alternating

deposition, and it is observed that the increment is larger at the dendrimer deposition step. The thickness increment per deposited double layer, $G_4(\text{NH}^+\text{Et}_2\text{Cl})_{96} + \text{HBPG}_{50}(\text{COO}^-\text{Na}^+)_{44}$, was calculated to be $\sim 13 \text{ \AA}$.

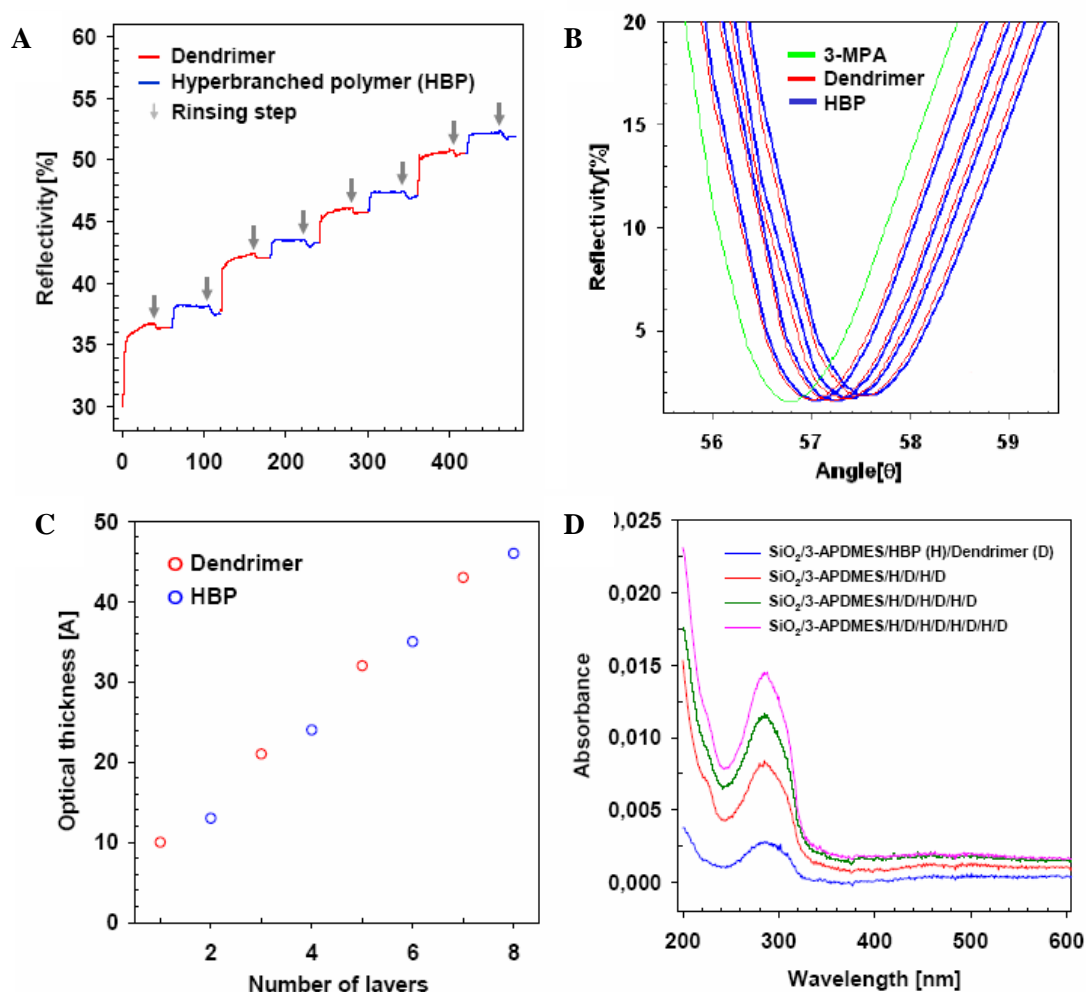


Figure 5. Kinetic mode (A) and scan mode (B) SPR profiles of the successive deposition of $G_4(\text{NH}^+\text{Et}_2\text{Cl})_{96}$ and $\text{HBPG}_{50}(\text{COO}^-\text{Na}^+)_{44}$ up to 4 bilayers. The red and blue curves represent the addition of $G_4(\text{NH}^+\text{Et}_2\text{Cl})_{96}$ and that of $\text{HBPG}_{50}(\text{COO}^-\text{Na}^+)_{44}$, respectively. In between each deposition, rinsing steps (indicated by arrows) removed small amounts of physically adsorbed material. The first step (sky blue curve) indicates the adsorption of 3-MPA onto an Au substrate. (C) Thickness of a four bilayer multilayer film [$(G_4(\text{NH}^+\text{Et}_2\text{Cl})_{96}/\text{HBPG}_{50}(\text{COO}^-\text{Na}^+)_{44})_4$] as a function of the number of deposited layers. Odd (red circle) and even layers (blue circle) are from $G_4(\text{NH}^+\text{Et}_2\text{Cl})_{96}$ and $\text{HBPG}_{50}(\text{COO}^-\text{Na}^+)_{44}$, respectively. (D) Monitoring the consecutive deposition of a four bilayer of $G_4(\text{NH}^+\text{Et}_2\text{Cl})_{96}/\text{HBPG}_{50}(\text{COO}^-\text{Na}^+)_{44}$ film onto a 3-APDMES modified SiO_2 substrate by UV-visible spectroscopy.

The growth of the multilayer with consecutive deposition steps was also monitored by UV-visible spectroscopy in the range of 200 ~ 600 nm, as depicted in **Figure 5.D**. A silicon dioxide (SiO_2) substrate was coated with 3-APDMES (3-aminopropyltrimethoxysilane) by placing the substrate in a closed glass vessel with a 3-APDMES reservoir at a temperature of 135°C for 3 h. The 3-APDMES layer

provides a positively charged surface, on which the first negatively charged HBP was directly deposited. The peak at ~ 285 nm is attributed to the π - π^* transition of the phenyl ring in the dendrimer molecules. The intensity of this peak exhibits a monotonic increase with the stepwise deposition, which is in good agreement with the results of the SPR spectroscopy.

Among the possible applications that these supramolecular multilayers may have, the capabilities of such films as scaffolds, by which hybrid organic multilayer/inorganic TiO₂ nanostructures are fabricated via chemical vapor deposition (CVD), have been explored. The strategy relies on a binary reaction mechanism between the TiCl₄ gas precursor and water molecules trapped inside the multilayers. Such a methodology has been shown to be a simple, facile route to generate TiO₂ nanoparticles in an organic matrix.¹⁶ For comparison, multilayers prepared from a salt containing dendrimer solution to control the porosity inside the films and utilized as templates were also fabricated. The effect of salt on the multilayers in terms of the permeability has been reported previously.¹⁷

The structural changes of the multilayers induced by the incorporation of the inorganic materials were investigated by X-ray reflectivity (XR) measurement. **Figure 6.A** shows the XR profiles of a four bilayer film prepared from pure water solutions (purple) and one prepared from a dendrimer solution containing 0.15M NaCl (pink). Since the total film thickness of a four bilayer film is on the order of ~ 5 nm according to the SPR results, a typical fringe pattern was not observed in the initial film. In contrast, an oscillating pattern appears in the salt-added multilayer film, indicating that the thickness of this film is larger than that of the salt-free film due to swelling effects.

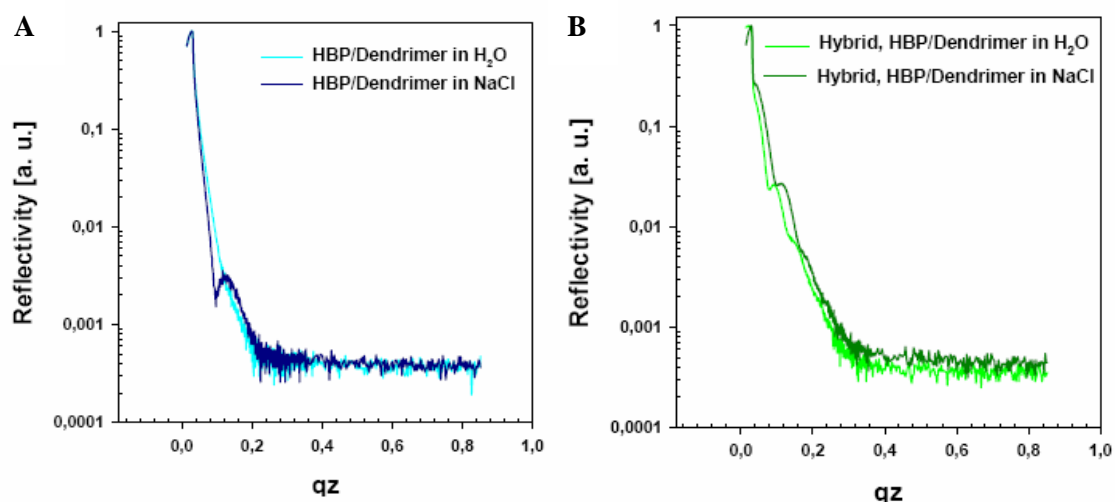


Figure 6. (A) X-ray reflectivity patterns of $(G_4(\text{NH}^+\text{Et}_2\text{Cl})_{96}/\text{HBPG}_{50}(\text{COO}^-\text{Na}^+)_{44})_4$ films prepared from pure water solutions (purple) and from salt-added dendrimer solution (pink), respectively. (B) X-ray reflectivity patterns of hybrid TiO_2 /multilayer films where $(G_4(\text{NH}^+\text{Et}_2\text{Cl})_{96}/\text{HBPG}_{50}(\text{COO}^-\text{Na}^+)_{44})_4$ films were prepared from pure water solutions (dark green) and from salt-added dendrimer solution (light green), respectively.

The XR profiles of the identical multilayer films (**Figure 6.A**) after reaction with TiCl_4 are displayed in **Figure 6.B**. It is clearly observed that the patterns of the hybrid multilayers change significantly, indicating that inorganic TiO_2 particles were successfully formed inside the films. The overall profile of the hybrid film prepared from a salt-added multilayer (light green) appears at higher angle, which is a characteristic feature of a film with a higher electron density, indicating that more amounts of TiO_2 were incorporated inside the swollen film. Here, a question may arise as to the distribution of TiO_2 inside the films. It appears that the TiO_2 particles are generated selectively in the HBP layers, considering the existence of hydroxyl groups in this building block. However, more in-depth analysis (e.g., cross-sectional TEM analysis) is being carried out to clarify this issue.

Of the various physical properties that these hybrid nanoarchitectures may exhibit, their photoluminescence (PL) properties are primarily interesting. **Figure 7** shows the PL spectra of the hybrid organic/ TiO_2 films prepared from salt-free (dark green) and salt-containing (light green) solutions, respectively, with an excitation wavelength of $\lambda = 350$ nm. It is clearly observed that the hybrid film prepared from a salt-containing precursor exhibits a noticeable characteristic emission due to the radiative recombination of self-trapped excitons localized within TiO_6 octahedra and oxygen vacancies.¹⁸ This verifies that the diffusion of TiCl_4 precursors into the interior of the

multilayer was facilitated in the swollen film, compared with the salt-free film, leading to the formation of larger amount of TiO_2 .

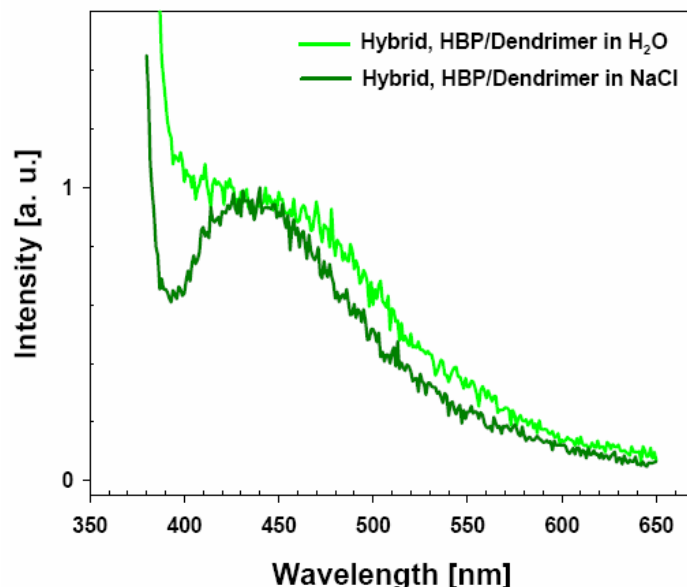


Figure 7. Photoluminescence ($\lambda=350$ nm) spectra of hybrid TiO_2 /multilayer films: The dark green and light green curves represent the profiles obtained from $(\text{G}_4(\text{NH}^+\text{Et}_2\text{Cl})_{96}/\text{HBPG}_{50}(\text{COO}^-\text{Na}^+)_{44})_4$ multilayers prepared from pure water solutions and from salt-added dendrimer solution respectively, after reaction with TiCl_4 .

8.5. Conclusion

The preparation of carboxylated hyperbranched polyglycerols was achieved by post-modification of the hydroxyl groups via Michael addition of acrylonitrile, followed by hydrolysis. High conversion could only be achieved for low molecular weight starting materials ($\text{HBPG } 520$ and $1,030 \text{ g}\cdot\text{mol}^{-1}$). The solution properties of such materials were investigated by DLS. The results show the formation of large aggregates with size depending on the pH value. After deposition on a negatively charge surface the structures observed by AFM show the coexistence of aggregates and unimers. In the case of the lower molecular weight sample ($\text{HBPG } 520 \text{ g}\cdot\text{mol}^{-1}$) extended and highly ordered terrace structures were formed, which can be of interest for specific deposition processes.

In the last part the materials were successfully employed for the fabrication of composite organic-inorganic multilayer thin films, using electrostatic layer-by-layer self-assembly coupled with chemical vapor deposition. The consecutive, alternating

deposition of multilayers led to linear growth behavior with increasing number of deposition steps. In order to generate TiO₂ moieties inside the multilayers, we exploited a binary reaction mechanism between water molecules trapped inside the film and TiCl₄ precursors. The amount of TiO₂ inside the films could be increased by increasing the porosity of the multilayers, which was controlled by adding a small amount of salts to the dendrimer solution. The resulting hybrid films exhibited characteristic photoluminescence properties.

8.6. Experimental part

Materials. Acetone, methanol, *tert*-butoxide, sodium hydroxide, sodium sulfite and 30% weight H₂O₂ solution were used as received from Fluka. Acrylonitrile and DMF were obtained from Fluka and distilled prior to use. For the layer-by-layer deposition, 3-Mercaptopropionic acid (3-MPA) was used as received from Aldrich. 3-aminopropyldimethylethoxysilane (3-APDMES) was purchased from ABCR GmbH.

Preparation of 3-(O-Polyglycerol)propanenitrile. Hyperbranched polyglycerol (500 mmol) was placed in a reactor and dissolved in 15 ml absolute DMF under argon atmosphere. Potassium *tert*-butoxide was added to the polymer solution to achieve 10% deprotonation of the hydroxyl groups. The reaction mixture was stirred and heated up to 80°C for 4 hours and then cooled down to 0°C. Distilled acrylonitrile (61 mmol) was slowly added via a syringe to the reactor and the temperature was kept at 0°C. After 4 hours the reactor was heated up to 5°C, the solution became slightly red. The reaction mixture was kept for another 20 hours at 5 °C and finally 48 hours at room temperature. Then 1 g of a cationic exchange resin was added to the reactor and that was stirred for 24 hours. After filtration DMF and the rest of acrylonitrile were distilled off. The modified polyglycerol was firstly dissolved in acetone and then precipitated in methanol. The both fractions were analyzed. The both fractions are brown. The acetone fraction is a solid and the methanol fraction is high viscous oil. The 3-(O-Polyglycerol)propanenitrile was dried in vacuum at 50°C.

$^1\text{H NMR}$ (300 MHz, d_6 -DMSO or d_6 -acetone, 25°C):

$\delta=3.9$ -3.3 ppm (m, $\text{CH}_3\text{-CH}_2\text{-C}(\text{CH}_2\text{-O})_3\text{-[PG-CH}_2\text{-CH}_2\text{-CN]}_x$), $\delta=2.7$ ppm (s, $\text{CH}_3\text{-CH}_2\text{-C}(\text{CH}_2\text{-O})_3\text{-[PG-CH}_2\text{-CH}_2\text{-CN]}_x$), $\delta=1.3$ ppm (m, $\text{CH}_3\text{-CH}_2\text{-C}(\text{CH}_2\text{-O})_3\text{-[PG-CH}_2\text{-CH}_2\text{-CN]}_x$), $\delta=0.87$ ppm (m, $\text{CH}_3\text{-CH}_2\text{-C}(\text{CH}_2\text{-O})_3\text{-[PG-CH}_2\text{-CH}_2\text{-CN]}_x$)

Preparation of 3-(O-Polyglycerol)propanoate

3-(O-Polyglycerol)propanenitrile (2g) was placed in 120 ml 3N sodium hydroxide solution. A 30% weight H_2O_2 solution (10 ml) was carefully added and the mixture was stirred for 1 hour at 70°C, then for 1 day at 80°C and finally cooled down to room temperature for 2 days. A 2M sodium sulfite solution was added and the reaction mixture was dialyzed for 2 days in water. Materials were precipitated in ethanol and the reaction was repeated until the conversion of the nitrile to carboxylate was high enough. The product is a slightly yellow solid.

$^1\text{H NMR}$ (300 MHz, D_2O , 25°C):

$\delta = 3.9$ -3.3 ppm (m, $\text{CH}_3\text{-CH}_2\text{-C}(\text{CH}_2\text{-O})_3\text{-[PG-CH}_2\text{-CH}_2\text{-COONa]}_x$), 2.4 ppm (s, $\text{CH}_3\text{-CH}_2\text{-C}(\text{CH}_2\text{-O})_3\text{-[PG-CH}_2\text{-CH}_2\text{-COONa]}_x$), 1.3 ppm (m, $\text{CH}_3\text{-CH}_2\text{-C}(\text{CH}_2\text{-O})_3\text{-[PG-CH}_2\text{-CH}_2\text{-COONa]}_x$), 0.87 ppm (m, $\text{CH}_3\text{-CH}_2\text{-C}(\text{CH}_2\text{-O})_3\text{-[PG-CH}_2\text{-CH}_2\text{-COONa]}_x$).

$^{13}\text{C NMR}$ (75.4 MHz, D_2O , 25°C): $\delta = 180$ ppm ($\text{CH}_3\text{-CH}_2\text{-C}(\text{CH}_2\text{-O})_3\text{-[PG-CH}_2\text{-CH}_2\text{-COONa]}_x$), 77-66 ppm ($\text{CH}_3\text{-CH}_2\text{-C}(\text{CH}_2\text{-O})_3\text{-[PG-CH}_2\text{-CH}_2\text{-COONa]}_x$), 61 ppm ($\text{CH}_3\text{-CH}_2\text{-C}(\text{CH}_2\text{-O})_3\text{-[PG-CH}_2\text{-CH}_2\text{-COONa]}_x$), 43 ppm ($\text{CH}_3\text{-CH}_2\text{-C}(\text{CH}_2\text{-O})_3\text{-[PG-CH}_2\text{-CH}_2\text{-COONa]}_x$), 37 ppm ($\text{CH}_3\text{-CH}_2\text{-C}(\text{CH}_2\text{-O})_3\text{-[PG-CH}_2\text{-CH}_2\text{-COONa]}_x$), 22 ppm ($\text{CH}_3\text{-CH}_2\text{-C}(\text{CH}_2\text{-O})_3\text{-[PG-CH}_2\text{-CH}_2\text{-COONa]}_x$), 7.5 ppm ($\text{CH}_3\text{-CH}_2\text{-C}(\text{CH}_2\text{-O})_3\text{-[PG-CH}_2\text{-CH}_2\text{-COONa]}_x$)

Phosphorous dendrimer

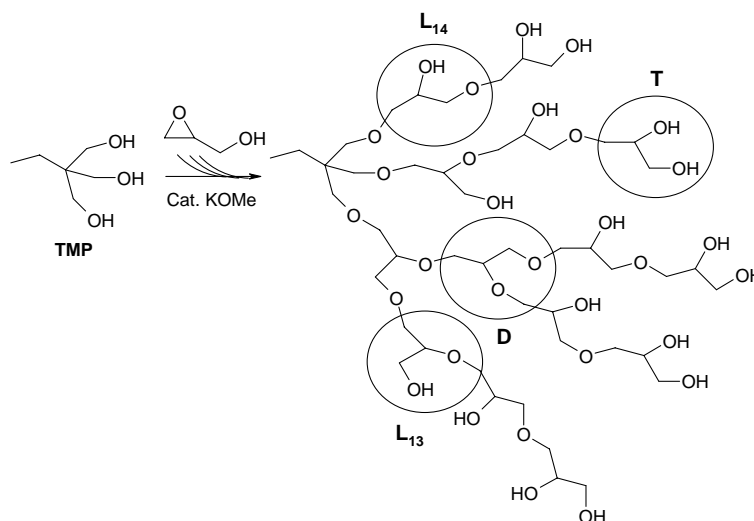
The cationic dendrimers used in this study were the N,N-disubstituted hydrazine phosphorus-containing dendrimers of the 4th generation having 96 functional groups on the surface with cationic character $\text{G}_4(\text{NH}^+\text{Et}_2\text{Cl})_{96}$.^{19,20}

8.7. References

- (1) Vögtle, F.; Gestermann, S.; Hesse, R.; Schwoerz, H.; Windisch, B. *Prog. Polym. Sci.* **2000**, *25*, 987.
- (2) Buhleier, E.; Wehner, W.; Vögtle, F. *Synthesis* **1978**, *155*, 8.
- (3) Wörner, C.; Mülhaupt, R. *Angew. Chem Int. Ed.* **1993**, *32*, 1306.
- (4) Brabander-van den Berg, E. M. M.; Meijer, E. W. *Angew. Chem Int. Ed.* **1993**, *32*, 1308.
- (5) van Hest, J. C. M.; Baars, M. W. P. L.; Elissen Román, C.; van Genderen, M. H. P.; Meijer, E. W. *Macromolecules* **1995**, *28*, 6689-6691.
- (6) Tsukruk, V. V. *Adv. Mater.* **1998**, *10*, 253.
- (7) Knopade, A. J.; Caruso, F. *Biomacromolecules* **2002**, *3*, 1154.
- (8) Kim, B. Y.; Bruening, M. L. *Langmuir* **2003**, *19*, 94.
- (9) Kim, D. H.; Hernandez-Lopez, J. L.; Liu, J.; Mihov, G.; Bauer, R. E.; Grebel-Köhler, D.; Klapper, M.; Müllen, K.; Weil, T.; Mittler, S.; Knoll, W. *Macromol. Chem. Phys.* **2005**, *206*, 52.
- (10) Kim, D. H.; Karan, P.; Göring, P.; Leclaire, J.; Caminade, A.-M.; Majoral, J.-P.; Gösele, U.; Steinhart, M.; Knoll, W. *Small* **2005**, *1*, 99.
- (11) Wu, X. C.; Bittner, A. M.; Kern, K. *Adv. Mater.* **2003**, *16*, 413.
- (12) He, J.-A.; Valluzzi, R.; Yang, K.; Dolukhanyan, T.; Sung, C.; Kumar, J.; Tripathy, S. K. *Chem. Mater.* **1999**, *11*, 3268.
- (13) Guo, Y.-G.; Hu, J.-S.; Liang, H.-P.; Wan, L.-J.; Bai, C.-L. *Adv. Funct. Mater.* **2005**, *15*, 196.
- (14) Sasaki, T.; Ebina, Y.; Tanaka, T.; Harada, M.; Watanabe, M.; Decher, G. *Chem. Mater.* **2001**, *13*, 4661.
- (15) Mitzi, D. B. *Chem. Mater.* **2001**, *13*, 3283.
- (16) Li, X.; Lau, K. H. A.; Kim, D. H.; Knoll, W. *Langmuir* **2005**, *21*, 5212.
- (17) Antipov, A. A.; Sukhorukov, G. B.; Möhwald, H. *Langmuir* **2003**, *19*, 2444.
- (18) Lei, Y.; Zhang, L. D.; Meng, G. W.; Li, G. H.; Zhang, X. Y.; Liang, C. H.; Chen, W.; Wang, S. X. *Appl. Phys. Lett.* **2001**, *78*, 1125.
- (19) Loup, P. C.; Zanta, M. A.; Caminade, A.-M.; Majoral, J.-P.; Meunier, B. *Chem. Eur. J.* **1999**, *5*, 3644.
- (20) Majoral, J.-P.; Caminade, A.-M.; Maraval, V. *Chem. Commun.* **2002**, 2929.

9. Summary and conclusions

The aim and the scope of this thesis was the development of new controlled architectures based on hyperbranched polyglycerol as building block, making use of the unusual properties of this compact building block. This includes hyperbranched oligomers, hyperbranched polyethers containing new initiator-cores at the focal point, well-defined linear-*b*-hyperbranched block copolymers as well as negatively charged hyperbranched polyelectrolytes. The synthesis of polyglycerol is based on an strategy established prior to the work of this thesis: the slow monomer addition of the highly reactive AB₂ monomer glycidol onto a multifunctional initiator-core (**Scheme 1**).



Scheme 1. Synthesis of hyperbranched polyglycerol from glycidol with 1,1,1-tris(hydroxymethyl)propane (TMP) as initiator-core.

Hyperbranched oligoglycerols versus industrial oligoglycerols

Hyperbranched oligoglycerols (HBPG) were successfully prepared via slow monomer addition of glycidol onto the partially activated initiator-core 1,1,1-tris(hydroxymethyl)propane (TMP). The two low molecular weight samples prepared ($\overline{DP}_n = 7$ and 14) exhibited low polydispersity (1.45) and monomodal elugrams by SEC. Characterization data regarding these novel low molecular weight polyglycerols are presented in **Table 1**. The molecular weights values obtained by different analytical methods (¹H NMR, ¹³C NMR, VPO and SEC) are in good concordance. Detailed ¹³C NMR studies showed that the degree of branching (DB) of the

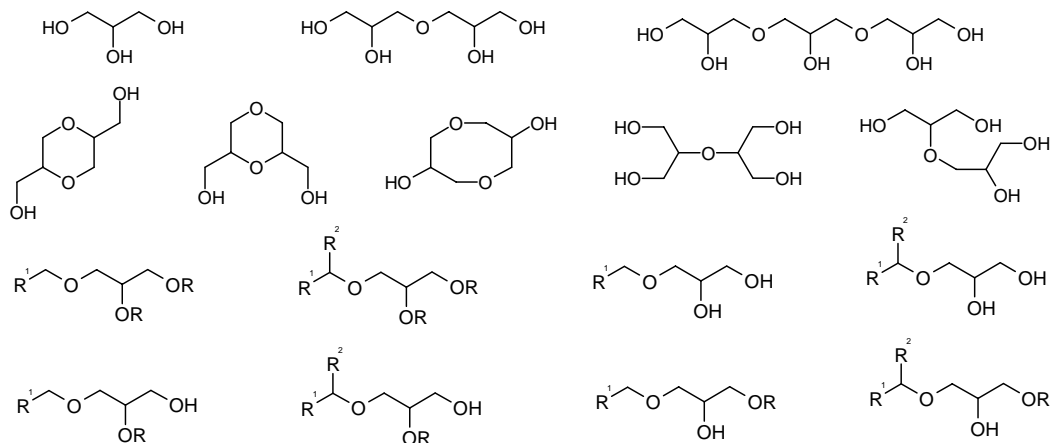
oligoglycerols is lower than the values for the higher molecular weight hyperbranched polyglycerols as expected.

Commercial oligoglycerols (SPG) exhibited narrow polydispersities but also multiple mode elugrams (see **Table 1**). The overall molecular weights obtained from VPO and SEC were similar, and branched structures are also present in the commercial samples SPG₃ and SPG₄.

Table 1. Characterization data of hyperbranched oligoglycerols (HBPG) and commercial oligoglycerols (SPG) (all molecular weights are given in g·mol⁻¹). [a] Calculated from monomer/initiator ratio; [b] calculated for $\overline{DP}_n = 2, 3$ and 4 (\overline{DP}_n depends on the reaction time); [c] \overline{M}_p is the corresponding molecular weight of the maximum(a) of the peak(s) visible in the SEC.

	Theory	¹ H NMR	VPO	SEC		¹³ C NMR		
	\overline{M}_n	\overline{M}_n	\overline{M}_n	\overline{M}_n	$\overline{M}_w / \overline{M}_n$	\overline{M}_p ^[c]	DB	\overline{DP}_n
HBPG ₇	500 ^[a]	640	496	650	1.45		44%	5.6
HBPG ₁₄	1,000 ^[a]	1,200	976	1,300	1.46		52%	11.2
SPG ₂	166 ^[b]	-	167	115	1.03	120	-	-
						180		
SPG ₃	240 ^[b]	-	241	160	1.24	115	-	-
						170		
						270		
SPG ₄	314 ^[b]	-	295	200	1.26	150	-	-
						260		

A detailed comparison of the composition of both series of materials was achieved by detailed ¹³C NMR and ESI studies.. According to the random reaction of the different hydroxyl groups during the polymerization different units can be obtained: (i) linear units, (ii) dendritic units, (iii) terminal units. Additionally, due to intramolecular homopolymerization, cyclic compounds were formed, particularly in the case of the technical samples. Some examples of compounds and structural units present are given in **Scheme 2**.



Scheme 2. Possible compounds and structural units present in hyperbranched and commercial oligoglycerols.

¹³C NMR experiments showed the presence of dendritic units in the commercial oligoglycerols, but the intensities of the respective signals were weak. Therefore it was not possible to calculate the degree of branching. The dendritic character of the commercial oligoglycerols is much less pronounced than that of hyperbranched polyglycerols, in which the signals corresponding to the dendritic **D** units are very intense. NMR spectroscopy could not provide information on the presence or absence of cyclization during the polymerization process, since the cyclic compounds comprise the same structural units as the others.

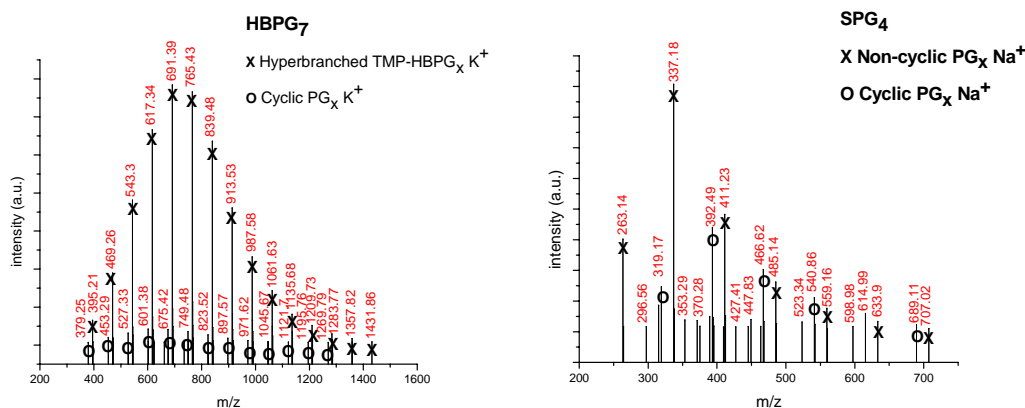


Figure 1: ESI mass spectra (methanol solution 1g·l⁻¹) of hyperbranched oligoglycerol sample HBPG₇ (left) and the commercial oligoglycerol sample SPG₄ (right).

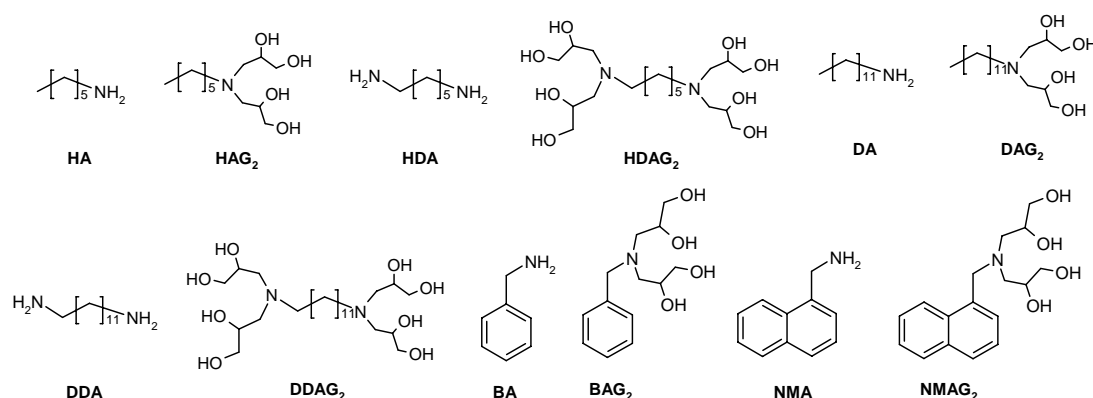
ESI mass spectrometry was performed on all samples. A very low fraction of macromolecules without core (cycles) are visible for the hyperbranched oligoglycerols hyperbranched macromolecules with TMP as initiator-core (**Figure 1 left**). On the contrary, commercial oligoglycerols comprise a large extent of cyclic

homopolymers (**Figure 1 right**). The polycondensation process promotes more cyclization than the ring-opening polymerization under slow monomer addition.

These results are important, since for very sensitive and demanding applications the homogeneity of the materials is a crucial requirement. In this regard the hyperbranched oligoglycerols are more appropriate than the industrial oligoglycerols.

New functional initiator-cores for hyperbranched polyglycerols

Amine initiator-cores have been used for the ROMBP of glycidol: mono- and bifunctional *n*-alkyl amines as well as photoactive cores such as benzylamine and 1-naphthylmethylamine (**Scheme 3**).



Scheme 3. *n*-Alkyl and UV-absorbing amine initiator-cores used.

The initiator-cores were used directly or were bisglycidolized prior to the polymerization. A systematic study on the influence of the initiator-cores on molecular weight control and molecular weight distribution permitted to conclude that the bisglycidolized amine initiator-cores lead to better results, since the polymerization started more homogeneously in this case (**Table 2**). Also the length of the *n*-alkyl chain of the amine has an impact on the molecular weight control and distribution. The C₁₂ amine leads to better control of the molecular weight than the C₆ amine, because the longest amine exhibits better solubility and stability towards sublimation than the short amines.

Table 2. Characterization data of hyperbranched polyglycerol samples with *n*-alkyl and UV absorbing amine initiator-cores. [a] \overline{M}_n in $\text{g}\cdot\text{mol}^{-1}$; [b] *NCS*: no core signals visible in ^1H NMR-spectra.

Core	Theory	^1H NMR	SEC	
	$\overline{M}_n^{[a]}$	$\overline{M}_n^{[a]}$	$\overline{M}_n^{[a]}$	$\overline{M}_w / \overline{M}_n$
No core	-		2,700	5.4
TMP	2,000	2,300	1,900	1.6
HA	2,000	<i>NCS</i> ^[b]	14,652	11.2
HAG ₂	2,000	6,800	5,600	1.5
HDA	2,000	3,500	1,110	3.6
HDAG ₂	2,000	3,100	2,850	1.65
DA	2,000	25,980	9,350	2.1
DAG ₂	2,000	4,500	2,000	1.5
DDA	2,000	6,200	3,340	5.4
DDAG ₂	2,000	3,580	1,500+(aggreg.)	1.9
BA	1,000	8,460	1,690	2.4
BAG ₂	1,000	1,560	1,200	1.8
BA	2,000	4,200	2,100	3.3
BAG ₂	2,000	3,290	2,900	1.8
BA	5,000	<i>NCS</i> ^[b]	67,400	3.5
BAG ₂	5,000	5,400	3,300	1.8

Using MALDI-ToF mass spectrometry the incorporation of initiator-core into the hyperbranched polyglycerols was investigated. Cyclic homopolymers were generally not present in the samples prepared with bisglycidolized amines (**Figure 2 top**), but were found in the majority of the polymers started with the amines directly (**Figure 2 bottom**). This observation indicates that cyclization is reduced when bisglycidolized amines are used.

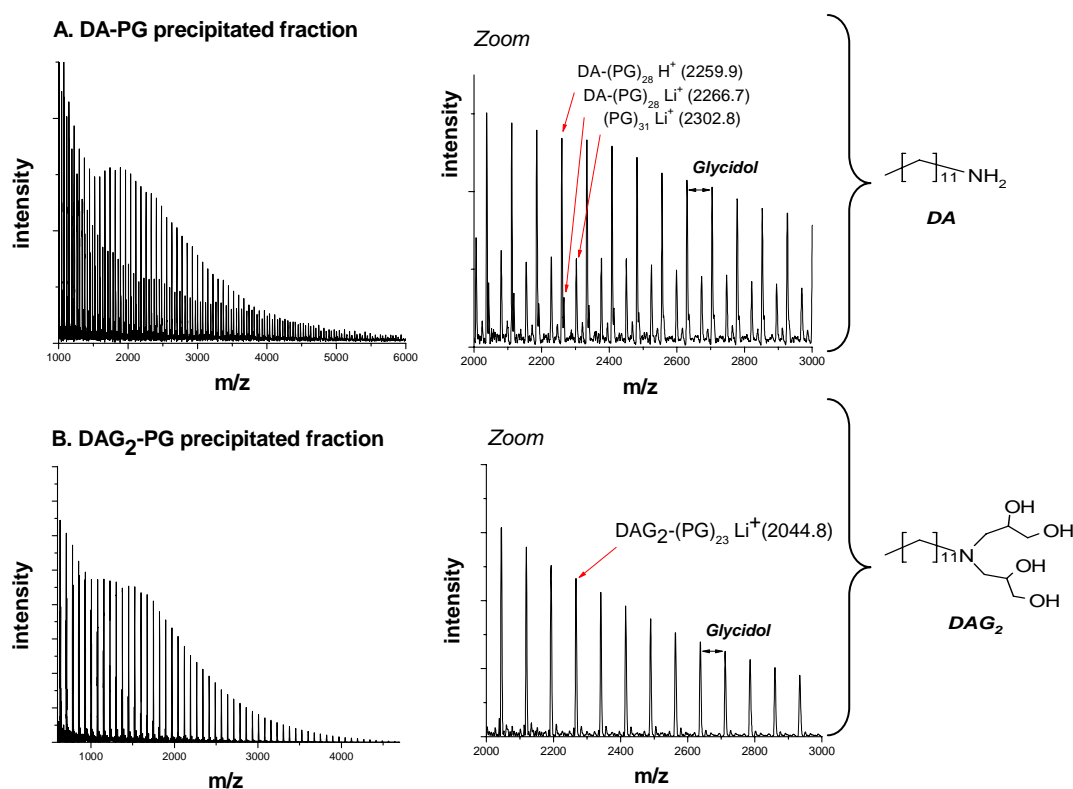


Figure 2. MALDI-ToF mass spectra of hyperbranched polyglycerols obtained with dodecylamine DA (*top*) and bisglycidolized benzylamine DAG₂ (*bottom*) initiator-cores, theoretical molecular weight 2,000 g·mol⁻¹.

UV-visible, steady state and time resolved fluorescence as well as pH-dependent fluorescence spectroscopy has been applied to confirm the presence of the naphthalene probe and the influence of the surrounding hyperbranched polymer on the optical and electronic properties of the encapsulated naphthalene core. A slight red shift and pronounced hypochromic shift (decrease of the intensity) in the hyperbranched spectra compared with the parent model compound have been observed (**Figure 3**). No electronic interactions between the polyglycerol branches and the naphthalene occurred in the ground state. However, fluorescence spectroscopy showed the importance of solvent access to the core, indicating the formation of relatively compact structure (**Figure 3**). At acidic pH, the emission fluorescence of the hyperbranched polymers increased strongly, resulting in rigid and compact structures.

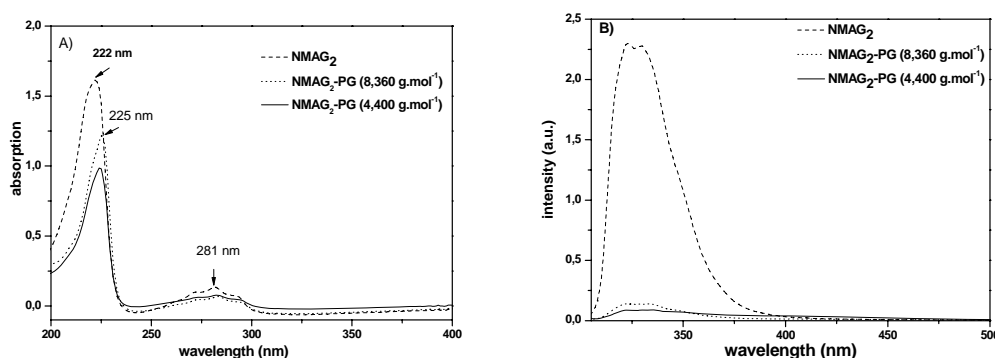


Figure 3. A) UV-*vis* spectra of NMAg₂ and hyperbranched polyglycerols with NMAg₂ as initiator-core recorded at 298K in millipore water. B) Fluorescence emission spectra at excitation wavelength, $\lambda_{\text{exc}} = 296 \text{ nm}$ of NMAg₂ and hyperbranched polyglycerols with NMAg₂ as initiator-core at 298K in millipore water. The samples were measured at fixed absorption, $\text{Abs}(\lambda_{\text{max}} = 296 \text{ nm}) = 0.3$.

Benzophenone, a typical triplet photosensitizer was employed as initiator-core. A series of samples with molecular weights ranging from 1,500 to 8,300 $\text{g}\cdot\text{mol}^{-1}$ ($\text{PDI} < 2$) was prepared (BP-PG). MALDI-ToF confirms the absence of cyclic homopolymers (without a benzophenone core) in the samples. The polarity of the functional end groups was modified (acetylation: BP-(PG-Ac)) in order to carry out a comparative study of the photochemical properties of these samples. UV-*vis* spectra showed a slight blue shift for all polymer samples in methanol compared with the simple tetraalkoxy core (**Figure 4**). Measurements recorded in a less polar solvent (i.e. CH₃CN) showed also a small blue shift for the acetylated polymers. Absorption maxima and molar extinction coefficients increase with the molecular weight of the hyperbranched polymer. The absence of a drastic influence of the surrounding hyperbranched polymer on the absorption spectra of the benzophenone core can be attributed to the open structure of the hyperbranched macromolecules in polar solvents (i.e. CH₃OH, CH₃CN), which prevents close contact of the branches with the benzophenone core.

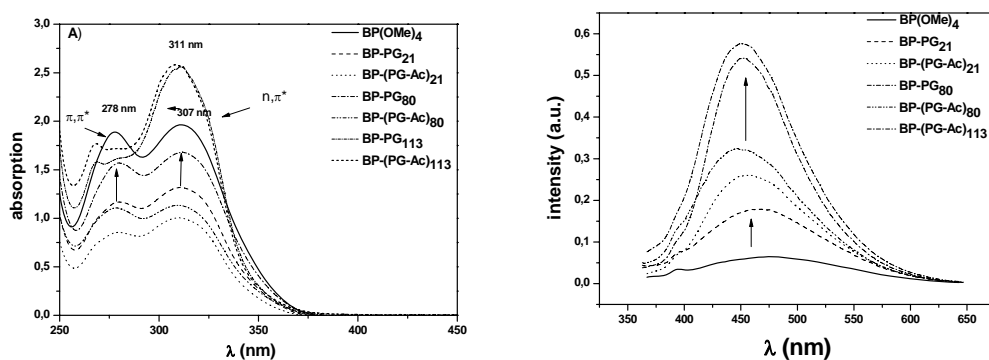
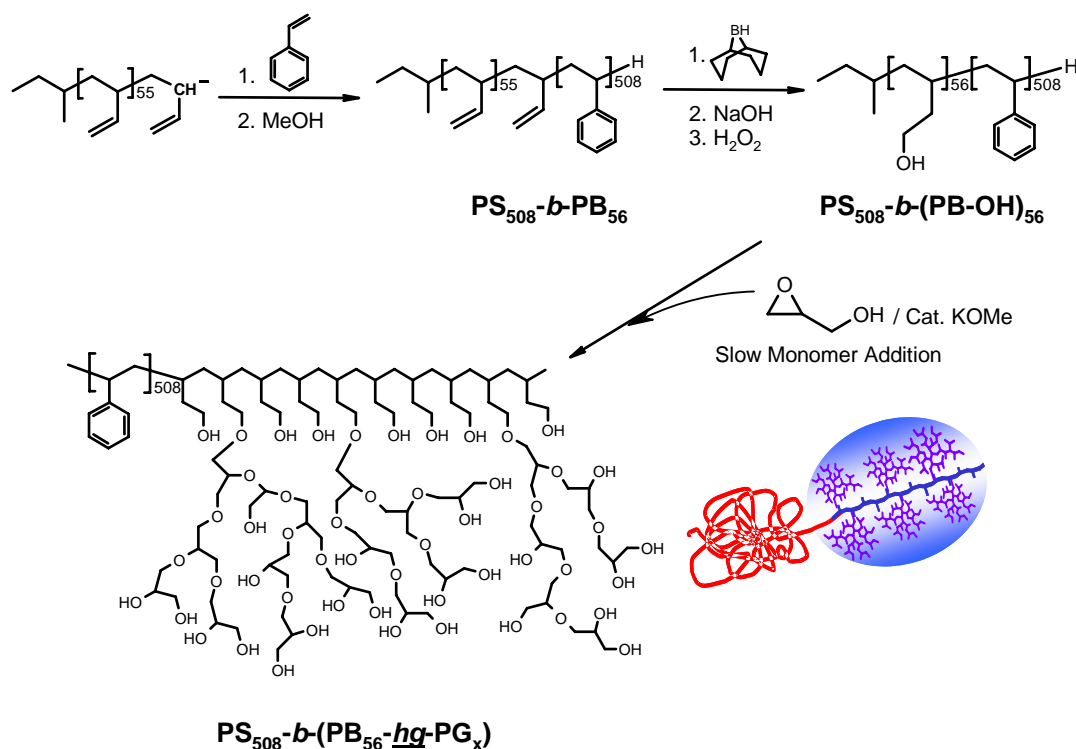


Figure 4. A) UV-*vis* spectra of hyperbranched polyglycerols containing benzophenone core normalized at $[BP] = 10^{-4} \text{M}$ at 298K: in methanol; B) fluorescence emission spectra at excitation wavelength $\lambda_{\text{exc}} = 355 \text{ nm}$ of hyperbranched polyglycerols containing benzophenone core in methanol normalized at $Ab_{355}(\text{BP}) = 0.3$.

Fluorescence measurements showed an increase of the emission intensity as the molecular weight increased (**Figure 4**). Emission spectra of the high molecular weight hyperbranched polymer BP-(PG-Ac)₁₁₃ displayed a clear negative blue shift (-56 nm). Also an increase of the emission maxima of the fluorescence intensity of the benzophenone core is observed with increasing molecular weights.. These results are very striking, since these materials exhibit a “dendritic effect” like in the case of dendrimers, which has not been observed for hyperbranched polymers before.

Linear-hyperbranched amphiphilic block copolymers

The strategy developed for the synthesis of linear-hyperbranched block copolymers is based on a well-defined AB-diblock copolymer with a short polyfunctional B-block that represents a macroinitiator for AB₂-type monomers. The polyfunctionality of the macroinitiator leads to a high degree of attachment of the hyperbranched structure and permits control of the molecular weight distribution as described in previous theoretical studies. As shown in **Scheme 3**, the first linear block copolymer used is polystyrene-*b*-1,2-polybutadiene (PS₅₀₈-*b*-PB₅₆), prepared by anionic polymerization and thus exhibiting a low polydispersity of 1.01. Subsequent to the synthesis of the diblock copolymer macroinitiator the vinyl groups of the polybutadiene block were fully hydroxylated by hydroboration/oxidation. In the third step of the synthesis, glycidol was slowly added to the partially deprotonated polyhydroxyl block. The size of the dendritic block could be controlled by the amount of glycidol grafted onto the AB-diblock copolymer.



Scheme 3. Synthetic strategy for the preparation of linear-hyperbranched amphiphilic block copolymers: $\text{PS}_{508}\text{-}b\text{-(PB}_{56}\text{-hg-PG}_x)$.

The precipitated polymers were dried and further characterized. Since the materials show strong aggregation in solution, they had to be persilylated. ^1H NMR spectra evidence grafting of glycidol onto the macroinitiator and permit to determine both the molecular weight of the hyperbranched block and the grafting efficiency. SEC measurements show narrow apparent molecular weight distributions for all samples (**Table 3**). This confirms that the well-defined polyfunctional macroinitiator acts as a template for the hypergrafting of the AB_2 monomer.

Table 3. Characterization data of the macroinitiator and the linear-hyperbranched block copolymers. SEC and ^1H NMR were performed on persilylated samples, [a] values from SEC include the TMS groups; [b] values in $\text{g}\cdot\text{mol}^{-1}$.

	SEC ^[a]		^1H NMR		
	$\overline{M}_n^{[b]}$	$\overline{M}_w / \overline{M}_n$	$\overline{M}_n^{[b]}$	wt. % PG	% Grafting
$\text{PS}_{508}\text{-}b\text{-PB}_{56}$	56,790	1.01	52,873 (PS) 3,017 (PB)	-	-
$\text{PS}_{508}\text{-}b\text{-(PB-OH)}_{56}$ ^[a]	52,900	1.01	56,840	-	-
$\text{PS}_{508}\text{-}b\text{-(PB}_{56}\text{-hg-PG}_{44})$ ^[a]	56,000	1.02	60,100	5.4%	60%
$\text{PS}_{508}\text{-}b\text{-(PB}_{56}\text{-hg-PG}_{86})$ ^[a]	56,760	1.02	63,140	10%	65%
$\text{PS}_{508}\text{-}b\text{-(PB}_{56}\text{-hg-PG}_{280})$ ^[a]	70,700	1.02	77,580	27%	65%
$\text{PS}_{508}\text{-}b\text{-(PB}_{56}\text{-hg-PG}_{840})$	120,640	1.74	119,020	52%	76%

In a second example linear polyisoprene was used as linear chain block and linear polyglycerol (LPG) as multifunctional short block. LPG can be obtained via ring-opening polymerization of an acetal-protected glycidol (ethoxy ethyl glycidyl ether). The polymerization of the protected monomer can be initiated by an alkoxide. A hydroxyl-terminated polyisoprene prepared via anionic polymerization was used as macroinitiator for the polymerization of the protected glycidol. The polydispersity of the different samples remains narrow (below 1.5). These results show the versatility of the hypergrafting strategy and its promising potential for the preparation of structurally different hybrid block copolymers.

The amphiphilic block copolymer, linear-hyperbranched polystyrene-*block*-(1,2-polybutadiene-*hypergrafted*-polyglycerol), exhibits interesting behavior in solution. PS₅₀₈-*b*-(PB₅₆-*hg* PG₂₈₀) forms interesting and homogeneous micellar aggregates in apolar solvents (chloroform and toluene). The block copolymer micelles are stabilized by the highly branched block. The size of the aggregates is solvent-dependent (smaller in chloroform than in toluene), but not concentration-dependent. The morphology of the aggregates depends on the solvent: in chloroform monodisperse spherical shape aggregates and in toluene ellipsoidal aggregates (and some cylindrical aggregates) are formed (LS).

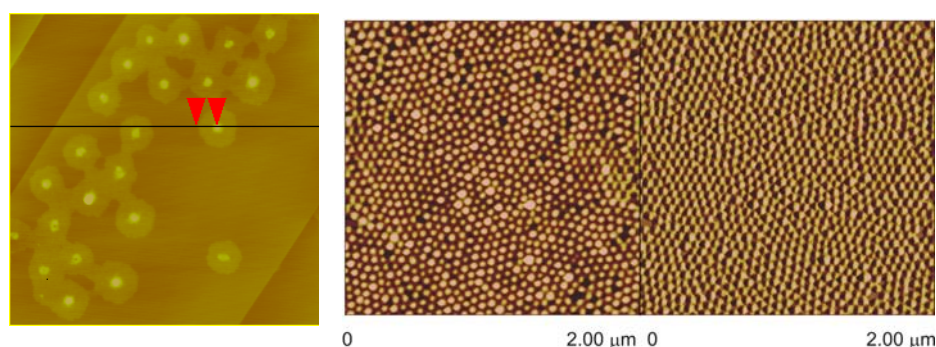


Figure 5. AFM-micrographs on a graphite substrate (tapping mode) (*left*) with corresponding height profile of PS₅₀₈-*b*-(PB₅₆-*hg* PG₂₈₀) (*right*) from toluene solution (0.5 g·l⁻¹) (*bottom*) of PS₅₀₈-*b*-(PB₅₆-*hg* PG₂₈₀) from toluene solution (1.5 g·l⁻¹).

The structures of the aggregates on graphite (HOPG) show highly regular domain structures. Deposition from chloroform leads to dense spherical micelles, but with broader polydispersity. Deposition from toluene solution led to well-defined core-shell structures. The shell consists of the polystyrene block and the core of the hyperbranched, polar polyglycerol block. The sample PS₅₀₈-*b*-(PB₅₆-*hg*-PG₂₈₀) showed

very homogeneous superstructures on graphite surface (**Figure 5**). By increasing the concentration it was possible to prepare an ultrathin film with the presence of packed domains. This is a promising result for the preparation of ordered nanoarrays via the self-assembly of these novel linear-hyperbranched block copolymers.

SAXS and TEM measurements have been performed in order to determine the morphology of the different linear-hyperbranched amphiphilic block copolymers. Since the hyperbranched polyglycerol block is bulky and possesses dense hydroxyl groups, it is presumably difficult for the structure to self-organize. The linear hyperbranched block copolymers containing polyisoprene as linear segment exhibited only one reflection in SAXS diffractograms. These materials behave like complex liquids due to the low T_g of both components. The bulk morphology of the polystyrene-block-(1,2-polybutadiene-*hg*-polyglycerol) samples was also investigated. Only the sample with 27% wt. of hyperbranched polyglycerol forms some lamellar phase domains in the solid state (**Figure 6**).

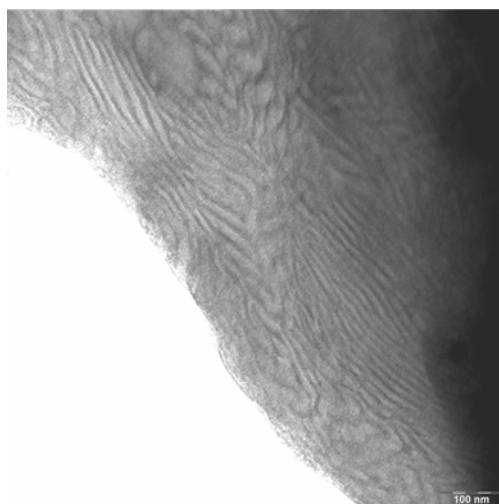
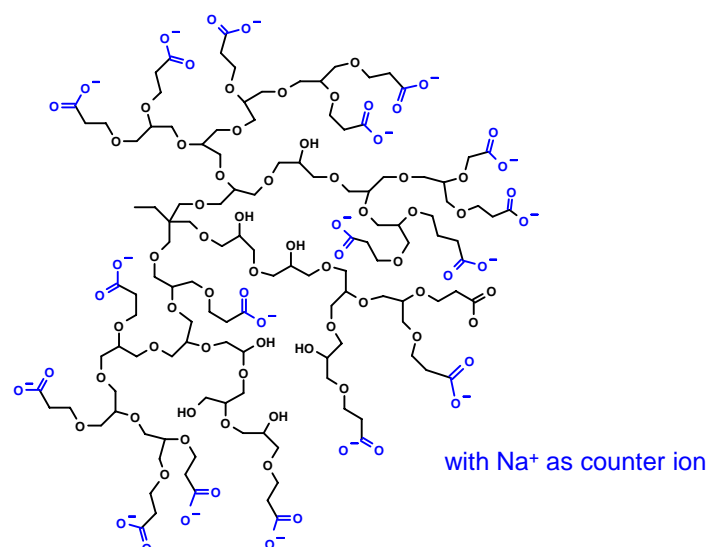


Figure 6. Transmission electron microscopy after staining with osmium tetroxide and dry cutting of $PS_{508}\text{-}b\text{-}(PB_{56}\text{-}hg\text{-}PG_{280})$.

Negatively charged hyperbranched polyglycerol polyelectrolytes

The preparation of carboxylated hyperbranched polyglycerols (**Scheme 4**) was achieved by post-modification of the hydroxyl groups via Michael addition of acrylonitrile, followed by hydrolysis. High conversion could only be achieved for low molecular weight starting materials ($PG\ 520$ and $1,030\text{ g}\cdot\text{mol}^{-1}$).



Scheme 4. Synthesis of carboxylated hyperbranched polyglycerol via Michael addition followed by hydrolysis.

The solution properties of such materials were investigated by DLS. The results show the formation of large aggregates with size depending on the pH value. After deposition on mica the structures observed by AFM show the coexistence of aggregates and unimers. In the case of the low molecular weight sample (PG 520 $\text{g}\cdot\text{mol}^{-1}$) extended and highly ordered terrace structures were formed at pH 10, which can be of interest for specific deposition processes (**Figure 7**).

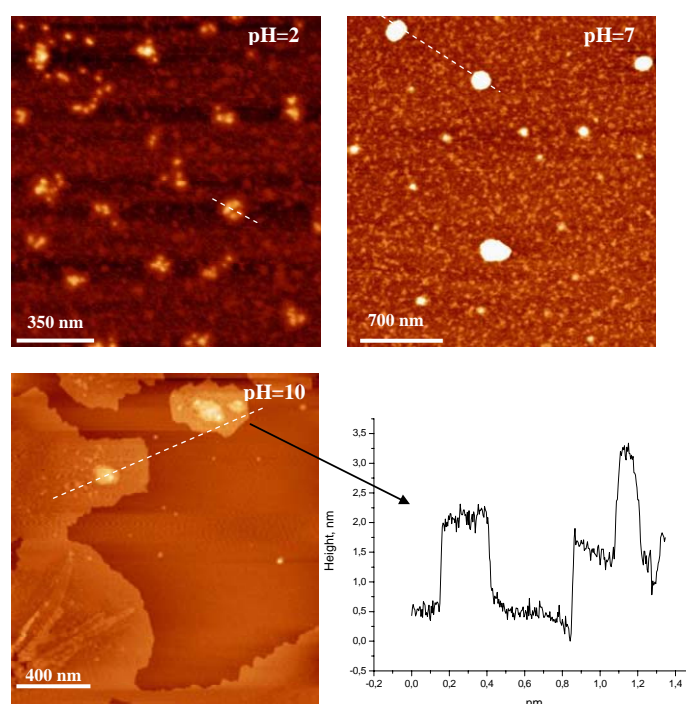


Figure 7. AFM-micrographs on a mica substrate of carboxylated hyperbranched polyglycerol (PG 520 $\text{g}\cdot\text{mol}^{-1}$) from an aqueous solution (1 $\text{g}\cdot\text{l}^{-1}$) at different pH (2, 7 and 10) and corresponding height profile for pH 10 (tapping mode).

The materials have been successfully employed for the fabrication of composite organic-inorganic multilayer thin films, using electrostatic layer-by-layer self-assembly coupled with chemical vapor deposition. The consecutive, alternating deposition of multilayers led to linear growth behavior with increasing number of deposition steps (**Figure 8**). In order to generate TiO₂ moieties inside the multilayers, a binary reaction mechanism between water molecules trapped inside the film and TiCl₄ precursors was exploited. The amount of TiO₂ inside the films could be increased by increasing the porosity of the multilayers, which was controlled by adding a small amount of salts to the polymer solution. The resulting hybrid films exhibited TiO₂-characteristic photoluminescence properties.

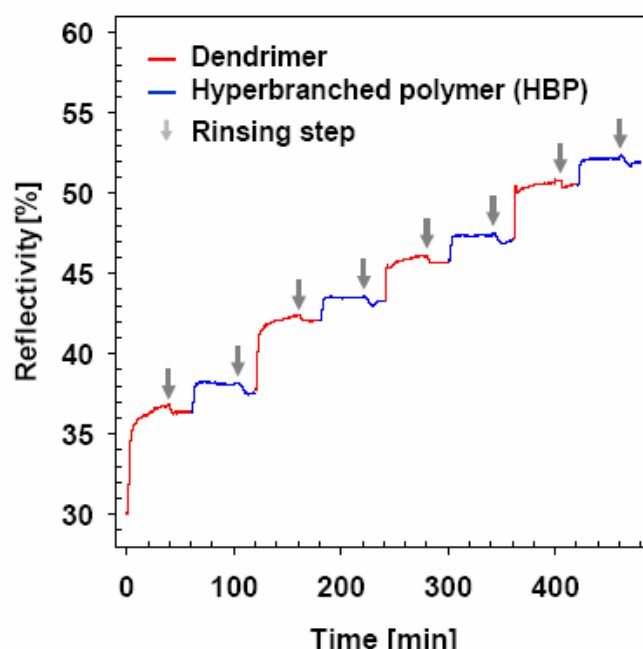


Figure 5. Kinetic mode scan mode of the successive deposition of the phosphorous dendrimer $G_4(NH^+Et_2Cl)_{96}$ and the carboxylated hyperbranched polyglycerol $HBPG_{50}(COO^-Na^+)_{44}$ up to 4 bilayers. In between each deposition, rinsing steps (indicated by arrows) removed small amounts of physically adsorbed material. The first step (sky blue curve) indicates the adsorption of 3-MPA onto an Au substrate.

10. Methods and instrumentation

10.1 Atomic force microscopy (AFM)

Chapter 6. AFM measurements were performed on a Multimode apparatus with (Digital Instruments, Santa Barbara) a Veeco IIIa controller in a tapping mode. Graphite (HOPG) was used as substrate for the AFM measurements.

Chapter 8. Samples are investigated in a dry state with a Multimode AFM instrument (Digital Instruments, Santa Barbara) operating with amplitude feedback in “light” tapping mode (amplitude set point in the range of 0.99-0.95). Silicon tips with a radius of 10-20 nm, spring constant of $0.3 \text{ N}\cdot\text{m}^{-1}$, and resonance frequency of 250-300 kHz were used after the calibration with gold nanoparticles (diameter 5.22 nm, Pelco AFM Gold Standard Kit.) to evaluate the tip radius. Most measurements were done with the tip radius $14.9 \pm 1.9 \text{ nm}$. The dimensions of structures obtained from AFM images were corrected (decreased) by the tip radius according to the standard procedure.²⁰ All measurements were done at ambient conditions (temperature $21 \pm 2^\circ \text{C}$; relative humidity 50-70%).

10.2 Differential scanning calorimetry (DSC)

DSC measurements were carried out on a Perkin-Elmer 7 series thermal analysis system in the temperature range from -70 to 150°C at heating rates of $10 \text{ K}\cdot\text{min}^{-1}$ under nitrogen.

10.3 Electron spray ionization (ESI) mass spectrometry

ESI mass spectra were recorded on a Micromass Q-TOF Ultima 3 from $1 \text{ g}\cdot\text{l}^{-1}$ solutions.

10.4 Fluorescence spectroscopy

Steady-state fluorescence. Spectra were acquired on a Photon Technology spectrofluorometer, equipped with a lamp power supply (LPS-220B), working at room temperature. The excitation wavelength for emission spectra and quantum yield measurements was 355 nm. Quantum yield measurements were measured and compared to quinine sulfate (dissolved in 0.1M sulfuric acid), for relative emission quantum yield measurements, the excitation bandwidth was 1 nm, and the absorbance of the sample solutions and the quinine sulfate dihydrate were fixed. Samples used for emission spectra and quantum yield determinations were dissolved in methanol, placed into quartz cells of 1 cm path length and purged with argon for 20 min.

Time-resolved fluorescence: Fluorescence decay data were collected on the same spectrofluorometer system equipped with a Time Master control module lamp filled with hydrogen. The decay curves were analyzed using the usual decay fit exponential analysis.

10.5 Infra-red (IR) spectrometry

FT-IR spectra were recorded on a Nicolet SDXC FT-IR spectrometer equipped with an ATR unit.

10.6 Light scattering (LS)

Chapter 6. Static light scattering (SLS) was performed with equipment composed of an ALV SP-86 goniometer, a Spectra Physics 2011-s Kr ion laser (647.1 nm wavelength, 500 mW output power) and an ALV-3000 correlator. Dynamic light scattering (DLS) was performed with an argon ion laser (Stabilite 2060-04, λ 514 nm, Spectra-Physics), a SP-125 goniometer, and an ALV-5000 multiple-tau digital correlator. The temperature was kept constant at 293 K for light scattering measurements.

Chapter 8. LS measurements were performed with a setup for combined static and dynamic light scattering consisting of an ALV/SP-86 goniometer and an ALV-5000/E multitan correlator. A He-Ne laser operating at a wavelength of 532 nm with a maximum output power of 375 mW was used as light source. Solutions were cleared by using a Millipore 0,22 μm pore size Teflon filter into 1cm diameter dust free quartz cells.

10.7 Matrix assisted laser desorption ionization - time of flight (MALDI-Tof)

Measurements were performed on with a Shimadzu Axima CFR MALDI-Tof mass spectrometer, equipped with a nitrogen laser delivering 3 ns laser pulses at 337 nm. α -cyanohydroxycinnamic acid (cca) was used as matrix. Samples were prepared by dissolving the polymer in methanol at a concentration of 10 $\text{g}\cdot\text{l}^{-1}$. A 10 μl aliquot of this solution was added to 10 μl of a 10 $\text{g}\cdot\text{l}^{-1}$ matrix solution and 1 μl of a LiCl solution (cationization agent). A 1 μl aliquot of the resulting mixture was applied to a multistage target to evaporate the methanol and create a thin matrix/analyte film. The samples were measured in positive reflectron and linear mode. A mixture of 6 peptides (Bradykinin 1-7, Angiotensin II, Angiotentin I, Pro₁₄ Arg, ACTH 1-7, ACTH 8-39) was used for an external calibration immediately before the measurement in reflectron mode.

10.8 Nuclear magnetic resonance spectroscopy (NMR)

^1H NMR spectra were recorded in $\text{d}_1\text{-CDCl}_3$, $\text{d}_3\text{-Methanol}$ and $\text{d}_6\text{-DMF}$ at concentrations of $100 \text{ g}\cdot\text{l}^{-1}$ on Bruker ARX 300 spectrometer or a Bruker ARX 400 spectrometer, operating at 400 MHz.

^{13}C NMR spectra were recorded on a Bruker ARX 400 spectrometer, operated at 75.4 MHz.

10.9 Photoluminescence (PL)

PL spectra were measured using SPEX FLUOROLOG II (212) instrument with an excitation wavelength of 350 nm.

10.10 Size exclusion chromatography (SEC)

SEC measurements were performed with a Shodex differential refractometer RI 71 in DMF with LiBr (75°C , column PSS GRAL e4/3/2) or chloroform (30°C , columns PSS SDV e4/3/2 and SDV e6/5/4) as eluent by injection of $150 \mu\text{l}$ of the polymer solution. Polystyrene standards were used for calibration.

10.11 Small angle X-ray scattering (SAXS)

The SAXS laboratory setup consisted of a Rigaku rotating anode X-ray source (Cu KR, 1.54 \AA) operated at 46 kV, 60 mA. The X-rays were monochromated using a nickel filter and focused onto the detector using a set of Franks mirrors. A 2-D CCD detector (512×512 pixels) at a sample to detector distance of 92.05 cm was used to record the scattering images. Images obtained from the block copolymers were integrated azimuthally for further analysis. To study the temperature dependence the samples were mounted on a heating stage with an accuracy of 0.1°C over the investigated temperature range.

10.12 Surface plasmon resonance spectroscopy (SPR)

The Kretschmann configuration is used with a gold (Au) film evaporated onto a glass substrate (LaSFN9), which is then optically matched to the base of a 90° LaSFN9 glass prism ($n=1.85$ at $\lambda = 632.8 \text{ nm}$). The plasmon surface polaritons are excited at the metal/dielectric interface, upon total internal reflection of the laser beam (HeNe, $\lambda = 632.8 \text{ nm}$, power 5 mW) at the prism base. By varying the angles of incidence the reflected intensity shows a sharp minimum at the resonance angle which depends upon the precise architecture of the metal/dielectric interface (scan mode). Adsorption processes occurring at the interface were followed up in real time by selecting an appropriate angle of incidence and monitoring the reflected intensity as a function of time (kinetic mode). Fresnel calculation was performed using the WINSPALL software (version 2.20) developed in the Max Planck Institute for Polymer Research in Germany.

10.13 Transmission electron microscopy (TEM)

Samples were sectioned ultrathin with a Leica Ultracut UCT microtome and stained with Ruthenium tetroxide. Bright field TEM micrographs were taken on a LEO 922 EFTEM operating at 200 kV.

10.14 Ultra violet-visible spectroscopy (UV-vis)

UV-vis spectra were recorded on an Agilent 8453 spectrophotometer equipped with a UV-vis scanning ChemStation software, operating at room temperature. A clean quartz plate of the same thickness as the substrate was used as the reference.

10.15 X-ray reflectivity measurement (XR)

X-ray reflectivity measurements were conducted at a Seifert XTD 3003 TT X-ray diffraction system operated in reflectivity mode equipped with a Goebel Mirror as a monochromator at a fixed wavelength of $\lambda = 1.54 \text{ \AA}$. Prior to the measurements the sample was aligned parallel to the primary beam with an accuracy of ($\Delta\Theta < 0.001^\circ$) and its surface was centered within the center of rotation ($\Delta z < 0.01\text{mm}$) using an iterative procedure. Starting from a coarse alignment of the z-translation ($\Delta z \sim 0.1\text{mm}$) the tilt offset ($\Delta\Theta$) and the z-translation were iteratively optimized until the required accuracy was met for both degrees of freedom.